2007

Probability density function formalism for multiphase flows

Madhusudan Gurpura Pai
Iowa State University

Probability density function formalism for multiphase flows

by

Madhusudan Gurpura Pai

A dissertation submitted to the graduate faculty

in partial fulfillment of the requirements for the degree of

DOCTOR OF PHILOSOPHY

Major: Mechanical Engineering

Program of Study Committee:
Shankar Subramaniam, Major Professor
James Evans
Rodney O. Fox
Theodore J. Heindel
James C. Hill
Richard H. Pletcher

Iowa State University

Ames, Iowa

2007

ProQuest Information and Learning Company
300 North Zeeb Road
P.O. Box 1346
Ann Arbor, MI 48106-1346

DEDICATION

To my wife Chandrika, my parents and my late mother–in–law Jayanthi Nayak.

TABLE OF CONTENTS

LIST OF TABLES

LIST OF FIGURES

ACKNOWLEDGEMENTS

It gives me great pleasure to acknowledge those individuals that have been instrumental in making my intellectual journey over the past five years most memorable. My sincere gratitude goes to my major professor Prof. Shankar Subramaniam for the innumerable discussions that sometimes ran into hours, through which he tirelessly taught me the systematic interpretation and explanation of ideas, the importance for rigor and the need for relentless attention to detail in any scientific endeavor. I am deeply grateful to him for enlightening me on the subtleties in description associated with the complex and challenging field of multiphase flows. I sincerely thank him for being an able mentor and a friend, and also for his invaluable guidance on professional matters.

I would like to express my heartfelt thanks to Profs. Rodney Fox and James Hill for agreeing to serve on my committee and providing insightful suggestions on my research and dissertation. I take this opportunity to thank them for the several mentoring sessions during two semesters in the Preparing Future Faculty program. My warmest regards goes to Profs. Richard Pletcher and Theodore Heindel for their invaluable time and their constructive comments on my work. I warmly thank Prof. James Evans for serving as my Minor representative and providing insight into my work from a physicist's perspective.

Many thanks go to Rahul Garg, Ying Xu and Sergiy Markutsya for collaborations and interesting discussions on research, course work, and other enlightening topics that were not even remotely connected to academics. During these years, I have been fortunate to be associated with my colleagues in the Computational Fluid Dynamics center, especially Anup Gokarn, Jin Sun and Kunlun Liu.

Several members of the Ames community have made this journey comfortable and enjoy-

able. My sincere thanks goes to Sunanda and Vijay Vittal, Simi and Horabail Venkatagiri, Kirthi and Srikanta Tirthapura, Kayal and Govindarasu Manimaran, and Rema and Sree Nilakanta.

I am indebted to my dear wife Chandrika for her inspiration and invaluable support during these past years. If it was not for her encouragement, understanding and patience, this would have been an impossible exercise. My sincere gratitude goes to my parents and my sister Pratima for their loving care, support and constant words of encouragement.

This work was partially supported by the US Department of Energy, ECPI Program, Grant No. DE–FG02–03ER25550.

ABSTRACT

A statistical description of multiphase flows is inevitable due to the inherent variability observed in such systems. The theoretical foundation for the Eulerian–Eulerian (EE) statistical representation of two–phase flows, which is the primary focus of the current study, is established using a probability density function formalism. It is shown that this probabilistic formalism leads naturally to the widely–used ensemble–averaged equations in the EE statistical representation. The relationship between the Lagrangian–Eulerian (LE) statistical representation and the EE formalism is clearly established. In particular, it is shown that the EE and the LE representations bear an exact relationship to each other only under restrictive conditions of local homogeneity of the two–phase flow. The correspondence between unclosed terms in the governing equations that are derived in the two statistical representations is presented. This correspondence allows one to transfer information from one representation to the other at the level of the means. A comparison of the two approaches reveals that the information content in the two representations is indeed different. The interchangeability between Lagrangian and Eulerian descriptions of the carrier phase is investigated. This exercise leads to the formulation of a new statistical representation, namely the Lagrangian–Lagrangian (LL) representation. In the LL formalism, it is shown that the only meaningful way to describe the carrier phase in a Lagrangian frame is through "surrogate" fluid particles. Together, the EE, LE and LL statistical representations presented in this study form a complete framework for the consistent single–point description of two–phase flows. Extension of the EE and LE statistical representations to systems with three and more co–existing phases is outlined. A clearly established theoretical foundation is indeed necessary; also essential is a concomitant improvement in the capability to model unclosed terms in the governing equations of a two–phase flow. Particle dispersion

and modulation of turbulent kinetic energy (TKE) by the dispersing particles are two important coupled phenomena that are observed in two–phase flows. Direct numerical simulations (DNS) of canonical homogeneous two–phase flows reveal that the timescales that govern these phenomena behave differently with Stokes number, which is an important non–dimensional quantity that characterizes the relative ease with which the dispersed phase responds to the disturbances in the carrier phase. A new dual–timescale Langevin model (DLM), which is essentially an LL model, is proposed. This model has the unique feature of *simultaneously* capturing the disparate timescale trends of particle dispersion and interphase TKE transfer with Stokes number. An important ingredient of DLM is a multiscale interaction timescale which is proposed to capture the multiscale nature of particle–turbulence interaction. The behavior of DLM in three canonical homogeneous particle–laden flows, namely freely–decaying turbulence, artificially–forced stationary turbulence and homogeneous shear, is investigated. The versatility of DLM is illustrated by its ability to capture the trends of important statistics that are observed in DNS of the aforementioned canonical two–phase flows with varying Stokes number and mass loading, which is another important non–dimensional quantity that characterizes the relative mass of each phase in a two–phase system. DLM can be extended to inhomogeneous flows with the help of the sound theoretical foundation for multiphase flows that has been established in this work.

CHAPTER 1. INTRODUCTION

1.1 Background

A multiphase flow is a physical system in which several thermodynamic phases (solid, liquid or gas) coexist. Common examples of multiphase flows that occur in nature are rain, snowfall, natural geysers, volcanoes and sandstorms. Multiphase flows find practical applications in a range of industries such as energy production, medicine and pharmaceutics. Internal combustion engines and gas turbines rely on a finely–atomized fuel spray injected into compressed air for efficient combustion and subsequent power generation. Nasal drug–delivery systems deliver a mist of life–saving medication either in the form of aerosols, or as a fine powder, to the deep recesses of the pulmonary environment via the respiratory tract. Particles are pneumatically conveyed over large distances in petrochemical industries. Emissions from automobiles and industry can be inadvertently transported over large distances, thus affecting a wide section of the population. The transport of bio–hazardous material either through the atmosphere or through large water bodies finds relevance in homeland security.

Given the socio–economic importance and wide–ranging applications of multiphase flows, there is a pressing need to gain a fundamental understanding of such flows in order to make current applications more efficient and exploit such flows further. Great strides have been achieved in probing multiphase flows (especially two–phase flows, which in the current context consists of either solid particles, bubbles or drops in a liquid or gas) by means of computer simulations and experiments. Interesting phenomena such as preferential concentration and clustering of particles [1] (Krol et al., 2000; Squires and Eaton, 1991b), and hydrodynamic interaction among droplets or particles – both of which affect macroscopic transport properties

[1] Hereafter, the word 'particle' can refer to both a solid particle or a droplet, unless specified in the context.

of the system – add to the complexity in describing such flows. Such phenomena are generally explained through an intuitive understanding of the factors that contribute to such phenomena. In order to understand precise mechanisms that lead to the such phenomena even in simple flows and extend this understanding to more complex industrial–size flows, there is a pressing need for advances in the understanding of the fundamental mathematical description of a multiphase flow.

Theoretical advances in the area of multiphase flows have been largely confined to a *first–order* description of the system. A first–order description contains information only at a single spatial location and time. However, the phenomena cited earlier are a manifestation of two–point or *second–order* [2] interactions. A mathematical description of such a system would require simultaneous information at two–points in the system. However, before embarking on developing a theory for a second–order description of a multiphase flow, it is first necessary to clearly understand the single–point description. Once a firm foundation for the single–point description has been established, it is straightforward to proceed to the next level of description. The absence of a unifying theoretical foundation for the single–point description of multiphase flows, and a need thereof, is the primary motivation behind this study.

Two–phase flows [3] lend themselves to a statistical description owing to several reasons. Firstly, the idea behind the use of a control volume, which is the starting point for a fundamental mathematical description of single–phase flows, cannot be extended in a straightforward manner to a two–phase flow. Depending on where the control volume is located in a dispersed two–phase flow, one can lose information of the other phase as the size of the control volume becomes arbitrarily small. Thus one cannot meaningfully characterize a two–phase flow using a single *realization* of the flow. One can however perform several realizations of the same two–phase flow. Since the initial conditions of the flow can only be specified nominally, one can expect that for a fraction of these realizations, this arbitrarily small control volume

[2] The terminology "second–order" is used in point process theory and refers to quantities that require simultaneous information at two physical locations in the system. This phrase should not be misinterpreted as referring to quantities whose effects are negligible compared to "first–order" quantities.

[3] In the rest of the document, the focus is on two–phase flows. The understanding gained from the study of two–phase flows can, in principle, be straightforwardly extended to multiphase flows.

is occupied by one phase and for the rest of these realizations, the same control volume is occupied by the other phase. Thus, a two–phase flow can be meaningfully described only by observing the same control volume across several realizations. This leads to the concept of an *ensemble* average, which is an average of a quantity over several independent realizations (see Figure 1.1). The fundamental starting point for a *tractable mathematical description* of a two–phase flow is, therefore, an average! The second reason why a statistical description of a flow is more reasonable is that engineers are seldom interested in how each particle behaves in a two–phase flow, but only need information on macroscopic mean quantities that describe such a flow. Although one could in principle adopt a simultaneous description of all dispersed particles and all fluid points in a two–phase flow for all time, such a description would contain much more information than is required for practical applications.

Existing statistical descriptions of two–phase flows can be classified into two broad categories: (*i*) Eulerian–Eulerian (EE) and (*ii*) Lagrangian–Eulerian (LE) representations. In the EE representation (Drew, 1983; Kataoka and Serizawa, 1989; Drew and Passman, 1999), the two phases are assumed to be interpenetrating continua. A continuum description is adopted for both the carrier phase (which is usually the bulk of the two–phase flow) and the dispersed phase. In the LE approach (Williams, 1958; Subramaniam, 2001c, 2000), although the continuum description of the carrier phase is generally assumed to be identical to that in the EE representation, the dispersed phase is treated as composed of discrete entities in the system. More precisely, the dispersed phase is described by means of an evolution equation for the distribution function (analogous to kinetic theory, although there are important differences between the kinetic treatment of gas–flows and two–phase flows), which is a function that gives the expected number of particles in an infinitesimal interval in state space [4].

In the context of the EE description of two–phase flows Drew (1983) employed an indicator function formalism to distinguish between the two–phases. Starting from the governing equations for a single–phase flow, he used the indicator function and ensemble averaging techniques to arrive at the so–called averaged equations for a two–phase flow. The fundamental descrip-

[4]The state space is generally composed of position, velocity and radius co–ordinates, but can have other variables like temperature, concentration, etc.

tion of the dispersed phase by means of a droplet–distribution function (ddf) was introduced by Williams (1958) and this theory forms the basis for the LE approach. Later, Subramaniam (2000, 2001c) established a firm mathematical foundation for the LE representation by resorting to the theory of stochastic point processes. The LE description is superior to the EE description for the dispersed phase due to the presence of an unambiguous radius phase space in the former. Size distributions in the dispersed phase can easily be accounted for in the LE approach. Moreover, as will be clearly shown in this work, insight into the unclosed terms in the governing equations for mean mass, mean momentum and turbulent kinetic energy (TKE) in the EE approach can be gained from the corresponding unclosed terms in the LE approach.

The issue of whether the Lagrangian and Eulerian descriptions of the carrier phase are interchangeable as in single–phase flows (Pope, 1985) is investigated in this work. It is shown that the carrier phase is represented consistently only by viewing it as a collection of "surrogate" fluid particles. This viewpoint results in a new statistical description called the Lagrangian–Lagrangian (LL) description of two–phase flows. The evolution equation for the carrier–phase Lagrangian probability density is derived and shown to be consistent with the corresponding Eulerian pdf equations.

The overarching goal of this work is to carefully develop the probability density function formalism for each of the three statistical representations of two–phase flow viz., EE, LE and LL. This involves clearly identifying fundamental events associated with a two–phase flow and defining probabilities corresponding to each event. Note that 'Eulerian' and 'Lagrangian' are only frames of reference, and therefore the outcome of a statistical description of a two–phase flow should not depend on the frame of reference. However, the level of information embedded in each representation can be different, and one may require consistency conditions to establish an equivalence between various representations. An equally important goal of this study is to show that the EE and LE probabilistic representations lead to distinct sets of governing equations for the two–phase flow.

The development of a fundamental and consistent mathematical description of two–phase flows is important and necessary. Inevitably, terms that are unclosed appear in such a de-

scription and analogous to that in single–phase flows the notorious closure problem is observed in the statistical description of two–phase flows. A mathematical theory for a physical phenomenon is complete and useful only when tractable models are proposed for the unclosed terms that arise from the mathematical description. In this work, we propose a new model in the context of the LL representation of two–phase flows called the dual–timescale Langevin model (DLM). This model has a unique feature that it can simultaneously capture certain fundamental timescales seen in two–phase flows and their disparate trends with certain non–dimensional quantities – a feature that is as yet unavailable in other two–phase models in literature. A new multiscale interaction timescale is also proposed that captures the multiscale nature of the particle–turbulence interaction in a two–phase flow.

Unclosed terms in the mathematical description of a two–phase flow usually shed light on the physical phenomena that such terms describe or how such terms drive the evolution of a physical quantity. However, the exact form of the models for these unclosed terms is not easily evident from the functional form of the unclosed terms. One then has to resort to datasets from carefully controlled computer simulations and experiments, where an attempt has been made to quantify the unclosed terms, to arrive at a workable model. These findings when combined with physical intuition yield simple and tractable models for the unclosed terms, yet possessing the capability of correctly reproducing trends of key two–phase statistical quantities such as phasic turbulent kinetic energy and velocity autocorrelations with non–dimensional quantities. It is worth noting that DLM is in fact a fruitful result of such an exercise. Thus findings from carefully constructed computer simulations and experiments form an integral part of the development of a mathematical description for two–phase flows.

Experiments give the most *realistic* insight into the behavior of a two–phase flow (see Poelma and Ooms (2006) for a recent review). Ensuring controlled ambient conditions, such as excluding gravity to probe particle–laden isotropic turbulence, under which experiments are performed is also important before attempting to derive conclusions from the study. Insight into the behavior of unclosed terms in the governing equations for a two–phase flow can be gained in simple experiments that isolate effects of gravity and flow inhomogeneities. Starting from

the classic experiments of Snyder and Lumley (1971) to the recent experiments by Hwang and Eaton (2006), important landmarks in understanding particle–laden flows such as the ability to negate effects of gravity and achievement of large turbulent Reynolds numbers have been realized. Recent experiments surmise that the local dissipation around particles contribute significantly towards turbulence attentuation in a turbulent particle–laden flow (Hwang and Eaton, 2006). Such refined experimental investigation would also further the development of high fidelity computational models for two–phase flows.

Direct numerical simulations (DNS), on the other hand, offer an alternative means of investigating a particle–laden turbulent flow. Speed and computer memory requirements are the only limiting factors for such simulations. Several DNS techniques are available in literature that can be classified broadly into those that solve for the flow around each particle ('true' DNS) and those that do not. Among the techniques that do not solve the flow around each particle, the point–particle (PP) approximation is the most popular and is valid only in simplified two–phase flow regimes (Sundaram and Collins, 1999; Boivin et al., 1998; Mashayek et al., 1997). In this approximation, the particles are evolved as per the particle velocity evolution equation proposed by Maxey and Riley (1983), while the carrier phase is solved using the full Navier–Stokes (NS) equations. The effect of the dispersed phase is taken into account through source terms in the gas–phase NS equations (two–way coupling). However, since the boundary layers around particles are not accounted for directly, its effect on the gas–phase turbulence is usually modeled (Sundaram and Collins, 1999), or neglected, as in most PP DNS. Hwang and Eaton (2006) conclude by means of their experiments that such PP DNS cannot account for the increased dissipation around particles that is essential for accurately quantifying the turbulence attenuation by particles. DNS techniques that do solve for the flow around each particle, on the other hand, are the fictitious domain methods (Patankar et al., 2000), discrete time immersed boundary methods (Yusof, 1996), continuous time immersed boundary methods (D. Goldstein and Sirovich, 1993) and Lattice–Boltzmann methods (Ten Cate et al., 2004). The benefit of such methods is that minimum modeling is involved in solving for the flow past immersed bodies, and most importantly, the flow around each particle can be

resolved accurately. The only modeling enters when the particles come close or collide. This is when lubrication forces or spring–damper analogies are used to rebound the colliding particles. Accurate estimates of the effect of the particles on the turbulence spectrum can be obtained using such methods. Although attractive, such DNS are limited to large particles (particle Reynolds numbers $\gg 1$). Body–fitted DNS, wherein the computational grid closely follows the shape of the immersed body, also come under the classification of true DNS. However, moving particles are very difficult to simulate using body–fitted grids and are computationally more expensive than immersed boundary methods.

The paucity of carefully controlled experiments or computations that report information useful and pertinent to the modeling community forces computational models to be based on findings from available published data in literature. Models proposed in this work rely on the findings from such experiments or computer simulations. Nevertheless, careful analysis of these findings reveal important and fundamental phenomena that any two–phase flow model must necessarily capture in order to be predictive in more complex flows.

Multiphase flows are sometimes referred to as multicomponent flows as in Drew and Passman (1999). Multicomponent in the context of mass transport phenomena (Bird et al., 2002) generally refers to the presence of several chemical species in a physical system which need not necessarily have several phases in it. For instance, a system of water and steam is a one–component two–phase flow, while a system of water and air bubbles is a two–component two–phase flow. In this study the term multiphase flow refers to a system containing two or more phases that have clearly identifiable boundaries or interfaces (at the continuum level of description) separating them. Constant density and variable–density multiphase flows are considered in this study. The thermodynamic state of the multiphase system which is important in evaporating droplet–laden flows is not discussed in this study. We also do not explicitly carry a scalar composition vector for the sake of brevity. Inclusion of a scalar composition vector into the theoretical development presented in this work is straightforward.

1.2 Research Objectives

A need to develop a unifying theoretical foundation for the single–point description of two–phase flows was identified earlier. A probabilistic formalism of the two–phase flow theory has several advantages. Quantities that are unclosed at the level of the means (such as triple velocity correlations, Reynolds stresses) are closed at the level of the pdf. The LL representation provides new insight into the description of the carrier phase. In this regard some of the pertinent questions on the representation of a two–phase that this work will focus on and attempt to answer are:

1. What are the fundamental events that characterize a two–phase flow in the EE and LE statistical represenations? What are the probabilities corresponding to each one of these events? What are the relations among these various probabilities? What is the minimum set of events and probabilities that is required to completely characterize a two–phase flow?

2. What are the consistency conditions that need to be satisfied in order to achieve a correspondence between the EE and LE representations? What is the level of information available in each representation? What is the ease or difficulty in going from one representation to the other?

3. What are the advantages and disadvantages of the LL description of a two–phase flow? At what level do the EE, LE and LL statistical representations correspond with each other?

At the outset it will be noted that significant contributions to the EE and LE statistical representations of a two–phase flow are available in literature (Drew, 1983; Drew and Passman, 1999). Rather than repeat the derivation of the governing equations for important two–phase flow quantities such as the mean mass, mean momentum and second moment using Drew's formalism, the focus of this work is to unify the existing statistical representations, show their correspondence with the LL representation and compare with existing statistical representa-

tions (such as Drew's formalism), all performed with the the fundamental probabilities as the basis.

Once a framework for the events and probabilities associated with a two–phase flow in the context of the EE, LE and LL statistical representations has been established, the next step is to derive transport equations for these probabilities. From the transport equations of the probabilities associated with the fundamental events, one can arrive at governing equations for the phasic mean mass, mean momentum and second moment. In this context, pertinent questions that this work will attempt to answer are:

1. What are the transport equations for the various probabilities corresponding to the fundamental events associated with a two–phase flow in the EE and LE representations?

2. What are important terms that drive the transport of these probabilities in phase space?

3. Can governing equations for the mean mass, mean momentum and TKE that are available in literature be related to those derived from the transport equations for the probabilities?

An exact description of a two–phase flow system will inevitably lead to terms in the governing equations for the mean mass, mean momentum and TKE that are unclosed. After careful identification of such terms, it is necessary that simple and tractable theoretical models be proposed for these terms in order for the theory to be useful to the engineering community. It is important to note that every such model in turn implies a modeled form of the exact governing equations for the mean mass, mean momentum and TKE in a two–phase flow. Determining appropriate models for unclosed terms is driven by the need to match predicted trends of important two–phase quantities with non–dimensional parameters that characterize the two–phase flow system available from direct numerical simulations or experiments on two–phase flows. Since in typical turbulent two–phase flows, the particles are influenced by a range of time and lengthscales of the carrier–phase turbulence, it is important for two–phase models that describe the evolution of mean quantities to capture this multiscale nature of particle–turbulence interaction. Since the number of unclosed terms tends to increase with the complexity of the system, the range of two–phase flows considered, as far as developing

tractable models is concerned, are restricted to particle–laden homogeneous turbulence. In this context, pertinent questions that this work will attempt to answer are:

1. Can tractable models that capture the multiscale nature of particle–turbulence interaction for a simple two–phase flow such as particle–laden homogeneous turbulence be proposed?

2. What are the evolution equations implied by such models and can one identify a correspondence between the exact and modeled governing equations?

3. How do model predictions match with datasets from direct numerical simulations or experiments?

Highlights of this study on the probability density function formalism for two–phase flows in terms of theory and modeling are shown pictorially in Figure 1.2. The carrier–phase description in the EE and LE approaches are identical, however the dispersed phase is represented as a random–field in the EE representation, while it is represented as a point process in the LE representation. The EE and LE representations lead to distinct governing equations for a two–phase flow, which in general cannot be simply related. The dispersed phase description in the LL representation is identical to that in the LE representation. However, the carrier phase is represented as a collection of "surrogate" fluid particles, in order to be consistent with the point process description of the dispersed phase. Corresponding to LE modeling, a new multiscale interaction timescale is developed to capture the multiscale interaction of the dispersed phase with a turbulent carrier phase, while a new dual–timescale Langevin model is proposed to simultaneouly capture the disparate timescales associated with dispersion and dynamics (interphase TKE transfer) in a two–phase flow. These models are validated by comparing with datasets from direct numerical simulations of canonical two–phase flows.

In summary, the principal objectives of this study are to:

1. *Develop a unifying theoretical foundation for the statistical representation of two–phase flows in the EE, LE and LL representations using the probability density function formalism*

2. *Develop models for unclosed terms that are validated by studying their ability to reproduce trends, observed in available DNS datasets, of important statistical quantities associated with a two–phase flow with non–dimensional parameters.*

1.3 Outline of the thesis

The thesis begins with a literature survey of the theoretical advances in the probabilistic formulations of two–phase flows in Chapter 2. Some of the so–called probability density function methods available in literature fall under the EE statistical representation, while the rest fall under the LE statistical representation of two–phase flows. There have been attempts to relate the EE representation to the LE representation through the use of a EE probabilistic formalism. The LE probabilistic formulation is based on the droplet distribution function and has a sound mathematical basis in the theory of point processes. All these approaches are reviewed in this chapter. Fundamental events and corresponding probabilities related to the EE representation are introduced in Chapter 3. Transport equations for the fundamental probabilities are derived in the same chapter. Evolution equations for the mean mass, mean momentum and phasic Reynolds stresses are derived from the transport equations for the probabilities. The LE probabilistic formalism is reviewed and the relation between the EE and LE approaches is presented here. Chapter 4 introduces the new LL statistical representation and investigates relationships with the EE and LE representations. Chapter 5 deals with modeling in the context of the LE statistical representation. A new multiscale interaction timescale is proposed to replace the particle response timescale which is generally used as a timescale for interphase momentum and interphase TKE transfer in widely–used LE implementations. A new dual–timescale Langevin model is proposed in Chapter 6 in the context of the LL representation of two–phase flows. The uniqueness of this model is in the existence of two timescales in a single model that can capture two fundamental and disparate timescale trends of key statistical quantities with non–dimensional parameters that characterize the two–phase flow system. Predictions of the model in particle–laden freely–decaying turbulence and homogeneous shear are presented here. Predictions from DLM for non–evaporating and evaporating

droplets in stationary turbulence are presented in Chapter 7. Chapter 8 presents the highlights and principal conclusions of this work. Some ideas on future work are outlined in the same chapter.

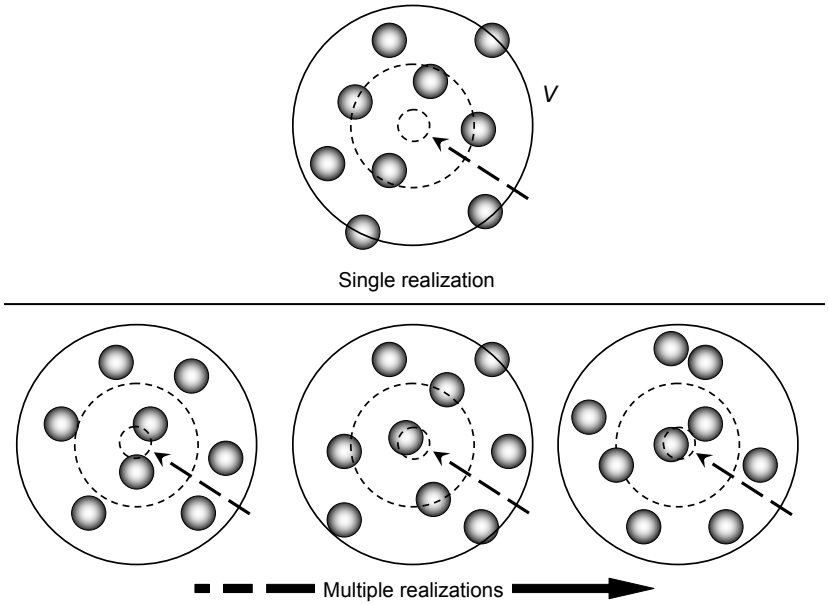

Figure 1.1 The top panel shows a snapshot of a single realization of a two–phase flow that is enclosed by a circular control volume V. As the size of the control volume is decreased (shown by the direction of the arrow) to an infinitesimal size, the volume may either completely occupy the carrier phase (as shown) or the dispersed phase. The lower panel shows various snapshots of multiple realizations the same two–phase flow. In this case, even if the volume is decreased to an infinitesimal size, it is not occupied entirely by one phase for all realizations (not considering pathological cases). Thus, meaningful statistics from the two–phase flow can be inferred only by observing several realizations of a two–phase flow. This observation leads to the concept of an *ensemble* average.

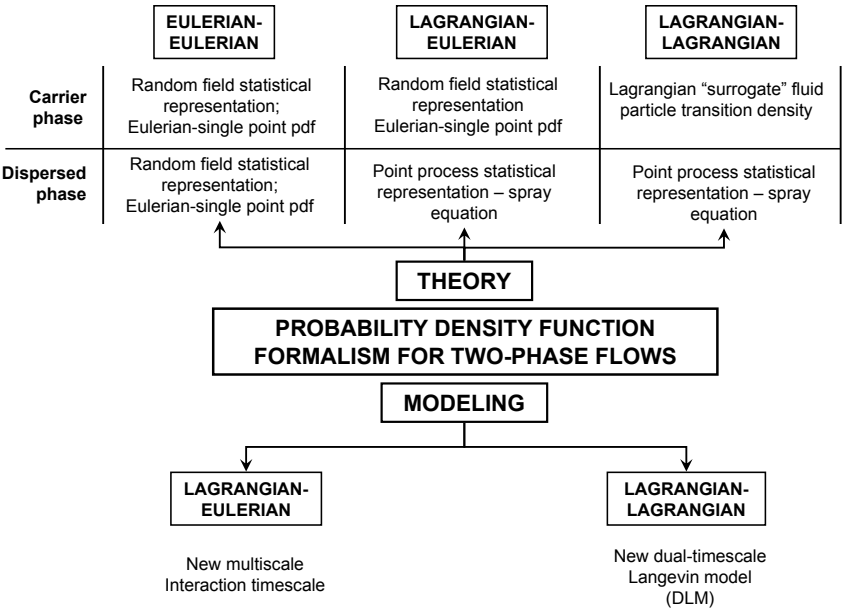

Figure 1.2 Pictorial overview of the thesis showing the principal outcomes of this work.

CHAPTER 2. LITERATURE REVIEW – PROBABILITY DENSITY FUNCTION METHODS FOR TWO–PHASE FLOWS

A literature search reveals that only a handful of researchers have embarked on developing the probability density function (pdf) formalism for two–phase flows. Most of these pdf methods can be grouped under the Eulerian–Eulerian (EE) statistical representation of two–phase flows, while a few others can be grouped under the Lagrangian–Eulerian (LE) statistical representation.

2.1 Eulerian–Eulerian statistical representation of two–phase flows

In this section, the following nomenclature will be adopted so that the notation is consistent throughout. The velocity of the two–phase flow field will be denoted $\mathbf{U}$, while the phasic velocity will be denoted $\mathbf{U}^{(\beta)}$. The indicator function that sifts the phase β from a two–phase flow will be denoted $I_\beta(\mathbf{x}, t)$ and defined as

$$I_\beta(\mathbf{x}, t) = \begin{cases} 1 & \text{if } \mathbf{x} \text{ is in phase } \beta \text{ at time } t \\ 0 & \text{if } \mathbf{x} \text{ is not in phase } \beta \text{ at time } t. \end{cases} \tag{2.1}$$

The volume fraction of the βth phase will be denoted α_β, which is given as the expectation of the indicator function $\alpha_\beta(\mathbf{x}, t) = \langle I_\beta(\mathbf{x}, t) \rangle$. Here the expectation implies an ensemble average, however, the exact meaning of the angled brackets will be clarified in each formalism.

2.1.1 Single–point pdf formalism

Zhu et al. (2000) proposed a single–time, single–point pdf for the gas and liquid phases. The starting point of their formalism is the concept of a level surface (Libby, 1976; Sethian,

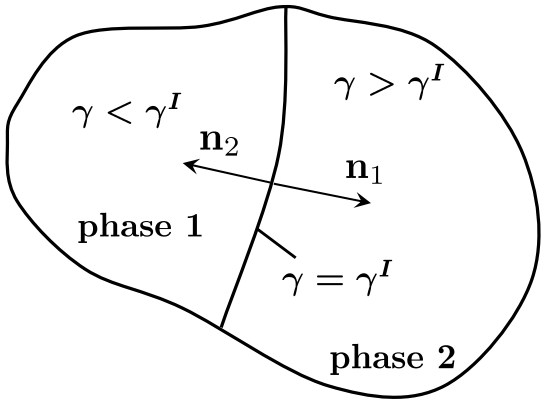

Figure 2.1 A region of the two–phase flow field containing an interface which is represented as a level surface γ. The region $\gamma < \gamma^I$ represents phase 1, $\gamma > \gamma^I$ represents phase 2 while $\gamma = \gamma^I$ represents the interface. Also shown are the normals $\mathbf{n}_1$ and $\mathbf{n}_2$ pointing away from the phases 1 and 2, respectively.

1996) denoted $\gamma(\mathbf{x}, t)$ in this work. In a two–phase flow field, the interface between the two phases is denoted γ^I with $\gamma < \gamma^I$ representing the region occupied by phase 1 and $\gamma > \gamma^I$ representing the region occupied by phase 2 (see Fig 2.1). The unit vectors normal to the interface are given as

$$\mathbf{n}^{(1)} = \frac{\nabla\gamma}{|\nabla\gamma|} \quad \text{and} \quad \mathbf{n}^{(2)} = -\mathbf{n}^{(1)} = -\frac{\nabla\gamma}{|\nabla\gamma|}.$$

At the level surface, the following governing equation for γ holds

$$\frac{\partial\gamma}{\partial t} + U_j^{(\beta)}\frac{\partial\gamma}{\partial x_j} = (U_j^I - U_j^{(\beta)})n_j^{(1)}|\nabla\gamma| \tag{2.2}$$

Using the level surface γ, they define an indicator function $I_\beta(\gamma)$ as

$$I_f(\gamma) = H(\gamma^I - \gamma) \tag{2.3}$$

$$I_d(\gamma) = 1 - H(\gamma^I - \gamma), \tag{2.4}$$

where H is the Heaviside function, and so $I_f + I_d = 1$. They derive an evolution equation for I_β as

$$\frac{\partial I_\beta}{\partial t} + U_j^{(\beta)}\frac{\partial I_\beta}{\partial x_j} = -(-1)^k(U_j^I - U_j^{(\beta)})n_j^{(1)}|\nabla\gamma|\delta(\gamma - \gamma^I) \tag{2.5}$$

where $k = 1$ if $\beta = f$ and $k = 2$ if $\beta = d$. Further, they define the two–phase flow density as

$$\rho = I_f(\gamma)\rho_f + I_d(\gamma)\rho_d \tag{2.6}$$

and the two–phase velocity as

$$\mathbf{U} = I_f(\gamma)\mathbf{U}^{(f)} + I_d(\gamma)\mathbf{U}^{(d)}. \tag{2.7}$$

Multiplying Eq. (2.2) by I_β and summing over $\beta = \{f, d\}$ results in an alternate equation for γ in terms of the two–phase velocity $\mathbf{U}$ as

$$\begin{aligned}\frac{\partial \gamma}{\partial t} + U_j \frac{\partial \gamma}{\partial x_j} &= (U_j^I - U_j^{(f)}) n_j^{(1)} |\nabla\gamma| - (U_j^I - U_j^{(d)}) n_j^{(1)} |\nabla\gamma| \\ &= -(U_j^{(f)} - U_j^{(d)}) n_j^{(1)} |\nabla\gamma| \end{aligned} \tag{2.8}$$

They then derive an evolution equation for the pdf of the two–phase velocity field $f_{\mathbf{U}\gamma}(\mathbf{V}, \gamma_s; \mathbf{x}, t)$ using the procedure outlined in Pope (1985) as

$$\frac{\partial f_{\mathbf{U}\gamma}}{\partial t} + \mathbf{V}_i \frac{\partial f_{\mathbf{U}\gamma}}{\partial x_i} = -\frac{\partial}{\partial V_i}\left[\langle A_i | \mathbf{V}, \gamma_s \rangle f_{\mathbf{U}\gamma}\right] - \frac{\partial}{\partial \gamma_s}\left[\langle B | \mathbf{V}, \gamma_s \rangle f_{\mathbf{U}\gamma}\right] \tag{2.9}$$

where $\mathbf{V}$ and γ_s are sample space variables corresponding to the random variables $\mathbf{U}$ and γ, respectively, and $B = -(U_j^{(f)} - U_j^{(d)}) n_j^{(1)} |\nabla\gamma|$. The probability that the phase β exists at point $\mathbf{x}$ is given as

$$\langle I_\beta \rangle = \iint I_\beta(\gamma_s) f_{\mathbf{U}\gamma}(\mathbf{V}, \gamma_s) d\mathbf{V} d\gamma_s \tag{2.10}$$

while the mean velocity in phase β is given as

$$\langle \mathbf{U}^{(\beta)} \rangle = \frac{1}{\langle I_\beta \rangle} \iint I_\beta(\gamma_s) \mathbf{V} f_{\mathbf{U}\gamma} d\mathbf{V} d\gamma_s \tag{2.11}$$

Velocity pdfs in each phase $f_{\mathbf{U}\gamma|I_\beta}(\mathbf{V}, \gamma_s | I_\beta; \mathbf{x}, t)$ are defined as

$$f_{\mathbf{U}\gamma|I_\beta} = \frac{I_\beta}{\langle I_\beta(\gamma) \rangle} f_{\mathbf{U}\gamma}. \tag{2.12}$$

The above velocity pdf evolves according to

$$\begin{aligned}\frac{\partial f_{\mathbf{U}\gamma|I_\gamma}}{\partial t} + \mathbf{V}_i \frac{\partial f_{\mathbf{U}\gamma|I_\gamma}}{\partial x_i} =& -\frac{\partial}{\partial V_i}\left[\langle A_i | \mathbf{V}, \gamma_s \rangle f_{\mathbf{U}\gamma|I_\gamma}\right] - \frac{\partial}{\partial \gamma_s}\left[\langle B | \mathbf{V}, \gamma_s \rangle f_{\mathbf{U}\gamma|I_\gamma}\right] \\ &+ (-1)^k \delta(\gamma - \gamma^I) \langle B | \mathbf{V}, \gamma_s \rangle f_{\mathbf{U}\gamma|I_\gamma} \end{aligned} \tag{2.13}$$

Zhu et al. (2000) attempt to relate their dispersed phase Eulerian pdf to the droplet distribution function (ddf) proposed by Williams (1958). They first integrate the earlier defined phase velocity pdf over all γ space, after introducing an additional radius phase space, as

$$f_{\mathbf{U}R|I_d}(\mathbf{V}, r|I_\beta; \mathbf{x}, t) = \int f_{\mathbf{U}R\gamma|I_\beta}(\mathbf{V}, r, \gamma_s|I_\beta; \mathbf{x}, t) d\gamma_s \tag{2.14}$$

and relate the ddf to the above pdf as

$$f(\mathbf{V}, \mathbf{x}, r, t) = f_{\mathbf{U}R|I_d}(\mathbf{V}, r|I_\beta; \mathbf{x}, t) n(\mathbf{x}, t). \tag{2.15}$$

Implicit in the above relation is the assumption that the Eulerian pdf $f_{\mathbf{U}R|I_d}$ is equal to the conditional joint pdf of velocity and radius (Subramaniam, 2001c, 2000):

$$f_{\mathbf{U}R|I_d}(\mathbf{V}, r|I_\beta; \mathbf{x}, t) = f^c_{\mathbf{V}R}(\mathbf{V}, r|\mathbf{x}, t). \tag{2.16}$$

It is shown in Section 3 that this relationship is valid only under restrictive conditions of homogeneous two–phase flow with monodisperse radius pdf, thereby rendering the work of Zhu et al. (2000) applicable only to a certain class of two–phase flows.

2.1.2 Two–point pdf formalism

The starting point for the pdf formalism proposed by Peirano and Minier (2002) is a two–point Lagrangian pdf defined such that (in the absence of scalars)

$$f^L_{fp}(\mathbf{y}_f, \mathbf{V}_f, \mathbf{y}_p, \mathbf{V}_p; t)\, d\mathbf{y}_f d\mathbf{V}_f d\mathbf{y}_p d\mathbf{V}_p$$

gives the probability of finding a pair of particles (one fluid point 'f'' and one 'dispersed' particle 'p'') with positions in the range $(\mathbf{y}_k, \mathbf{y}_k + d\mathbf{y}_k)$, velocities in the range $(\mathbf{V}_k, \mathbf{V}_k + d\mathbf{V}_k)$, and a so–called two–point Eulerian distribution function defined such that

$$f^E_{fp}(\mathbf{V}_f, \mathbf{V}_p; \mathbf{x}_f, \mathbf{x}_p, t)\, d\mathbf{V}_f d\mathbf{V}_p$$

is the probability that at time t and at positions $\mathbf{x}_f$ and $\mathbf{x}_p$, a fluid–point and a particle exist with velocities in the range $(\mathbf{V}_k, \mathbf{V}_k + d\mathbf{V}_k)$. This is not a pdf since one cannot guarantee with probability 1 that there is a fluid point at point $\mathbf{x}_f$ and a particle at point $\mathbf{x}_p$.

Two marginal Lagrangian pdfs are defined as

$$f_{\beta}^{L}(\mathbf{V}_{\beta}, \mathbf{y}_{\beta}; t) = \int f_{fp}^{L}(\mathbf{y}_f, \mathbf{V}_f, \mathbf{y}_p, \mathbf{V}_p; t)\, d\mathbf{y}_{\beta^c} d\mathbf{V}_{\beta^c} \tag{2.17}$$

where β^c is the complement of β (i.e. when $\beta = f$, then $\beta^c = p$). Two marginal Eulerian distribution functions can be defined as

$$f_{\beta}^{E}(\mathbf{V}_{\beta}; \mathbf{x}, t) = \int f_{fp}^{E}(\mathbf{V}_f, \mathbf{V}_p; \mathbf{x}_f, \mathbf{x}_p, t)\, d\mathbf{V}_{\beta^c} d\mathbf{x}_{\beta^c}. \tag{2.18}$$

by taking the limit $\mathbf{x}_f = \mathbf{x}_p = \mathbf{x}$. At the same point $\mathbf{x}$, the marginal Eulerian distribution functions satisfy a relation

$$\int f_{f}^{E}(\mathbf{V}_f; \mathbf{x}, t) d\mathbf{V}_f + \int f_{p}^{E}(\mathbf{V}_p; \mathbf{x}, t) d\mathbf{V}_p = 1, \tag{2.19}$$

and

$$\alpha_{\beta}(\mathbf{x}, t) = \int f_{\beta}^{E}(\mathbf{V}_{\beta}; \mathbf{x}, t) d\mathbf{V}_{\beta}, \tag{2.20}$$

which leads to the relation

$$\alpha_f(\mathbf{x}, t) + \alpha_p(\mathbf{x}, t) = 1, \tag{2.21}$$

where α_β is the probability that the point $\mathbf{x}$ is occupied by the phase β. They further propose a relationship between the Eulerian and Lagrangian representations analogous to that in single–phase flows, with the Lagrangian pdf serving as a transition density. Upon adopting a trajectory point of view for the fluid and dispersed phases, they derive a Fokker–Planck equation for the evolution of the Lagrangian joint fluid–particle pdf f_{fp}^{L}. From this evolution equation, they derive the mean field equations in each phase.

As far as the Lagrangian approach is considered, it is shown by Subramaniam (2000) that in developing the Lagrangian description of the dispersed phase, the notion of a single–droplet or particle is lost. This is due to an intermediate symmetrization of the Liouville pdf corresponding to the dispersed phase that is essential to arrive at a unique single–particle pdf. Therefore, the single–particle pdf does not characterize events associated with a single–particle (or droplet), but events associated with surrogate particles. It is then unclear as to what events the "Lagrangian" pdf for the dispersed phase in the two–point pdf formalism of Peirano and

Minier (2002) characterizes. Moreover, a prescription for a Lagrangian description of the dispersed phase should make a connection with the spray equation formalism which has a sound foundation in the theory of point processes (Subramaniam, 2000). Such a connection is not made in the work of Peirano and Minier (2002).

The relationship between the Eulerian joint pdf of velocity and radius in the dispersed phase and the joint pdf of velocity and radius from the Lagrangian (spray equation) formalism bear a complicated relationship with each other; these relationships are clearly laid out in this work. It is therefore essential to revisit the formalism of Peirano and Minier (2002) in the light of the observations made in this work.

In order to derive the mean field equations in the two–fluid formalism, Peirano and Minier (2002) use a Fokker–Planck equation, which essentially implies that the starting point for the derivation of the mean equations is a model. In this work, it is shown that no such assumptions are required to derive the mean field equations in the Eulerian–Eulerian statistical representation. Starting from an exact evolution equation for the single–point phasic Eulerian pdf, the ensemble averaged mean equations are derived and these are shown to be identical to the averaged equations of Drew (1983).

2.1.3 Kinetic equation formalism

A concise review of the kinetic equation formalism (see for instance, Derevich and Zaichik, 1988; Zaichik, 1999; Reeks, 1992) is available in Mashayek and Pandya (2003). The starting point of the kinetic equation formalism is the Lagrangian equation of motion for a particle suspended in a turbulent flow:

$$\frac{d}{dt}\mathbf{X}_p = \mathbf{V}_p \tag{2.22}$$

$$\frac{d}{dt}\mathbf{V}_p = \mathbf{A}_p, \tag{2.23}$$

where $\mathbf{X}_p$, $\mathbf{V}_p$ and $\mathbf{A}_p$ are the particle position, velocity and acceleration, respectively. On defining a fine–grained density as

$$f'(\mathbf{x}, \mathbf{v}, t) = \delta(\mathbf{x} - \mathbf{X})\delta(\mathbf{v} - \mathbf{V}),$$

where δ is the Dirac delta (see Appendic C in Pope (2000)), the evolution equation for the fine–grained density can be obtained, in the absence of collisions, as

$$\frac{\partial f'}{\partial t} + \frac{\partial (v_i f')}{\partial x_i} + \frac{\partial (A_i f')}{\partial v_i} = 0 \tag{2.24}$$

If Stokes drag is assumed for the particle, then a drag model of the form

$$\frac{d}{dt}\mathbf{V}_p = \Omega_p(\mathbf{U}_f - \mathbf{V}_p)$$

holds, where Ω_p is the particle response frequency and $\mathbf{U}_f$ is the fluid–phase velocity. Decomposing the mean velocity of the fluid phase as $\mathbf{U}_f = \langle \mathbf{U}_f \rangle + \mathbf{u}'_f$ and substituting into Eq. (2.24) results in, after ensemble averaging,

$$\frac{\partial f}{\partial t} + \frac{\partial (v_i f)}{\partial x_i} + \frac{\partial}{\partial v_i}\left[\Omega_p(\langle U_{f_i} \rangle - v_i) f\right] = -\frac{\partial}{\partial v_i}\left[\Omega_p \langle u'_i f \rangle\right], \tag{2.25}$$

where f is the so–called 'phase–space' density which is defined as $f = \langle f' \rangle$ and $-\partial \left[\Omega_p \langle u'_i f \rangle\right] / \partial v_i$ is called the 'phase–space diffusion current' (Reeks, 1991). Much of the effort in the kinetic equation formalism has been devoted to determining appropriate closures for the term containing the correlation between the fluctuating velocity and the phase–space density $\langle u'_i f \rangle$. An implicit assumption in this formalism is that the mean velocity in the fluid–phase is known from a Reynolds–averaged solution.

Reeks (1992) employed the Lagrangian history direct interaction approximation due to Kraichnan (1965) and proposed a general form for the phase space diffusion current as

$$\Omega_p \langle u'_i f \rangle = -\left[\mu_{ji}\frac{\partial}{\partial v_j} + \lambda_{ji}\frac{\partial}{\partial x_j} + \gamma_i\right] f$$

that is invariant to a random Galilean transformation (Kraichnan, 1977), which amounts to applying a random translational velocity (in magnitude) to the carrier phase velocity that varies for each realization of the flow but is otherwise constant in space and time. The terms $\boldsymbol{\lambda}$, $\boldsymbol{\mu}$ and $\boldsymbol{\gamma}$ are called the dispersion tensors and, for homogeneous flows, are given as

$$\begin{aligned}
\lambda_{ji} &= \langle \Delta x_j(\mathbf{x}, \mathbf{v}, t|t_0) \Omega_p u'_i(\mathbf{x}, t) \rangle \\
\mu_{ji} &= \langle \Delta v_j(\mathbf{x}, \mathbf{v}, t|t_0) \Omega_p u'_i(\mathbf{x}, t) \rangle \\
\gamma_i &= -\left\langle \Delta x_j(\mathbf{x}, \mathbf{v}, t|t_0) \frac{\partial}{\partial x_j} \Omega_p u'_i(\mathbf{x}, t) \right\rangle,
\end{aligned}$$

where

$$\Delta x_j(\mathbf{v},\mathbf{x},t|t_0) = \int_0^t e^{\Omega_p(s-t)} u_j'(\mathbf{x},\mathbf{v},t|s)\, ds$$
$$\Delta v_j(\mathbf{v},\mathbf{x},t|t_0) = \Omega_p^{-1} \int_0^t (1 - e^{\Omega_p(s-t)}) u_j'(\mathbf{x},\mathbf{v},t|s)\, ds$$

represent changes in position and velocity due to the fluctuations $\Omega_p u_i'$ along the particle trajectory starting from time t_0 and passing through the point $(\mathbf{x},\mathbf{v})$ at time t.

If $\mathbf{u}'$ is assumed to be a Gaussian random variate, the Furutsu–Novikov–Donsker formula (FND) can be used to determine an analytical expression for the correlation $\langle u_i' f\rangle$. The FND formula is given as:

$$\langle u_i' f\rangle = \int \langle u_i'(\mathbf{x},t) u_j'(\mathbf{x}',t')\rangle \left\langle \frac{\delta f}{\delta u_j(\mathbf{x}',t') d\mathbf{x}' dt'} \right\rangle d\mathbf{x}' dt'$$

where $\langle \delta f/(\delta u_j(\mathbf{x}',t) d\mathbf{x}' dt)\rangle$ is the functional derivative of f with respect to $\mathbf{u}'$. Derevich (2000), Zaichik (1999) and Hyland et al. (1999a) use the FND formula to derive the closed phase density transport equation. The final expression for the phase–space diffusion current derived by Hyland et al. (1999a) using the FND formula is identical to that derived by Reeks (1992). Details can be found in Hyland et al. (1999a) and Mashayek and Pandya (2003). Predicted particle phase Reynolds stresses from the kinetic equation formalism have been compared with a LES of two–phase flow in a simple shear with overall good agreement in Hyland et al. (1999a,b). In that study, the carrier phase mean quantities like the fluid Reynolds stresses, turbulent kinetic energy and turbulent dissipation rate that are required in the dispersion tensors $\boldsymbol{\lambda}$, $\boldsymbol{\mu}$ and $\boldsymbol{\gamma}$ are all taken as input from the LES. Derevich (2000) uses the fluctuating dispersed–phase velocity as the phase space variable and derives a closure for the phase space diffusion current. Pozorski and Minier (1999) derive a closure for the same term using the cumulant expansion method of Van Kampen (1992) for linear stochastic differential equations. Since the original form of the kinetic equation contains information only at the level of the dispersed phase, Pozorski and Minier (1999) propose an extension of the phase space by including the fluid velocity 'seen' by the particles as an additional phase space variable. They

propose a model similar to the generalized Langevin model (Haworth and Pope, 1986) for the fluid velocity 'seen' by the particles. Pandya and Mashayek (2001, 2003) have extended kinetic equation formalism to non–isothermal flows by including temperature as an additional phase space variable.

The work done in the kinetic equation formalism is notable since this is an attempt to connect kinetic theory with the theory of particle–laden flows. However, there are several issues that need to be considered like the affect of ordering, finite number of particles and the need for an intermediate symmetrization of the distribution function (see Subramaniam (2000) for more details) that precludes a straightforward extension of the transport equation for the distribution function used in kinetic theory to particle–laden flows. Although the kinetic equation formalism is often referred to as a 'probability density function' method, no information on the ensemble of events and fundamental probabilities corresponding to the events associated with a particle–laden flow are presented.

2.2 Lagrangian–Eulerian statistical representation of two–phase flows

2.2.1 Spray equation formalism

The spray equation is an evolution equation for the droplet distribution function $f(\mathbf{x}, \mathbf{v}, r, t)$ (Williams, 1958), which is defined such that

$$f(\mathbf{x}, \mathbf{v}, r, t)\, d\mathbf{x}\, d\mathbf{v}\, dr$$

gives the expected number of droplets with positions in the range $\mathbf{x}, \mathbf{x} + d\mathbf{x}$, velocities in the range $\mathbf{v}, \mathbf{v}+d\mathbf{v}$ and radii in the range $r, r+dr$ at time t. Williams noted that if the droplets have a low velocity relative to the gas with small inter droplet collision duration times compared to the time between collisions, droplets can be considered spherical and a single parameter – radius r – can be used to characterize the size and shape of the dispersed phase. O'Rourke (1981) extended the phase space over which the ddf is defined to include effects of sphericity, droplet oscillation and temperature. In his seminal work, O'Rourke laid a detailed framework for theory and computation of evaporating droplet–laden flows with chemical reactions based

on the spray equation. The popular KIVA family of codes (Amsden et al., 1989) is based on this work.

The mathematical foundation for the LE formalism based on the spray equation was rigorously derived by Subramaniam (2001c, 2000) using the theory of point processes. In this dissertation, the LE formalism based on Williams' spray equation is considered as a fundamental description of the dispersed phase. As such, a detailed description of this formalism is deferred until Section 3.

As the name suggests, the spray equation formalism was originally proposed for sprays. However, its theoretical development is general and is applicable to any particle-laden or bubbly flows that satisfy certain restrictions of size on the dispersed phase elements.

2.2.2 Sectional method formalism

Based on Williams' spray equation (Williams, 1958), the essence of the sectional method is to divide the size distribution of the dispersed–phase elements (DPE) into several 'sections', instead of representing the entire size distribution either through a particle method such as the one used in the popular KIVA family of codes (Amsden et al., 1989). First proposed by Greenberg et al. (1993), this method involves writing sectional conservation equations that govern the evolution of the spray properties such as velocity, radius (or spray volume), vaporization and coalescense in each section. This method is not a unique theory in itself, but relies on the spray equation formalism for its foundation. It is essentially a means to efficiently seek solutions to the spray equation. A brief synopsis of the sectional method follows.

Greenberg et al. (1993) begin with the spray equation proposed by Williams which is an evolution equation for the droplet distribution function (ddf) given as

$$\frac{\partial f}{\partial t} + \frac{\partial (Rf)}{\partial v} + \frac{\partial (u_i f)}{\partial x_i} + \frac{\partial (F_i f)}{\partial u_i} = \Psi.$$

The notation used in the spray equation above is taken from Greenberg et al. (1993). According to them, v is the volume corresponding to each DPE, R is the rate of volume change of the dispersed–phase element, $\mathbf{F}$ is the 'drag force' exerted on the droplet and Ψ are source terms

corresponding to vaporization, collision and coalescence[1]. The symbol $\mathbf{u}$ is used here to denote velocity. They divide the DPE volume distribution into N sections such that

$$\text{Section } I = \{v | v_{L_I} \leq v \leq v_{H_I}\}, \;\; I = 1, 2, \ldots, N.$$

Instead of working on the ddf $f(\mathbf{x}, \mathbf{v}, v, t)$, which contains a dependence on the velocity, they integrate out the velocity dependence from the spray equation and define a number density in position and volume phase space as

$$\hat{f}(\mathbf{x}, v, t) = \int f(\mathbf{x}, \mathbf{u}, v, t) d\mathbf{v}.$$

Note that the radius phase space has been replaced by a volume phase space in the definition of the ddf. The spray is characterized by means of the following general function

$$q(\mathbf{x}, v, t) = \alpha v^{\xi} \hat{f}(\mathbf{x}, v, t).$$

When $\xi = 0$ and $\alpha = 1$, q is the number density defined earlier; when $\xi = 1$ and $\alpha = \rho_d$, where ρ_d is the thermodynamic density of the dispersed phase, and $\xi = 1$, q is the mass concentration in phase space. Thus, the total spray property in any section can be computed as

$$Q_I(\mathbf{x}, t) = \int_{v_{L_i}}^{v_{H_i}} q(\mathbf{x}, v, t)\, dv \;\; \text{for } I = 1, 2, \ldots, N$$

The evolution equation for the quantity Q_I is then derived as

$$\frac{\partial Q_i}{\partial t} + \int_{v_{L_i}}^{v_{H_i}} \alpha v^{\xi} \frac{\partial (\tilde{R} \hat{f})}{\partial v} dv + \frac{\partial}{\partial x_i} \int_{v_{L_i}}^{v_{H_i}} \widetilde{W}_i \hat{f} \alpha v^{\xi} dv = \int_{v_{L_i}}^{v_{H_i}} \alpha v^{\xi} \tilde{\Psi} dv$$

where

$$\begin{aligned}
\hat{f} &= \int_{\mathbf{u}} f \, d\mathbf{u} \\
\tilde{R} &= \frac{1}{\hat{f}} \int_{\mathbf{u}} R f \, d\mathbf{u} \\
\widetilde{W} &= \frac{1}{\hat{f}} \int_{\mathbf{u}} \mathbf{u} f \, d\mathbf{u} \\
\widetilde{\Psi} &= \frac{1}{\hat{f}} \int_{\mathbf{u}} \Psi f \, d\mathbf{u}
\end{aligned}$$

[1]In Chapter 3, it will be shown that quantities such as the drag force and vaporization rate are conditional expectations and are not as intuitive as is presented by Greenberg et al. (1993)

Greenberg et al. (1993) make a series of assumptions such as invoking the d^2 law for vaporization, assuming that $\hat{f}$ is uniform in each section, and that coalescence of two droplets results in a new droplet, where the two droplets can be either from two different sections or from the same section, resulting finally in the so called 'spray sectional conservation' equation. More details are available in Greenberg et al. (1993).

2.3 Summary

Although several researchers have studied the pdf formalism for two–phase flows, it is unclear from these attempts that there are essentially two distinct approaches in the EE and LE formalism, respectively, to such a formalism. Some researchers attempt to make a connection between their pdf formalism and the spray equation formalism, however, it is shown in this work that such a connection cannot be established in general for a two–phase flow. A two–point pdf formalism is intuitively attractive and can potentially provide a high–fidelity description of a two–phase flow. However, in proposing a two–point pdf formalism, one has to ensure that the single–point limit of such a formalism is correctly connected to established single–point descriptions of two–phase flows. The kinetic equation formalism makes an important connection between kinetic theory of gases and particle–laden flows. However, this connection is based on several assumptions which are in general not satisfied by two–phase flows encountered in reality. A rigorously–established LE description of a two–phase flow is the spray–equation formalism, which has been derived starting from the theory of point processes and forms the basis for the LE description proposed in this work.

Since the major emphasis of this work in on developing a consistent theoretical description of two–phase flows, a literature review of current modeling strategies in the LE and LL formalism is deferred to the chapters on modeling viz., Chapter 5–7.

Also the modeling advances presented in this work are in the context of the LE and LL statistical representations of two–phase flows. For currently–used modeling strategies in the EE formalism, the reader is referred to reviews by Crowe et al. (1996); Shirolkar et al. (1996); Drew (1983); Drew and Passman (1999). It is noteworthy that the LE and LL models proposed

in this work also imply models in the EE formalism.

CHAPTER 3. PROBABILISTIC REPRESENTATION OF TWO–PHASE FLOWS

This chapter is a manuscript in preparation titled "A comprehensive probability density function formalism for multiphase flows" co–authored with S. Subramaniam.

A theoretical foundation for two widely–used statistical representations of multiphase flows, namely the Eulerian–Eulerian (EE) and Lagrangian–Eulerian (LE) representations, is established in the framework of the probability density function formalism. Consistency relationships between fundamental statistical quantities in the EE and LE representations are rigorously established. It is shown that these fundamental quantities in the two statistical representations bear a simple relationship with one another only under conditions of spatial homogeneity. Transport equations for the fundamental probability densities in each statistical representation are derived. Governing equations for the mean mass, mean momentum and second moment of velocity are derived from these transport equations. In particular, for the EE representation, the fundamental pdf formalism is shown to naturally lead to the widely–used ensemble averaged equations for two–phase flows. Galilean invariant combinations of unclosed terms in the governing equations which need to be modeled are clearly identified. The correspondence between unclosed terms in each statistical representation is established, which serves in transferring information from one representation to the other, and in proposing new models in either representation. Advantages and limitations of each statistical approach are identified. The results of this work can serve as a guiding framework for direct numerical simulations of two–phase flows, which can now be exploited to precisely quantify unclosed terms in the governing equations in the two statistical representations.

3.1 Introduction

Statistical models of multiphase flow are inevitable because of the statistical variability inherent in most multiphase flow applications. Moreover, information from single realizations of a multiphase flow contain information that far exceeds the amount required for engineering purposes. Therefore, averaged statistics of multiphase flows are of interest to the engineering community. Widely–used statistical representations of two–phase flows [1] can be broadly classified as Eulerian–Eulerian (EE) or Lagrangian–Eulerian (LE), depending on the reference frames underlying their formulation.

Historically, the EE statistical representation refers to a statistical approach wherein the two–phases are represented at the level of the means, such as the mean densities, volume fractions, mean momentum and second moments in each phase, with source terms due to interphase interactions. A lucid account of this approach is given by Drew (1983) (see also Drew and Passman (1999)) and extensions have been developed by Kataoka and Serizawa (1989). A notable example of an ensemble–averaged EE implementation for chemically reacting or inert multiphase flows is CFDLib (Kashiwa and Rauenzahn, 1994; Kashiwa and Gaffney, 2003).

The LE statistical representation refers to a statistical approach that represents the dispersed phase in a Lagrangian frame by a number density based on the location of dispersed–phase element (DPE) [2] centers. The origin of this representation can be traced back to Williams (1958) who proposed the droplet distribution function (ddf) and derived the spray equation, which is the evolution equation for the ddf, from physical principles. In numerical implementations of the LE statistical approach, the spray equation is indirectly solved using particle–based methods. Generally, the two primary components of such a particle–method solution are (i) Lagrangian particles, with modeled drag and vaporization terms, that represents the ddf, and (ii) a single–phase Reynolds averaged Navier–Stokes (RANS) closure for the carrier phase with additional source terms representing the effects of the dispersed phase. An example of such an

[1] For simplicity, only two–phases are considered in this study. However, extension to multiphase flows is straightforward.

[2] In this work, the phrase 'dispersed–phase element' is a generic term used to denote either rigid particles, drops or bubbles.

approach is the KIVA series of codes (Amsden et al. (1989); Amsden (1993)) used widely in the automotive industry.

It is natural to seek a probability density function (pdf) formalism to describe two–phase flows, given their statistical variability. There have been recent studies by several authors (see for instance, Pozorski and Minier, 1999; Zhu et al., 2000; Peirano and Minier, 2002) to extend pdf methods, which have been successful in single–phase turbulent reactive flows (Lundgren, 1969; Libby and Williams, 1980; Pope, 1985), to two–phase flows. In particular, Zhu et al. (2000) derive an evolution equation for the Eulerian joint pdf for velocity and radius in the dispersed phase, and show that this is identical to the evolution of the joint pdf of velocity and radius in Williams' spray–equation formalism. The so–called "kinetic equation" formalism for the pdf of the dispersed–phase velocity has been studied by several researchers (see for instance, Derevich and Zaichik, 1988; Zaichik, 1999; Reeks, 1992). Reeks (1992) used the pdf kinetic equation formalism to arrive at continuum equations that describe the dispersed phase in dilute particle–laden flows. In this approach, the acceleration term in the pdf kinetic equation is simplified by assuming Stokes drag and the resulting phase–space "diffusion current" (Reeks, 1991) is closed using elaborate techniques (see Mashayek and Pandya (2003) for details on the techniques used by various researchers to close this diffusion–current term). Simonin (1996) proposed a kinetic equation for the probable number of particles in an infinitesimal volume in position and velocity phase space (Lagrangian approach) that is similar to the spray equation. He derives mean equations from the transport equation, while making an assumption that the dispersed–phase volume fraction can be simply related to the number density, and refers to these mean equations as "Eulerian" closures. Although the mean equations derived from the spray equation are Eulerian quantities, his approach implicitly does not take into account of the fact that there is a distinct EE approach to deriving "Eulerian" mean equations for the two–phase flow.

It is noteworthy that researchers who studied the kinetic equation formalism attempt to make an important connection between kinetic theory and particle–laden flows. However, the several assumptions that the kinetic theory of gases is based upon fail to hold in almost all

two–phase flows that are encountered in reality. There are several considerations unique to particle–laden flows, such as (*i*) finite number of particles, (*ii*) non–negligible fluctuations of particle number about the mean, (*iii*) non–identical distributions of particle positions that results in ordering–dependent Liouville densities, and (*iv*) symmetrization of the Liouville pdf to arrive at unique single–particle densities (Subramaniam, 2001c), that preclude a straightforward extension of kinetic theory to such flows.

It is also not clear from the aforementioned studies that there are two approaches – one in the EE and the other in the LE statistical representation – to a pdf formalism for two–phase flows. Yet, since the EE and LE statistical representations are essentially the description of a two–phase flow in two reference frames, it is natural to expect that these representations are related. A major challenge in describing two–phase flows, therefore, is to establish the precise relationship between these two modeling approaches. Furthermore, the conditions under which such a relationship holds, and conditions under which they do not, need to be clearly established.

Establishing the exact form of the relationship between the two statistical representations has far–reaching implications. Subramaniam and O'Rourke (1998) noted that computations of some two–phase applications such as fuel sprays can potentially benefit by using the EE modeling approach in the near–nozzle region, and the LE approach in the dispersed spray region. Figure 3.1 shows a schematic for one such recipe for handover from a EE representation to a LE representation in a typical spray. A pertinent question that arises in this context is how would one transfer information from one representation to the other. The answer lies in the exact relationship between these two approaches which will allow a consistent transfer of flow information at the common boundary of the two regions. Some recent studies on sprays in which the liquid core is represented using a Refined Level Set Grid method while the atomized droplets are modeled using Lagrangian DPEs have been pursued (Kim et al., 2006). In such calculations, if the consistency between the liquid core and the Lagrangian DPEs is enforced at the level of the means, then the transfer of information from one representation to the other will be dictated by the relationships between the EE and the LE representations.

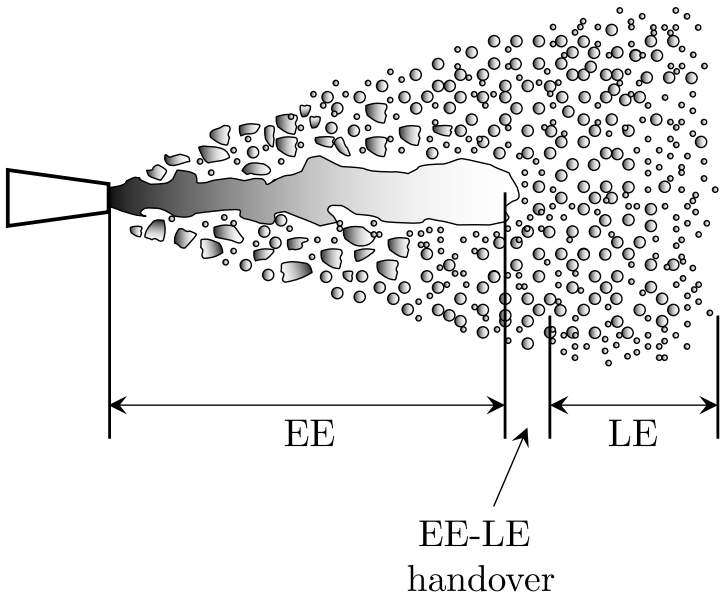

Figure 3.1 Schematic of a typical spray indicating the region where a handover between the EE and the LE description is appropriate. This handover requires consistency conditions to be satisfied between the two statistical representations at the common boundary of the two regions.

Ning et al. (2007) has proposed a new spray model using the Eulerian–Lagrangian Spray and Atomization (ELSA) model after Blokkeel et al. (2003) in which an Eulerian description of the spray for the region close to the injector and a Lagrangian description in the dilute regions of the spray is used. The transfer of information from the Eulerian to the Lagrangian description in such computations will require the knowledge of the relationships between corresponding mean quantities and unclosed terms in the two representations.

More importantly, the exact form of such a relationship also enables us to address several important, but hitherto unresolved, modeling issues such as:

(i) How can model predictions from both approaches be compared with one another? If the EE and LE modeling approaches are employed to describe the same two–phase flow, then under what conditions can predictions of key two–phase flow statistics from either approach be directly compared?

(ii) How, and under what conditions, are the modeled terms in both approaches related, and how can this relationship be used to guide model development in both approaches?

The primary objective of this work is to address these fundamental issues related to the theoretical underpinnings of two–phase flows. In order to achieve this objective, the foundation for the EE and the LE representations is first established in the context of the pdf formalism using fundamental events and corresponding probabilities. It is shown in this work that the EE probabilistic formalism naturally leads to the ensemble–averaged equations of a two–phase flow. Although the LE formalism also results in mean equations, these equations are not identical to the averaged equations in the EE formalism. It is shown in this work that fundamental quantities in the EE and LE representations bear a simple relationship with one another only under restrictive conditions of spatial uniformity (or statistical homogeneity) of the two–phase flow, thereby rendering the work of Zhu et al. (2000) and Simonin (1996) applicable only to a certain class of flows. This work also identifies a correspondence between the unclosed terms in the governing equations for the mean mass, mean momentum and second moment equations in the two representations. This correspondence enables one to transfer information seamlessly from one representation to the other. The relationship between modeled terms is

also useful in constructing improved models for the unclosed terms using data from direct numerical simulations (DNS) of two–phase flows. An important contribution of this work is the identification of Galilean invariant (GI) combinations of unclosed interphase interaction terms that need to be modeled. No attempt is made to propose models for the unclosed terms in this study. Rather, the precise form of the unclosed terms is derived, thereby establishing a framework for appraising existing two–phase models and guiding future modeling efforts.

The rest of the paper is organized as follows. The foundation for the EE statistical representation of a two–phase flow is established in Section 3.2 by identifying fundamental events and corresponding probabilities. An important highlight of this section is the definition of the pdf of instantaneous velocity conditional on the presence of a particular phase in a two–phase flow. The basis for the LE statistical representation is also presented and key equalities in this representation that are useful in the rest of the work are summarized in this section. Relationships between fundamental quantities in the EE and LE statistical representations are developed in Section 3.3. Evolution equations corresponding to the pdf of instantaneous velocity conditional on the presence of each phase in the EE representation, and the droplet distribution function in the LE representation, are derived in Section 3.4. These evolution equations are used to derive governing equations for the mean mass, mean momentum and second moment of velocity in each representation in Section 3.5. In the same section, the correspondence between various unclosed terms in the governing equatons is identified. GI forms of the unclosed terms in the governing equations that need to be modeled are also identified. The advantages and limitations of each approach are discussed in Section 3.6. Section 3.7 summarizes the achievements and conclusions of this work.

3.2 Statistical Representations of Two–Phase Flow

The statistical representation of a two–phase flow using the EE and the LE approaches is described. In the EE approach, the two–phase flow field is represented as a *random field* (Drew, 1983; Zhang and Prosperetti, 1994) while in the LE approach the dispersed phase is represented as a *marked point process* (Edwards and Marx, 1996; Subramaniam, 2001c) imbedded in a car-

rier flow. While the ensemble–averaged equations in the EE representation have been reported in literature, this work provides insight into the underlying pdf framework. Fundamental events and corresponding probabilities associated with a two–phase flow in the EE and LE framework are developed in this section.

3.2.1 Random–field representation

Consider a realization of a two–phase flow with two distinct thermodynamic phases: a carrier phase and a dispersed phase. Each realization can be thought of as an element of a sample space Ω, which is the space of all possible realizations. See Figure 3.2. In a single realization, and at a single space–time location, the phases are distiguished using an indicator function $I_\beta(\mathbf{x}, t)$ for the βth phase, defined as

$$I_\beta(\mathbf{x}, t) = \begin{cases} 1 & \text{if } \mathbf{x} \text{ is in phase } \beta \text{ at time } t \\ 0 & \text{if } \mathbf{x} \text{ is not in phase } \beta \text{ at time } t. \end{cases} \tag{3.1}$$

In two–phase flows, the phase indicator functions satisfy the relation

$$\sum_{\beta=\{f,d\}} I_\beta(\mathbf{x}, t) = 1, \tag{3.2}$$

where f represents the carrier phase and d represents the dispersed phase, for all $(\mathbf{x}, t)$. The instantaneous two–phase velocity field $\mathbf{U}(\mathbf{x}, t)$, which is defined in all the phases is a vector field that is defined at each point $\mathbf{x}$ in the flow domain in physical space $\mathcal{D}$. Similarly $\rho(\mathbf{x}, t)$ is the thermodynamic mass density field that is defined in all the phases. It is assumed that (i) the density difference between the two phases is sufficiently large so that the density field can be used to distinguish between the two phases (i.e., the thermodynamic state of the fluid is not close to the critical point), and (ii) the characteristic length scale of the interface over which this density change occurs is so small that in a continuum description the density changes discontinuously at the interface.

Different events can be used to characterize the state of a two–phase flow at a single space–time location $(\mathbf{x}, t)$, and each leads to different probabilities and pdf's. A complete Eulerian

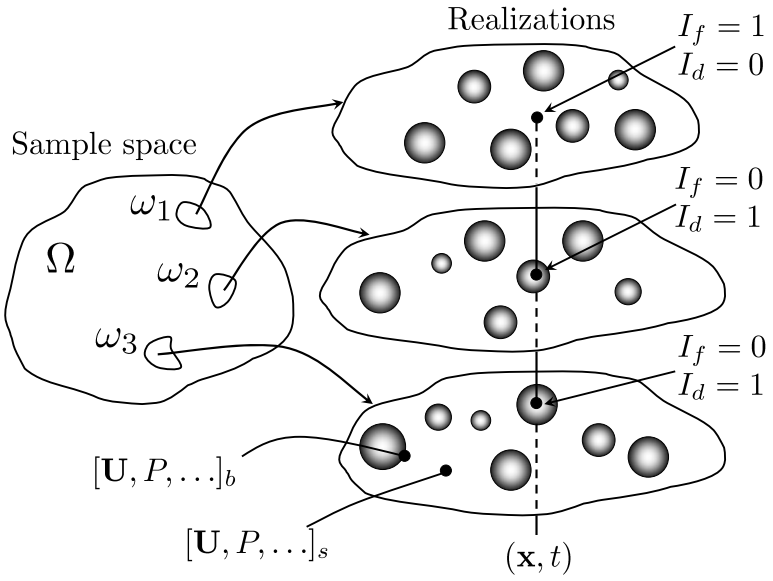

Figure 3.2 Schematic of the sample space Ω of all possible realizations of a two–phase flow from which three realizations $\{\omega_1, \omega_2, \omega_3\}$ are shown. The indicator function $I_\beta(\mathbf{x}, t)$ at a point $(\mathbf{x}, t)$, where $\beta = \{f, d\}$, as defined in Section 3.2.1 is shown for each of the three realizations. Also, primitive variables $\mathbf{U}$ – velocity and P – pressure at the DPE surface (subscript s) and in the bulk (subscript b) are shown. As discussed in Section 3.4, a single–point statistical representation cannot distinguish between these two locations in a two–phase flow.

single–point pdf description of the two–phase flow will require the knowledge of the event

$$E_1 = [\mathbf{U} \in (\mathbf{u}, \mathbf{u} + d\mathbf{u}), I_f(\mathbf{x}, t) = 1]\,, \tag{3.3}$$

which is the event corresponding to the joint occurence of $\mathbf{U}$ falling in the range $(\mathbf{u}, \mathbf{u}+d\mathbf{u})$ at a point $\mathbf{x}$ and the fluid phase being present at the same point. Here $\mathbf{u}$ is the sample space variable corresponding to the random variable $\mathbf{U}$. Note that $I_f(\mathbf{x}, t) = 1$ automatically precludes the occurence of the dispersed phase at that same point (i.e., $I_d(\mathbf{x}, t) = 0$ at the same point $\mathbf{x}$). It is noteworthy that (Sundaram and Collins, 1994a,b) have explored the simultaneous two–point description of a two–phase flow in the random–field representation. We focus on the single–point representation in this study since single–point models are more tractable, although there is a loss of scale information when moving from the two–point to the single–point description.

Corresponding to the joint event E_1, two unconditional events are:

$$E_2 = [\mathbf{U}(\mathbf{x}, t) \in (\mathbf{u}, \mathbf{u} + d\mathbf{u})]$$
$$E_3^{(\beta)} = [I_\beta(\mathbf{x}, t) = 1],$$

where E_2 is the event that $\mathbf{U}(\mathbf{x}, t)$ belongs to $(\mathbf{u}, \mathbf{u} + d\mathbf{u})$ regardless of whether the phase β is located at $\mathbf{x}$, while $E_3^{(\beta)}$ is the event that the phase β exists at $\mathbf{x}$. Two conditional events are also important

$$E_4 = [\mathbf{U}(\mathbf{x}, t) \in (\mathbf{u}, \mathbf{u} + d\mathbf{u}) | I_\beta = 1] \tag{3.4a}$$

$$E_5 = [I_\beta(\mathbf{x}, t) = 1 | \mathbf{U} = \mathbf{u}], \tag{3.4b}$$

where E_4 is the event that $\mathbf{U}(\mathbf{x}, t)$ belongs to $(\mathbf{u}, \mathbf{u} + d\mathbf{u})$ conditional on the presence of phase β at location $\mathbf{x}$, while E_5 is the event that the location $\mathbf{x}$ is occupied by phase β conditional on $\mathbf{U} = \mathbf{u}$ at the same location.

Let the Eulerian joint pdf of $\mathbf{U}$ be denoted $f_{\mathbf{U}}(\mathbf{u}; \mathbf{x}, t)$, where $\mathbf{x}$ and t are parameter–space variables. The probabilities corresponding to each of the above events are (Subramaniam,

2005):

$$
\begin{aligned}
P[E_2] &= P[\mathbf{U}(\mathbf{x},t) \in (\mathbf{u}, \mathbf{u}+d\mathbf{u})] && = f_{\mathbf{U}}(\mathbf{u};\mathbf{x},t)d\mathbf{u} \\
P[E_5] &= P[I_\beta(\mathbf{x},t) = 1 | \mathbf{U} = \mathbf{u}] && = p_\beta(\mathbf{u};\mathbf{x},t) \\
P[E_1] &= P[I_\beta(\mathbf{x},t) = 1 | \mathbf{U} = \mathbf{u}]\, P[\mathbf{U}(\mathbf{x},t) \in (\mathbf{u}, \mathbf{u}+d\mathbf{u})] && = p_\beta(\mathbf{u};\mathbf{x},t) f_{\mathbf{U}}(\mathbf{u},\mathbf{x},t)d\mathbf{u} \\
P[E_3^{(\beta)}] &= \int P[I_\beta = 1 | \mathbf{U} = \mathbf{u}] f_{\mathbf{U}}(\mathbf{u})d\mathbf{u} = \int p_\beta f_{\mathbf{U}}(\mathbf{u})d\mathbf{u} && = \alpha_\beta(\mathbf{x},t) \\
P[E_4] &= P[\mathbf{U}(\mathbf{x},t) \in (\mathbf{u}, \mathbf{u}+d\mathbf{u}) | I_\beta = 1] && = \frac{p_\beta(\mathbf{u}) f_{\mathbf{u}}(\mathbf{u};\mathbf{x},t)}{\alpha_\beta(\mathbf{x},t)} d\mathbf{u},
\end{aligned}
$$

where $p_\beta(\mathbf{u};\mathbf{x},t)$ is a phase probability function. Note that $P[E_3^{(\beta)}]$ defines a probability *field* $\alpha_\beta(\mathbf{x},t)$:

$$\alpha_\beta(\mathbf{x},t) \equiv P[I_\beta(\mathbf{x},t) = 1]. \tag{3.6}$$

It is important to note that $\alpha_\beta(\mathbf{x},t)$ is *not* a probability density in $\mathbf{x}$. However, α_β is a probability mass function in I_β, which takes values $\{0,1\}$. Another property of I_β is that $P[I_\beta(\mathbf{x},t) = 1] = \langle I_\beta \rangle$

Since $f_{\mathbf{U}}$ is a pdf it has to satisfy the normalization condition:

$$\int f_{\mathbf{U}}(\mathbf{u};\mathbf{x},t)d\mathbf{u} = 1.$$

Also, let the probability $P[E_4]$ be denoted $f_{\mathbf{U}|I_\beta}d\mathbf{u}$, so that the Eulerian joint pdf of velocity conditioned on the presence of phase β at $\mathbf{x}$, $f_{\mathbf{U}|I_\beta}$ is given as:

$$f_{\mathbf{U}|I_\beta} = \frac{p_\beta(\mathbf{u}) f_{\mathbf{U}}(\mathbf{u})}{\alpha_\beta(\mathbf{x},t)}. \tag{3.7}$$

One may define the following expectations:

$$\langle \mathbf{U} \rangle(\mathbf{x},t) = \int \mathbf{u} f_{\mathbf{U}} d\mathbf{u}$$

and

$$\langle \mathbf{U}^{(\beta)} \rangle = \int \mathbf{u} f_{\mathbf{U}|I_\beta} d\mathbf{u},$$

where $\langle \mathbf{U} \rangle$ is the mixture mean velocity field and is related to the phasic mean velocity $\langle \mathbf{U}^{(\beta)} \rangle$ as

$$\langle \mathbf{U} \rangle = \alpha_f \langle \mathbf{U}^{(f)} \rangle + \alpha_d \langle \mathbf{U}^{(d)} \rangle.$$

Note that the following relations hold:

$$P[I_f = 1] + P[I_d = 1] = 1$$
$$\alpha_f + \alpha_d = 1$$
$$p_f(\mathbf{u}; \mathbf{x}, t) + p_d(\mathbf{u}; \mathbf{x}, t) = 1.$$

Also, the phase probability function and the pdf $f_{\mathbf{U}}$ can be written as (Subramaniam, 2005)

$$p_f(\mathbf{u}; \mathbf{x}, t) = \frac{\alpha_f(\mathbf{x}, t) f_{\mathbf{U}|I_f}}{\alpha_f(\mathbf{x}, t) f_{\mathbf{U}|I_f} + \alpha_d(\mathbf{x}, t) f_{\mathbf{U}|I_d}} \tag{3.8}$$

$$f_{\mathbf{U}}(\mathbf{u}; \mathbf{x}, t) = \alpha_f(\mathbf{x}, t) f_{\mathbf{U}|I_f} + \alpha_d(\mathbf{x}, t) f_{\mathbf{U}|I_d}, \tag{3.9}$$

showing that the knowledge of one of α_f or α_d and the phasic probability pdfs $f_{\mathbf{U}|I_\beta}$ for $\beta = \{f, d\}$ is sufficient for a complete one–point description of a isothermal non–reacting two–phase system. This description corresponds to the *minimal* and *complete single–point Eulerian description* (Subramaniam, 2005) of the two–phase system.

3.2.2 Point–process representation

The starting point for the point process or the LE description of a two–phase flow is the ddf proposed by Williams (1958). The spray equation, which is the evolution equation of the ddf, can be rigorously derived starting from the Lagrangian evolution equations of droplet position, velocity and radius (Subramaniam, 2001c). Although the ddf was initially conceived to describe a fuel spray in internal combustion engines (and hence the name 'droplet' distribution function), it can be used to describe any two–phase flow wherein the dispersed phase can be modeled as a collection of discrete entities. Thus, the LE representation is a valid statistical representation of a two–phase flow. While the salient aspects of this statistical description that are relevant to the current discussion are given here, details may be found in Subramaniam (2000, 2001c).

In the following, we consider the DPEs to be droplets, although the discussion is equally valid for other DPEs. Consider a two–phase flow in a finite flow domain $\mathcal{D}$ in physical space as an ensemble of droplets. It is assumed that one can associate a characteristic length scale with each droplet, which is the radius in the case of spherical droplets. At time t the total

number of droplets $N(t)$ is a non–negative integer–valued random variable, which is finite with probability 1. The ith DPE is characterized by its position vector $\mathbf{X}_{(i)}(t)$ (which is defined as the center of mass of the droplet), its velocity vector $\mathbf{V}_{(i)}(t)$, and its radius $R_{(i)}(t)$ ($R_{(i)}(t) > 0$). The position, velocity, and radius of a droplet are called the droplet properties, and the droplet property vector associated with each droplet is a 7–dimensional random vector in this representation. Additional droplet properties may be included as required, but they do not fundamentally alter the formulation, other than increasing the dimension of the space of droplet properties. The properties associated with the ith droplet evolve by the following equations:

$$\frac{d\mathbf{X}_{(i)}}{dt} = \mathbf{V}_{(i)} \tag{3.10}$$

$$\frac{d\mathbf{V}_{(i)}}{dt} = \mathbf{A}_{(i)} \tag{3.11}$$

$$\frac{dR_{(i)}}{dt} = \Theta_{(i)}, \tag{3.12}$$

where $\mathbf{A}_{(i)}$ is the acceleration experienced by the droplet, and $\Theta_{(i)}$ is the rate of radius change due to vaporization.

The ensemble of droplets is characterized in the 7–dimensional position–velocity–radius space $[\mathbf{x}, \mathbf{v}, r]$ by its Klimontovich fine–grained density function f' which is defined as:

$$f'(\mathbf{x}, \mathbf{v}, r, t) \equiv \sum_{i=1}^{N(t)} \delta(\mathbf{x} - \mathbf{X}_{(i)}(t))\delta(\mathbf{v} - \mathbf{V}_{(i)}(t))\delta(r - R_{(i)}(t)). \tag{3.13}$$

Note that $[\mathbf{X}_{(i)}, \mathbf{V}_{(i)}, R_{(i)}]$ are the Lagrangian coordinates of the ith droplet, whereas $[\mathbf{x}, \mathbf{v}, r]$ are the Eulerian coordinates. The Klimontovich fine–grained density function f' represents the density of droplets in a 7–dimensional $[\mathbf{x}, \mathbf{v}, r]$ space. If the number of droplets in any region B_+ in $[\mathbf{x}, \mathbf{v}, r_+]$ space [3] is denoted $N(B_+; t)$, it is obtained by integrating f' over the region B_+ such that:

$$N(B_+; t) = \int_{B_+} f'(\mathbf{x}, \mathbf{v}, r, t)\, d\mathbf{x}\, d\mathbf{v}\, dr. \tag{3.14}$$

Since f' is composed of delta functions it is not a smooth function in $[\mathbf{x}, \mathbf{v}, r]$ space.

[3] Since only droplets with non–zero radius belong to the spray system, if for convenience of notation we denote r_+ to be the positive r–axis ($r > 0$), then it is sufficient to integrate over regions only in $[\mathbf{x}, \mathbf{v}, r_+]$ space.

The statistical description of a spray in terms of f' contains far more information than is necessary for engineering calculations. In order to obtain information concerning the average properties of the spray, it is advantageous to consider the ensemble average of f'. The ensemble average of f' is denoted $f(\mathbf{x}, \mathbf{v}, r, t)$, and it *defines* the ddf:

$$f(\mathbf{x}, \mathbf{v}, r, t) \equiv \left\langle f'(\mathbf{x}, \mathbf{v}, r, t) \right\rangle = \left\langle \sum_{i=1}^{N(t)} \delta(\mathbf{x} - \mathbf{X}_{(i)}(t)) \delta(\mathbf{v} - \mathbf{V}_{(i)}(t)) \delta(r - R_{(i)}(t)) \right\rangle . \tag{3.15}$$

Since the ddf is defined to be the ensemble–average of f' (cf. Eq. (3.15)), it follows that if the expected number of droplets in a region B_+ of $[\mathbf{x}, \mathbf{v}, r_+]$ space is denoted $\langle N(B_+; t) \rangle$, it is obtained by integrating the ddf $f(\mathbf{x}, \mathbf{v}, r, t)$ over the region B_+ such that:

$$\langle N(B_+; t) \rangle = \int_{B_+} f(\mathbf{x}, \mathbf{v}, r, t) \, d\mathbf{x} \, d\mathbf{v} \, dr. \tag{3.16}$$

The ddf is the fundamental quantity in the Lagrangian statistical representation. If $\langle N(t) \rangle$ represents the expected total number of spray droplets at time t, then the droplet distribution function $f(\mathbf{x}, \mathbf{v}, r, t)$ when integrated over the entire $[\mathbf{x}, \mathbf{v}, r_+]$ space, must yield $\langle N(t) \rangle$, such that:

$$\int_{[\mathbf{x}, \mathbf{v}, r_+]} f(\mathbf{x}, \mathbf{v}, r, t) \; d\mathbf{x} \, d\mathbf{v} \, dr = \langle N(t) \rangle. \tag{3.17}$$

Note that f does not possess the normalization property of a probability density function, since it does not integrate to unity over the space on which it is defined.

If the droplet distribution function is integrated over only $[\mathbf{v}, r_+]$ space, the density (in physical space) of the expected number of spray droplets $n(\mathbf{x}; t)$ is obtained:

$$n(\mathbf{x}; t) \equiv \int_{[\mathbf{v}, r_+]} f(\mathbf{x}, \mathbf{v}, r, t) \, d\mathbf{v} \, dr. \tag{3.18}$$

If the multiphase flow is modeled as a marked point process, then the theory of point processes can be used to express the ddf as the product of the number density in physical space $n(\mathbf{x}; t)$ and $f^c_{\mathbf{V}R}(\mathbf{v}, r \mid \mathbf{x}; t)$, the joint probability density function (jpdf) of velocity and radius conditional on physical location $\mathbf{x}$, such that (Subramaniam, 2001c):

$$f(\mathbf{x}, \mathbf{v}, r, t) = n(\mathbf{x}; t) \; f^c_{\mathbf{V}R}(\mathbf{v}, r \mid \mathbf{x}; t). \tag{3.19}$$

Unlike the ddf, $f^c_{\mathbf{V}R}(\mathbf{v}, r \mid \mathbf{x}; t)$ is a pdf, and when it is integrated over $[\mathbf{v}, r_+]$ space it yields unity.

In pdf modeling of constant–density turbulent flows the Lagrangian jpdf of fluid particle position $\mathbf{X}^+(t)$ and velocity $\mathbf{U}^+(t)$ can be related to the Eulerian jpdf of the Eulerian velocity field $\mathbf{U}(\mathbf{x}, t)$ by using a conditioning argument as shown by Dreeben and Pope (1997b). There the conditioning is on the position of the fluid particle being at the field location $\mathbf{x}$, i.e., the conditioning is on the event $[\mathbf{X}^+(t) = \mathbf{x}]$. In contrast, the jpdf $f^c_{\mathbf{V}R}(\mathbf{v}, r \mid \mathbf{x}; t)$ does not correspond to conditioning on the event that a droplet's position is at the field location $\mathbf{x}$. In other words, the jpdf $f^c_{\mathbf{V}R}(\mathbf{v}, r \mid \mathbf{x}; t)$ is not an Eulerian jpdf since it does not characterize the probability of an Eulerian event (in the sense of $\mathbf{U}(\mathbf{x}, t)$ being an Eulerian event in a random–field model of turbulent flow).

In the LE approach one cannot meaningfully associate a density with each droplet in the spray, since information about individual droplets is lost in the course of the derivation of the ddf (Subramaniam, 2001c). However, the ddf can be related to single–particle densities associated with "surrogate" droplets as (Subramaniam, 2000):

$$f(\mathbf{x}, \mathbf{v}, r, t) \; = \sum_{k \geq 1} q_k \; f^{(k)}(\mathbf{x}, \mathbf{v}, r; t) = \sum_{k \geq 1} k \; q_k \; f^{(k)}_{1s}(\mathbf{x}, \mathbf{v}, r; t), \tag{3.20}$$

where k is the integer value that $N(t)$ takes with probability $q_k = P[N(t) = k]$, $f^{(k)}$ is the density of expected number of droplets in phase space, conditional on the event $[N(t) = k]$, i.e., conditional on there being a total of k droplets in the ensemble, and $f^{(k)}_{1s}(\mathbf{x}, \mathbf{v}, r; t)$ is the single–particle density of identically–distributed surrogate droplets, conditional on the event $[N(t) = k]$. The single–particle density of identically–distributed surrogate droplets $f^{(k)}_{1s}(\mathbf{x}, \mathbf{v}, r; t)$ is related to the droplet properties by the relation

$$f^{(k)}_{1s}(\mathbf{x}, \mathbf{v}, r; t) = \frac{1}{k} f^{(k)}(\mathbf{x}, \mathbf{v}, r, t) = \frac{1}{k} \left\langle \sum_{i=1}^{k} \delta(\mathbf{x} - \mathbf{X}_{(i)}(t)) \delta(\mathbf{v} - \mathbf{V}_{(i)}(t)) \delta(r - R_{(i)}(t)) \right\rangle. \tag{3.21}$$

It is impossible to characterize events associated with a *single* droplet in the LE approach. This is primarily because here one is dealing with a ddf that is the superposition of several surrogate–droplet densities (cf. Eq. (3.20)). Nevertheless, even in the LE representation one

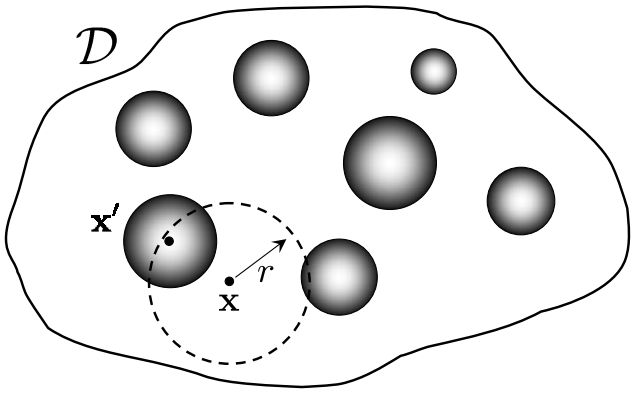

Figure 3.3 A schematic of the region of integration in Eq. (3.22) given by $[\mathbf{x}', r : \mathbf{x}' \in b(\mathbf{x}, r)]$. The point $\mathbf{x}$ is the location where the volume fraction α_d is desired, $\mathbf{x}'$ is the center of the DPE under consideration, and r is the radius of the ball centered at $\mathbf{x}$.

can characterize number–weighted statistical moments of the particle ensemble, and write conservation equations for mean mass and momentum in an Eulerian reference frame (see Section 3.5).

We have now established the foundation for the EE and LE statistical representations and defined the necessary equalities required in the rest of this work. We now proceed to establish a relationship between the two approaches.

3.3 Relationship Between the Eulerian–Eulerian and Lagrangian–Eulerian Description

In order to establish a relationship between the two representations, we consider *first–order* [4] quantities of the point–process (LE) and random–field (EE) statistical descriptions of a two–phase flow. Since the volume fraction $\alpha_d(\mathbf{x}, t)$ and the phasic pdfs $f_{\mathbf{U}|I_\beta}$ correspond to the minimal and complete description of a two–phase flow in the EE representation (cf. Eq. (3.9)), it is natural to seek expressions for the corresponding quantities in the LE representation.

[4] In this work, the phrase "first–order" is used to describe quantities that are defined at a single space–time location. Second–order quantities, which simultaneously characterizes the state of the point field at two different space–time locations (Stoyan et al., 1995), such as the pair–correlation function are not considered in this work.

If we assume *spherical* DPE's, then we can relate $\alpha_d(\mathbf{x},t)$ to the fundamental description as follows (Subramaniam, 2001a):

$$\begin{aligned}\alpha_d(\mathbf{x},t) &= \sum_{k\geq 1} q_k\ k \int_{\mathcal{X}_\mathcal{R}} \int_{\mathbf{v}} f_{1s}^{(k)}(\mathbf{x},\mathbf{v},r,t) d\mathbf{v}\, d\mathbf{x}'\, dr \\ &= \sum_{k\geq 1} q_k \int_{\mathcal{X}_\mathcal{R}} \int_{\mathbf{v}} \left\langle \sum_{i=1}^{k} \delta(\mathbf{x}' - \mathbf{X}_{(i)}(t)) \delta(\mathbf{v} - \mathbf{V}_{(i)}(t)) \delta(r - R_{(i)}(t)) \right\rangle d\mathbf{v}\, d\mathbf{x}'\, dr, \quad (3.22)\end{aligned}$$

where the region of integration $\mathcal{X}_\mathcal{R} = [\mathbf{x}', r : \mathbf{x}' \in b(\mathbf{x},r)]$. Here, $b(\mathbf{x},r)$ is the disk of radius r centered at $\mathbf{x}$. See Fig. 3.3. The above equation states that the event $E_0^{(d)} = P[I_d(\mathbf{x},t) = 1]$ can arise from all possible combinations of DPE location and radius that result in $\mathbf{x}$ being covered by the DPE. For a constant number of DPEs $n = N$ in the system, $q_k = \delta_{kn}$ for $k = N$ otherwise. With the additional assumption of identically distributed monodispersed DPEs, the above expression simplifies to

$$\alpha(\mathbf{x},t) = \sum_{i=1}^{N} \left\langle H\left(\frac{\sigma}{2} - \left|\mathbf{x} - \mathbf{X}_{(i)}(t)\right|\right)\right\rangle, \quad (3.23)$$

where $H(\mathbf{x})$ is the Heaviside function defined as

$$H(\mathbf{x}) = \begin{cases} 1 & \text{if } \mathbf{x} \geq 0 \\ 0 & \text{if } \mathbf{x} < 0, \end{cases} \quad (3.24)$$

and σ is the diameter of the DPE. Equation 3.23 is identical to the expression for the expected indicator function available in literature (see for instance, Zhang and Prosperetti, 1994; Sundaram and Collins, 1994a). Equation 3.22 is more general compared to Eq. (3.23) because (a) the total number of DPE's is assumed to be a random variable (an assumption that extends previous analyses to physical problems in which the expected total number of DPEs can change in time), (b) the important effect of polydispersity is considered, and (c) the effects of statistical inhomogeneity are also considered.

It is convenient to express $\alpha_d(\mathbf{x},t)$ in Eq. (3.22) in terms of the ddf using Eq. (3.20) as (Subramaniam, 2001a)

$$\alpha_d(\mathbf{x},t) = \int_{[\mathbf{x}', r\,:\,\mathbf{x}' \in b(\mathbf{x},r)]} \int_{\mathbf{v}} f(\mathbf{x}',\mathbf{v},r,t)\, d\mathbf{v}\, d\mathbf{x}'\, dr. \quad (3.25)$$

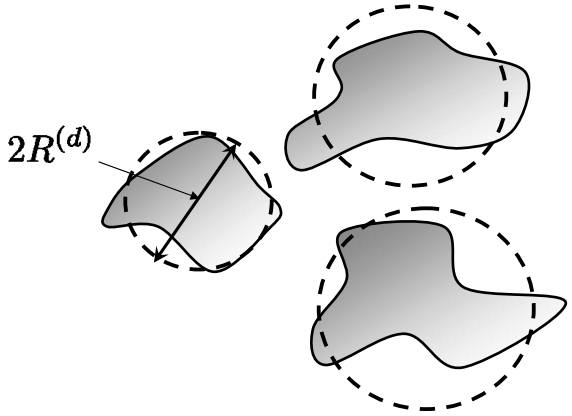

Figure 3.4 Schematic of a representative spherical DPE (dashed line) with radius $R^{(d)}$ corresponding to the dispersed phase (shaded) in the EE representation.

Using the decomposition in Eq. (3.19), expressing

$$f^c_{\mathbf{V}R}(\mathbf{v}, r \mid \mathbf{x}; t) \; = f^c_{\mathbf{V} \mid R}(\mathbf{v} \mid r, \mathbf{x}; t) \; f^c_R(r \mid \mathbf{x}; t) \; ,$$

and noting that $f^c_{\mathbf{V} \mid R}(\mathbf{v} \mid r, \mathbf{x}; t)$ integrates to unity over all velocity space, we find as expected that $\alpha_d(\mathbf{x}, t)$ depends only on the number density and the radius pdf (Subramaniam, 2001a):

$$\alpha_d(\mathbf{x}, t) \; = \int_{[\mathbf{x}', r \,:\, \mathbf{x}' \in b(\mathbf{x}, r)]} n(\mathbf{x}'; t) \, f^c_R(r \mid \mathbf{x}', t) \, d\mathbf{x}' \, dr. \tag{3.26}$$

Later, we consider special cases where assumptions of statistical homogeneity in $n(\mathbf{x}, t)$ and f^c_R result in simpler forms of Eq. (3.26).

Next we relate the Eulerian events with the conditional jpdf of velocity and radius arising from the ddf description of the spray. To this end, we write the event E_2 as (Subramaniam, 2001a)

$$E_2 = [\mathbf{U}(\mathbf{x}, t) \in (\mathbf{u}, \mathbf{u} + d\mathbf{u}), R^{(d)}(\mathbf{x}, t) \in (r, r + dr)],$$

where the event has been augmented with an additional radius phase space $R^{(d)}$ to allow for a consistent comparison with the LE approach. It is implicitly assumed that the dispersed phase is represented as equivalent spherical DPEs (see Fig.3.4). The phasic velocity pdf conditional

on the presence of phase β, $f_{\mathbf{U}|I_\beta}$ (cf. Eq. (3.7)) is now written as $f^E_{\mathbf{U}R|I_\beta}$ such that

$$P\Big[\,\mathbf{U}(\mathbf{x},t)\in(\mathbf{u},\mathbf{u}+d\mathbf{u}),R^{(d)}(\mathbf{x},t)\in(r,r+dr)\mid I_\beta(\mathbf{x},t)=1\,\Big]=f^E_{\mathbf{U}R|I_\beta}(\mathbf{u},r\,;\mathbf{x},t)\;d\mathbf{v}\,dr, \tag{3.27}$$

where $f^E_{\mathbf{U}R|I_\beta}(\mathbf{u},r\,;\mathbf{x},t)$ represents the Eulerian conditional joint pdf of velocity and radius [5]. An additional E superscript has been included compared to Eq. (3.7) to denote explicitly in the subsequent comparisons with the LE approach that $f^E_{\mathbf{U}R|I_\beta}(\mathbf{u},r\,;\mathbf{x},t)$ arises from the EE representation. We then define the probability of the event $[E_2\bigcap E_3^{(d)}]$ (Subramaniam, 2001a):

$$P\Big[\,\mathbf{U}(\mathbf{x},t)\;\in(\mathbf{u},\mathbf{u}+d\mathbf{u}),R^{(d)}(\mathbf{x},t)\in(r,r+dr),I_d(\mathbf{x},t)=1\Big]=\sum_{k\geq1}k\;q_k\;\int_{[\mathbf{x}'\,:\,\mathbf{x}'\in b(\mathbf{x},r)]}f^{(k)}_{1s}(\mathbf{x}',\mathbf{v},r;t)\,d\mathbf{x}'. \tag{3.28}$$

Now using the definition of conditional probability, we can write

$$P\,\Big[\,\mathbf{U}(\mathbf{x},t)\in(\mathbf{u},\mathbf{u}+d\mathbf{u}),R^{(d)}(\mathbf{x},t)\in(r,r+dr)\mid I_d(\mathbf{x},t)=1\,\Big]=\frac{P\,\big[\,\mathbf{U}(\mathbf{x},t)\in(\mathbf{u},\mathbf{u}+d\mathbf{u}),R^{(d)}(\mathbf{x},t)\in(r,r+dr),I_d(\mathbf{x},t)=1\,\big]}{P\,[\,I_d(\mathbf{x},t)=1\,]}. \tag{3.29}$$

Therefore the Eulerian jpdf of velocity and radius conditional on the dispersed phase, $f^E_{\mathbf{U}R|I_d}(\mathbf{u},r\,;\mathbf{x},t)$ is given by (Subramaniam, 2001a)

$$\begin{aligned}f^E_{\mathbf{U}R|I_d}(\mathbf{u},r\,;\mathbf{x},t)\;&=\frac{1}{\alpha_d(\mathbf{x},t)}\int_{[\mathbf{x}'\,:\,\mathbf{x}'\in b(\mathbf{x},r)]}f(\mathbf{x}',\mathbf{v},r,t)\,d\mathbf{x}'\\&=\frac{1}{\alpha_d(\mathbf{x},t)}\int_{[\mathbf{x}'\,:\,\mathbf{x}'\in b(\mathbf{x},r)]}n(\mathbf{x}',t)f^c_{\mathbf{V}R}(\mathbf{v},r\mid\mathbf{x}';t)\,d\mathbf{x}',\end{aligned} \tag{3.30}$$

which clearly shows that in general it is different from the jpdf of velocity and radius $f^c_{\mathbf{V}R}(\mathbf{v},r\mid\mathbf{x};t)$ obtained in the Lagrangian approach (cf. Eq. (3.19)). The relationships given by Eq. (3.26) and Eq. (3.30) form the two fundamental equalities that relate two–phase flow quantities across the EE and LE statistical representations.

3.3.1 Simplified relations under special conditions

In this subsection, we consider special conditions under which simple relations between the EE and LE descriptions exist. This involves determining the conditions under which a simple

[5] For the carrier phase where R is always defined to be zero, this essentially reduces to a pdf of velocity, i.e., $f^E_{\mathbf{U}R\,|I_f}(\mathbf{v},r\,;\mathbf{x},t)=f^E_{\mathbf{U}|I_f}(\mathbf{v}\,;\mathbf{x},t)\cdot\delta(r)$.

relation between $\alpha_d(\mathbf{x},t)$ and $n(\mathbf{x};t)$, and between $f^E_{\mathbf{U}R|I_d}(\mathbf{u},r\,;\mathbf{x},t)$ and $f^c_{\mathbf{V}R}(\mathbf{v},r\mid\mathbf{x};t)$ exist, and under what conditions such relationships are precluded. The simplest situation in which to study these relationships is *statistically homogeneous* two–phase flow. In two–phase flows there are two sources of statistical inhomogeneity. This is implicit in the decomposition expressed in Eq. (3.19), which shows that spatial inhomogeneity of the ddf has two different sources: namely, inhomogeneity can arise from either $n(\mathbf{x};t)$ in physical space, or from $f^c_{\mathbf{V}R}(\mathbf{v},r\mid\mathbf{x};t)$. It is clear from Eq. 3.26 that only the statistical properties of the radius pdf $f^c_R(r\mid\mathbf{x};t)$ affect the relation between $\alpha_d(\mathbf{x},t)$ and the point–process quantities, whereas Eq. (3.30) shows that the relationship between $f^E_{\mathbf{U}R|I_d}(\mathbf{u},r\,;\mathbf{x},t)$ and $f^c_{\mathbf{V}R}(\mathbf{v},r\mid\mathbf{x};t)$ also depends on the statistical properties of the jpdf $f^c_{\mathbf{V}\,|\,R}(\mathbf{v}\mid r,\mathbf{x};t)$.

With this in mind, the simplifications that result from a statistically homogeneous number density with statistically homogeneous radius pdf and velocity–radius jpdf are considered, details of which are given in Appendix B. The principal findings from these simplifications are summarized below. Also given in Appendix B are considerations required to extend these relations to inhomogeneous number density, radius and velocity–radius jpdf.

3.3.1.1 Statistically homogeneous cases

The simplified relationships arising from the cases corresponding to the statistically homogeneous cases are shown in Table 3.1. Two–phase flows with monodisperse DPE's are included as a special subset of the homogeneous radius pdf case. The principal findings are as follows (Subramaniam, 2001a):

(i) The relation between $\alpha_d(\mathbf{x},t)$ and $n(\mathbf{x};t)$ for the case of statistically homogeneous number density and statistically homogeneous radius pdf is

$$\alpha_d(\mathbf{x},t) = n(t)\,\overline{\mathcal{V}}_D(t) = n(t)K_D\,\langle R^D(t)\rangle, \tag{3.31}$$

where $K_1 = 2, K_2 = \pi$, and $K_3 = 4\pi/3$, and $K'_D = DK_D$. The above expression reveals that while $\alpha_d(\mathbf{x},t)$ depends on the dimensionality D of physical space, $n(\mathbf{x};t)$ does not [6].

[6] A detailed derivation of this relation is given in Appendix B.

Statistically homogeneous number density $n(t)$ and point–process radius pdf $f_R^c(r;t)$	
Monodisperse	Polydisperse
$\alpha_d(t) = n(t) K_D r_0^D$	$\alpha_d(t) = n K_D \langle R^D(t) \rangle$
$f_R^E(r) = f_R^c(r) = \delta(r - r_0)$	$f_R^E(r;t) = r^D \dfrac{f_R^c(r;t)}{\langle R^D(t) \rangle}$
Statistically homogeneous $f^c_{\mathbf{V}\,\vert\,R}(\mathbf{v} \mid r;t)$	
$f^E_{\mathbf{U}R\,\vert\,d}(\mathbf{v},r;t) = f^c_{\mathbf{V}R}(\mathbf{v},r;t)$	$f^E_{\mathbf{U}R\,\vert\,d}(\mathbf{v},r;t) = \dfrac{r^D\, f^c_{\mathbf{V}R}(\mathbf{v},r;t)}{\langle R^D(t) \rangle}$

Table 3.1 Relationship between first–order statistics and velocity–radius jpdf's of point–process and random–field representations for the statistically homogeneous cases. $K_1 = 2; K_2 = \pi; K_3 = 4\pi/3$.

This fact alone clearly shows that the LE and EE statistical representations contain different information.

(ii) For the statistically homogeneous number density and statistically homogeneous $f_R^c(r \mid \mathbf{x};t)$ m the following simplified relation between the EE and LE radius pdf's results:

$$f^E_{R\,\vert\,d}(r;t) = \frac{r^D\, f_R^c(r;t)}{\langle R^D(t) \rangle}. \tag{3.32}$$

(iii) If $f^c_{\mathbf{V}\,\vert\,R}(\mathbf{v} \mid r, \mathbf{x};t)$ is also statistically homogeneous then the velocity–radius jpdf's satisfy the following relation:

$$f^E_{\mathbf{U}R\,\vert\,d}(\mathbf{v},r;t) = \tilde{f}^c_{\mathbf{V}R}(\mathbf{v},r;t) \equiv \frac{r^D\, f^c_{\mathbf{V}R}(\mathbf{v},r;t)}{\langle R^D(t) \rangle}, \tag{3.33}$$

where $\tilde{f}^c_{\mathbf{V}R}(\mathbf{v},r;t)$ is the volume–weighted–pdf corresponding to $f^c_{\mathbf{V}R}(\mathbf{v},r;t)$.

(iv) For a monodisperse size distribution with DPEs of radius r_0, these relations further simplify to

$$\alpha_d(\mathbf{x},t) = n(t) K_D\ r_0^D \tag{3.34}$$

$$f^E_{\mathbf{U}R\,\vert\,d}(\mathbf{v},r;t) = f^c_{\mathbf{V}\,\vert\,R}(\mathbf{v} \mid r;t)\, \delta(r - r_0). \tag{3.35}$$

It has already been noted that the velocity–radius jpdf's in each representation are not equal in general. As noted earlier, Zhu et al. (2000) derive an evolution equation for $f^c_{\mathbf{V}R}(\mathbf{v}, r \mid \mathbf{x}; t)$ from the transport equation for $f^E_{\mathbf{U}R}(\mathbf{v}, r\,; \mathbf{x}, t)$ under an assumption that these two quantities are equal for a general spray. However, it is shown here that only under rather restrictive assumptions of spherical monodisperse DPE's and a statistically isotropic and homogeneous point process does a simple relationship between $f^c_{\mathbf{V}R}(\mathbf{v}, r; t)$ and $f^E_{\mathbf{U}R}(\mathbf{v}, r; t)$ exist.

3.3.2 Validity of assumptions necessary for exact relations

The exact equalities between first–order quantities in the LE and EE approach that are derived in the earlier section hold only under certain conditions and assumptions that can restrict the applicability of the exact equalities in general two–phase flows.

3.3.2.1 Spatial inhomogeneities in the two–phase flow

Spatial inhomogeneities in $n(\mathbf{x}; t)$ and $f^c_R(r \mid \mathbf{x}; t)$ that exist either at initial time or develop as a two–phase flow evolves could preclude the validity of the exact equalities. Two examples of such flows are:

1. Fuel sprays: In the near–nozzle region of the fuel spray injector, the dispersed–phase number density $n(\mathbf{x}; t)$ can have steep gradients. Also, $f^c_R(r \mid \mathbf{x}; t)$ can be spatially inhomogeneous due to a spatially varying size distribution of the dispersed phase. Under such conditions, even assumptions of local homogeneity may cease to hold. Furthermore, in regions close to the injector, $n(\mathbf{x}; t)$ and $f^c_R(r \mid \mathbf{x}; t)$ may remain inhomogeneous even as time evolves. Under such conditions, the relationship between the EE and LE representations have to be interpreted only as approximate relations.

2. Particle–laden mixing layers: Particle–laden mixing layers form an important class of canonical problems studied by researchers through multiphase DNS and experiments (See for eg. Lázaro and Lasheras, 1992a,b; Okong'o and Bellan, 2004). Consider a particle–laden mixing layer with two monodispersed streams of particles, with each stream having a different particle radius. The particle positions in the two streams are such that the

initial number density is statistically homogeneous. The region near the centerline of the mixing layer will have a locally inhomogeneous $f_R^c(r \mid \mathbf{x}; t)$. Once the flow starts to evolve, the number density may develop inhomogeneities as well. Again under such conditions, the equalities presented in the earlier section between the EE and LE representations have to be interpreted only as approximate relations.

3.3.2.2 Spherical shape assumption

An important assumption of spherical DPEs has been made in the development of the exact equalities (see Appendix B). This is implicit in the assumption of an isotropic point process for the DPE positions that results in Eq. (B.1). In general however, the DPE locations need not form an isotropic point process and thus the exact inequalities may fail to hold.

3.3.2.3 Internal circulation in a droplet

Implicit in the representation of the spray in terms of a ddf is the assumption of uniform velocity inside a DPE. This assumption is also implicit in the equations of motion for a droplet given by Eqs. (3.10)–(3.12). In other words, the form of the Eulerian jpdf of velocity and radius expressed in terms of the point–process representation given by Eq. (3.30) assumes that the two–phase flow is composed of rigid DPEs, or DPEs in which the internal velocity field is uniform. However, if the dispersed phase is a fluid (as in droplets or bubbles) then the velocity field internal to the DPE need not be constant because of internal circulation effects. Under these conditions, the Eulerian jpdf as defined in its general form by Eq. (3.27) is capable of representing such internal circulation effects. However, its form in Eq. (3.30) as derived from the point–process representation will not be equal to that given by Eq. (3.27) when the velocity field is non–uniform inside the DPEs.

3.3.3 Example to show relationship between statistical representations

The difference between $f^E_{\mathbf{U}R|I_d}(\mathbf{u}, r\ ; \mathbf{x}, t)$ in the EE representation and $f^c_{\mathbf{V}R}(\mathbf{v}, r \mid \mathbf{x}; t)$in the LE representation is illustrated by means of a simple example (Subramaniam, 2001a). Also,

a comparison between the information contained in the number density $n(\mathbf{x},t)$ and $\alpha_d(\mathbf{x},t)$ is presented.

Consider an idealized two–phase flow comprising spherical DPEs in the unit interval in the x–coordinate. The total number of DPEs N in the unit interval is deterministic and is always equal to k^*, i.e., $q_{k^*} = 1$. For simplicity only the position and radius properties of DPEs are considered. The two–phase flow can be interpreted as being composed of two streams of DPEs: one stream has DPEs of radius r_0, and the pdf of their position decreases linearly from unity to zero with increasing x in the unit interval; while the other stream has DPEs of radius $10r_0$, and the pdf of their position increases linearly from zero to unity with increasing x in the same unit interval. The single–particle density for this example problem is given by (cf. Eq. (3.21))

$$f_{1s}^{(k^*)}(x,r;t) = \delta(r-10r_0)\cdot x + \delta(r-r_0)\cdot(1-x). \tag{3.36}$$

Using Eq. (3.20) the ddf corresponding to this idealized problem is

$$f(x,r,t) = k^*\left[\delta(r-10r_0)\cdot x + \delta(r-r_0)\cdot(1-x)\right] \tag{3.37}$$

Integrating the ddf over all r_+ space, results in a statistically homogeneous number density

$$n(x;t) = k^*\left\{x + (1-x)\right\} = k^*, \tag{3.38}$$

which was the intent in constructing this example (see Figure 3.3.3).

In the LE approach, the pdf of radius conditional on physical location as obtained from the ddf is given by

$$f_R^c(r \mid \mathbf{x};t) \ = \delta(r-10r_0)\cdot x + \delta(r-r_0)\cdot(1-x), \tag{3.39}$$

which is a simple linear combination of the two droplet streams. For instance at the mid–point of the unit interval, it is composed of two delta–functions at r_0 and $10r_0$ each weighted by 0.5, i.e., on a number–basis there is equal probability of finding a droplet of radius r_0 or $10r_0$.

In the EE representation, the probability that the dispersed phase is located at x as obtained from its definition Eq. (3.22) (or, from Eq. (3.25)) is given by [7]

$$\alpha_d(x,t) = k^* \ \ 2r_0 \ \ (9x+1), \tag{3.40}$$

[7]The limit $[x', r : x' \in b(x,r)]$ in Eq. (3.22) can be decomposed into two double integrals; one with limits $r = [0,\infty)$ and $x' = [x, x-r]$, and the other with limits $r = [0,\infty)$ and $x' = [x+r, x]$.

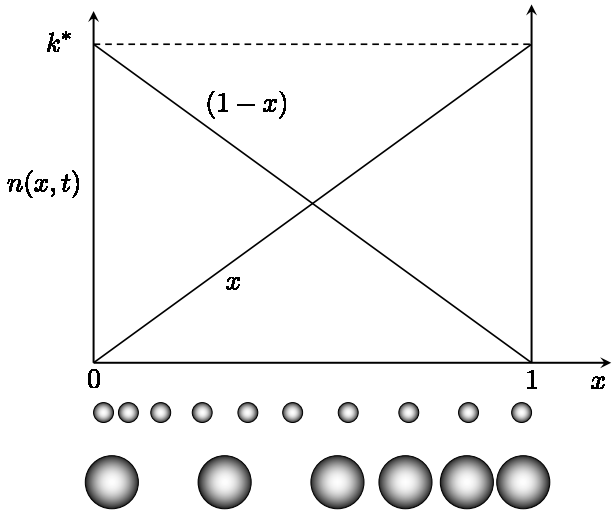

Figure 3.5 Variation of number density with position shown for an idealized two–phase flow composed of two streams of droplets. Droplets with radius r_0 have a position pdf which decreases linearly from unity to zero, while droplets with radius $10r_0$ have a position pdf which increases linearly from zero to unity. The resulting number density is homogeneous and equal to k^*.

which reveals that the probability of being in the liquid phase increases with x because the larger DPEs are occurring more frequently. Substituting the above expressions for $\alpha_d(x,t)$ and $f_R^c(r \mid x;t)$ into Eq. (3.30), the Eulerian pdf of radius conditional on the liquid phase, $f_R^E(r;x,t)$ is found to be

$$f_R^E(r;x,t) = \frac{\{\delta(r-10r_0)\cdot 10x + \delta(r-r_0)\cdot(1-x)\}}{(1+9x)}. \tag{3.41}$$

Clearly this Eulerian pdf of radius is different from its Lagrangian counterpart Eq. (3.39). For instance at the mid–point of the unit interval it evaluates to

$$f_R^E(r\,;\mathbf{x},t) \;= \{0.91\,\delta(r-10r_0) + 0.09\,\delta(r-r_0)\}\,,$$

which reveals that the larger droplets are considerably more probable on the basis of presence of liquid at that point. This simple example illustrates, as noted ealier, that $\alpha_d(\mathbf{x},t)$ and $f_{\mathbf{U}R}^E(\mathbf{v},r\,;\mathbf{x},t)$ depends on the dimensionality of the physical space defining the flow domain (1–D in this example), whereas the radius pdf in the Lagrangian approach $f_{\mathbf{V}R}^c(\mathbf{v},r \mid \mathbf{x};t)$does

not.

A related problem widely studied using two–phase DNS is that of monodispersed DPEs whose number density can vary in space. A linear dependence of $n(x,t)$ on x is the simplest form of inhomogeneity that can occur in two–phase flows. Assuming that the dispersed phase is composed of DPEs of size r_0, and the number density is varying as a function of x as $n(x,t) = k^* x$, then the single–particle density is given by

$$f_{1s}^{(k^*)} = \delta(r - r_0)x,$$

and the corresponding ddf is

$$f(x,r,t) = k^* \delta(r - r_0)x.$$

The pdf of radius conditional on location in the LE approach is

$$f_R^c(r \mid x;t) = \delta(r - r_0).$$

Following the same procedure as earlier, the volume fraction α_d corresponding to the inhomogeneous number density is

$$\alpha_d(x,t) = k^* \; 2r_0 \; x,$$

which shows that the volume fraction is also linear in x (and thus, inhomogeneous). The above expression also shows that for simple integrable forms of the inhomogeneity in number density (cf. Eq. (3.26)) and simplifying assumptions on the radius pdf, exact expressions for the volume fraction can be derived. However, if the number density variation in space is a complex non–integrable function of x, then the volume fraction cannot be expressed in terms of a simple function of number density. Finally, the Eulerian pdf of radius $f_R^E(r;x,t)$ can be derived:

$$f_R^E(r;x,t) = \delta(r - r_0).$$

Note that for a linear number density and monodispersed size distribution, the pdf f_R^c in the LE approach is the same as the Eulerian pdf $f_R^E(r;x,t)$ in the EE approach.

Having established a clear foundation for the EE and the LE statistical representations, along with an understanding of the relationship between the two representations, we now derive the evolution equations corresponding to the densities in each approach.

3.4 Evolution Equations for the Probability Densities

The primary objective of this section is to derive the evolution equations for densities $f_{\mathbf{U}|I_\beta}$ and $f(\mathbf{x}, \mathbf{v}, r, t)$ that were introduced in Section 3.2 corresponding to the EE and LE statistical representations. Evolution equations for the densities developed in this section form the basis for the derivation of the governing equations for the mean mass, mean momentum and second–moment of velocity in the two statistical representations.

3.4.1 Random–field statistical representation

Analogous to single–phase flows, it is convenient to work with mass–weighted or Fàvre quantities in two–phase flows. The Fàvre fine–grained mass density conditional on the phase β is defined as

$$\mathcal{F}'_{\mathbf{U}|I_\beta} = \rho\, I_\beta \delta(\mathbf{U} - \mathbf{u})$$

Here, ρ is the instantaneous density of the two–phase flow at $\mathbf{x}$. The expectation of the $\mathcal{F}_{\mathbf{U}|I_\beta}$ defines the Fàvre mass density conditional on phase β:

$$\mathcal{F}_{\mathbf{U}|I_\beta} \equiv \langle \mathcal{F}'_{\mathbf{U}|I_\beta} \rangle, \tag{3.42}$$

where the angled brackets $\langle \cdot \rangle$ represents an expectation over all possible realizations in the $\mathbf{U}$ space. Since the fundamental events defined in Section 3.2.1 are in terms of $f_{\mathbf{U}}$, the following relations establish the connection between $\mathcal{F}_{\mathbf{U}|I_\beta}$ and the fundamental events:

$$\begin{aligned}
\mathcal{F}_{\mathbf{U}|I_\beta} = \langle \rho I_\beta \delta(\mathbf{U} - \mathbf{u}) \rangle &= \int \left\langle \rho I_\beta \delta(\mathbf{U} - \mathbf{u}) | \mathbf{U} = \mathbf{u}' \right\rangle f_{\mathbf{U}}(\mathbf{u}') d\mathbf{u}' \\
&= \int \delta(\mathbf{u}' - \mathbf{u}) \left\langle \rho I_\beta | \mathbf{U} = \mathbf{u}' \right\rangle f_{\mathbf{U}}(\mathbf{u}') d\mathbf{u}' \\
&= \langle \rho I_\beta | \mathbf{U} = \mathbf{u} \rangle\, f_{\mathbf{U}}(\mathbf{u}).
\end{aligned} \tag{3.43}$$

Integrating $\mathcal{F}_{\mathbf{U}|I_\beta}$ over all velocity space results in

$$\int_{\mathbf{U}} \mathcal{F}_{\mathbf{U}|I_\beta} d\mathbf{u} = \langle \rho I_\beta \rangle.$$

One can show that $\mathcal{F}_{\mathbf{U}|I_\beta} = \langle \rho I_\beta \rangle \tilde{f}_{\mathbf{U}|I_\beta}$. Density–weighted means can be defined as

$$\widetilde{\langle Q(\mathbf{U}) \rangle} = \frac{1}{\langle \rho I_\beta \rangle} \int Q(\mathbf{u}) \mathcal{F}_{\mathbf{U}|I_\beta}\, d\mathbf{u} = \int Q(\mathbf{u}) \tilde{f}_{\mathbf{U}|I_\beta}\, d\mathbf{u}, \tag{3.44}$$

where $\tilde{f}_{\mathbf{U}|I_\beta}$ is analogous to the phasic pdf $f_{\mathbf{U}|I_\beta}$ defined in Section 3.2.1. Likewise, unweighted means can also be defined as

$$\langle Q(\mathbf{U})\rangle = \int Q(\mathbf{u}) f_{\mathbf{U}|I_\beta}\, d\mathbf{u} = \int Q(\mathbf{u}) \frac{\tilde{f}_{\mathbf{U}|I_\beta}}{\langle \rho I_\beta | \mathbf{u}\rangle}\, d\mathbf{u}. \tag{3.45}$$

In the above development, the dependence on $\mathbf{x}$ and t has been omitted for the sake of brevity. The evolution equation for the fine–grained mass density is obtained by forming the substantial derivative of $\mathcal{F}'_{\mathbf{U}|I_\beta}$ as

$$\frac{D}{Dt}\mathcal{F}'_{\mathbf{U}|I_\beta} = \frac{\partial}{\partial t}\mathcal{F}'_{\mathbf{U}|I_\beta} + U_i \frac{\partial}{\partial x_i}\mathcal{F}'_{\mathbf{U}|I_\beta}, \tag{3.46}$$

where $\mathbf{U}$, the instantaneous two–phase flow velocity, is the convection velocity of the mass density in $\mathbf{x}$–space. Using a standard procedure of differentiating delta functions (Pope, 2000), the temporal and spatial derivatives of $\mathcal{F}'_{\mathbf{U}|I_\beta}$ can be derived from the corresponding fine–grained density as

$$\frac{\partial \mathcal{F}'_{\mathbf{U}|I_\beta}}{\partial t} = -\frac{\partial}{\partial V_i}\left(\frac{\partial U_i}{\partial t}\mathcal{F}'_{\mathbf{U}|I_\beta}\right) + \mathcal{F}'_{\mathbf{U}|I_\beta}\frac{1}{I_\beta}\frac{\partial I_\beta}{\partial t} + \mathcal{F}'_{\mathbf{U}|I_\beta}\frac{1}{\rho}\frac{\partial \rho}{\partial t} \tag{3.47}$$

and

$$\frac{\partial \mathcal{F}'_{\mathbf{U}|I_\beta}}{\partial x_i} = -\frac{\partial}{\partial V_i}\left(\frac{\partial U_i}{\partial x_i}\mathcal{F}'_{\mathbf{U}|I_\beta}\right) + \mathcal{F}'_{\mathbf{U}|I_\beta}\frac{1}{I_\beta}\frac{\partial I_\beta}{\partial x_i} + \mathcal{F}'_{\mathbf{U}|I_\beta}\frac{1}{\rho}\frac{\partial \rho}{\partial x_i}. \tag{3.48}$$

Substituting Eq. (3.47) and Eq. (3.48) into Eq. (3.46) and rearranging results in

$$\begin{aligned}\frac{D}{Dt}\mathcal{F}'_{\mathbf{U}|I_\beta} = &-\frac{\partial}{\partial u_k}\left[\left(\frac{\partial U_k}{\partial t} + U_i\frac{\partial U_k}{\partial x_i}\right)\mathcal{F}'_{\mathbf{U}|I_\beta}\right] \\ &+ \frac{\mathcal{F}'_{\mathbf{U}|I_\beta}}{I_\beta}\left(\frac{\partial I_\beta}{\partial t} + U_i\frac{\partial I_\beta}{\partial x_i}\right) + \frac{\mathcal{F}'_{\mathbf{U}|I_\beta}}{\rho}\left(\frac{\partial \rho}{\partial t} + U_i\frac{\partial \rho}{\partial x_i}\right),\end{aligned} \tag{3.49}$$

which can be rewritten as

$$\frac{D}{Dt}\mathcal{F}'_{\mathbf{U}|I_\beta} = -\frac{\partial}{\partial u_k}\left[\left(\frac{\partial U_k}{\partial t} + U_i\frac{\partial U_k}{\partial x_i}\right)\mathcal{F}'_{\mathbf{U}|I_\beta}\right] + \frac{\mathcal{F}'_{\mathbf{U}|I_\beta}}{\rho I_\beta}\left(\frac{\partial(\rho I_\beta)}{\partial t} + U_i\frac{\partial(\rho I_\beta)}{\partial x_i}\right). \tag{3.50}$$

The convective part of $D\mathcal{F}'_{\mathbf{U}|I_\beta}/Dt$ in Eq. (3.49) can been written as:

$$\begin{aligned}U_i\frac{\partial}{\partial x_i}\mathcal{F}'_{\mathbf{U}|I_\beta} &= \frac{\partial}{\partial x_i}\left(U_i\mathcal{F}'_{\mathbf{U}|I_\beta}\right) - \mathcal{F}'_{\mathbf{U}|I_\beta}\frac{\partial U_i}{\partial x_i} \\ &= u_i\frac{\partial}{\partial x_i}\left(\mathcal{F}'_{\mathbf{U}|I_\beta}\right) - \mathcal{F}'_{\mathbf{U}|I_\beta}\frac{\partial U_i}{\partial x_i},\end{aligned}$$

where the instantaneous two–phase velocity is not assumed to be solenoidal. The random variable U_i in the first equality can be replaced by the sample space variable u_i due to the sifting property of the delta function in $\mathcal{F}_{\mathbf{U}|I_\beta}$. The last term on the right hand side of the above equation can be combined with the last term on the right hand side of Eq. (3.50) to give

$$\frac{\partial \mathcal{F}_{\mathbf{U}|I_\beta}}{\partial t} + u_i \frac{\partial}{\partial x_i}\left(\mathcal{F}'_{\mathbf{U}|I_\beta}\right) = -\frac{\partial}{\partial u_k}\left[\left(\frac{\partial U_k}{\partial t} + U_i \frac{\partial U_k}{\partial x_i}\right)\mathcal{F}'_{\mathbf{U}|I_\beta}\right] + \frac{\mathcal{F}'_{\mathbf{U}|I_\beta}}{\rho I_\beta}\left(\frac{\partial(\rho I_\beta)}{\partial t} + \frac{\partial(\rho I_\beta U_i)}{\partial x_i}\right). \tag{3.51}$$

Since, the velocity field $\mathbf{U}$ is the instantaneous two–phase velocity field in the two–phase flow, it satisfies the instantaneous continuity in each phase at every location $\mathbf{x}$ in the domain, as long as this location does not fall on the interface. Thus, on each realization the following is true away from the interface

$$\frac{\partial \rho}{\partial t} + \frac{\partial(\rho U_i)}{\partial x_i} = 0. \tag{3.52}$$

In order to incorporate the effect of the interface, it is instructive to multiply both sides of the above equation by I_β, use the product rule and rearrange:

$$I_\beta\left[\frac{\partial \rho}{\partial t} + \frac{\partial(\rho U_i)}{\partial x_i}\right] = 0 \tag{3.53}$$

$$\left[\frac{\partial(\rho I_\beta)}{\partial t} + \frac{\partial(\rho I_\beta U_i)}{\partial x_i}\right] = \rho\left[\frac{\partial I_\beta}{\partial t} + U_i \frac{\partial I_\beta}{\partial x_i}\right] \tag{3.54}$$

The material derivative of I_β on the right hand side of the above equation can been simplified as

$$\begin{aligned}\frac{\partial I_\beta}{\partial t} + U_i \frac{\partial I_\beta}{\partial x_i} &= \left[\frac{\partial I_\beta}{\partial t} + \left(U_i - U_i^{(I)} + U_i^{(I)}\right)\frac{\partial I_\beta}{\partial x_i}\right] \\ &= \left[\frac{\partial I_\beta}{\partial t} + U_i^{(I)}\frac{\partial I_\beta}{\partial x_i}\right] + \left(U_i - U_i^{(I)}\right)\frac{\partial I_\beta}{\partial x_i}\end{aligned}$$

where $\mathbf{U}^{(I)}$ is the velocity of the phasic interface, with the additional observation that the topological equation (Drew, 1983) holds:

$$\frac{\partial I_\beta}{\partial t} + U_i^{(I)}\frac{\partial I_\beta}{\partial x_i} = 0.$$

Thus, the instaneous mass conservation at any location in the two–phase flow is

$$\left[\frac{\partial(\rho I_\beta)}{\partial t} + \frac{\partial(\rho I_\beta U_i)}{\partial x_i}\right] = \rho\left[\left(U_i - U_i^{(I)}\right)\frac{\partial I_\beta}{\partial x_i}\right]. \tag{3.55}$$

The above development shows that the instantaneous mass conservation in each phase has a source term due to the difference between the interface velocity and the instantaneous two–phase velocity which commonly occurs in two–phase flows with vaporization or interphase mass transfer. An interesting observation from Eq. (3.54) is that in flows with zero interphase mass transfer, the indicator function behaves like a conserved scalar:

$$\frac{D}{Dt}I_\beta = \frac{\partial I_\beta}{\partial t} + U_i\frac{\partial I_\beta}{\partial x_i} = 0.$$

With the above simplifications, Eq. (3.51) becomes

$$\frac{\partial \mathcal{F}_{\mathbf{U}|I_\beta}}{\partial t} + u_i\frac{\partial}{\partial x_i}\left(\mathcal{F}'_{\mathbf{U}|I_\beta}\right) = -\frac{\partial}{\partial u_k}\left[\left(\frac{\partial U_k}{\partial t} + U_i\frac{\partial U_k}{\partial x_i}\right)\mathcal{F}'_{\mathbf{U}|I_\beta}\right] + \frac{\mathcal{F}'_{\mathbf{U}|I_\beta}}{\rho I_\beta}\left[\rho\left(U_i - U_i^{(I)}\right)\frac{\partial I_\beta}{\partial x_i}\right]. \tag{3.56}$$

Taking the expectation of Eq. (3.56) and using the definition Eq. (3.42) leads to the evolution equation for the phasic mass density in each phase β:

$$\frac{\partial \mathcal{F}_{\mathbf{U}|I_\beta}}{\partial t} + u_i\frac{\partial \mathcal{F}_{\mathbf{U}|I_\beta}}{\partial x_i} = -\frac{\partial}{\partial u_k}\left[\left\langle \rho I_\beta \frac{DU_k}{Dt}\middle|\mathbf{u}\right\rangle \frac{\mathcal{F}_{\mathbf{U}|I_\beta}}{\langle \rho I_\beta|\mathbf{u}\rangle}\right] + \frac{\mathcal{F}_{\mathbf{U}|I_\beta}}{\langle \rho I_\beta|\mathbf{u}\rangle}\left\langle \rho\left(U_i - U_i^{(I)}\right)\frac{\partial I_\beta}{\partial x_i}\middle|\mathbf{u}\right\rangle \tag{3.57}$$

where $\langle\cdot|\mathbf{U}=\mathbf{u}\rangle$ is abbreviated as $\langle\cdot|\mathbf{u}\rangle$. The description of each term in the above equation is as follows: the two terms on the left hand side represent the unsteady and convective derivative of the phasic mass density; on the right hand side, the first term represents the transport in velocity space and the second term represents a source in the transport equation due to a regressing interface (in case of evaporating sprays). This term leads to the interphase mass transfer source term in the phasic mean mass conservation (see Eq. (3.77)), the contribution to the mean momentum due to interphase mass transfer (see Eq. (3.89) and Eq. (3.90)) and the contribution to the phasic Reynolds stresses due to interphase mass transfer (see Eq. (3.107)).

The terms representing transport in velocity space and the mass source in Eq. (3.57) are unclosed, i.e., they are not known in terms of the phasic mass density. Since the mass density transport equation is a one–point description of the two–phase flow, the unclosed terms are also evaluated at a single location in space–time co–ordinates. However, closures for such terms are almost always non–local in the sense that information at a particular location can depend

on the state at other locations in the two–phase flow. For instance, as discussed in Sec. 3.5.3, the drag experienced by a DPE depends on the pressure and state of fluid stress at its surface. Such information is absent in the mass density transport equation given in Eq. (3.57), since non–local information cannot be captured in a one–point description of the two–phase flow. In fact, a one–point description cannot distinguish between a location on the surface of a particle and one in the bulk (see schematic in Fig. 3.2). This has lead some researchers to propose functions that represent the shortest distance to the nearest interface (Zhu et al., 2000) in their single–point pdf formulation. To rigorously define such a distance function in a two–phase flow, one should know the spatial locations of all the DPEs from a reference point and the morphology of each DPE with respect to (say) its centroid. Such a description would require, at a minimum, a two–point description of the system.

In order to gain insight into Eq. (3.57) in terms of the decomposition $\mathcal{F}_{\mathbf{U}|I_\beta} = \langle \rho I_\beta \rangle \tilde{f}_{\mathbf{U}|I_\beta}$, we form

$$\langle \rho I_\beta \rangle \frac{\partial \tilde{f}_{\mathbf{U}|I_\beta}}{\partial t} = \frac{\partial \mathcal{F}_{\mathbf{U}|I_\beta}}{\partial t} - \tilde{f}_{\mathbf{U}|I_\beta} \frac{\partial \langle \rho I_\beta \rangle}{\partial t},$$

to derive the evolution of $f_{\mathbf{U}|I_\beta}$. The second term on the right hand side is the evolution equation of $\langle \rho I_\beta \rangle$ obtained by integrating Eq. (3.57) over all velocity space (see Eq. (3.77) in Section 3.5). Substituting Eq. (3.57) and Eq. (3.77) into the above equation, using the decomposition $\mathbf{u} = \mathbf{u}''^{(\beta)} + \langle \mathbf{U}^{(\beta)} \rangle$ and rearranging, results in

$$\begin{aligned} \frac{\partial \tilde{f}_{\mathbf{U}|I_\beta}}{\partial t} + u_i \frac{\partial \tilde{f}_{\mathbf{U}|I_\beta}}{\partial x_i} = &- \frac{\partial}{\partial u_k} \left[\left\langle \rho I_\beta \frac{DU_k}{Dt} \middle| \mathbf{u} \right\rangle \frac{\tilde{f}_{\mathbf{U}|I_\beta}}{\langle \rho I_\beta | \mathbf{u} \rangle} \right] + \frac{\tilde{f}_{\mathbf{U}|I_\beta}}{\langle \rho I_\beta | \mathbf{u} \rangle} \left\langle \rho \left(U_i - U_i^{(I)} \right) \frac{\partial I_\beta}{\partial x_i} \middle| \mathbf{u} \right\rangle \\ &- \tilde{f}_{\mathbf{U}|I_\beta} \frac{D}{Dt} \ln \langle \rho I_\beta \rangle, \end{aligned} \tag{3.58}$$

where

$$\frac{D}{Dt} \langle \rho I_\beta \rangle = \frac{\partial}{\partial t} \langle \rho I_\beta \rangle + u_k \frac{\partial \langle \rho I_\beta \rangle}{\partial x_k}$$

is the material derivative following the instantaneous two–phase velocity.

Defining

$$\langle \mathbf{A}^{(\beta)} | \mathbf{u} \rangle = \frac{1}{\langle \rho I_\beta | \mathbf{u} \rangle} \left\langle \rho I_\beta \frac{D\mathbf{U}}{Dt} \middle| \mathbf{u} \right\rangle,$$

as the acceleration conditional on velocity in phase β,

$$\langle S_\rho^{(\beta)} \mid \mathbf{u}\rangle = \left\langle \rho\left(U_i - U_i^{(I)}\right)\frac{\partial I_\beta}{\partial x_i}\Big|\mathbf{u}\right\rangle,$$

as the source term due to interphase mass transfer conditional on velocity, Eq. (3.58) can be rewritten as

$$\frac{\partial \tilde{f}_{\mathbf{U}|I_\beta}}{\partial t} + u_i\frac{\partial \tilde{f}_{\mathbf{U}|I_\beta}}{\partial x_i} + \frac{\partial}{\partial u_k}\langle A_k^{(\beta)}|\mathbf{u}\rangle\tilde{f}_{\mathbf{U}|I_\beta} = \frac{\tilde{f}_{\mathbf{U}|I_\beta}}{\langle\rho I_\beta|\mathbf{u}\rangle}\langle S_\rho^{(\beta)} \mid \mathbf{u}\rangle - \tilde{f}_{\mathbf{U}|I_\beta}\frac{D}{Dt}\ln\langle\rho I_\beta\rangle$$

One may verify using the above equation that $\tilde{f}_{\mathbf{U}|I_\beta}$ satisfies normalization for all time. Integrating both sides of the above equation over $\mathbf{u}$ space, we get

$$\begin{aligned}\frac{\partial}{\partial t}\int \tilde{f}_{\mathbf{U}|I_\beta}\,d\mathbf{u} + \underbrace{\frac{\partial}{\partial x_i}\int u_i\tilde{f}_{\mathbf{U}|I_\beta}\,d\mathbf{u}}_{a} + \underbrace{\int \frac{\partial}{\partial u_k}\langle A_k^{(\beta)}|\mathbf{u}\rangle\tilde{f}_{\mathbf{U}|I_\beta}\,d\mathbf{u}}_{b} \\ = \underbrace{\int \frac{\tilde{f}_{\mathbf{U}|I_\beta}}{\langle\rho I_\beta|\mathbf{u}\rangle}\langle S_\rho^{(\beta)} \mid \mathbf{u}\rangle\,d\mathbf{u}}_{c} - \underbrace{\int \tilde{f}_{\mathbf{U}|I_\beta}\frac{D}{Dt}\ln\langle\rho I_\beta\rangle\,d\mathbf{u}}_{d}\end{aligned} \tag{3.59}$$

Term a evaluates to

$$\frac{\partial}{\partial x_i}\int u_i\tilde{f}_{\mathbf{U}|I_\beta}\,d\mathbf{u} = \frac{\partial}{\partial x_i}\widetilde{\left\langle U_i^{(\beta)}\right\rangle}.$$

Term b evaluates to zero, since the pdf $\tilde{f}_{\mathbf{U}|I_\beta}$ has compact support. Term c evaluates to

$$\int \frac{\tilde{f}_{\mathbf{U}|I_\beta}}{\langle\rho I_\beta|\mathbf{u}\rangle}\langle S_\rho^{(\beta)} \mid \mathbf{u}\rangle\,d\mathbf{u} = \langle S_\rho^{(\beta)}\rangle.$$

Term d evaluates to

$$\int \tilde{f}_{\mathbf{U}|I_\beta}\frac{D}{Dt}\ln\langle\rho I_\beta\rangle\,d\mathbf{u} = \frac{\tilde{D}^{(\beta)}}{\tilde{D}^{(\beta)}t}\ln\langle\rho I_\beta\rangle.$$

Substituting these simplifications into Eq. (3.59) results in

$$\frac{\partial}{\partial t}\int \tilde{f}_{\mathbf{U}|I_\beta}\,d\mathbf{u} + \frac{\partial}{\partial x_i}\widetilde{\left\langle U_i^{(\beta)}\right\rangle} = \langle S_\rho^{(\beta)}\rangle - \frac{\tilde{D}^{(\beta)}}{\tilde{D}^{(\beta)}t}\ln\langle\rho I_\beta\rangle. \tag{3.60}$$

The phasic mean mass conservation, obtained by integrating Eq. (3.57) over $\mathbf{u}$ space, is

$$\frac{\tilde{D}^{(\beta)}}{\tilde{D}^{(\beta)}t}\ln\langle\rho I_\beta\rangle + \frac{\partial}{\partial x_i}\widetilde{\left\langle U_i^{(\beta)}\right\rangle} = \langle S_\rho^{(\beta)}\rangle.$$

Thus, Eq. (3.60) shows that the source term on the right hand side involving the material derivative of $\ln\langle\rho I_\beta\rangle$ ensures that $\tilde{f}_{\mathbf{U}|I_\beta}$ retains its normalization property for all time.

A note on the mean velocities in the EE representation

In the statistical representation of variable density two–phase flows, one can define a density–weighted phasic mean velocity as

$$\widetilde{\left\langle \mathbf{U}^{(\beta)} \right\rangle} = \frac{1}{\langle \rho I_\beta \rangle} \int \mathbf{u}\, \mathcal{F}_{\mathbf{U}|I_\beta}\, d\mathbf{u} = \frac{\langle \rho I_\beta \mathbf{U} \rangle}{\langle \rho I_\beta \rangle} \tag{3.61}$$

and a density–weighted mixture mean velocity as

$$\widetilde{\left\langle \mathbf{U}^{(m)} \right\rangle} = \frac{1}{\langle \rho \rangle} \left(\int \mathbf{u} \mathcal{F}_{\mathbf{U}|I_f} d\mathbf{u} + \int \mathbf{u} \mathcal{F}_{\mathbf{U}|I_d} d\mathbf{u} \right) \tag{3.62}$$

$$= \frac{1}{\langle \rho \rangle} \left[\langle \rho I_f \mathbf{U} \rangle + (\langle \rho I_f \mathbf{U} \rangle] \right, \tag{3.63}$$

where

$$\langle \rho \rangle = \langle \rho I_f \rangle + \langle \rho I_d \rangle \tag{3.64}$$

$$= \langle \rho | I_f = 1 \rangle\, \alpha_f + \langle \rho | I_d = 1 \rangle\, \alpha_d \tag{3.65}$$

is the mixture density.

We can gain insight into the nature of the above mean velocity fields by forming the mean mass evolution equation by integrating Eq. (3.57) over $\mathbf{u}$ space to obtain

$$\frac{\partial \alpha_\beta \langle \rho | I_\beta = 1 \rangle}{\partial t} + \frac{\partial}{\partial x_i} (\alpha_\beta \langle \rho | I_\beta = 1 \rangle \widetilde{\langle U_i^{(\beta)} \rangle}) = \langle S_\rho^{(\beta)} \rangle, \tag{3.66}$$

where

$$\langle S_\rho^{(\beta)} \rangle = \left\langle \rho \left(U_i - U_i^{(I)} \right) \frac{\partial I_\beta}{\partial x_i} \right\rangle \tag{3.67}$$

is the source term due to interphase mass transfer, and then summing the above equation over $\beta = \{f, d\}$ to obtain

$$\frac{\partial \langle \rho \rangle}{\partial t} + \frac{\partial}{\partial x_i} \left(\langle \rho \rangle \widetilde{\left\langle U_i^{(m)} \right\rangle} \right) = 0. \tag{3.68}$$

In the above development, the relation $\langle \rho I_\beta Q(\mathbf{U}) \rangle = \alpha_\beta \langle \rho Q(\mathbf{U}) | I_\beta = 1 \rangle$ has been used for simplification. The conditioning $I_\beta = 1$ imply that such terms are evaluated in phase β.

Rearranging the above equation shows that

$$\frac{\partial}{\partial x_i} \widetilde{\left\langle U_i^{(m)} \right\rangle} = -\frac{\tilde{D}^{(m)}}{\tilde{D}^{(m)} t} \ln \langle \rho \rangle \,,$$

where $\tilde{D}^{(m)}/\tilde{D}^{(m)}t$ is the material derivative following the mixture mean velocity:

$$\frac{\tilde{D}^{(m)}}{\tilde{D}^{(m)}t} = \frac{\partial}{\partial t} + \widetilde{\left\langle U_i^{(m)} \right\rangle} \frac{\partial}{\partial x_i}.$$

In other words, the mixture mean velocity field is not solenoidal in variable density two–phase flows.

Rearranging Eq. (3.66) result in the following expression for the divergence of the phasic mean velocity field:

$$\frac{\partial}{\partial x_i} \widetilde{\langle U_i^{(\beta)} \rangle} = -\frac{\tilde{D}^{(\beta)}}{\tilde{D}^{(\beta)}t} \ln \alpha_\beta \langle \rho | I_\beta = 1 \rangle + \frac{1}{\alpha_\beta \langle \rho | I_\beta = 1 \rangle} \left\langle \rho \left(U_i - U_i^{(I)} \right) \frac{\partial I_\beta}{\partial x_i} \right\rangle, \tag{3.69}$$

where $\tilde{D}^{(\beta)}/\tilde{D}^{(\beta)}t$ is the material derivative following the phasic mean velocity:

$$\frac{\tilde{D}^{(\beta)}}{\tilde{D}^{(\beta)}t} = \frac{\partial}{\partial t} + \widetilde{\left\langle U_i^{(\beta)} \right\rangle} \frac{\partial}{\partial x_i}.$$

Thus, the phasic mean velocity is also not solenoidal. Moreover, the divergence of the phasic mean velocity field depends on a term that represents the interphase mass transfer.

Interesting simplifications result under assumptions of constant density two–phase flows. Under this assumption,

$$\langle \rho | I_\beta = 1 \rangle = \alpha_\beta \, \rho_\beta$$

where ρ_β is the thermodynamic density of phase β. Since ρ_β is not a function of space or time in this case, the evolution equation for α_β simplifies to

$$\frac{\partial \alpha_\beta}{\partial t} + \frac{\partial}{\partial x_i} (\alpha_\beta \langle U_i^{(\beta)} \rangle) = 0, \tag{3.70}$$

where

$$\langle U_i^{(\beta)} \rangle = \frac{\langle I_\beta U_i \rangle}{\langle I_\beta \rangle} = \widetilde{\langle U_i^{(\beta)} \rangle}.$$

is the unweighted phasic mean velocity. Summing the above equation over the phases results in the observation that the mixture mean velocity field is solenoidal:

$$\nabla \cdot \left\langle \mathbf{U}^{(m)} \right\rangle = 0.$$

However, the phasic mean velocity field is not solenoidal even in the case of constant density two–phase flows:

$$\frac{\partial}{\partial x_i} \widetilde{\langle U_i^{(\beta)} \rangle} = -\frac{D^{(\beta)}}{D^{(\beta)}t} \ln \alpha_\beta, \tag{3.71}$$

where $D^{(\beta)}/D^{(\beta)}t$ is the material derivative following the unweighted phasic mean velocity.

3.4.2 Lagrangian statistical representation

Starting from the Klimontovich fine–grained density Eq. (3.13), and using the droplet evolution equations Eqs. (3.10)–(3.12), an evolution equation for the droplet distribution function $f(\mathbf{x}, \mathbf{v}, r, t)$, also widely known as Williams' spray equation, can be derived (Subramaniam, 2001c):

$$\frac{\partial f}{\partial t} + \frac{\partial}{\partial x_j}[v_j f] + \frac{\partial}{\partial v_j}\left[\langle A_j | \mathbf{x}, \mathbf{v}, r; t\rangle f\right] + \frac{\partial}{\partial r}\left[\langle \Theta | \mathbf{x}, \mathbf{v}, r; t\rangle f\right] = 0. \tag{3.72}$$

For the sake of brevity, a detailed derivation of the ddf evolution equation is not reproduced here and can be found in Subramaniam (2001c). In Eq. (3.130), $\langle \mathbf{A} | \mathbf{x}, \mathbf{v}, r; t\rangle$ is the expected acceleration conditional on the location $\mathbf{x}$, velocity $\mathbf{v}$ and radius r, and $\langle \Theta | \mathbf{x}, \mathbf{v}, r; t\rangle$ is the expected vaporization rate conditional on location, velocity and radius.These quantitites are given as (Subramaniam, 2001c)

$$\langle \mathbf{A} \mid \mathbf{x}, \mathbf{v}, r; t\rangle = \frac{1}{f(\mathbf{x}, \mathbf{v}, r, t)} \left\{ \sum_{k \geq 1} q_k \left\langle \mathbf{A}^{(k)} \middle| \mathbf{x}, \mathbf{v}, r, t) \right\rangle f^{(k)}(\mathbf{x}, \mathbf{v}, r, t) \right\} \tag{3.73}$$

if $f > 0$, and zero otherwise; and

$$\left\langle \Theta \middle| \mathbf{x}, \mathbf{v}, r; t \right\rangle = \frac{1}{f(\mathbf{x}, \mathbf{v}, r, t)} \left\{ \sum_{k \geq 1} q_k \left\langle \Theta^{(k)} \middle| \mathbf{x}, \mathbf{v}, r, t) \right\rangle f^{(k)}(\mathbf{x}, \mathbf{v}, r, t) \right\} \tag{3.74}$$

q if $f > 0$, and zero otherwise. Furthermore, in the above expressions,

$$\left\langle \mathbf{A}^{(k)} \middle| \mathbf{x}, \mathbf{v}, r; t \right\rangle = \frac{1}{f^{(k)}(\mathbf{x}, \mathbf{v}, r, t)} \left\{ \left\langle \sum_{i=1}^{k} \mathbf{A}_{(i)} f_i'(\mathbf{x}, \mathbf{v}, r, t) \right\rangle \right\} \tag{3.75}$$

if $f^{(k)} > 0$, and zero otherwise, and

$$\left\langle \Theta^{(k)} \middle| \mathbf{x}, \mathbf{v}, r; t \right\rangle = \frac{1}{f^{(k)}(\mathbf{x}, \mathbf{v}, r, t)} \left\{ \left\langle \sum_{i=1}^{k} \Theta_{(i)} f_i'(\mathbf{x}, \mathbf{v}, r, t) \right\rangle \right\} \tag{3.76}$$

if $f^{(k)} > 0$, and zero otherwise.

As the above expressions suggest, $\langle \mathbf{A} | \mathbf{x}, \mathbf{v}, r; t\rangle$ is not the acceleration corresponding to a *single* DPE (cf. $\mathbf{A}_{(i)}$ in Eq. (3.75)), but is the expected acceleration contribution at a point $\mathbf{x}$ due to an ensemble of (infinite) realizations of the two–phase flow under consideration. Similarly, $\langle \Theta | \mathbf{x}, \mathbf{v}, r; t\rangle$ is not the vaporization rate corresponding to a single droplet (cf. $\Theta_{(i)}$ in Eq. (3.76)), but is the expected vaporization rate contribution at a point $\mathbf{x}$ due to an ensemble

of (infinite) realizations of the same two–phase flow. Note that there are two intermediate stages of averaging performed on the droplet acceleration and vaporization rate (cf. Eqs. (3.75) and (3.73) for $\mathbf{A}_{(i)}$, and Eqs. (3.76) and (3.74) for $\Theta_{(i)}$). Therefore, it is incorrect to refer to $\langle \mathbf{A}|\mathbf{x},\mathbf{v},r,t\rangle$ and $\langle \Theta|\mathbf{x},\mathbf{v},r,t\rangle$ as the *droplet* acceleration and the *droplet* vaporization rate, respectively, for a general spray.

Using the decomposition $f = n f^c_{\mathbf{V}R}$ and an analogous approach as in Sec.(3.4.1), we can form the transport equation for $f^c_{\mathbf{V}R}$ as (cf. Eq. (66) in Subramaniam (2001c)):

$$\frac{\partial f^c_{\mathbf{V}R}}{\partial t} + \frac{\partial}{\partial x_k} v_k f^c_{\mathbf{V}R} + \frac{\partial}{\partial v_k}[\langle A_k|\mathbf{x},\mathbf{v},r,t\rangle f^c_{\mathbf{V}R}] + \frac{\partial}{\partial r}[\langle \Theta|\mathbf{x},\mathbf{v},r,t\rangle f^c_{\mathbf{V}R}] = -f^c_{\mathbf{V}R}\frac{D}{Dt}\ln n(\mathbf{x},t)$$

Analogous to the EE representation, the source term involving the material derivative of $\ln n$ ensures that $f^c_{\mathbf{V}R}$ retains its normalization property for all time.

Transport equations for the probability densities in the EE and LE statistical representations have now been established. It is now straightforward to derive the governing equations for the mean mass and momentum, as well as second moment equations in each statistical representation from these transport equations.

3.5 Governing Equations for a Two–Phase Flow

3.5.1 Mean mass conservation

3.5.1.1 Random field statistical representation

As noted earlier, integrating Eq. (3.57) over $\mathbf{u}$ space results in the mean mass conservation in each phase:

$$\frac{\partial \alpha_\beta \langle \rho | I_\beta = 1\rangle}{\partial t} + \frac{\partial}{\partial x_i}(\alpha_\beta \langle \rho | I_\beta = 1\rangle \widetilde{\langle U_i^{(\beta)}\rangle}) = \langle S_\rho^{(\beta)}\rangle. \tag{3.77}$$

3.5.1.2 Number–density based Lagrangian approach

If a constant thermodynamic density of the dispersed phase ρ_d is assumed, then the mean mass conservation equation implied by the ddf evolution equation can be obtained using the

following development. Multiplying Eq. (3.130) by $(4/3)\pi r^3\rho_d$ results in

$$\frac{\partial(4/3)\pi r^3\rho_d f}{\partial t}+\frac{\partial}{\partial x_j}[v_j(4/3)\pi r^3\rho_d f]+\frac{\partial}{\partial v_j}\left[(4/3)\pi r^3\rho_d\langle A_j|\mathbf{x},\mathbf{v},r;t\rangle f\right] + \frac{\partial}{\partial r}\left[(4/3)\pi r^3\rho_d\langle\Theta|\mathbf{x},\mathbf{v},r;t\rangle f\right]-(4/3)\pi 3r^2\rho_d\langle\Theta|\mathbf{x},\mathbf{v},r;t\rangle f=0. \tag{3.78}$$

Integrating over $\mathbf{v}, r_+$ space

$$\underbrace{\frac{\partial}{\partial t}\int_{\mathbf{v},r_+}(4/3)\pi r^3\rho_d f d\mathbf{v}dr}_{a}+\underbrace{\frac{\partial}{\partial x_j}\int_{\mathbf{v},r_+}v_j(4/3)\pi r^3\rho_d f d\mathbf{v}dr}_{b} + \underbrace{\frac{\partial}{\partial v_j}\int_{\mathbf{v},r_+}(4/3)\pi r^3\rho_d\langle A_j|\mathbf{x},\mathbf{v},r;t\rangle f d\mathbf{v}dr}_{c}+\underbrace{\int_{\mathbf{v},r_+}\frac{\partial}{\partial r}\left[(4/3)\pi r^3\rho_d\langle\Theta|\mathbf{x},\mathbf{v},r;t\rangle f\right]d\mathbf{v}dr}_{d} - \underbrace{\int_{\mathbf{v},r_+}(4/3)\pi 3r^2\rho_d\langle\Theta|\mathbf{x},\mathbf{v},r;t\rangle f d\mathbf{v}dr}_{e}=0. \tag{3.79}$$

Using the decomposition, $f=nf^c_{\mathbf{V}R}$ and performing the integration, we get:

Term a

$$\frac{\partial}{\partial t}\int_{\mathbf{v},r_+}(4/3)\pi r^3\rho_d f d\mathbf{v}dr=\frac{\partial}{\partial t}\left[\frac{4}{3}\pi\langle R^3\rangle\rho_d\ n\right]$$

Term b:

$$\begin{aligned}\frac{\partial}{\partial x_j}\int_{\mathbf{v},r_+}v_j(4/3)\pi r^3\rho_d f d\mathbf{v}dr&=\frac{4}{3}\pi\rho_d\frac{\partial}{\partial x_j}\left[n\int_{r_+}r^3\left(\int_{\mathbf{v}}v_j f^c_{\mathbf{V}|R}d\mathbf{v}\right)f^c_R dr\right]\\&=\frac{4}{3}\pi\rho_d\frac{\partial}{\partial x_k}\left[n\int_{r_+}r^3\langle V_k|R\rangle f^c_R(r)dr\right]\\&=\frac{\partial}{\partial x_j}\left[\frac{4}{3}\pi\langle R^3\rangle\langle\widetilde{V}_j\rangle\rho_d\ n\right],\end{aligned}$$

where $\Omega=\Theta/R$ and the volume–weighted average of any smooth function $Q(\mathbf{v},r)$ is defined as:

$$\langle\widetilde{Q}\rangle\equiv\frac{\langle R^3Q\rangle}{\langle R^3\rangle}.$$

Term c:

$$\frac{\partial}{\partial v_j}\int_{\mathbf{v},r_+}(4/3)\pi r^3\rho_d\langle A_j|\mathbf{x},\mathbf{v},r;t\rangle f d\mathbf{v}dr=0.$$

Term d:

$$\begin{aligned}
\int_{\mathbf{v},r_+} \frac{\partial}{\partial r}\left[(4/3)\pi r^3 \rho_d \langle \Theta|\mathbf{x},\mathbf{v},r;t\rangle f\right] d\mathbf{v}dr &= \int_{\mathbf{v},r_+} \frac{\partial}{\partial r}\left[(4/3)\pi r^3 \rho_d \langle \Theta|\mathbf{x},\mathbf{v},r;t\rangle n f^c_{\mathbf{V}R}\right] d\mathbf{v}dr \\
&= (4/3)\pi\rho_d n \int_{\mathbf{v},r_+} \frac{\partial}{\partial r}\left[r^3 \langle \Theta|\mathbf{x},\mathbf{v},r;t\rangle f^c_{\mathbf{V}|R} f^c_R\right] d\mathbf{v}dr \\
&= (4/3)\pi\rho_d n \int_{r_+} \frac{\partial}{\partial r}\left[r^3 \int_{\mathbf{v}} \langle \Theta|\mathbf{x},\mathbf{v},r;t\rangle f^c_{\mathbf{V}|R} d\mathbf{v} f^c_R\right] dr \\
&= (4/3)\pi\rho_d n \int_{r_+} \frac{\partial}{\partial r}\left[r^3 \langle \Theta|\mathbf{x},r;t\rangle f^c_R\right] dr \\
&= (4/3)\pi\rho_d n \int_{r_+} \frac{\partial}{\partial r}\left[\langle \Theta R^3|\mathbf{x},r;t\rangle f^c_R\right] dr \\
&= -(4/3)\pi\rho_d n \langle R^3\rangle \langle \widetilde{\Theta}|\mathbf{x},r=0_+;t\rangle f^c_R(r=0_+;t).
\end{aligned}$$

Term e:

$$\begin{aligned}
\int_{\mathbf{v},r_+} (4/3)\pi 3 r^2 \rho_d \langle \Theta|\mathbf{x},\mathbf{v},r;t\rangle f d\mathbf{v}dr &= \int_{\mathbf{v},r_+} (4/3)\pi 3 r^3 \rho_d \left\langle \frac{\Theta}{R}|\mathbf{x},\mathbf{v},r;t \right\rangle f d\mathbf{v}dr \\
&= \int_{\mathbf{v},r_+} (4/3)\pi 3 \rho_d \left\langle R^3\Omega|\mathbf{x},\mathbf{v},r;t\right\rangle f d\mathbf{v}dr \\
&= (4/3)\pi 3 \rho_d \langle R^3\rangle \left\langle \widetilde{\Omega} \mid \mathbf{x};t\right\rangle
\end{aligned}$$

Thus, the mean mass evolution equation in the dispersed phase using the LE statistical representation is

$$\begin{aligned}
&\frac{\partial}{\partial t}\left[\frac{4}{3}\pi\langle R^3\rangle \rho_d\, n\right] + \frac{\partial}{\partial x_k}\left[\frac{4}{3}\pi\langle R^3\rangle\langle \widetilde{V}_k\rangle \rho_d\, n\right] = \\
&\qquad n\frac{4}{3}\pi\rho_d\, \langle R^3\rangle \left\{ 3\langle\widetilde{\Omega} \mid \mathbf{x};t\rangle + \langle \widetilde{\Theta} \mid \mathbf{x}, r=0_+;t\rangle f^c_R(r=0_+ \mid \mathbf{x};t)\right\}, \qquad (3.80)
\end{aligned}$$

The source term on the right hand side of Eq. (3.80) contains two parts. One part corresponds to a loss of mean mass due to evaporation. The other part represents the depletion of number density due to a flux of droplets across the $r = 0_+$ boundary, which corresponds to the smallest radius below which a drop is considered evaporated.

3.5.1.3 Correspondence for locally homogeneous flows

For statistically homogeneous number density (but inhomogeneous radius pdf), we have shown that

$$\alpha_d(\mathbf{x},t) = n(t)\frac{4}{3}\pi\langle R^3(\mathbf{x},t)\rangle \tag{3.81}$$

$$f_R^E(r;\mathbf{x},t) = r^3 f_R^c(r;\mathbf{x},t)/\langle R^3(\mathbf{x},t)\rangle, \tag{3.82}$$

where the last equality holds only for fluid–rigid particle two–phase flows, or for two–phase flows with fluid dispersed phase elements where we neglect internal fluid motion of the fluid DPE. Using the first of the above relations, Eq. (3.80) can be written as

$$\frac{\partial}{\partial t}\left[\alpha_d\ \rho_d\ \right] + \frac{\partial}{\partial x_k}\left[\alpha_d\ \rho_d\ \langle\widetilde{V}_k\rangle\right] = \alpha_d\ \rho_d\ 3\langle\widetilde{\Omega}\mid\mathbf{x};t\rangle + \alpha_d\ \rho_d\ \langle\widetilde{\Theta}\mid\mathbf{x},r=0_+;t\rangle f_R^c(r=0_+\mid\mathbf{x};t)\ . \tag{3.83}$$

If Eq. (3.82) holds, then it is true that

$$\widetilde{\langle\mathbf{U}^\beta\rangle} = \widetilde{\langle\mathbf{V}\rangle}.$$

Then Eq. (3.83) can be directly compared with the constant thermodynamic density version of the phase mass conservation equation arising from the random–field approach written for the dispersed phase ($\beta = d$):

$$\frac{\partial}{\partial t}[\alpha_d\rho_d] + \frac{\partial}{\partial x_k}[\alpha_d\rho_d\widetilde{\langle U_i^{(\beta)}\rangle}] = \langle S_\rho^{(d)}\rangle, \tag{3.84}$$

thereby leading to the correspondence of the terms (Subramaniam, 2001a):

$$\langle S_\rho^{(d)}\rangle \Longleftrightarrow \alpha_d\ \rho_d\ \left\{3\langle\widetilde{\Omega}\mid\mathbf{x};t\rangle + \langle\widetilde{\Theta}\mid\mathbf{x},r=0_+;t\rangle f_R^c(r=0_+\mid\mathbf{x};t)\ \right\}.$$

If the number density retains spatial homogeneity as the flow evolves, then the above correspondence becomes an equality. However, if the number density develops spatial inhomogeneities as the flow evolves, then relation given by Eq. (3.81) no longer holds, and the correspondence given above should be treated only as an approximation.

3.5.2 Mean momentum conservation

3.5.2.1 Random field statistical representation

Multiplying Eq. (3.57) by u_i and integrating over $\mathbf{u}$ space results in

$$\frac{\partial \langle \rho I_\beta \rangle \widetilde{\langle U_i^{(\beta)} \rangle}}{\partial t} + \frac{\partial}{\partial x_j} \langle \rho I_\beta \rangle \widetilde{\langle U_i^{(\beta)} U_j^{(\beta)} \rangle} = \left\langle \rho I_\beta \frac{DU_i}{Dt} \right\rangle + \left\langle \rho U_i \left(U_j - U_j^{(I)} \right) \frac{\partial I_\beta}{\partial x_j} \right\rangle \tag{3.85}$$

If the fluctuation with respect to the Fàvre –averaged phasic velocity is defined as $\mathbf{u}''^{(\beta)} = \mathbf{U} - \widetilde{\langle \mathbf{U}^{(\beta)} \rangle}$ [8], then the above expression can be simplified as

$$\begin{aligned} \frac{\partial \langle \rho I_\beta \rangle \widetilde{\langle U_i^{(\beta)} \rangle}}{\partial t} + \frac{\partial}{\partial x_j} \langle I_\beta \rho \rangle \widetilde{\langle U_i^{(\beta)} \rangle} \widetilde{\langle U_j^{(\beta)} \rangle} &= -\frac{\partial}{\partial x_j} \left\langle I_\beta \rho \; u_i''^{(\beta)} u_j''^{(\beta)} \right\rangle \\ &+ \left\langle \rho I_\beta \frac{DU_i}{Dt} \right\rangle + \left\langle \rho U_i \left(U_j - U_j^{(I)} \right) \frac{\partial I_\beta}{\partial x_j} \right\rangle \end{aligned} \tag{3.86}$$

The above mean momentum equation is identical to that derived using the indicator function formalism of Drew (1983).

The second term on the right hand side of Eq. (3.86) essentially evaluates to the divergence of the stress tensor evaluated in the βth phase:

$$\left\langle \rho I_\beta \frac{DU_i}{Dt} \right\rangle = \left\langle I_\beta \frac{\partial \tau_{ji}}{\partial x_j} \right\rangle .$$

The mean momentum equations as given by Eq. (3.86) are not Galilean invariant (GI) forms. One can rewrite Eq. (3.86) as:

$$\begin{aligned} &\frac{\partial}{\partial t} [\alpha_\beta \langle \rho \mid I_\beta = 1 \rangle \widetilde{\langle U_i^{(\beta)} \rangle}] + \frac{\partial}{\partial x_j} [\alpha_\beta \langle \rho \mid I_\beta = 1 \rangle \widetilde{\langle U_i^{(\beta)} \rangle} \widetilde{\langle U_j^{(\beta)} \rangle}] \\ &= \; -\frac{\partial}{\partial x_j} [\alpha_\beta \langle \rho \mid I_\beta = 1 \rangle \widetilde{R}_{ij}^{(\beta)}] + \left\langle \frac{\partial}{\partial x_j} (I_\beta \tau_{ji}) \right\rangle + \langle I_\beta \rho b_j \rangle + \langle S_{Mi}^{(\beta)} \rangle \end{aligned} \tag{3.87}$$

where

$$\widetilde{R}_{ij}^{(\beta)} \equiv \frac{\left\langle I_\beta \rho \; u_i''^{(\beta)} u_j''^{(\beta)} \right\rangle}{\langle I_\beta \rho \; \rangle}$$

is the Reynolds stress in the βth phase. We do not assume Gauss rule to hold for the second term on the right hand side of Eq. (3.87), i.e., the expectation and derivative are not assumed to commute.

[8] The reader is cautioned against confusing the fluctuation $\mathbf{u}''^{(\beta)}$ with the sample space variable $\mathbf{u}$ corresponding to the random variable $\mathbf{U}$. The choice of the fluctuating velocity is discussed in Sec. 3.5.3.

It is convenient to decompose the interfacial momentum source term $\langle \mathbf{S}_M^{(\beta)} \rangle$ into two part, one attributable to interphase mass transfer arising from phase change $\langle \mathbf{S}_M^{(\beta)(PC)} \rangle$, and the other to the interfacial stress $\langle \mathbf{S}_M^{(\beta)(IS)} \rangle$, that is nonzero even in the absence of interphase mass transfer, and these are defined as (Subramaniam, 2001a):

$$\langle S_{Mi}^{(\beta)(PC)} \rangle \equiv \left\langle \rho U_i \left(U_j - U_j^{(I)} \right) \frac{\partial I_\beta}{\partial x_j} \right\rangle \tag{3.88}$$

$$\langle S_{Mi}^{(\beta)(IS)} \rangle \equiv - \left\langle \tau_{ji} \frac{\partial I_\beta}{\partial x_j} \right\rangle . \tag{3.89}$$

The one arising from interfacial stress $\langle S_{Mj}^{(\beta)(IS)} \rangle$ is in GI form, whereas $\langle S_{Mj}^{(\beta)(PC)} \rangle$, the term arising from interfacial mass transfer, is not in GI form.

Substituting Eq. (3.77) into Eq. (3.86) results in:

$$\begin{aligned} &\alpha_\beta \langle \rho \mid I_\beta = 1 \rangle \frac{\tilde{D}_\beta \widetilde{\langle U_j^{(\beta)} \rangle}}{\tilde{D}_\beta t} + \frac{\partial}{\partial x_i} [\alpha_\beta \langle \rho \mid I_\beta = 1 \rangle \widetilde{R}_{ij}^{(\beta)}] - \left\langle \frac{\partial}{\partial x_i} (I_\beta \tau_{ij}) \right\rangle - \langle I_\beta \rho b_j \rangle \\ &= \langle S_{Mj}^{(\beta)(IS)} \rangle + \left\{ \langle S_{Mj}^{(\beta)(PC)} \rangle - \langle \widetilde{U}_j^{(\beta)} \rangle \langle S_\rho^{(\beta)} \rangle \right\} \end{aligned} \tag{3.90}$$

Each term on the left hand side of Eq. (3.90) is in GI form, and so is $\langle S_{Mj}^{(\beta)(IS)} \rangle$, therefore it follows that the term $\left\{ \langle S_{Mj}^{(\beta)(PC)} \rangle - \langle \widetilde{U}_j^{(\beta)} \rangle \langle S_\rho^{(\beta)} \rangle \right\}$ on the right hand side of Eq. (3.90) should also be in GI form. Therefore, it is this term that should be modeled in the mean momentum equation for two–phase flows with interphase mass transfer.

Evolution of mixture mean velocity

One can derive the evolution of the mixture mean velocity as defined in Eq. (3.63) by summing Eq. (3.87) over all β phases as

$$\begin{aligned} &\underbrace{\frac{\partial}{\partial t} [\sum_\beta \alpha_\beta \langle \rho \mid I_\beta = 1 \rangle \widetilde{\langle U_i^{(\beta)} \rangle}]}_{a} + \underbrace{\frac{\partial}{\partial x_j} [\sum_\beta \alpha_\beta \langle \rho \mid I_\beta = 1 \rangle \widetilde{\langle U_i^{(\beta)} \rangle} \widetilde{\langle U_j^{(\beta)} \rangle}]}_{b} \\ &= \underbrace{- \frac{\partial}{\partial x_j} [\sum_\beta \alpha_\beta \langle \rho \mid I_\beta = 1 \rangle \widetilde{R}_{ij}^{(\beta)}]}_{c} + \underbrace{\sum_\beta \left\langle \frac{\partial}{\partial x_j} (I_\beta \tau_{ji}) \right\rangle}_{d} + \underbrace{\sum_\beta \langle I_\beta \rho b_j \rangle}_{e} + \underbrace{\sum_\beta \langle S_{Mi}^{(\beta)} \rangle}_{f} \end{aligned} \tag{3.91}$$

Term a simplifies to

$$\frac{\partial}{\partial t} [\sum_\beta \alpha_\beta \langle \rho \mid I_\beta = 1 \rangle \widetilde{\langle U_i^{(\beta)} \rangle}] = \frac{\partial}{\partial t} \langle \rho \rangle \left\langle U_i^{(m)} \right\rangle .$$

In order to simplify term b, we first define a velocity difference between the phasic mean velocity and the mixture mean velocity as

$$\widetilde{\langle V_i^{(\beta)}\rangle} = \widetilde{\langle U_i^{(\beta)}\rangle} - \widetilde{\langle U_i^{(m)}\rangle}. \tag{3.92}$$

The tilde on $\langle V_i^{(\beta)}\rangle$ reminds us that this velocity is derived from density–weighted mean velocities. Using this definition, the product $\widetilde{\langle U_i^{(\beta)}\rangle}\widetilde{\langle U_j^{(\beta)}\rangle}$ can be re–expressed as

$$\widetilde{\langle U_i^{(\beta)}\rangle}\widetilde{\langle U_j^{(\beta)}\rangle} = (\widetilde{\langle V_i^{(\beta)}\rangle} + \widetilde{\langle U_i^{(m)}\rangle})(\widetilde{\langle V_j^{(\beta)}\rangle} + \widetilde{\langle U_j^{(m)}\rangle}) \tag{3.93}$$

$$= \widetilde{\langle V_i^{(\beta)}\rangle}\widetilde{\langle V_j^{(\beta)}\rangle} + \widetilde{\langle U_i^{(m)}\rangle}\widetilde{\langle V_j^{(\beta)}\rangle} + \widetilde{\langle U_i^{(m)}\rangle}\widetilde{\langle V_j^{(\beta)}\rangle} + \widetilde{\langle U_i^{(m)}\rangle}\widetilde{\langle U_j^{(m)}\rangle} \tag{3.94}$$

Taking the summation over $\beta = \{f, d\}$ of $\alpha_\beta\langle\rho|I_\beta = 1\rangle$ times the right hand side of the above expression is

$$\sum_\beta \alpha_\beta\langle\rho|I_\beta = 1\rangle\widetilde{\langle U_i^{(\beta)}\rangle}\widetilde{\langle U_j^{(\beta)}\rangle} = \sum_\beta \Bigg\{\alpha_\beta\langle\rho|I_\beta = 1\rangle \Bigg(\widetilde{\langle V_i^{(\beta)}\rangle}\widetilde{\langle V_j^{(\beta)}\rangle} \tag{3.95}$$

$$+\widetilde{\langle U_i^{(m)}\rangle}\widetilde{\langle V_j^{(\beta)}\rangle} + \widetilde{\langle U_i^{(m)}\rangle}\widetilde{\langle V_j^{(\beta)}\rangle} + \widetilde{\langle U_i^{(m)}\rangle}\widetilde{\langle U_j^{(m)}\rangle}\Bigg)\Bigg\} \tag{3.96}$$

One can show that

$$\sum_\beta \left\{\alpha_\beta\langle\rho|I_\beta = 1\rangle \left(\widetilde{\langle U_i^{(m)}\rangle}\widetilde{\langle V_j^{(\beta)}\rangle}\right)\right\} = \widetilde{\langle U_i^{(m)}\rangle}\sum_\beta \left\{\alpha_\beta\langle\rho|I_\beta = 1\rangle \left(\widetilde{\langle V_j^{(\beta)}\rangle}\right)\right\} = 0,$$

which follows from Eq. (3.92).x

Thus, term b simplifies to

$$\frac{\partial}{\partial x_j}[\sum_\beta \alpha_\beta\langle\rho \mid I_\beta = 1\rangle\widetilde{\langle U_i^{(\beta)}\rangle}\widetilde{\langle U_j^{(\beta)}\rangle}] = \frac{\partial}{\partial x_j}\sum_\beta \alpha_\beta \langle\rho|I_\beta = 1\rangle \left\{\widetilde{\langle U_i^{(m)}\rangle}\widetilde{\langle U_j^{(m)}\rangle} + \widetilde{\langle V_i^{(\beta)}\rangle}\widetilde{\langle V_j^{(\beta)}\rangle}\right\}.$$

Term c can be combined with term b. To simplifiy term d we need to make the assumption that Gauss' rule, i.e., the expectation and derivative operator commute. This is a very significant assumption since one can show using simple examples that, for instance, $\langle\partial I_\beta/\partial x_i\rangle \neq \partial\alpha_\beta/\partial x_i$ in general Aplin and Subramaniam (2003). However, under assumptions of local homogeneity and for conditions under which the dispersed phase is entirely inside the volume over which local homogeneity is assumed, Gauss' rule can hold.

Thus, invoking the Newtonian constitutive relation

$$\begin{aligned}\sum_\beta \frac{\partial}{\partial x_j}\langle I_\beta \tau_{ji}\rangle &= \sum_\beta \frac{\partial}{\partial x_j}\langle I_\beta(-p\delta_{ji} + \lambda\left(\frac{\partial U_k}{\partial x_k}\right)\delta_{ji} + 2\mu S_{ji})\rangle \\ &= -\frac{\partial}{\partial x_j}\sum_\beta \langle I_\beta p\rangle + \frac{\partial}{\partial x_j}\sum_\beta \left\langle \lambda I_\beta \left(\frac{\partial U_k}{\partial x_k}\right)\delta_{ji} + 2\mu I_\beta S_{ji}\right\rangle \\ &= -\frac{\partial}{\partial x_j}\langle p^{(m)}\rangle + \lambda\frac{\partial}{\partial x_i}\sum_\beta \left\langle I_\beta\left(\frac{\partial U_k}{\partial x_k}\right)\right\rangle + 2\mu\frac{\partial}{\partial x_j}\langle S_{ji}^{(m)}\rangle, \end{aligned} \tag{3.97}$$

where $\langle p^{(m)}\rangle$ is the mean mixture pressure defined as

$$\langle p^{(m)}\rangle = \langle I_f p\rangle + \langle I_f p\rangle$$

and

$$\langle S_{ji}^{(m)}\rangle = \langle I_f S_{ji}\rangle + \langle I_d S_{ji}\rangle$$

is the mean deviatoric part of the Newtonian stress tensor. In the above development, λ is the bulk viscosity coefficient which is related to the shear viscosity through $\lambda = (2/3)\mu$.

For a constant body force, which is usually the case, term e simplifies to $\langle\rho\rangle b_j$. Term f is summation of the interphase momentum transfer over the two phases, and since the interphase momentum transfer is equal and opposite in a two–phase flow,

$$\sum_\beta \langle S_{Mi}^{(\beta)}\rangle = 0. \tag{3.98}$$

Substituting the above simplifications into Eq. (3.91), and rearranging we get

$$\begin{aligned} -\frac{\partial}{\partial x_i}\langle p^{(m)}\rangle &= \frac{\partial}{\partial x_j}\sum_\beta \alpha_\beta \langle\rho|I_\beta = 1\rangle \widetilde{\langle U_i^{(m)}\rangle}\widetilde{\langle U_j^{(m)}\rangle} - \lambda\frac{\partial}{\partial x_i}\sum_\beta\left\langle I_\beta\left(\frac{\partial U_k}{\partial x_k}\right)\right\rangle - 2\mu\frac{\partial}{\partial x_j}\langle S_{ji}^{(m)}\rangle \\ &+ \frac{\partial}{\partial x_j}\sum_\beta \alpha_\beta\langle\rho|I_\beta = 1\rangle\left\{\widetilde{\langle V_i^{(\beta)}\rangle}\widetilde{\langle V_j^{(\beta)}\rangle} + \widetilde{R}_{ij}^{(\beta)}\right\} - \frac{\partial}{\partial t}\langle\rho\rangle\left\langle U_i^{(m)}\right\rangle - \langle\rho\rangle b_i. \end{aligned} \tag{3.99}$$

Taking the divergence of both sides of the above equation results in

$$\begin{aligned} -\frac{\partial^2}{\partial x_i\partial x_i}\langle p^{(m)}\rangle &= \frac{\partial^2}{\partial x_i\partial x_j}\sum_\beta \alpha_\beta\langle\rho|I_\beta = 1\rangle\widetilde{\langle U_i^{(m)}\rangle}\widetilde{\langle U_j^{(m)}\rangle} - \lambda\frac{\partial^2}{\partial x_i x_j}\sum_\beta\left\langle I_\beta\left(\frac{\partial U_k}{\partial x_k}\right)\right\rangle \\ &- 2\mu\frac{\partial^2}{\partial x_i\partial x_j}\langle S_{ji}^{(m)}\rangle + \frac{\partial^2}{\partial x_i\partial x_j}\sum_\beta\alpha_\beta\langle\rho|I_\beta = 1\rangle\left\{\widetilde{\langle V_i^{(\beta)}\rangle}\widetilde{\langle V_j^{(\beta)}\rangle} + \widetilde{R}_{ij}^{(\beta)}\right\} \\ &- \frac{\partial}{\partial t}\left(\frac{\partial}{\partial x_i}\langle\rho\rangle\left\langle U_i^{(m)}\right\rangle\right) - b_i\frac{\partial}{\partial x_i}\langle\rho\rangle, \end{aligned} \tag{3.100}$$

which is the Poisson equation for the mean mixture pressure in a two–phase variable density flow.

3.5.2.2 Number–density based Lagrangian approach

The mean momentum conservation equation implied by the ddf evolution equation Eq. (3.130) is obtained by multiplying Eq. (3.130) by $(4/3)\pi r^3 \rho_d v_j$ and integrating over all $[\,\mathbf{v}, r_+]$:

$$\frac{\partial}{\partial t}[n\frac{4}{3}\pi\rho_d\langle R^3\rangle\langle\widetilde{V}_j\rangle] + \frac{\partial}{\partial x_k}[n\frac{4}{3}\pi\rho_d\ \langle R^3\rangle\langle\widetilde{V_jV_k}\rangle] = n\frac{4}{3}\pi\rho_d\ \langle R^3\rangle\langle\widetilde{A}_j \mid \mathbf{x};t\rangle + n\frac{4}{3}\pi\rho_d\ \langle R^3\rangle\left\{3\langle\widetilde{V_j\Omega} \mid \mathbf{x};t\rangle + \langle\widetilde{V_j\Theta} \mid \mathbf{x}, r=0_+;t\rangle f_R^c(r=0_+ \mid \mathbf{x};t)\ \right\}. \tag{3.101}$$

where mass–weighted averages have been used as in Eq. (3.80). The last term on the right hand side of the above equation corresponds to a loss of mean momentum due to evaporation, and the depletion of mean momentum due to a flux of droplets across the $r = 0_+$ boundary.

Substituting Eq. (3.80) into the Eq. (3.101) results in:

$$\begin{aligned} n\frac{4}{3}\pi\rho_d\langle R^3\rangle\left\{\frac{\partial\langle\widetilde{V}_j\rangle}{\partial t} + \widetilde{V}_k\frac{\partial\langle\widetilde{V}_j\rangle}{\partial x_k}\right\} = \\ n\frac{4}{3}\pi\rho_d\ \langle R^3\rangle\langle\widetilde{A}_j \mid \mathbf{x};t\rangle - \frac{\partial}{\partial x_k}\left[n\frac{4}{3}\pi\rho_d\ \langle R^3\rangle\left\langle\widetilde{v_j''v_k''}\right\rangle\right] \\ + n\frac{4}{3}\pi\rho_d\ \langle R^3\rangle\left\{3\langle\widetilde{V_j\Omega} \mid \mathbf{x};t\rangle + \langle\widetilde{V_j\Theta} \mid \mathbf{x}, r=0_+;t\rangle f_R^c(r=0_+ \mid \mathbf{x};t)\right\} \\ - n\frac{4}{3}\pi\rho_d\ \langle R^3\rangle\left\{3\langle\widetilde{V}_j\rangle\langle\widetilde{\Omega} \mid \mathbf{x};t\rangle + \langle\widetilde{V}_j\rangle\langle\widetilde{\Theta} \mid \mathbf{x}, r=0_+;t\rangle f_R^c(r=0_+ \mid \mathbf{x};t)\right\}. \end{aligned} \tag{3.102}$$

where

$$\left\langle\widetilde{v_j''v_k''}\right\rangle \equiv \int_{[\,\mathbf{v},r_+]}\left(v_j - \langle\widetilde{V}_j\rangle\right)\left(v_k - \langle\widetilde{V}_j\rangle\right)\frac{r^3 f_{\mathbf{V}R}^c(\mathbf{v}, r \mid \mathbf{x};t)}{\langle R^3(\mathbf{x},t)\rangle}d\mathbf{v}\,dr,$$

The following are the GI combinations of unclosed terms are:

$$\left\{\langle\widetilde{V_j\Omega} \mid \mathbf{x};t\rangle - \langle\widetilde{V}_j\rangle\langle\widetilde{\Omega} \mid \mathbf{x};t\rangle\right\},$$

and

$$\left\{\langle\widetilde{V_j\Theta} \mid \mathbf{x}, r=0_+;t\rangle - \langle\widetilde{V}_j\rangle\langle\widetilde{\Theta} \mid \mathbf{x}, r=0_+;t\rangle\right\}.$$

Particle method solutions to the ddf equation that model $\langle\mathbf{A}|\mathbf{x},\mathbf{v},r;t\rangle$ and $\langle\Theta|\mathbf{x},\mathbf{v},r;t\rangle$ automatically guarantee GI modeling of the above terms in the mean momentum equation.

3.5.2.3 Correspondence for locally homogeneous flows

Under the assumptions of statistical homogeneity of $n(\mathbf{x};t)$ and $f^c_{\mathbf{V}R}(\mathbf{v},r \mid \mathbf{x};t)$, and spherical DPE's, we can substitute $\alpha_d = (4/3)\pi\langle R^3\rangle n$ into Eq. (3.102) to obtain:

$$\begin{aligned}\alpha_d\ \rho_d\ \left[\frac{\partial\langle\widetilde{V}_j\rangle}{\partial t} + \langle\widetilde{V}_k\rangle\frac{\partial\langle\widetilde{V}_j\rangle}{\partial x_k}\right] &= \alpha_d\ \rho_d\ \langle\widetilde{A}_j \mid \mathbf{x};t\rangle - \frac{\partial}{\partial x_k}\left[\alpha_d\ \rho_d\ \left\langle\widetilde{v''_j v''_k}\right\rangle\right] \\ &+ \alpha_d\ \rho_d\ \left\{3\langle\widetilde{V_j\Omega} \mid \mathbf{x};t\rangle + \langle\widetilde{V_j\Theta} \mid \mathbf{x},r=0_+;t\rangle f^c_R(r=0_+ \mid \mathbf{x};t)\ \right\} \\ &- \alpha_d\ \rho_d\ \left\{3\langle\widetilde{V}_j\rangle\langle\widetilde{\Omega} \mid \mathbf{x};t\rangle + \langle\widetilde{V}_j\rangle\langle\widetilde{\Theta} \mid \mathbf{x},r=0_+;t\rangle f^c_R(r=0_+ \mid \mathbf{x};t)\right\}. \qquad (3.103)\end{aligned}$$

This equation can be directly compared with the constant thermodynamic density version of the phase mass conservation equation arising from the random–field approach written for the dispersed phase ($\beta = d$):

$$\alpha_d\rho_d\frac{\tilde{D}_d\widetilde{\langle U^{(d)}_j\rangle}}{\tilde{D}_\beta t} = \langle S^{(d)(IS)}_{Mj}\rangle + \langle I_d\rho b_j\rangle - \frac{\partial}{\partial x_i}[\alpha_d\rho_d\widetilde{R^{(d)}_{ij}}] + \left\{\langle S^{(d)(PC)}_{Mj}\rangle - \widetilde{\langle U^{(d)}_j\rangle}\langle S^{(d)}_\rho\rangle\right\}, \qquad (3.104)$$

where now the stress term drops out because the velocity field is uniform in the DPE (it being a rigid particle, or a fluid DPE where internal flow is assumed uniform).

A comparison of Eqs. (3.103) and (3.104) leads to the correspondence of the terms ($\beta = d$) (Subramaniam, 2001a):

$$\begin{aligned}\langle S^{(\beta)(IS)}_{Mj}\rangle + \langle I_\beta\rho b_j\rangle &\Longleftrightarrow \alpha_d\ \rho_d\ \langle\widetilde{A}_j\rangle \\ \widetilde{R}^{(\beta)}_{ij} &\Longleftrightarrow \left\langle\widetilde{v''_j v''_k}\right\rangle \\ \langle S^{(\beta)(PC)}_{Mj}\rangle &\Longleftrightarrow \alpha_d\ \rho_d\ \left\{3\langle\widetilde{V_j\Omega} \mid \mathbf{x};t\rangle + \langle\widetilde{V_j\Theta} \mid \mathbf{x},r=0_+;t\rangle f^c_R(r=0_+ \mid \mathbf{x};t)\right\} \\ -\langle\widetilde{U}^{(\beta)}_j\rangle\langle S^{(\beta)}_\rho\rangle &\Longleftrightarrow -\alpha_d\ \rho_d\ \left\{3\langle\widetilde{V}_j\rangle\langle\widetilde{\Omega} \mid \mathbf{x};t\rangle + \langle\widetilde{V}_j\rangle\langle\widetilde{\Theta} \mid \mathbf{x},r=0_+;t\rangle f^c_R(r=0_+ \mid \mathbf{x};t)\right\}\end{aligned}$$

If the number density retains spatial homogeneity as the flow evolves, then the above correspondence becomes an equality. However, if the number density develops spatial inhomogeneities as the flow evolves, then relation given by Eq. (3.81) no longer holds, and the correspondence given above should be treated only as an approximation.

3.5.3 Second moment equations

3.5.3.1 Random–field based Eulerian approach

Prior to deriving second–moment evolution equations for velocity we need to define the fluctuating velocity field. In single–phase turbulent flow there are two ways in which velocity fluctuations can be defined: (1) the fluctuation defined with respect to the mean velocity, (2) the Fàvre fluctuation velocity defined with respect to the density–weighted mean. The two fluctuating velocity fields are identical for constant density flows, but for variable density flows the equations are considerably simpler when written in terms of Fàvre fluctuating velocities and associated second moments (Jones, 1980; Libby and Williams, 1993). Therefore Fàvre averaging is the more general averaging approach, and is preferred for variable density flows, in spite of the difficulties encountered in modeling the unclosed terms and comparison with experimentally measured velocity moments.

In two–phase flows there are *four* ways in which velocity fluctuations can be defined (Subramaniam, 2001a): (1) the fluctuation defined with respect to the mean velocity of that phase, (2) the Fàvre fluctuation velocity defined with respect to the density–weighted mean velocity of that phase, (3) the fluctuation defined with respect to the mean velocity of the two–phase mixture, and (4) the Fàvre fluctuation velocity defined with respect to the density–weighted mean velocity of the two–phase mixture. It is preferable to adopt the more general definition of fluctuation velocity with respect to mean velocity in a particular phase. The most useful definition of fluctuating velocity is the Fàvre fluctuation in phase β:

$$u_i''^{(\beta)} \equiv U_i - \widetilde{\langle U_i^{(\beta)} \rangle}, \tag{3.105}$$

as was defined earlier. As in single–phase flows, the equations for second moments based on Fàvre fluctuation velocity are considerably simpler than those based on other definitions.

The Fàvre –averaged Reynolds stress $\widetilde{R_{ij}^{(\beta)}}$ in phase β is defined in terms of $u_i''^{(\beta)}$as

$$\widetilde{R}_{ij}^{(\beta)} \equiv \frac{\left\langle I_\beta \rho \; u_i''^{(\beta)} u_j''^{(\beta)} \right\rangle}{\langle I_\beta \rho \; \rangle} = \int_{\mathbf{U}} v_i''^{(\beta)} v_j''^{(\beta)} \; \mathcal{F}_{\mathbf{U}|I_\beta} \; d\mathbf{V}. \tag{3.106}$$

In order to derive the evolution equation for $\tilde{R}_{ij}^{(\beta)}$, we multiply Eq. (3.57) by $v'^{(\beta)}_i v'^{(\beta)}_j$ and integrate over **u** space, along with manipulations as detailed in Appendix A, to obtain:

$$\begin{aligned}
\langle I_\beta \rho \rangle \underbrace{\frac{\tilde{D}}{\tilde{D}t}\widetilde{R}_{ij}^{(\beta)}}_{1} + \underbrace{\frac{\partial}{\partial x_k}\langle \rho I_\beta u_i''^{(\beta)} u_j''^{(\beta)} u_k''^{(\beta)} \rangle}_{2} = \\
+ \underbrace{\left\{ \langle \rho I_\beta u_i''^{(\beta)} u_k''^{(\beta)} \rangle \widetilde{\frac{\partial \langle U_j^{(\beta)} \rangle}{\partial x_k}} + \langle \rho I_\beta u_j''^{(\beta)} u_k''^{(\beta)} \rangle \widetilde{\frac{\partial \langle U_i^{(\beta)} \rangle}{\partial x_k}} \right\}}_{3} \\
+ \underbrace{\left\langle u_i''^{(\beta)} \frac{\partial \left(I_\beta \tau_{kj} \right)}{\partial x_k} \right\rangle}_{4} + \underbrace{\left\langle u_j''^{(\beta)} \frac{\partial \left(I_\beta \tau_{ki} \right)}{\partial x_k} \right\rangle}_{5} \\
+ \underbrace{\left\langle u_i''^{(\beta)} \left(S_{Mj}^{(\beta)} - U_j S_\rho^{(\beta)} \right) \right\rangle}_{6} + \underbrace{\left\langle u_j''^{(\beta)} \left(S_{Mi}^{(\beta)} - U_i S_\rho^{(\beta)} \right) \right\rangle}_{7} \\
+ \underbrace{\left\langle u_i''^{(\beta)} u_j''^{(\beta)} S_\rho^{(\beta)} \right\rangle - \widetilde{R}_{ij}^{(\beta)} \left\langle S_\rho^{(\beta)} \right\rangle}_{8}.
\end{aligned} \tag{3.107}$$

Term 1 above is the material derivative that convects at the Fàvre –averaged mean flow velocity, term 2 is the triple velocity correlation, term 3 corresponds to production due to mean flow gradients, terms 4 and 5 correspond to the fluctuating velocity–stress correlations, terms 6 and 7 correspond to the fluctuating velocity–interfacial force correlations, and term 8 is the source in Reynolds stress equation due to phase change. The above equation has been written in GI form; in particular, the GI forms of unclosed terms that need to be modeled (note that they are also symmetric in indices i and j) are: term 4 and 5; term 6 and 7, and term 8.

3.5.3.2 Number–density based Lagrangian approach

In order to derive the second–moment equation in the LE approach, it is instructive to define the volume–weighted (analogous to mass–weighting in the Fàvre average presented earlier) ddf

of fluctuating velocity $\tilde{g}(\mathbf{x},\mathbf{w},r,t)$ as (Subramaniam, 2001a, 2003)

$$\begin{aligned}\tilde{g}(\mathbf{x},\mathbf{w},r,t) &= \tilde{f}(\mathbf{x},\langle\widetilde{\mathbf{V}}\mid\mathbf{x};t\rangle+\mathbf{w},r,t)\\ &= r^3 f(\mathbf{x},\mathbf{v},r,t) \qquad (3.108)\\ &= \langle R^3(\mathbf{x};t)\rangle n(\mathbf{x};t)\ \tilde{f}^c_{\mathbf{V}R}(\langle\widetilde{\mathbf{V}}\mid\mathbf{x};t\rangle+\mathbf{w},r\mid\mathbf{x};t) \qquad (3.109)\\ &= \langle R^3(\mathbf{x};t)\rangle n(\mathbf{x};t)\ \tilde{g}^c(\mathbf{w},r\mid\mathbf{x};t), \qquad (3.110)\end{aligned}$$

where

$$\mathbf{w}=\mathbf{v}-\langle\widetilde{\mathbf{V}}\mid\mathbf{x};t\rangle,$$

where $\tilde{g}^c(\mathbf{w},r|\mathbf{x};t)$ is the r^3–weighted or volume weighted pdf of fluctuating velocity.

The evolution equation of $\tilde{g}$ is can be derived from Eq. (3.130) (see Appendix C for a derivation) (Subramaniam, 2001a, 2003):

$$\begin{aligned}\frac{\partial\tilde{g}}{\partial t}+\left(\langle\widetilde{V}_k\rangle+w_k\right)\frac{\partial\tilde{g}}{\partial x_k} &= w_k\frac{\partial\tilde{g}}{\partial w_l}\frac{\partial\langle\widetilde{V}_l\rangle}{\partial x_k}-\frac{\partial}{\partial w_l}\left[\langle A_l\mid\mathbf{x},\mathbf{v},r;t)\rangle\tilde{g}-\tilde{g}\frac{\partial\langle\widetilde{V}_l\rangle}{\partial t}-\tilde{g}\langle\widetilde{V}_k\rangle\frac{\partial\langle\widetilde{V}_l\rangle}{\partial x_k}\right]\\ &\quad-\frac{\partial}{\partial r}\left\{\langle\Theta\mid\mathbf{x},\mathbf{v},r;t\rangle\tilde{g}\right\}+3\langle\Omega\mid\mathbf{x},\mathbf{v},r;t\rangle\tilde{g}. \qquad (3.111)\end{aligned}$$

The second moment equation can be obtained by multiplying the $\tilde{g}$ evolution equation by w_iw_j and integrating over all $[\mathbf{w},r_+]$ space to obtain:

$$\begin{aligned}&\underbrace{\kappa n\langle R^3\rangle\left\{\frac{\partial\langle\widetilde{v_i''v_j''}\rangle}{\partial t}+\langle\widetilde{V}_k\rangle\frac{\partial\langle\widetilde{v_i''v_j''}\rangle}{\partial x_k}\right\}}_{1}+\underbrace{\kappa\frac{\partial}{\partial x_k}\left[n\langle R^3\rangle\langle\widetilde{v_i''v_j''v_k''}\rangle\right]}_{2}=\\ &\underbrace{-\kappa n\langle R^3\rangle\left\{\langle\widetilde{v_j''v_k''}\rangle\frac{\partial\langle\widetilde{V}_i\rangle}{\partial x_k}+\langle\widetilde{v_i''v_k''}\rangle\frac{\partial\langle\widetilde{V}_j\rangle}{\partial x_k}\right\}}_{3}\\ &\underbrace{+\kappa n\langle R^3\rangle\left\{\left\langle\widetilde{A_iv_j''}\right\rangle+\left\langle\widetilde{A_jv_i''}\right\rangle\right\}}_{4}\\ &\underbrace{+\kappa n\langle R^3\rangle\left[3\left\langle\widetilde{v_i''v_j''\Omega}\;\middle|\;\mathbf{x};t\right\rangle+\left\langle\widetilde{v_i''v_j''\Theta}\;\middle|\;\mathbf{x},r=0_+;t\right\rangle f^c_R(r=0_+\mid\mathbf{x},t)\right]}_{5}\\ &\underbrace{-\kappa n\langle R^3\rangle\langle\widetilde{v_i''v_j''}\rangle\left\{3\left\langle\widetilde{\Omega}\;\middle|\;\mathbf{x};t\right\rangle+\left\langle\widetilde{\Theta}\;\middle|\;\mathbf{x},r=0_+;t\right\rangle f^c_R(r=0_+\mid\mathbf{x},t)\right\}}_{6}, \qquad (3.112)\end{aligned}$$

where additionally, the above equation has been multiplied throughout by $\kappa=(4/3)\pi\rho_d$. The description of each term is as follows: term 1 is material derivative (following the mass–weighted

mean flow) of the dispersed–phase Reynolds stress, term 2 is the triple velocity correlation term, term 3 is the production due to mean velocity gradients, term 4 is the fluctuating velocity–acceleration correlation and terms 5 and 6 correspond to the net Reynolds stress change due to interphase mass transfer. Note that the terms in the above equation are automatically in GI form.

In homogeneous two–phase flows with neither production nor interphase mass transfer, the only terms that remain in Eq. (3.112) are (i) the time derivative of the Reynolds stress and (ii) the acceleration–fluctuating velocity correlations. The acceleration–fluctuating velocity correlation can be written in terms of $\tilde{g}^c(\mathbf{w}, r|\mathbf{x}; t)$ as (Subramaniam, 2005)

$$\left\langle \widetilde{A_i v_j''} \right\rangle = \frac{1}{\langle R^3(\mathbf{x}, t)\rangle} \int_{[\mathbf{v},r]} r^3 \langle A_i|\mathbf{x}, \mathbf{v}, r; t\rangle w_j \tilde{g}^c(\mathbf{w}, r|\mathbf{x}; t) d\mathbf{w} dr,$$

where the expected acceleration $\langle A_i|\mathbf{x}, \mathbf{v}, r; t\rangle$ is completely determined by Eq.(3.10)–(3.11) and the ddf. The center–of–mass acceleration of the DPE with radius r_0 in turn depends on the state of the stress $\boldsymbol{\tau}$ at the DPE surface through the expression (cf. Eq. (3.75))

$$\mathbf{A}_{(i)}(\mathbf{x}, t) = \frac{1}{m} \int_{\mathcal{S}} \mathbf{n}(\mathbf{y}) \boldsymbol{\tau}(\mathbf{y}, t) dA_s,$$

where $\mathbf{y} = \mathbf{x} + \mathbf{e}_r r_0$ is a point on the surface, $\mathbf{x}$ is the DPE center, $\mathbf{e}_r$ is the unit vector directed radially outward from $\mathbf{x}$ and dA_s is the differential surface area of the DPE [9]. Thus, the acceleration–fluctuating velocity correlation $\langle \widetilde{A_i v_j''} \rangle$ depends on two–point information: the velocity at $\mathbf{x}$, and the state of fluid stress at the DPE surface. This observation has important implications in modeling two–phase flows. Unlike in single–phase flows, wherein single–point models suffice to close unclosed terms in the governing equation for the Reynolds stress [10], closures for terms such as the $\langle \widetilde{A_i v_j''} \rangle$ in two–phase flows require *two–point* information. A widely–used single–point closure for the DPE acceleration in particle–method solutions to the spray equation (See for eg. Amsden et al., 1989) is of the form

$$\mathbf{A}_p(t) = \frac{d\mathbf{V}_p(t)}{dt} = \frac{\mathbf{U}_f(\mathbf{X}_p, t) - \mathbf{V}_p}{\tau_p} C_d(Re_p), \tag{3.113}$$

[9] For a Newtonian fluid, $\boldsymbol{\tau}(\mathbf{y}, t) = -p(\mathbf{y}, t)\mathbf{I} + 2\mu\mathbf{D}(\mathbf{y}, t)$, where p is the mechanical pressure, $\mathbf{I}$ is the identity tensor, μ is the absolute viscosity of the carrier phase and $\mathbf{D}$ is the deviatoric part of the stress tensor.

[10] This is true everywhere except near the walls where it is known that non–local closures for the conditional acceleration are necessary to take wall effects into account correctly Dreeben and Pope (1997a).

where $\mathbf{A}_p$ is a model for $\mathbf{A}_{(i)}$ in Eq. (3.11), $\mathbf{V}_p$ is the modeled dispersed–phase velocity, $\mathbf{U}_f$ is the carrier–phase velocity at the particle *center* $\mathbf{X}_p$, τ_p is the particle response timescale and C_d is the drag coefficient which is a function of the particle Reynolds number Re_p. Clearly, such models do not include surface statistics or two–point information in them, thereby making them applicable only to a restricted class of flows wherein the point particle approximation is valid.

3.5.3.3 Correspondence for locally homogeneous flows

Invoking the assumptions Eq. (3.81) and Eq. (3.82), a direct comparison of the equations Eq. (3.107) and Eq. (3.112) leads to the following correspondence of the terms to be modeled ($\beta = d$) (Subramaniam, 2001a):

$$\frac{\partial}{\partial x_k}\left\langle I_\beta \rho\, u_i''^{(\beta)} u_j''^{(\beta)} u_k''^{(\beta)} \right\rangle \Longleftrightarrow \frac{4}{3}\pi\rho_d\, \frac{\partial}{\partial x_k}\left[n\langle R^3\rangle \langle \widetilde{v_i'' v_j'' v_k''}\rangle \right] \tag{3.114}$$

$$\left\langle u_i''^{(\beta)} \frac{\partial\left(I_\beta \tau_{kj}\right)}{\partial x_k} \right\rangle + \left\langle u_i''^{(\beta)} \left(S_{Mj}^{(\beta)} - U_j S_\rho^{(\beta)} \right) \right\rangle \Longleftrightarrow \frac{4}{3}\pi\rho_d\, n\langle R^3\rangle \left\langle \widetilde{A_i v_j''} \right\rangle \tag{3.115}$$

$$\left\langle u_j'' \frac{\partial\left(I_\beta \tau_{ki}\right)}{\partial x_k} \right\rangle + \left\langle u_j''^{(\beta)} \left(S_{Mi}^{(\beta)} - U_i S_\rho^{(\beta)} \right) \right\rangle \Longleftrightarrow \frac{4}{3}\pi\rho_d\, n\langle R^3\rangle \left\langle \widetilde{A_j v_i''} \right\rangle \tag{3.116}$$

$$\begin{aligned} \left\langle u_i''^{(\beta)} u_j''^{(\beta)} S_\rho^{(\beta)} \right\rangle \Longleftrightarrow \frac{4}{3}\pi\rho_d\, n\langle R^3\rangle \Big[3 \Big\langle \widetilde{v_i'' v_j'' \Omega} \;\Big|\; \mathbf{x}; t \Big\rangle \\ + \Big\langle \widetilde{v_i'' v_j'' \Theta} \;\Big|\; \mathbf{x}, r = 0_+; t \Big\rangle f_R^c(r = 0_+ \mid \mathbf{x}, t) \Big] \end{aligned} \tag{3.117}$$

$$\begin{aligned} -\widetilde{R}_{ij}^{(\beta)} \left\langle S_\rho^{(\beta)} \right\rangle \Longleftrightarrow -\frac{4}{3}\pi\rho_d\, n\langle R^3\rangle \langle \widetilde{v_i'' v_j''}\rangle \times \\ \Big\{ 3 \Big\langle \widetilde{\Omega} \;\Big|\; \mathbf{x}; t \Big\rangle + \Big\langle \widetilde{\Theta} \;\Big|\; \mathbf{x}, r = 0_+; t \Big\rangle f_R^c(r = 0_+ \mid \mathbf{x}, t) \Big\} \end{aligned} \tag{3.118}$$

This correspondence allows one to compare statistics from the EE statistical representation with those in the LE statistical representation, or vice versa.

3.6 Comparison of Advantages and Limitations

The EE and LE probabilistic descriptions of two–phase flows contain different information. In this section, the advantages and limitations of each approach are compared in terms of the information contained in each statistical representation.

3.6.1 Eulerian–Eulerian

1. The fundamental description of a two–phase flow in the EE statistical representation starts from a phase probability field $\alpha_\beta(\mathbf{x},t)$ and pdf $f^E_{\mathbf{U}R|I_\beta}(\mathbf{u},r\,;\mathbf{x},t)$, where $\beta=\{f,d\}$, that are defined in both phases. The governing equations for the mean mass, momentum and second–moment that are derived from the transport equation for the phasic pdf are also defined in both phases. Thus, a coupling between the fluid dynamic equations in both phases is clearly retained in the EE representation.

2. The complete single–point EE description in terms of phase probability fields and pdf contains no explicit representation of *shape or number* of dispersed–phase elements. This informs us that very different two–phase flows can have the same phase probability fields α_β and pdf $f^E_{\mathbf{U}R|I_\beta}(\mathbf{u},r\,;\mathbf{x},t)$.

3. The EE representation is valid in each phase regardless of the size of the dispersed phase element. Internal circulation effects inside a droplet or bubble can be captured by the EE statistical description in terms of Eq.(3.27).

4. A noteworthy limitation of the pdf $f^E_{\mathbf{U}R|I_\beta}(\mathbf{u},r\,;\mathbf{x},t)$ is its inability to distinguish between the flow at a point near the dispersed phase surface and the flow in the bulk. Experiments and body–fitted grid simulations clearly indicate that velocity gradients very close to the particle surface can be very different compared to those in the bulk. A one–point pdf description of a two–phase flow does not possess the capability of capturing such velocity gradients. Such velocity gradients can be captured using a two–point pdf formalism.

3.6.2 Lagrangian–Eulerian

1. Since the LE representation is primarily a description of the dispersed phase, no information on the carrier phase is directly available in the ddf or the spray equation. Thus, a coupling between the dispersed phase and the carrier phase in the LE approach is not rigorously justified. However, one should note that terms such as $\langle\mathbf{A}|\mathbf{x},\mathbf{v},r,t\rangle$ in Eq.(3.130) need to be correctly interpreted as the expected acceleration of the dispersed

phase conditional on position, velocity and radius and also the state of the carrier phase, where the carrier phase information is assumed to be known.

2. The ddf contains both shape and number information of the dispersed–phase elements. However, the shape of the dispersed phase elements is modeled (such as assuming that a characteristic radius r describes the DPE).

3. The ddf cannot capture internal circulation effects since it assumes that a DPE can be described by a single velocity, usually at the particle center–of–mass. As such, rigid particles of any size, and drops and bubbles in which internal circulation effects are not important can be modeled using the ddf. This implicitly imposes a restriction on the size of droplets or bubbles that the ddf is capable of modeling. For instance, the dispersed phase structures that peel off the solid core near the fuel injector during primary atomization may not be amenable to a description by the ddf since such structures could have significant internal circulation effects and may be insufficiently characterized by a single velocity at their center of mass.

4. The implicit restriction on the size of the DPE (droplet or bubble) in (3) should not be misconstrued as a limitation of the ddf to model dense flows. In fact, the ddf does not rely on the assumption of diluteness (or denseness) of a two–phase flow in its definition (Subramaniam, 2001c). It is the models used in existing EE and LE formulations that invoke the assumption of diluteness. The ddf is perfectly valid to model a dense two–phase flow composed of droplets or bubbles in which (i) the DPEs do not have any internal circulation effects (ii) the DPEs can be described by a characteristic length scale.

5. For two–phase flows where the LE statistical description is valid, unclosed quantities in the EE governing equations can be estimated using the corresponding unclosed terms in the LE approach. We invoke the following assumptions: (i) the model for the DPE drag is given by Eq. (3.113) (ii) a constant number of DPEs N, (iii) no interphase mass transfer, (iv) a monodispersed size distribution with radius R_0, and (v) no body forces such as gravity. Under these assumptions, we have for the interphase momentum transfer

term

$$\langle \mathbf{S}_M^{(d)} \rangle(\mathbf{x},t) = \iint \frac{4}{3}\pi r^3 \rho_d \, \langle \mathbf{A} | \mathbf{x},\mathbf{v},r,t \rangle \, f(\mathbf{x},\mathbf{v},r,t) \; d\mathbf{v} \; dr. \tag{3.119}$$

Here

$$\begin{aligned}
\langle \mathbf{A} | \mathbf{x},\mathbf{v},r,t \rangle &= \frac{1}{f} \left\langle \sum_{i=1}^{N} \mathbf{A}_{(i)} \delta(\mathbf{x} - \mathbf{X}_{p(i)}) \delta(\mathbf{v} - \mathbf{V}_{p(i)}) \delta(r - R_0) \right\rangle \\
&= \frac{1}{f} \left\langle \sum_{i=1}^{N} \left(\frac{\mathbf{U}_f(\mathbf{X}_{p(i)},t) - \mathbf{V}_{p(i)}}{\tau_p} \right) \delta(\mathbf{x} - \mathbf{X}_{p(i)}) \delta(\mathbf{v} - \mathbf{V}_{p(i)}) \delta(r - R_0) \right\rangle .
\end{aligned}$$

Substituting in Eq. (3.119) results in

$$\langle \mathbf{S}_M^{(d)} \rangle(\mathbf{x},t) = \iint \frac{4}{3}\pi r^3 \rho_d \left\langle \sum_{i=1}^{N} \left(\frac{\mathbf{U}_f(\mathbf{X}_{p(i)},t) - \mathbf{v}}{\tau_p} \right) \delta_{\mathbf{X}_{p(i)}} \delta_{\mathbf{V}_{p(i)}} \delta_{R_0} \right\rangle \; d\mathbf{v} \; dr,$$

where $\delta_{\mathbf{X}_{p(i)}} = \delta(\mathbf{x} - \mathbf{X}_{p(i)})$, $\delta_{\mathbf{V}_{p(i)}} = \delta(\mathbf{v} - \mathbf{V}_{p(i)})$ and $\delta_{R_0} = \delta(r - R_0)$.

Thus,

$$\begin{aligned}
\langle \mathbf{S}_M^{(d)} \rangle(\mathbf{x},t) &= \iint \frac{4}{3}\pi r^3 \rho_d \left\langle \sum_{i=1}^{N} \left(\frac{\mathbf{U}_f(\mathbf{X}_{p(i)},t) - \mathbf{v}}{\tau_p} \right) \delta_{\mathbf{X}_{p(i)}} \delta_{\mathbf{V}_{p(i)}} \delta_{R_0} \right\rangle \; d\mathbf{v} \; dr, \\
&= \iint \frac{4}{3}\pi r^3 \rho_d \left(\frac{\langle \mathbf{U} \mid \mathbf{x},t \rangle - \langle \mathbf{V} \mid \mathbf{x},t \rangle}{\tau_p} \right) f(\mathbf{x},\mathbf{v},r,t) \; d\mathbf{v} \; dr, \\
&= \iint \frac{4}{3}\pi r^3 \rho_d \left(\frac{\langle \mathbf{U} \mid \mathbf{x},t \rangle - \langle \mathbf{V} \mid \mathbf{x},t \rangle}{\tau_p} \right) n(\mathbf{x},t) f^c_{\mathbf{V}|R} \delta(r - R_0) \; d\mathbf{v} \; dr, \\
&= \frac{4}{3}\pi R_0^3 \; \rho_d \; n(\mathbf{x},t) \left(\frac{\langle \mathbf{U} \mid \mathbf{x},t \rangle - \langle \mathbf{V} \mid \mathbf{x},t \rangle}{\tau_p} \right),
\end{aligned} \tag{3.120}$$

where $\langle \mathbf{U} \mid \mathbf{x},t \rangle$ and $\langle \mathbf{V} \mid \mathbf{x},t \rangle$ are the expected carrier phase and dispersed phase velocities, respectively, conditional on location $\mathbf{x}$ at time t. Thus, under the assumptions noted earlier, a model for the particle drag in the LE framework implies a model for interphase momentum transfer term in the EE representation. Interestingly, the right hand side of Eq. (3.120) can also be extracted from DNS of particle–laden flows that are performed under the same assumptions (also widely known as the point–particle approximation), and thus EE models for the interphase momentum transfer term $\langle \mathbf{S}_M^{(d)} \rangle(\mathbf{x},t)$ can be evaluated using the above equality by comparing with DNS data. A significant observation from the above development is that single–point models such as the one used for $\mathbf{A}_{(i)}$ do not contain any multiscale information. This has implications in accurately modeling interphase TKE transfer in two–phase flows (see Chapter 7).

3.7 Summary and Conclusions

Unlike for a single–phase flow, two distinctly different statistical representations, namely the Eulerian–Eulerian and Lagrangian–Eulerian statistical representations, exist for a two–phase flow. This work clearly shows that the EE and LE probabilistic representations of two–phase flow bear a complicated relationship with each other, unlike the relatively simpler relationship for single–phase flow (Pope, 1985). This work establishes the foundation for the pdf approach to two–phase flows by unifying the EE and LE statistical representations. The following summarizes the principal achievements and conclusions of this work.

1. Fundamental events and corresponding probabilities associated with a two–phase flow in the EE statistical representation are established. Once this is done, it is then straightforward to derive an evolution equation for the fundamental single–point pdf for the instantaneous velocity conditional on the presence of phase β, where $\beta = \{f, d\}$, for a two–phase flow. Governing equations for the mean mass, mean momentum and second moment that are derived from the evolution equation for the EE mass density are shown to be identical to widely–used ensemble–averaged equations for two–phase flows. This level of consistency is absent in two–phase flow pdf formulations available in literature.

2. Fundamental to the LE statistical representation is the droplet distribution function whose evolution equation has been rigorously derived using the theory of point processes (Subramaniam, 2000, 2001c). Based on the droplet distribution function, the pdf of fluctuating velocity $\tilde{g}$ can be defined. The transport equation for $\tilde{g}$ forms the basis for the derivation of mean mass, mean momentum and second–moment equations for the dispersed phase in the LE representation.

3. Consistency conditions are established between the fundamental quantities in the EE (viz. α_β and $f^E_{\mathbf{U}R|I_\beta}(\mathbf{u}, r\,; \mathbf{x}, t)$) and the LE (viz. $n(\mathbf{x}, t)$ and $f^c_{\mathbf{V}R}(\mathbf{v}, r \mid \mathbf{x}, t)$) representations. It is noteworthy that these quantities bear a simple relationship with one another only under conditions of statistical homogeneity of number density and radius pdf. Example two–phase flows where the exact relations between the EE and LE statistical representations

fail to hold are enumerated.

4. By comparing unclosed terms in the governing equations for the mean mass, mean momentum and second–moment in each statistical representation, correspondence between the unclosed terms is established. Galilean invariant forms of unclosed terms in the governing equations in both the statistical representations are identified. This work also serves as a framework for comparing existing two–phase flow models with the Galilean invariant forms of the unclosed terms presented in this work, and also as a guide for proposing new models. The correspondence also aids in estimating unclosed terms in the governing equations in the EE representation using corresponding terms in the LE representation.

5. A comparison between the two statistical representations reveals that the information content in the two approaches is indeed different. The inability of the ddf to capture internal circulation effects in drops or bubbles imposes a restriction on the class of DPEs that can be modeled by the ddf.

DNS of particle-laden flows can significantly benefit from the correspondence between the EE and LE representations presented in this work. This work also provides the necessary consistency relations that need to be satisfied in combined EE–LE formulations in which information is handed over from one representation to the other at a common boundary.

3.8 Extension to multiphase flows

The development of a statistical description for multiphase flows thus far was restricted to two–phase flows. We now briefly outline the considerations that are essential to extend this theoretical framework to multiphase flows. In particular, we consider the extension of the EE and the LE statistical description to three–phase flows. This discussion should also lay the foundation for the extension of the theoretical framework to multiphase flows with four and more interacting phases. In the following we consider a carrier phase denoted f and two dispersed phases denoted d_1 and d_2, respectively.

3.8.1 Eulerian–Eulerian statistical representation

The definition for the indicator function given in Eq. (3.1) remains valid regardless of the number of phases. At any location $\mathbf{x}$, the sum of the indicator function over all the phases is unity:

$$\sum_{\beta=\{f,d_1,d_2\}} I_\beta = 1 \tag{3.121}$$

The fundamental joint event in the case of three phase flow is (cf. Eq. (3.3))

$$E_1 = [\mathbf{U} \in (\mathbf{u}, \mathbf{u} + d\mathbf{u}), I_\beta = 1] \tag{3.122}$$

Corresponding to this joint event, conditional and marginal events are identical to those declared in Sec. 3.2.1. The definitions for the phase probability function p_β, volume fraction α_β and the phasic velocity pdf $f_{\mathbf{U}|I_\beta}$ are all identical to those defined earlier as well. The following relations hold in the case of three phase flows:

$$\sum_{\beta=\{f,d_1,d_2\}} \alpha_\beta = 1 \tag{3.123}$$

$$\sum_{\beta=\{f,d_1,d_2\}} p_\beta = 1 \tag{3.124}$$

$$f_{\mathbf{U}} = \sum_{\beta=\{f,d_1,d_2\}} \alpha_\beta f_{\mathbf{U}|I_\beta} \tag{3.125}$$

The minimal and complete single–point description for a three–phase flow now refers to the knowledge of two of the three α_β's and the phasic velocity pdfs $f_{\mathbf{U}|I_\beta}$ corresponding to all the phases. The following relationships can be used to obtain the phase probability function from the knowledge of $f_{\mathbf{U}|I_\beta}$ and α_β:

$$p_\beta = \frac{f_{\mathbf{U}|I_\beta}\alpha_\beta}{\sum_{\beta=\{f,d_1,d_2\}} \alpha_\beta f_{\mathbf{U}|I_\beta}}.$$

Note that only two of the three volume fractions α_β are independent.

The definition and evolution equation for the mass density $\mathcal{F}_{\mathbf{U}|I_\beta}$ are identical to those presented in Sec.3.4.1 for $\beta = \{f, d_1, d_2\}$ (cf. Eq. (3.42) and Eq. (3.57)). It is noteworthy that for the carrier phase $\beta = f$, the source term due to interphase mass transfer in Eq. (3.57) now represents the regression of the interface for the phases $\beta = d_1$ and $\beta = d_2$. While the mean

mass conservation equation Eq. (3.77) remains valid for three–phase flow, note that since the total mass in the closed three–phase system is conserved, the source terms due to interphase mass transfer sum to zero:

$$\sum_{\beta=\{f,d_1,d_2\}} \left\langle \rho \left(U_i - U_i^{(I)} \right) \frac{\partial I_\beta}{\partial x_i} \right\rangle = 0.$$

The mean momentum equation Eq. (3.87) is also valid for the three–phase system under consideration. For the interphase momentum transfer term, we have the following relationship:

$$\sum_{\beta=\{f,d_1,d_2\}} \left\langle \rho U_i \left(U_j - U_j^{(I)} \right) \frac{\partial I_\beta}{\partial x_j} \right\rangle - \left\langle \tau_{ji} \frac{\partial I_\beta}{\partial x_j} \right\rangle = 0, \tag{3.126}$$

which follows since $I_f = 1 - I_{d_1} - I_{d_2}$. An interpretation of this result is that the sum of the interphase momentum transfer associated with phase d_1 and d_2 is equal and opposite to that associated with phase f. The second moment equation Eq. (3.107) also holds for the three–phase system.

3.8.2 Lagrangian–Eulerian statistical representation

In the LE statistical representation, the ddf is the fundamental starting point for the description of the dispersed phase. For two dispersed phases in a three–phase system, one would have to define the two ddfs as

$$f_{d_1}(\mathbf{x}, \mathbf{v}, r, t) = \left\langle f'_{d_1}(\mathbf{x}, \mathbf{v}, r, t) \right\rangle = \left\langle \sum_{i=1}^{N_{d_1}} \delta(\mathbf{x} - \mathbf{X}_{d_1}^{(i)}) \delta(\mathbf{v} - \mathbf{V}_{d_1}^{(i)}) \delta(r - R_{d_1}^{(i)}) \right\rangle \tag{3.127}$$

$$f_{d_2}(\mathbf{x}, \mathbf{v}, r, t) = \left\langle f'_{d_2}(\mathbf{x}, \mathbf{v}, r, t) \right\rangle = \left\langle \sum_{j=1}^{N_{d_2}} \delta(\mathbf{x} - \mathbf{X}_{d_2}^{(j)}) \delta(\mathbf{v} - \mathbf{V}_{d_2}^{(j)}) \delta(r - R_{d_2}^{(j)}) \right\rangle \tag{3.128}$$

where the subscripts d_1 and d_2 distinguishes properties associated with each phase. Proceeding in the same manner as in Sec. 3.4, one can derive two evolution equations, one for each ddf defined above, as

$$\frac{\partial f_{d_1}}{\partial t} + \frac{\partial}{\partial x_j}[v_j f_{d_1}] + \frac{\partial}{\partial v_j}\left[\langle A_{d_1 j} | \mathbf{x}, \mathbf{v}, r; t \rangle f_{d_1} \right] + \frac{\partial}{\partial r}\left[\langle \Theta_{d_1} | \mathbf{x}, \mathbf{v}, r; t \rangle f_{d_1} \right] = 0 \tag{3.129}$$

$$\frac{\partial f_{d_2}}{\partial t} + \frac{\partial}{\partial x_j}[v_j f_{d_2}] + \frac{\partial}{\partial v_j}\left[\langle A_{d_2 j} | \mathbf{x}, \mathbf{v}, r; t \rangle f_{d_2} \right] + \frac{\partial}{\partial r}\left[\langle \Theta_{d_2} | \mathbf{x}, \mathbf{v}, r; t \rangle f_{d_2} \right] = 0. \tag{3.130}$$

One should bear in mind that the conditional acceleration $\langle A_{d_1 j}|\mathbf{x}, \mathbf{v}, r; t\rangle$ for phase d_1 is implicitly conditional upon the presence of the other phase d_2. A similar observation holds for $\langle A_{d_2 j}|\mathbf{x}, \mathbf{v}, r; t\rangle$ and the conditional evaporation rates. In this three–phase system containing two dispersed phases, one may need to take into account collisions between the dispersed phases. To account for such collisions (say, in dispersed phase d_1), the conditional acceleration $\langle \mathbf{A}_{d_1}\rangle$ can be considered to be composed of three parts: (i) a part that is known in terms of the ddf, (ii) a part that is unknown, but is modeled in terms of how the dispersed phase d_2 is spatially distributed with respect to d_1, and (iii) a part that is also unknown, but is modeled in terms of how the dispersed phase d_1 is spatially distributed. The term (ii) accounts for interphase collisions, while term (iii) accounts for intraphase collisions.

The mean mass, mean momentum and second–moment equations associated with each dispersed phase can now be derived in a straightforward manner as presented for a single dispersed phase in Sec.(3.5). Coupling between the dispersed phases is accounted through the conditional acceleration terms and the conditional vaporization terms corresponding to the evolution equation in each dispersed phase.

In a single–point description of a three–phase system, information is available only at the level of the means (for instance, mean number density in each dispersed phase at each physical location). Since there is no other means to distinguish between phases than using mean information, the procedure to establish the relationship between the EE and the LE representation is identical to that presented in Sec. 3.3. In particular, the volume fraction associated with phase d_1 can be related to the ddf f_{d_1} and the volume fraction associated with phase d_2 can be related to the ddf f_{d_2} using the method outlined in that section. Similarly, the Eulerian phasic velocity pdf in each dispersed phase can be related to the conditional joint pdf of velocity and radius corresponding to the ddf in each phase as outlined in the same section.

CHAPTER 4. A NEW LAGRANGIAN–LAGRANGIAN REPRESENTATION OF TWO-PHASE FLOWS

A new statistical representation for a two–phase flow called the Lagrangian–Lagrangian (LL) description that is based on a Lagrangian description of both the carrier phase and the dispersed phase is proposed. The description of the dispersed phase in terms of the droplet distribution function is retained in this formalism. Since the droplet distribution function can be expressed as a sequence of single "surrogate" droplet pdfs, the corresponding Lagrangian description of the carrier phase is properly interpreted as describing the evolution of single "surrogate" fluid particles. Such a Lagrangian interpretation of the carrier phase follows naturally from an intermediate symmetrization done on the Liouville multi–particle pdf of the dispersed phase (Subramaniam, 2000). Implicit in the symmetrization of the dispersed phase Liouville pdf is an analogous symmetrization of the multipoint pdf description of the carrier phase. The relationship between the new LL description and a recently formulated Eulerian–Eulerian (EE) pdf formalism for two–phase flows is presented. In particular, it is shown that in the context of two–phase flows the relationship between Eulerian and Lagrangian quantities in the two phases is not as straightforward as in single–phase flows, but has to be interpreted carefully. A framework for the consistent statistical representation of two–phase flows in the EE, LE, and LL statistical representations is established.

4.1 Lagrangian representation in single–phase flows

Before we delve into developing a framework for the Lagrangian description of the carrier phase in a two–phase flow, it is instructive to review the Lagrangian representation in single–phase flows. This section will help us appreciate the difference between the Lagrangian

representation in single phase flows and that in two–phase flows.

In the context of low–Mach number gaseous flow (Pope, 1985), the state of the fluid at any physical location is completely described by the velocity vector $\mathbf{U}$ and a composition vector $\boldsymbol{\phi} = \{\phi_1, \phi_2, \ldots, \phi_\sigma\}$, which is composed of $\sigma = s + 1$ scalars, where s is the number of species corresponding to the species mass fractions, and the remaining scalar is the enthalpy. Conservation equations of mass and momentum are

$$\frac{\partial \rho}{\partial t} + \frac{\partial \rho U_i}{\partial x_i} = 0 \tag{4.1}$$

$$\rho \frac{DU_j}{Dt} = \frac{\partial \tau_{ij}}{\partial x_i} - \frac{\partial p}{\partial x_j} + \rho g_j \tag{4.2}$$

while the evolution of the scalars can be succinctly written as

$$\rho \frac{D\phi_\alpha}{Dt} = -\frac{\partial J_i^\alpha}{\partial x_i} + \rho S_\alpha, \quad \alpha = 1, 2, \ldots, \sigma, \tag{4.3}$$

where $\mathbf{J}^\alpha$ is the diffusive mass flux vector of species α and S_α is the mass rate of addition of species α due to reaction. Given a reference pressure p_0, the density and reaction source term are completely determined by the composition vector $\rho = \rho(\boldsymbol{\phi})$ and $S_\alpha = S_\alpha(\boldsymbol{\phi})$. This has implications in the definition of the Lagrangian joint pdf of velocity and scalar as a transition density for the Eulerian pdf (see Eq. (4.12) and later).

The velocities and compositions form a $3+\sigma$ dimensional random vector in a turbulent flow. The complete single–point description of the turbulent flow is characterized by the velocity–composition joint pdf $f_{\mathbf{U}\boldsymbol{\phi}}(\mathbf{V}, \boldsymbol{\phi})$. In term of the fine–grained density, $f_{\mathbf{U}\boldsymbol{\phi}}$ can be written as (Pope, 1985)

$$f_{\mathbf{U}\boldsymbol{\phi}} = \langle \delta(\mathbf{U} - \mathbf{V}) \delta(\boldsymbol{\phi} - \boldsymbol{\psi}) \rangle \,. \tag{4.4}$$

where $\mathbf{V}$ and $\boldsymbol{\psi}$ are the sample space variables corresponding to the random variables $\mathbf{U}$ and $\boldsymbol{\phi}$, respectively. One can define the density–weighted joint pdf $\tilde{f}$ as

$$\tilde{f}(\mathbf{V}, \boldsymbol{\psi}) = \frac{\rho(\boldsymbol{\psi})}{\langle \rho \rangle} f(\mathbf{V}, \boldsymbol{\psi}) \tag{4.5}$$

In the context of variable–density single–phase flows, it is instructive to define a mass density function as (Pope, 1985)

$$\mathcal{F}(\mathbf{V}, \boldsymbol{\psi}, \mathbf{x}, t) = \rho(\boldsymbol{\psi}) \; f_{\mathbf{U}\boldsymbol{\phi}}(\mathbf{V}, \boldsymbol{\psi}; \mathbf{x}, t) = \langle \rho \rangle \; \tilde{f}_{\mathbf{U}\boldsymbol{\phi}}(\mathbf{V}, \boldsymbol{\psi}; \mathbf{x}, t). \tag{4.6}$$

Using the expected mass of fluid M in a region of volume V, one can represent the mass density discretely through N notional particles, each particle representing a mass $\Delta m = M/N$. The discrete mass density function $\mathcal{F}_N$ is then defined by (Pope, 1985)

$$\mathcal{F}_N = \Delta m \sum_{i=1}^{N} \delta(\mathbf{U}^{(i)} - \mathbf{V})\delta(\boldsymbol{\phi}^{(i)} - \boldsymbol{\psi})\delta(\mathbf{X}^{(i)} - \mathbf{x}). \tag{4.7}$$

The N particles are identically distributed and hence the expected mass density is (Pope, 1985)

$$\langle \mathcal{F}_N \rangle = \Delta m \sum_{i=1}^{N} \left\langle \delta(\mathbf{U}^{(i)} - \mathbf{V})\delta(\boldsymbol{\phi}^{(i)} - \boldsymbol{\psi})\delta(\mathbf{X}^{(i)} - \mathbf{x}) \right\rangle. \tag{4.8}$$

A consequence of the above development is that the position pdf of the notional particles is proportional to the mean density:

$$h(\mathbf{x}) = \frac{\langle \rho(\mathbf{x}) \rangle}{M}. \tag{4.9}$$

If $f^*(\mathbf{V}, \boldsymbol{\psi}|\mathbf{x})$ is the joint pdf of $\mathbf{U}^{(i)}$ and $\boldsymbol{\phi}^{(i)}$ conditional on the particles being at position $\mathbf{x}$, then

$$f^*(\mathbf{V}, \boldsymbol{\psi}|\mathbf{x}) = \frac{\mathcal{F}(\mathbf{V}, \boldsymbol{\psi}, \mathbf{x})}{\langle \rho(\mathbf{x}) \rangle} = \tilde{f}(\mathbf{V}, \boldsymbol{\psi}; \mathbf{x}). \tag{4.10}$$

The above relation shows that the pdf of notional particle properties at a given location must be equal to the density–weighted pdf of fluid properties for the relation $\langle \mathcal{F}_N \rangle = \mathcal{F}$ to hold.

The evolution of the mass density function $\mathcal{F}(\mathbf{V}, \boldsymbol{\psi}, \mathbf{x}, t)$ is given as (Pope, 1985)

$$\frac{\partial \mathcal{F}}{\partial t} + V_j \frac{\partial \mathcal{F}}{\partial x_j} = -\frac{\partial}{\partial V_j}[\langle A_j|\mathbf{V}, \boldsymbol{\psi}\rangle \mathcal{F}] - \frac{\partial}{\partial \psi_\alpha}[\langle \Theta_\alpha|\mathbf{V}, \boldsymbol{\psi}\rangle \mathcal{F}], \tag{4.11}$$

where

$$\rho A_j(\mathbf{x}, t) = \frac{\partial \tau_{ij}}{\partial x_i} - \frac{\partial p}{\partial x_j} + \rho g_j$$
$$\rho \Theta_\alpha(\mathbf{x}, t) = -\frac{\partial J_i^\alpha}{\partial x_i} + \rho S_\alpha.$$

The expectations $\langle \mathbf{A} \rangle$ and $\langle \boldsymbol{\Theta} \rangle$ are not random variables, and therefore Eq. (4.11) is a deterministic equation. This brings forth an important observation that many different stochastic systems can be described by the same mass density function evolution. Such *stochastically equivalent* systems (in this case, the fluid particle system and the notional particle system form

stochastically equivalent systems) form an important basis in the Lagrangian description of the single–phase flow.

The concept of a fluid particle is the starting point for the Lagrangian description in single–phase flows. Since the mass of a material element of fluid remains unchanged, the ratio of the volume occupied by the material element at time t_0 to the volume at t can be expressed as

$$\frac{dV(t)}{dV(t_0)} = \frac{\partial \mathbf{X}^+}{\partial \mathbf{Y}} = \frac{\rho(\mathbf{Y}, t_0)}{\rho(\mathbf{X}^+(t, \mathbf{Y}), t)} \tag{4.12}$$

where $\mathbf{X}^+$ is the Lagrangian position of the fluid particle at time t, and $\mathbf{Y}$ is its initial position. In augmented state space (Pope, 1985), the evolution of the state of a fluid particle be represented as $[\mathbf{V}, \psi, \mathbf{x}] = [\mathbf{U}^+, \phi^+, \mathbf{X}^+]$ given that the initial position of the particle is $\mathbf{Y}$. In a turbulent flow, the particle paths in augmented state space can cross each other, since the state vector $[\mathbf{U}^+, \phi^+, \mathbf{X}^+]$ does not uniquely determine the rate of change vector $[\mathbf{A}, \Theta, \mathbf{U}^+]$.

The Lagrangian conditional joint pdf $f_L(\mathbf{V}, \boldsymbol{\psi}, \mathbf{x}; t|\mathbf{V}_0, \boldsymbol{\psi}_0, \mathbf{x}_0)$ is the joint probability of the event (Pope, 1985)

$$S_t \equiv \{\mathbf{U}^+(t, \mathbf{Y}) = \mathbf{V}, \boldsymbol{\phi}^+(t, \mathbf{Y}) = \boldsymbol{\psi}, \mathbf{X}^+(t, \mathbf{Y}) = \mathbf{x}\}, \tag{4.13}$$

conditional on the event

$$S_0 \equiv \{\mathbf{U}^+(t_0, \mathbf{Y}) = \mathbf{U}(\mathbf{Y}, t_0) = \mathbf{V}_0, , \boldsymbol{\phi}^+(t_0, \mathbf{Y}) = \boldsymbol{\phi}(t, \mathbf{Y}) = \boldsymbol{\psi}_0\}. \tag{4.14}$$

The Lagrangian joint pdf f_L is shown to be the transition density in that the mass density at time t can be determined from its value at t_0 through the relation (Pope, 1985)

$$\mathcal{F}(\mathbf{V}, \boldsymbol{\psi}, \mathbf{x}; t) = \iiint f_L(\mathbf{V}, \boldsymbol{\psi}, \mathbf{x}; t|\mathbf{V}_0, \boldsymbol{\psi}_0, \mathbf{Y})\, \mathcal{F}(\mathbf{V}_0, \boldsymbol{\psi}_0, \mathbf{Y}; t)\, d\mathbf{V}_0\, d\boldsymbol{\psi}_0\, d\mathbf{Y}. \tag{4.15}$$

The transition density f_L evolves according to (Pope, 1985)

$$\frac{\partial f_L}{\partial t} + \frac{\partial [V_i f_L]}{\partial x_i} + \frac{\partial}{\partial V_i}[f_L \langle A_i|S_t, S_0\rangle] + \frac{\partial}{\partial \psi_\alpha}[f_L \langle \Theta_\alpha|S_t, S_0\rangle] = 0. \tag{4.16}$$

Using Eq. (4.15) the evolution of $\mathcal{F}$ can be derived to be

$$\frac{\partial \mathcal{F}}{\partial t} + \frac{\partial [V_i \mathcal{F}]}{\partial x_i} + \frac{\partial}{\partial V_i}[\mathcal{F} \langle A_i|\mathbf{V}, \boldsymbol{\psi}\rangle] + \frac{\partial}{\partial \psi_\alpha}[\mathcal{F} \langle \Theta_\alpha|\mathbf{V}, \boldsymbol{\psi}\rangle] = 0. \tag{4.17}$$

Corresponding to the evolution equation of $\mathcal{F}$, one can envisage a set of notional particles that evolve according to a deterministic set of Lagrangian equations

$$\frac{\partial}{\partial t}\begin{bmatrix} \widehat{\mathbf{U}} \\ \widehat{\boldsymbol{\phi}} \\ \widehat{\mathbf{x}} \end{bmatrix} = \begin{bmatrix} \langle \mathbf{A}|\mathbf{V},\boldsymbol{\psi}\rangle \\ \langle \boldsymbol{\Theta}|\mathbf{V},\boldsymbol{\psi}\rangle \\ \langle \mathbf{U}|\mathbf{V},\boldsymbol{\psi}\rangle \end{bmatrix}. \tag{4.18}$$

These notional particles are referred to as "conditional particles" in Pope (1985). The quantities on the right hand side of Eq. (4.18) depend on the initial state $\mathbf{V}_0, \boldsymbol{\psi}_0, \mathbf{x}_0$, and since the quantities on the right hand side of Eq. (4.18) are conditional expectations, the evolution of a conditional particle is uniquely determined by its initial state. As such conditional particle paths cannot cross. A computationally feasible method of solving the joint pdf equation is possible through using the idea of conditional particles. Pope (1985) shows that if the mass density $\mathcal{F}$ is represented discretely using a collection of N conditional particles at initial time, then their evolution given by Eq. (4.18) ensures that the mass density can be approximated by a large number of conditional particles for all time.

While the idea of conditional particles is beneficial to appreciate the fact that the fluid particle system and the conditional particle system have the same pdf, the method of solution through the evolution of Eq. (4.18) is not a satisfactory means to solve the pdf equation since in general the right hand side is unknown. Using the principle of stochastic equivalence, systems of *stochastic particles* can be constructed whose pdf evolves in the same way as that of the fluid particles. It is important to note that unlike conditional particles, stochastic particle paths can cross. Using a Markov process (Pope, 2000) as a stochastic model, the implied evolution equations of the Lagrangian transition density and the mass density function can be derived. For the mass density implied by the model at initial time to remain a valid mass density for all time, essentially two conditions need to be satisfied (Pope, 1985): (i) realizability, which is guaranteed if $\mathcal{F} > 0$ and (ii) normalization

$$\iint \mathcal{F}(\mathbf{V},\boldsymbol{\psi},\mathbf{x};t)\, d\mathbf{V}\, d\boldsymbol{\psi} = \langle \rho(\mathbf{x},t)\rangle$$

and consistency

$$\iint \frac{1}{\rho(\boldsymbol{\psi})}\mathcal{F}(\mathbf{V},\boldsymbol{\psi},\mathbf{x};t)\, d\mathbf{V}\, d\boldsymbol{\psi} = 1,$$

which are equivalent. Realizability is guaranteed if the model can be expressed in terms of the evolution of the discrete mass density function F_N (see Eq. (4.8)). The satisfaction of the mean continuity equation is necessary and sufficient to satisfy the consistency condition, and the mean continuity is satisfied for all time if and only if the mean pressure satisfies a Poisson equation.

In summary, the Lagrangian description in single–phase flows has a clear physical meaning in terms of fluid particles. The Eulerian pdf at time t is known in terms of the Eulerian pdf at initial time t_0 and the Lagrangian pdf. Hence the Lagrangian pdf serves as a transition density for the Eulerian pdf. The principle of stochastic equivalence allows one to model the fluid particles in terms of a collection of Lagrangian notional particles whose pdf evolves in the same way as the pdf corresponding to the fluid particles. These notional particles must satisfy certain constraints and consistency conditions in order for the implied mass density at initial time to remain a valid mass density for all time.

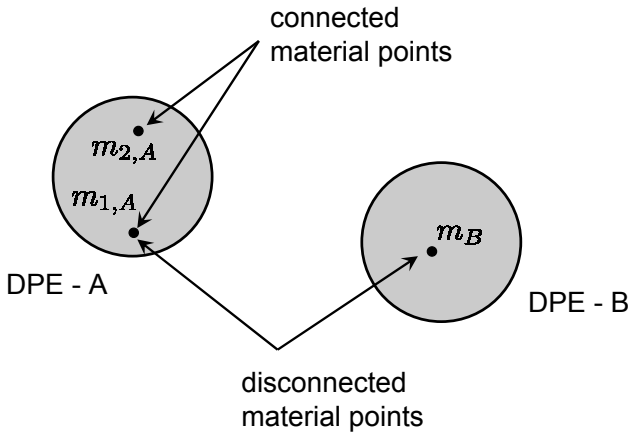

Figure 4.1 Schematic showing two DPEs A and B taken from a snapshot of a two–phase flow. Three material points $m_{1,A}$, $m_{2,A}$ and m_B, all in the dispersed phase, are shown. A single–point Lagrangian description based on material points in a two–phase flow cannot distinguish between the connectedness of $m_{1,A}$ and $m_{2,A}$, and also the fact that m_B is not connected to the DPE A.

It is natural to seek a straightforward extension of the Lagrangian treatment of single–phase

flows to two–phase flows in terms of material points in the two phases. Consider a schematic of a two–phase flow in Fig. 4.1 that contains, for simplicity, a solid dispersed phase. Let us follow two material points $m_{1,A}$ and $m_{2,A}$ in the dispersed–phase element (DPE) denoted A and one material point m_B in the DPE denoted B each with a Lagrangian state $[\mathbf{X}^+(t,\mathbf{Y}), \mathbf{U}^+(t,\mathbf{Y})]$ along with an indicator function $I_d^+(t,\mathbf{Y})$ to distinguish whether the material point is in the dispersed phase or not. The material points $m_{1,A}$ and $m_{2,A}$ are connected since they form a part of the same solid DPE, while the material point m_B is not connected with either $m_{1,A}$ or $m_{2,A}$ since it is in a different DPE. A single–point description of a two–phase flow cannot capture the fact that $m_{1,A}$ and $m_{2,A}$ are connected, while m_B is disconnected with the other two material points. The issue of connectedness of material points that constitute a DPE (such as a droplet, solid particle or bubble) in a 1–pt description of the two–phase flow can be resolved by using topological information, such as characteristic radius of the DPE. In other words, one needs to associate a characteristic radius to each DPE and a reference center, in order to capture the connectedness between material points in a DPE. Topological information such as the characteristic radius is important in closure models for the drag and vaporization, since these phenomena predominantly occur at the surface of the DPE. However, once one introduces the notion of a characteristic radius associated with each DPE center in a Lagrangian description of the dispersed phase, the relationship between such a description and the spray equation formalism (Subramaniam, 2001c) needs to be clearly established.

We therefore conclude that the only tractable single–point Lagrangian statistical description of the dispersed phase is the spray equation formalism. In this description (see Subramaniam (2001c, 2000) and also Section 3.2.2), we have already noted that using the ddf one cannot meaningfully characterize single droplet events. However by performing a symmetrization of the N–particle Liouville density and successive intergration over all $N-1$ spaces, one can indeed obtain a single–particle density of "surrogate" particles (Subramaniam, 2001c, 2000). These considerations for the dispersed phase impose certain restrictions on the Lagrangian description of the carrier phase in a two–phase flow.

In a single–point statistical description of a two–phase flow therefore, the statistics of a

single fluid particle (or material point in the carrier phase) are lost in the symmetrization process. Since in describing the carrier phase, one needs to condition on the state of the dispersed phase, it is instructive to seek a joint description of the two–phases. It is worthwhile to note that Edwards (2000) has explored such a simultaneous joint description of the fluid and dispersed phase in the context of dense sprays. From such a joint description of the two–phases, one can define an unambiguous initial state which forms the basis for the Lagrangian description of the carrier phase.

In the following, we first briefly review the Lagrangian description of the dispersed phase, and then establish the foundation for the Lagrangian description of the carrier phase.

4.2 Lagrangian description of the dispersed phase

The complete multiparticle description of the dispersed phase conditional on the presence of $N = k$ DPEs in the system is given by the Liouville probability density (Subramaniam, 2000)

$$f_{[N=k]}(\mathbf{x}_1, \mathbf{v}_1, \ldots, \mathbf{x}_k, \mathbf{v}_k, t) \equiv \left\langle \prod_{i=1}^{N=k} \delta(\mathbf{x}_i - \mathbf{X}^{(i)}(t))\delta(\mathbf{v}_i - \mathbf{V}^{(i)}(t)) \right\rangle, \tag{4.19}$$

where $\mathbf{X}^{(i)}$ and $\mathbf{V}^{(i)}$ are the position and velocity of the ith DPE at time t. The Liouville density is the joint multiparticle density which characterizes all joint (multiparticle) events of the ensemble for a fixed total number of DPEs $N = k$. In kinetic theory, the $N = k$ Liouville density can be straightforwardly related to the single–particle Klimontovich density by deriving a succession of marginal densities leading to the BBGKY hierarchy. However, the Liouville density that characterizes the dispersed phase in a two–phase flow cannot be simply related to the Klimontovich density owing to several reasons (Subramaniam, 2000): (*i*) this Liouville density is ordering dependent (*ii*) fluctuations of the total number of particles about the mean in realistic two–phase flows are non–negligible (*iii*) the total number of particles is finite and can change in time (*iv*) dispersed–phase elements are not independently distributed as large volume fractions in a two–phase flow preclude such an independence. As far as (*iv*) is concerned, in the dense limit and in the context of monodispersed size distribution of the dispersed phase, one could use the radial distribution function to account for spatial correlations

between particle positions as employed in the theory of dense gases (Chapman and Cowling, 1990) .

In order to relate the Liouville density to the Klimontovich density associated with the dispersed phase in a two–phase flow, or simply, to derive the single particle density from the multiparticle Liouville density, an intermediate symmetrization of Eq. (4.19) needs to be performed. Details on the symmetrization procedure applied to Eq. (4.19) are given in Subramaniam (2000). The resulting symmetrized Liouville density is

$$f^{\text{sym}}_{[N(t)=k]}(\mathbf{x}_1, \mathbf{v}_1, \ldots, \mathbf{x}_k, \mathbf{v}_k; t) = \frac{1}{k!} \sum_{\text{perm}} f_{[N(t)=k]}(\mathbf{x}_1, \mathbf{v}_1, \ldots, \mathbf{x}_k, \mathbf{v}_k; t) \tag{4.20}$$

From this symmetrized Liouville density, it is straightforward to derive a unique single–particle probability density:

$$f_{1s}^{[N(t)=k]}(\mathbf{x}_1, \mathbf{v}_1; t) \equiv \int f^{\text{sym}}_{[N(t)=k]}(\mathbf{x}_1, \mathbf{v}_1, \ldots, \mathbf{x}_k, \mathbf{v}_k; t) d\mathbf{x}_2 d\mathbf{v}_2 \ldots d\mathbf{x}_k d\mathbf{v}_k.$$

The droplet distribution function is related to the single–particle density through

$$f(\mathbf{x}, \mathbf{v}, t) = \sum_{k \geq 1} q_k k f_{1s}^{[N(t)=k]}(\mathbf{x}, \mathbf{v}; t) = \sum_{k \geq 1} q_k f^k(\mathbf{x}, \mathbf{v}; t) \tag{4.21}$$

where q_k is the probability that there are $N = k$ DPEs in the system. Using Eq. (4.21), one can show that

$$n(\mathbf{x}, t) = \sum_{k \geq 1} q_k n^{(k)}(\mathbf{x}, t), \tag{4.22}$$

where $n^{(k)}$ is the number density conditional on the presence of k droplets in the system.

4.3 Framework for the Lagrangian description of the fluid phase

A prerequisite for the Lagrangian description of the fluid phase is the characterization of the initial state of the two–phase system. In single–phase flows, the initial state is characterized in terms of the fluid particle. The initial state vector S_0 (cf. Eq. (4.14) and Eq. (4.13)) (Pope, 1985):

$$S_0 = \left\{ \mathbf{U}^+(t_0, \mathbf{Y}) = \mathbf{U}(\mathbf{Y}_0, t_0) \right\},$$

where $\mathbf{U}^+$ is the velocity following the fluid particle, $\mathbf{Y}$ is the initial position of the fluid particle and $\mathbf{U}$ is the Eulerian velocity at the location $\mathbf{Y}_0$ at time t_0, uniquely characterizes (in the absence of scalars) the initial state of the single–phase flow.

A straightforward extension of this idea to two–phase flows is not possible. This is primarily because the presence of the dispersed phase adds complexity to the unique characterization of the initial state in a two–phase flow. Given a physical domain containing a two–phase flow, the carrier phase and dispersed phase each occupy a region of the domain whose measure (or, volume) is itself a random variable. A meaningful statistical description of a two–phase flow therefore will require an intermediate averaging, which is not required in the statistical description of single–phase flows.

Another hurdle in extending the idea of the Lagrangian pdf in single–phase flows to two–phase flows is the information content in the Lagrangian pdf associated with a fluid particle. In single–phase flows, Dreeben and Pope (1997b) show that the Eulerian pdf can be inferred from Lagrangian pdf by simply dividing the Lagrangian pdf by the position pdf of the fluid particles. One can think of $\mathcal{F}$ as the unconditional, unnormalized Lagrangian pdf associated with a fluid particle, and $\tilde{f}_{\mathbf{U}\phi}$ as the Eulerian pdf corresponding to $\mathcal{F}$. The mass density $\mathcal{F}$ contains all the information required for its normalization $\langle\rho\rangle$ at any time. However, in the context of two–phase flows, all the normalization information is not contained in the Lagrangian state of a material point with the knowledge of its current phase information.

In single–phase flows, the ensemble of realizations can be thought of as a set of delta functions, each corresponding to the state of a fluid particle. In two–phase flows, we could extend the same idea and define the Lagrangian state of the fluid particle at initial time in terms of a fine–grained Lagrangian density as

$$f'_{L,f} = I_f^+ \delta(\mathbf{X}^+(t_0, \mathbf{Y}) - \mathbf{x})\delta(\mathbf{U}^+(t_0, \mathbf{Y}) - \mathbf{u}).$$

Here I_f^+ is actually $I_f(\mathbf{Y}, t; \omega)$, where ω is a realization from the sample space of all realizations and signifies a particular configuration of the DPEs. However, one should note that in the above definition $\mathbf{Y}$ is restricted to be in the carrier phase only in each realization ω. Since each realization has a certain probability of ocurring, the only tractable method of obtaining useful

information from the two–phase flow is to average information from individual realizations as

$$\int I_f(\mathbf{X}, t; \omega) dP_\omega = \langle I_f \rangle = \langle \alpha_f \rangle$$

where dP_ω is the probability measure associated with each realization. Since α_f can occur at any location in the two–phase flow, the concept of a fluid particle is no longer a tractable means to describe the Lagrangian state of a two–phase flow. It is then useful to associate a "notional" fluid particle with each location of the two–phase flow that corresponds to the fluid–phase volume fraction field.

4.3.1 Multipoint description of the carrier phase

The earlier discussion suggests that it is imperative to account for the presence of a dispersed phase when seeking a Lagrangian description of the carrier phase in a two–phase flow. It is instructive to start from a multipoint description of the carrier phase, conditional on the presence of $N = k$ DPEs. Such a multipoint description would require the knowledge of the event $[\mathbf{U}(t), I_f^k(t)]$. Here $\mathbf{U}(t)$ represents the random *field* of velocities at all points occupied by the fluid phase (see Monin and Yaglom (1971) for a discussion on the simultaneous N_f point description of the random velocity field in a turbulent flow). The random field corresponding to the fluid indicator field is denoted $I_f^k(t)$. Let the probability corresponding to the above event be denoted $P^{[N=k]}[\mathbf{U}(t), I_f^k(t)]$.

This multipoint description of the fluid phase is analogous to the Liouville density for the dispersed phase. Considerations of ordering–dependence impose a requirement of symmetrization on the Liouville density corresponding to the dispersed phase. A unique single particle density is then obtained by successive integration of the symmetrized Liouville density over $k-1$ spaces (Subramaniam, 2000). The symmetrization of the dispersed–phase Liouville density imposes an analogous requirement on the multipoint description of the fluid phase. Thus one can envision a corresponding symmetrized multipoint Eulerian probability description for the fluid phase conditional on there being $N = k$ DPEs as

$$P_s^{[N=k]}[\mathbf{U}^{(s)}(t), I_f^{k,s}(t)]. \tag{4.23}$$

Analogous to the single "surrogate" particle density in the dispersed phase, a single point "surrogate" Eulerian density can be defined for the carrier phase. Corresponding to the symmetrized multipoint Eulerian density conditional on the presence of k DPEs, the single–point surrogate probability description is denoted

$$P_{1,s}^{[N=k]}[\mathbf{U}^{(s)}(\mathbf{x},t) \in (\mathbf{u}, \mathbf{u}+d\mathbf{u}), I_f^{k,s}(\mathbf{x},t) = 1], \tag{4.24}$$

where $\mathbf{u}^{(s)}$ is the sample space variable corresponding to the random variable $\mathbf{U}^{(s)}$. The probability density, if it exists, corresponding to the symmetrized probability description when integrated over all $N_f - 1$ locations in the field results in the single–point surrogate fluid indicator field. This surrogate indicator field no longer possesses the sharpness of the initial fluid indicator field. This field is essentially the volume fraction $\alpha_f^{(k)}(\mathbf{x},t)$ at the location $\mathbf{x}$, conditional on $N = k$ DPEs. Thus, $P[I_f^{k,s}(\mathbf{x},t) = 1] = \alpha_f^{(k)}(\mathbf{x},t)$. We believe that the symmetrization of the multipoint description and successive integration over $N_f - 1$ locations would require mathematical tools involving functionals (Monin and Yaglom, 1971). We do not pursue the details of this mathematical procedure here, as this is not central to the discussion and objective of this study, but provide only an outline.

The single–point surrogate density taking into consideration the fact that $N(t)$ can be random is therefore

$$\begin{aligned} &P_{1,s}[\mathbf{U}^{(s)}(\mathbf{x},t) \in (\mathbf{u}, \mathbf{u}+d\mathbf{u}), I_f^{k,s}(\mathbf{x},t) = 1] \\ &\qquad = \sum_{k\geq 1} q_k P_{1,s}^{[N(t)=k]}[\mathbf{U}^{(s)}(\mathbf{x},t) \in (\mathbf{u}, \mathbf{u}+d\mathbf{u}), I_f^{k,s}(\mathbf{x},t) = 1], \end{aligned} \tag{4.25}$$

corresponding to which one may define the volume fraction α_f as

$$\alpha_f(\mathbf{x},t) = P[I_f^s(\mathbf{x},t) = 1] = \sum_{k\geq 1} q_k \alpha_f^{(k)}(\mathbf{x},t).$$

Here q_k is the probability that there are $N(t) = k$ DPEs in the two–phase system.

4.3.2 Surrogate fluid–particles

The symmetrization procedure performed on the multipoint Eulerian density and the successive integration leading to the definition of a single point "surrogate" Eulerian density

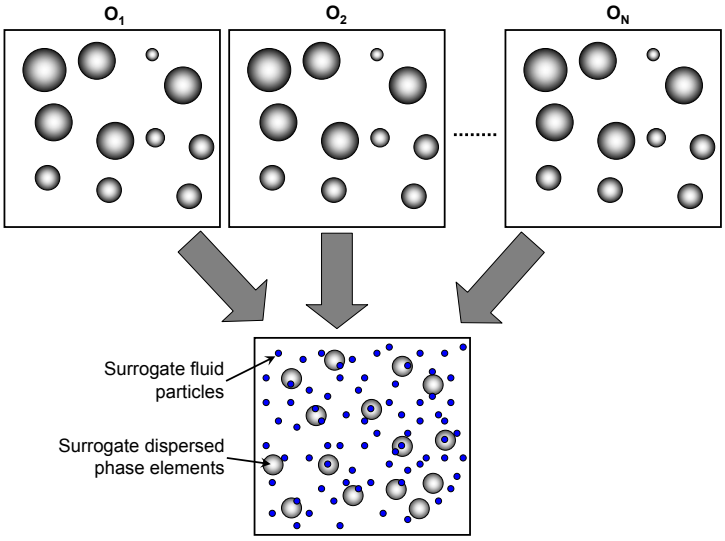

Figure 4.2 Schematic showing several orderings of the dispersed phase in a two–phase flow (top panel) and the corresponding surrogate system (bottom panel) showing the surrogate fluid particles, which can occupy any physical location, and the surrogate dispersed–phase elements. The above schematic corresponds to a typical two–phase flow at initial time. See discussion in Sec. 4.3.2 for details.

enables one to visualize the two–phase flow at initial time as a collection of surrogate fluid particles with interspersed surrogate DPEs. See Fig. 4.2 for a schematic of the surrogate two–phase system that is derived by performing a symmetrization over N orderings of the two–phase flow. Since the surrogate fluid particles represent averaged information, they can be present at any location in space – even coinciding with the location of the surrogate DPE.

Since the topological information contained in each realization of the two–phase system is lost, and two–phase system is correctly viewed as an ensemble of surrogate fluid particles and DPEs, no physical interpretation of the surrogate two–phase system is possible. As a result, these notional particles can be thought of as analogous to computational particles in the context of single–phase turbulent flows. In other words, the Lagrangian representation corresponding to the carrier phase in a two–phase flow is essentially a *modeled* representation

of the carrier phase.

4.3.3 Fluid–phase Lagrangian density

We now know that when a Lagrangian description of the fluid phase is required in the context of a two–phase flow, it is futile to consider each realization and follow a Lagrangian "fluid" particle. The fluid phase is correctly interpreted as a collection of surrogate fluid particles. This brings us to an unambiguous definition of the Lagrangian pdf for the carrier phase in terms of surrogate fluid particles: it is the probability density of the event

$$S_t = [\mathbf{U}^{+,(s)}(t, \mathbf{Y}^{(s)}) = \mathbf{u}, \mathbf{X}^{+,(s)}(t, \mathbf{Y}^{(s)}) = \mathbf{x}]$$

conditional on the event that

$$S_0 = [\mathbf{U}^{+,(s)}(t_0, \mathbf{Y}^{(s)}) = \mathbf{u}_0]$$

We denote this surrogate fluid–particle Lagrangian density as $f_L^{(s)}(\mathbf{u}, \mathbf{x}; t \mid \mathbf{u}_0, \mathbf{Y})$.

4.3.4 Consistency between Lagrangian and Eulerian descriptions of the carrier phase

In single–phase flows, the concept of a physical fluid particle introduces the notion of a Lagrangian transition density. The mass of a material element is conserved, and hence one can determine the Eulerian pdf at any later time with the knowledge of Eulerian pdf at initial time using the Lagrangian density. In each realization of a two–phase flow, the analogous definition of the material element for the carrier phase of a two–phase flow remains valid. However, in the light of the discussion thus far, the carrier phase is meaningfully represented as surrogate fluid particles. Since these are notional particles, it is not necessary that they individually satisfy any mass constraint. However, the statistical information represented by these surrogate fluid particles need to satisfy certain constraints.

This leads us to an important consideration of whether the carrier–phase Lagrangian density in two–phase flows can function as a transition density of the Eulerian pdf in a manner

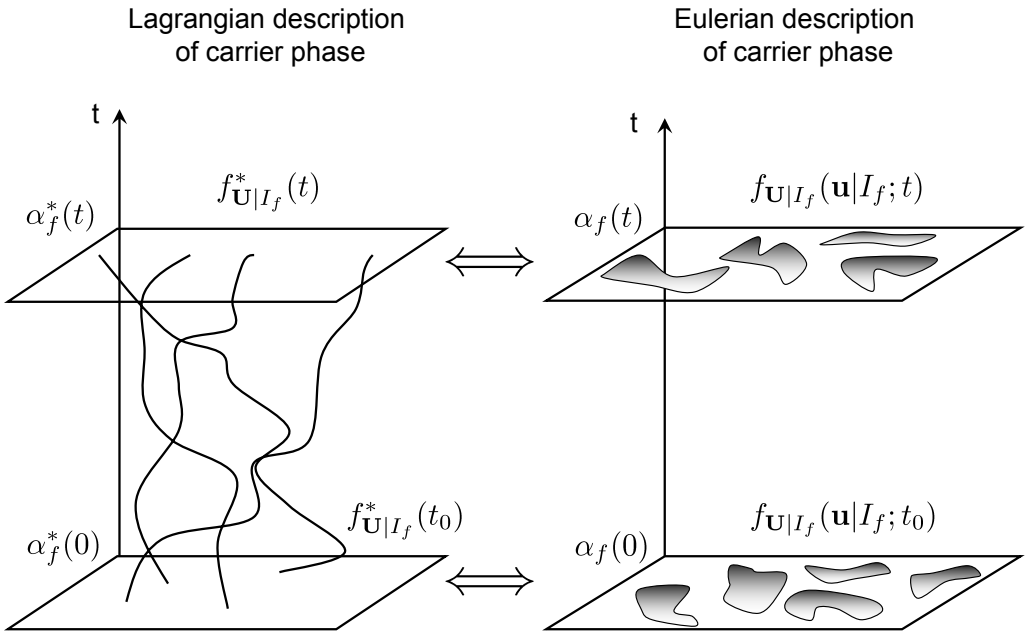

Figure 4.3 Schematic showing the requirement for consistency between the Lagrangian description of the carrier phase as an ensemble of surrogate fluid particles and the corresponding Eulerian description. At initial time, the right panel shows a particular initial condition in terms of α_f and $f_{\mathbf{U}|I_f}$. The notional particle ensemble corresponding to this state should be consistent with α_f and $f_{\mathbf{U}|I_f}$. As the notional particles evolve (shown using surrogate particle trajectories), the consistency has to be enforced at any future time instant t.

similar to that in single–phase flows. In other words, is a relation of the form

$$f_{\mathbf{U}|I_f}(\mathbf{u}|I_f;\mathbf{x},t) = \int f_L^{(s)}\left(\mathbf{u},\mathbf{x};t \mid \mathbf{u}_0,\mathbf{Y}\right) f_{\mathbf{U}|I_f}(\mathbf{u}_0|I_{f0};\mathbf{Y},t_0)d\mathbf{Y}d\mathbf{u}_0 \tag{4.26}$$

valid for two–phase flows?

It turns out that since the carrier phase is viewed as an ensemble of surrogate fluid particles or notional particles, such a physical interpretation of $f_L^{(s)}$ as the transition density for the pdf $f_{\mathbf{U}|I_f}$ is not meaningful. However, $f_L^{(s)}$ can be considered the transition density for the Eulerian density implied by surrogate fluid particles.

The observation that $f_L^{(s)}$ is not a meaningful transition density for $f_{\mathbf{U}|I_f}$ does not imply that the evolution of the surrogate fluid particles can be arbitrarily specified; the surrogate two–

phase system must evolve in such a way that it is consistent with the corresponding statistical description of the two–phase flow in the EE representation. Figure 4.3 shows a schematic of the consistency requirement that needs to be satisfied by the Lagrangian system at all time. At initial time, the surrogate fluid particles are initialized such that they imply a volume fraction $\alpha_f^*(t = 0)$ (the dependence on position is suppressed for brevity) and an Eulerian phasic pdf $f^*_{\mathbf{U}|I_f}(\mathbf{u}|I_f; t_0)$ (or the mass density $\mathcal{F}^*_{\mathbf{U}|I_f}(\mathbf{u}|I_f; t)$). The same correspondence needs to be respected at later time t. In the figure and in the rest of this work, modeled Eulerian quantities are represented with a $*$ superscript. The paths traversed by the notional particles can cross each other since the state of the particle at future time is not uniquely determined by its state at initial time. As noted earlier in this study, these notional particles can occupy any physical location in the two–phase system.

Another consequence of the above interpretation of $f_L^{(s)}$ is that there could be several Lagrangian transition densities that can correspond to the Eulerian description of the carrier phase. In other words, to any initial state S_0 described by an Eulerian one–point pdf (at any later time), there can correspond several Lagrangian densities of the surrogate fluid particles. Thus, the correspondence viz., Lagrangian surrogate fluid particles $\longrightarrow$ single–point Eulerian pdf, is a many–to–one mapping.

4.3.5 Modeled mass density corresponding to Lagrangian notional fluid particles

We have noted that the Lagrangian surrogate particles are meaningfully viewed as computational particles. Since the computational particles have to evolve in such a manner that their implied mass density corresponds to the Eulerian mass density, we can think of a system of N particles

$$\mathcal{F}'^*_s(\mathbf{u}, \mathbf{x}, t) = \sum_{i=1}^{N} \mu^{(i)} \delta(\mathbf{u} - \mathbf{U}^{(i)}) \delta(\mathbf{x} - \mathbf{X}^{(i)}), \tag{4.27}$$

where $\mu^{(i)}$ is the mass associated with each notional fluid particle, and $\mathbf{U}^{(i)}$ and $\mathbf{X}^{(i)}$ are the (Lagrangian) velocity and (Lagrangian) position associated with each notional particle, respectively. The subscript s denotes surrogate and superscript * denotes modeled quantities. We could ideally require this mass density to be consistent with $\mathcal{F}_{\mathbf{U}|I_f}$. However, due to the

presence of unclosed terms in the mass density evolution equation in the EE representation, we can only require the modeled mass density implied by the Lagrangian notional particles to be consistent with the modeled Eulerian mass density $\mathcal{F}^*_{\mathbf{U}|I_f}$. In other words, we require

$$\left\langle \mathcal{F}'^*_s \right\rangle = \mathcal{F}^*_s = \mathcal{F}^*_{\mathbf{U}|I_f}. \tag{4.28}$$

This implies that the mean mass represented by the computational particles must correspond to $\langle \rho I_f \rangle^*$, which is the modeled mean mass in the fluid phase:

$$\int \left\langle \mathcal{F}'^*_s \right\rangle d\mathbf{u} = \int \mathcal{F}^*_{\mathbf{U}|I_f} d\mathbf{u} \tag{4.29}$$

or

$$\sum_{i=1}^{N} \left\langle \mu^{(i)} \delta(\mathbf{x} - \mathbf{X}^{(i)}) \right\rangle = \langle \rho I_f \rangle^* , \tag{4.30}$$

where the expectation can be taken inside the summation since the notional particles are independent and identically distributed. The left hand side of Eq. (4.30) can be written as

$$\sum_{i=1}^{N} \left\langle \mu^{(i)} \delta(\mathbf{x} - \mathbf{X}^{(i)}) \right\rangle = n_c \langle \mu \rangle, \tag{4.31}$$

where n_c is the number density of computational particles corresponding to the carrier phase, and $\langle \mu \rangle$ is the mean mass associated with each computational particle.

Thus,

$$n_c \langle \mu \rangle = \langle \rho I_f \rangle^* \tag{4.32}$$

$$\frac{n_c}{\langle N_s \rangle} \langle \mu \rangle \langle N_s \rangle = \langle \rho I_f \rangle^* \tag{4.33}$$

$$f_{\mathbf{X},c} = \frac{\langle \rho I_f \rangle^*}{\langle \mu \rangle \langle N_s \rangle}, \tag{4.34}$$

where $f_{\mathbf{X},c}$ is the position pdf of the computational particles corresponding to the carrier phase. The final relation above suggests that in a computational cell of the two–phase flow domain, the position pdf of the surrogate fluid particles is given by the ratio of the modeled mean mass as implied by the Eulerian mass density to the mean total mass corresponding to the computational particles.

Starting from the definition of the mass density implied by the surrogate fluid particles Eq. (4.27), one can derive the evolution equation for the $\mathcal{F}_s^*$ by the usual method of taking the time derivative of Eq. (4.27) to give

$$\frac{\partial \mathcal{F}_s^*}{\partial t} + u_k \frac{\partial \mathcal{F}_s^*}{\partial x_k} + \frac{\partial}{\partial u_k}\left[\left\langle \frac{\partial}{\partial t} U_k^{(i)} \Big| \mathbf{u}, \mathbf{x} \right\rangle f_{s,\mathbf{U}}^*\right] = f_{s,\mathbf{U}}^* \left\langle \frac{\partial \ln \mu^{(i)}}{\partial t} \Big| \mathbf{u}, \mathbf{x} \right\rangle, \tag{4.35}$$

where $f_{s,\mathbf{U}}^*$ is the instantaneous two–phase velocity pdf modeled by the surrogate fluid particles. The above equation can be compared with a modeled form of the Eulerian mass density

$$\frac{\partial \mathcal{F}_{\mathbf{U}|I_f}^*}{\partial t} + u_k \frac{\partial \mathcal{F}_{\mathbf{U}|I_f}^*}{\partial x_k} + \frac{\partial}{\partial u_k}\left[A_k^* f_{\mathbf{U}}^*\right] = f_{\mathbf{U}}^* \left\langle S_\rho^* | \mathbf{u} \right\rangle. \tag{4.36}$$

Integrating Eq. (4.35) over velocity space results in the evolution equation for the implied mean mass corresponding to the surrogate fluid particles:

$$\frac{\partial n_c \langle \mu \rangle}{\partial t} + \frac{\partial \left\langle U_k \right\rangle_s n_c \langle \mu \rangle}{\partial x_k} = \left\langle \frac{\partial \ln \mu^{(i)}}{\partial t} \Big| \mathbf{x} \right\rangle. \tag{4.37}$$

Similarly, integrating Eq. (4.36) over velocity space results in the evolution equation for the modeled mean mass:

$$\frac{\partial \left\langle \rho I_f \right\rangle^*}{\partial t} + \frac{\partial \left\langle U_k^* \right\rangle \left\langle \rho I_f \right\rangle^*}{\partial x_k} = \left\langle S_\rho^* \right\rangle \tag{4.38}$$

A comparison of the last two equations reveals that in order for the mean mass represented by the surrogate fluid particles to correspond to the modeled mean mass, the mean velocity $\langle \mathbf{U} \rangle_s$ should be equal to $\langle \mathbf{U}^* \rangle$, and the mass corresponding to the surrogate fluid particles must evolve such that

$$\left\langle \frac{\partial \ln \mu^{(i)}}{\partial t} \Big| \mathbf{x} \right\rangle = \left\langle S_\rho^* \right\rangle. \tag{4.39}$$

For constant density flows, $\left\langle S_\rho^* \right\rangle = 0$ and so the mass $\mu^{(i)}$ corresponding to the surrogate fluid particles must not evolve in time.

Although the carrier phase is represented as an ensemble of computational particles, one would expect that an underlying pressure solution (in constant density flows) is necessary to obtain the mean pressure fields. This mean pressure field is then used in the evolution of the computational particles. One would then require a consistency between the mean pressure Poisson equation implied by Eq. (4.35) and the pressure solution on an underlying grid (typically obtained from Eq. (4.36)). Details on this consistency condition will be presented as a part of future work.

4.4 Summary

In the following a summary of the development of the Lagrangian description of the carrier phase in a two–phase flow is presented.

1. In a Lagrangian statistical description of the carrier phase, it is not tractable to follow a fluid particle as is done in single–phase flows.

2. The statistical description of dispersed phase in terms of the Liouville density requires an intermediate symmetrization to be performed. A unique single–particle surrogate density is then obtained by successive integration of the symmetrized Liouville density. Analogous to the multiparticle Liouville description of the dispersed phase, a multipoint description of the fluid phase is sought. The symmetrization of the dispersed–phase Liouville density implies an analogous requirement on the carrier phase multipoint pdf. The unique single–point surrogate pdf obtained by successive integration of the symmetrized multipoint pdf characterizes the state of the carrier phase in a two–phase flow.

3. During the course of the symmetrization and successive integration, the carrier phase loses its identity as being composed by a continuum of fluid particles. The end result is that the carrier phase is envisaged as being composed of surrogate fluid particles. In the light of this observation, it is fruitful to visualize the carrier phase as composed of notional particles or computational particles.

4. The Lagrangian description in terms of the initial state and the state of the carrier phase at a future time is written in terms of the surrogate fluid particles. A Lagrangian pdf is defined in terms of the surrogate particles. However, this pdf cannot be thought of as a transition density corresponding to the Eulerian pdf analogous to single–phase flows; it is a transition density corresponding to the surrogate fluid particles.

5. Since the Lagrangian density is defined in terms of notional particles, several different Lagrangian densities can correspond to the same Eulerian one–point pdf or mass density. Herein lies the important distinction from the Lagrangian density in single phase flows:

in single phase flows, the Lagrangian density corresponding to an Eulerian one–point pdf is unique.

6. The mass density implied by the Lagrangian notional particles has to satisfy certain consistency conditions both at initial time and at any future time. At future time, Lagrangian densities of surrogate fluid particles that satisfy this consistency condition can be related to the Eulerian pdf corresponding to the state at that time. Thus, the mapping between the Lagrangian densities and the Eulerian pdf is many–to–one.

7. The mass of a computational particle corresponding to the carrier phase has to evolve such that the mean mass implied by the computational particles is consistent with the mean mass corresponding to the modeled Eulerian mass density.

In summary, in two-phase flows, one cannot go from the Lagrangian to the Eulerian description of the carrier phase as is easily done in the context of single-phase flows. In fact, the Lagrangian description of the carrier phase depends on the EE description for its definition and evolution.

4.4.1 Consistent statistical representation of two–phase flows

The Lagrangian statistical representation of the carrier phase was presented. With this a statistical description connecting the EE, LE and LL representations has been established. The connection between the EE and the LE representations was presented in Chapter 3. Advantages and limitations of each representation were reviewed in the light of the relationship between the two representations. In this chapter the connection between the LL and the other two statistical representations was presented. In particular, the Lagrangian description of the dispersed phase in terms of the droplet distribution function is retained in the LL formalism, primarily because we believe that spray equation formalism has been rigorously analyzed and its theoretical basis established based on sound physical principles. The Eulerian description of the carrier phase is identical in both the EE and LE formalisms. In this chapter, the Lagrangian description of the carrier phase is shown to be connected to the Eulerian description. However, it is shown that the Lagrangian description of the carrier phase is not tractable in terms of physical fluid

particles, but is correctly interpreted in terms of surrogate fluid particles or notional particles. It is noted that the mass density implied by the notional particles has to be equal to the Eulerian description of the carrier phase, in order for the evolution of the notional particles to be consistent with the evolution of the two–phase flow.

The theory behind the LL representation motivates one to seek a particle–method solution to the governing equations for the carrier phase in a two–phase flow. One such recipe is proposed in Chapter 6 in the form of a dual–timescale Langevin model. This model is a system of two stochastic differential equations (SDE) for the fluctuating velocities, one in the carrier phase and the other in the dispersed phase. The Fokker–Planck equation corresponding to the carrier–phase SDE can be considered to be a model of the type given by Eq. (4.36).

The remaining chapters are devoted to modeling in the context of the LE and LL statistical representations of two–phase flows.

CHAPTER 5. AN IMPROVED TURBULENCE MODEL FOR LAGRANGIAN–EULERIAN COMPUTATIONS

In this chapter on modeling in turbulent multiphase flows, a new multiscale interaction timescale for particle–turbulence interaction is proposed that can capture the multiscale interaction of particles and the carrier–phase turbulence.

A significant part of this chapter has appeared in 'M. G. Pai and S. Subramaniam, Modeling Interphase Turbulent Kinetic Energy Transfer in Lagrangian-Eulerian Spray Computations, Atomization and Sprays, vol. 16. pp. 807–826, 2006.'

Modeling turbulent multiphase flows is a major challenge owing to droplet (or solid–particle) interactions with a wide range of turbulence length and timescales. In a broad class of Lagrangian–Eulerian models, the instantaneous Lagrangian dispersed phase velocity evolves on a timescale that is proportional to the particle response time $\tau_p = \rho_d d^2/18\mu_f$. Numerical simulations of a model from this class reveal a non-monotonic and unphysical increase of the TKE in the dispersed phase k_d that is not seen in direct numerical simulations (DNS) of decaying, homogeneous turbulence laden with solid particles. Analysis of this class of models shows that for a linear drag law corresponding to the Stokes regime, the entire class of models will predict an anomalous increase in k_d for decaying turbulent flow laden with solid particles or droplets. Even though the particle response time is the appropriate time scale to characterize momentum transfer between sub–Kolmogorov size dispersed phase particles and the smallest turbulent eddies (for droplet/particle Reynolds number less than one), it is incapable of capturing the range of time and length scale interactions that are reflected in the evolution of k_d. A new model that employs a timescale based on a multiscale analysis is proposed. This model succeeds in capturing the dispersed phase TKE and fluid phase TKE

evolution observed in DNS. The model also correctly predicts the trends of TKE evolution in both phases for different Stokes numbers.

5.1 Introduction

Turbulence in the ambient gas is important in determining the evolution of a spray. It affects the rate of entrainment of ambient gas into the spray cone, which in turn strongly influences the spray angle and other global characteristics like the spray penetration length. The turbulent two–phase flow at the edge of a spray is a very complex physical phenomenon involving high shear rates, large fluctuations in instantaneous liquid volume fraction and interphase mass transfer (in the case of vaporizing sprays). It is recognized that statistical models of sprays must represent the evolution of velocity fluctuations in the gas as well as the droplets in order to predict global spray properties, but current models for these quantities are still in need of improvement.

This study focuses on a considerably simpler turbulent two–phase flow problem of sub–Kolmogorov size *solid* particles evolving in zero–gravity, constant–density, decaying homogeneous turbulence. The goal is to understand and assess current Lagrangian–Eulerian (LE) models and to propose model improvements. The choice of this simple problem is motivated by two reasons. One is that this problem isolates two important flow processes: (i) the interphase transfer of turbulent kinetic energy (TKE), and (ii) the dissipation rate of TKE in the carrier fluid, which enables a detailed evaluation of existing models. The second reason is that direct numerical simulation (DNS) datasets are available from carefully controlled studies of this flow in decaying turbulence (Sundaram and Collins, 1999). Although turbulent flows laden with solid particles will behave differently from droplet–laden turbulent flows in general, all features of the models we consider are identical in the limit of sub–Kolmogorov size non–vaporizing droplets evolving in zero–gravity, constant–density, homogeneous turbulence. While in the more general case spray models must account for phenomena like droplet vaporization and its effect on turbulence, we find that there is considerable scope for model improvement even in non–vaporizing cases like the simple flow considered here.

The LE approach is based on Williams' spray equation (Williams, 1958), which is an evolution equation for the droplet distribution function (ddf) the theoretical foundations of which are now rigorously established and understood (Subramaniam, 2000, 2001c). The evolution equation for the second moment of dispersed phase velocity in the LE approach has also been derived from the spray equation by Subramaniam (2003), and forms the theoretical basis of this investigation. In this work, the focus is on testing and evaluating specific models in a simple flow to determine whether the predicted evolution of the TKE in each phase is physically consistent with DNS results. Based on these findings we propose an improved model.

It is important to note that all the LE models considered here are *first–order* models based on the average number density. This is of course a direct consequence of their being a solution approach to the spray equation. A first–order model cannot represent certain physical phenomena like preferential concentration of droplets (or solid particles) in homogeneous turbulence. The proper description of such phenomena will require the consideration of *second–order* statistics like the pair–correlation function. This is not to imply that *second–order* effects such as preferential concentration are not important, but rather that our current modeling capabilities are still in need of further development before they can represent these phenomona.

The rest of the chapter is organized as follows. A model problem involving particles (or non–evaporating droplets) evolving in homogeneous turbulence is described in Section 5.2. The evolution equation for the dispersed phase TKE simplifies for the homogeneous problem, and depends solely on the particle acceleration-velocity covariance, which needs to be modeled. Details of DNS results available from a homogeneous particle–laden turbulent flow that are used to assess model predictions are given in Section 5.3. A drag model based on the particle response time that is widely used in LE implementations is presented in Section 5.4. Evolution equations for the dispersed phase TKE as implied by this drag model, and the modeled evolution equation for the TKE in the fluid phase are derived. Model predictions for freely decaying particle–laden turbulence are reported in Section 5.5. A theoretical analysis reveals that the particle–response time is not an appropriate timescale for interphase TKE transfer. A multiscale interaction timescale is then proposed that improves model predictions for the decaying

turbulence case. The implications of the study are discussed in Section 5.8 and conclusions are drawn in the final section.

5.2 Homogeneous two-phase flow model problem

A canonical problem that is useful in assessing the behavior of turbulent two–phase flow models is now described. The problem consists of sub–Kolmogorov size particles evolving in zero–gravity, constant–density, homogeneous turbulence. If gravity is neglected then the mean pressure gradient must also be zero and the mean momentum equation admits a trivial solution of zero mean velocity in each phase, which in turn implies a zero mean slip velocity. The evolution of TKE in each phase can then be studied *independent* of the mean flow quantities.

Exact governing equations for the second moment of dispersed phase velocity for an inhomogeneous system of evaporating droplets with no coalescence, collisions or break–up is given in Eq. (3.112). The equation for the dispersed phase TKE is then obtained by contracting the second–moment equation. With the assumptions of zero interphase mass transfer, constant density, and statistical homogeneity, Eq. (3.112) simplifies to

$$\frac{\partial \widetilde{\langle v_i'' v_j'' \rangle}}{\partial t} = \left[\widetilde{\langle A_i v_j'' \rangle} + \widetilde{\langle A_j v_i'' \rangle} \right], \tag{5.1}$$

where $\widetilde{\langle A_j v_i'' \rangle}$ is the acceleration–fluctuating velocity correlation. In the canonical homogeneous problem the evolution of the second moment of particle velocity is solely determined by the model for the acceleration–fluctuating velocity covariance (the right hand side of Eq. (5.1)).

Taking one half the trace of Eq. (5.1) results in the evolution equation for the TKE in the dispersed phase $\tilde{k}_d = (1/2)\widetilde{\langle v_i'' v_i'' \rangle}$ as

$$\frac{\partial \tilde{k}_d}{\partial t} = \widetilde{\langle A_i v_i'' \rangle}. \tag{5.2}$$

The *tilde* in the above equations represent mass weighting (or volume weighting for constant thermodynamic density in the dispersed phase)[1]. Mass–weighting of terms is necessary to consistently account for the interphase TKE terms that appear in the evolution equation for the TKE and dissipation in the gas phase (cf. Eq. (5.13) and Eq. (5.14)). Moreover, mass–weighted

[1]See Appendix D for the definitions of mass weighting and number weighting

governing equations from the LE approach have a direct correspondence with their counterparts in the Eulerian–Eulerian or two–fluid approach. Since the dispersed–phase thermodynamic density is constant, the distinction between volume weighting and mass weighting is not needed in the rest of the paper. Furthermore, since this study focuses on monodispersed particles with no evolution of their radii in time, number-weighted quantities are the same as their weighted counterparts. Hence, the tilde can be dropped in Eqs. (5.1)–(5.2), and in the equations in the rest of the paper.

5.3 DNS results for the homogeneous model problem

Several researchers (Sundaram and Collins, 1999; Mashayek et al., 1997; Boivin et al., 1998) have performed DNS of particle–laden homogeneous turbulence. These DNS results can be used to validate two–phase turbulence models. Sundaram and Collins (1999) have performed a study on particle–laden freely decaying turbulence in the absence of gravity for several Stokes numbers. The Stokes number St_η is defined as the ratio of the particle response timescale τ_p to the Kolmogorov timescale τ_η, and characterizes the tendency of a particle to follow the turbulent fluctuations of the carrier phase. The particle response timescale is defined as $\tau_p = (\rho_d d^2)/(\rho_f 18\nu_f)$ and the Kolmogorov timescale is given by $\tau_\eta = (\nu_f/\varepsilon_f)^{1/2}$. The system is volumetrically dilute, with particles in the sub–Kolmogorov size range and collisions among particles, if any, are assumed to be elastic. Particles are assumed to be point sources/sinks and the simulation is two–way coupled, i.e., the effect of the particles on fluid phase momentum conservation is also accounted for. Parameters of the homogeneous model problem are given in Tables 5.1-5.2. In Table 5.1 u' is the initial turbulence intensity in the fluid phase and v' is the initial turbulence intensity in the dispersed phase. These intensities are related to the respective TKE in each phase at initial time through $u'^2 = (2/3)k_f(0)$ and $v'^2 = (2/3)k_d(0)$. The following section describes LE models that can be used to model this turbulent two–phase flow.

5.4 Lagrangian models for particle velocity

LE models indirectly solve the ddf evolution equation using a particle method for reasons of computational efficiency and ease of modeling. In this approach, an ensemble of N identically distributed computational particles is used to indirectly represent the modeled ddf. With each computational particle we associate a position vector $\mathbf{X}_p^{(i)}$, velocity vector $\mathbf{V}_p^{(i)}$, radius $R_p^{(i)}$ and a statistical weight $w_p^{(i)}$.[2] The evolution equation for the particle velocity implies a modeled evolution equation for the ddf of fluctuating velocity and the second moment Eq. (3.112). The particle velocity evolution equation

$$\mathbf{A}^* = \frac{d\mathbf{V}_p^*}{dt} = \Omega_p^* \left(\mathbf{U}_f^* - \mathbf{V}_p^* \right) + \mathbf{g} \tag{5.3}$$

defines a class of Lagrangian models that subsumes the vast majority of models (Sundaram and Collins, 1999; Amsden et al., 1989; Ormancey and Martinon, 1984; Brown and Hutchinson, 1979; Gosman and Ioannides, 1983) in the literature. In Eq. (5.3), $\mathbf{A}^*$ is the modeled particle acceleration, $\mathbf{U}_f^*$ and $\mathbf{V}_p^*$ are the modeled gas phase and dispersed phase instantaneous velocities respectively, $\mathbf{g}$ is the acceleration due to gravity and Ω_p^* is a characteristic particle response frequency[3]. The particle response frequency depends the drag coefficient C_D, which is a function of particle Reynolds number Re_p. Models proposed in literature for Ω_p^* (see Amsden et al. (1989) for example) can be cast in the following form:

$$\Omega_p^* = \frac{1}{\tau_p} f(Re_p), \tag{5.4}$$

where $f(Re_p)$ represents a functional dependence of the model for C_D on Re_p. This form (cf. Eq. (5.3)) of the particle acceleration model is based on the equation of motion of a sphere in a fluid under the influence of only drag and body forces Maxey and Riley (1983). The models in this class differ only in terms of the particle response frequency model, and the model for the gas phase velocity.

[2]The definition of the statistical weight $w_p^{(i)}$ is not unique, but the sum of weights over all computational particles must sum to unity: $\sum_{i=1}^{N} w_p^{(i)} = 1$. In KIVA Amsden et al. (1989), the statistical weight is defined as $w_p^{(i)} = n_s^{(i)}/\langle N_s \rangle$, where $n_s^{(i)}$ is the number of droplets represented by each computational particle and $\langle N_s \rangle$ is the mean total number of droplets represented by the ensemble.

[3]The superscript '*' in Eq. (5.3), and in the rest of this work is used to denote modeled quantities, which are only approximations to their exact unclosed counterparts. For example, $\mathbf{A}^*$ in Eq. (5.3) is a model for $\mathbf{A}$ in Eq. (3.130).

The instantaneous gas phase velocity is decomposed into a mean component $\langle \mathbf{U}_f \rangle^*$, and a fluctuating component $\mathbf{u}_f'^*$, which are related by

$$\mathbf{U}_f^* = \langle \mathbf{U}_f \rangle^* + \mathbf{u}_f'^*. \tag{5.5}$$

In the Lagrangian–Eulerian approach, the solution to the averaged Eulerian equations in the gas phase yields a mean gas phase velocity $\langle \mathbf{U}_f \rangle^*$ while the fluctuation in the gas phase velocity $\mathbf{u}_f'^*$ is modeled. Together the mean and fluctuating gas phase velocities form a model for the instantaneous gas phase velocity $\mathbf{U}_f^*$.

The particle–velocity evolution model implemented in KIVA (Amsden et al., 1989) also belongs to the general class of Lagrangian models considered here. The particle acceleration $\mathbf{A}^*$ in KIVA (Amsden et al., 1989) is modeled as

$$\frac{d\mathbf{V}_p^*}{dt} = \frac{3}{8}\frac{\rho_f}{\rho_d}\frac{|\langle \mathbf{U}_f \rangle^* + \mathbf{u}_f'^* - \mathbf{V}_p^*|}{R_p}(\langle \mathbf{U}_f \rangle^* + \mathbf{u}_f'^* - \mathbf{V}_p^*)C_D + \mathbf{g}. \tag{5.6}$$

The drag coefficient C_D is given by,

$$C_D = \begin{cases} \dfrac{24}{Re_p}\left(1 + \dfrac{Re_p^{2/3}}{6}\right) & Re_p < 1000 \\ 0.424 & Re_p > 1000, \end{cases} \tag{5.7}$$

where the particle Reynolds number

$$Re_p = \frac{2\rho_f |\langle \mathbf{U}_f \rangle^* + \mathbf{u}_f'^* - \mathbf{V}_p^*| R_p}{\mu_f} \tag{5.8}$$

and μ_f is the dynamic viscosity of the gas. The limit of Stokes drag results in $C_D Re_p = 24$ corresponding to a particle Reynolds number $Re_p \ll 1$. Note that Stokes drag is a remarkably good approximation even for $Re_p \sim 1$ since at this particle Reynolds number, the Stokes law predicts a drag that is only 10% in error (see (Bird et al., 2002), pg. 61).

Models for fluctuating gas phase velocity

The fluctuating gas phase velocity $\mathbf{u}_f'^*$ is usually sampled from a joint–normal probability density with zero mean and covariance equal to $(2k_f/3)\delta_{ij}$ under the assumption that the

turbulence is isotropic. This velocity is kept constant over a time interval, called the turbulence correlation time, which is taken to be the minimum of an eddy traverse time t_R and an eddy–life time t_E. At the end of the time interval the renewal time is reached, and a new value of fluctuating velocity $\mathbf{u}'^*_f$ is sampled. This is intended to capture the effect of crossing trajectories as a particle shoots across successive eddies. Such models for the fluctuating gas phase velocity are commonly known as *eddy life time* models (ELT). Brown and Hutchinson (1979), and Gosman and Ioannides (1983) used a linearized form of the equation of motion of a droplet to arrive at an eddy traverse time $t_R = -\tau_p \ln(1.0 - l_e/(\tau_p|\mathbf{U}^*_f - \mathbf{V}^*_p|))$, where the characteristic length scale of the eddy $l_e = C_\mu^{1/2} {k_f}^{3/2}/\varepsilon_f$. They also proposed a model for the eddy life time as $t_E = l_e/|\mathbf{u}'^*_f|$. Ormancey and Martinon (1984) proposed that the time intervals over which $\mathbf{u}'^*_f$ remains constant be exponentially distributed (Poisson model), with the mean time interval equal to the Lagrangian integral time scale of turbulence T_L. Amsden et al. (1989) used a model similar to Hutchinson's but with $t_E = k_f/\varepsilon_f$ and $t_R = C_{ps}({k_f}^{3/2}/\varepsilon_f)|\langle\mathbf{U}_f\rangle^* + \mathbf{u}'^*_f - \mathbf{V}^*_p|^{-1}$, where C_{ps} is a model constant equal to 0.16432 ($= C_\mu^{3/4}$). This model has been incorporated into the popular KIVA family of codes (Amsden et al., 1989).

Implied evolution of dispersed phase TKE

The velocity covariance evolution implied by the class of particle velocity evolution models discussed in the previous section (including the KIVA model) can be analyzed for the homogeneous model problem. With assumptions of statistical homogeneity [4] and a monodisperse size distribution of solid particles (or droplets), the mean and second–moment equations implied by such drag models are considerably simplified.

From Eq. (5.6) one can infer an instantaneous particle response frequency Ω^*_p as

$$\Omega^*_p = \frac{3}{8}\frac{\rho_f}{\rho_d}\frac{|\langle\mathbf{U}_f\rangle^* + \mathbf{u}'^*_f - \mathbf{V}^*_p|}{R_p} C_D. \tag{5.9}$$

The evolution equation for the second moments of the dispersed phase velocity as implied by Eq. (5.6) can be derived to be

[4] The assumption of statistical homogeneity implies that the position property need not be retained.

$$\begin{aligned}\frac{d\langle v_i'^* v_j'^* \rangle}{dt} =& \langle v_i'^* \omega^* \rangle \langle U_{f\,j} \rangle^* + \langle v_j'^* \omega^* \rangle \langle U_{f\,i} \rangle^* \\ &- \langle v_i'^* \omega^* \rangle \langle V_{p\,j}^* \rangle - \langle v_j'^* \omega^* \rangle \langle V_{p\,i}^* \rangle \\ &- \langle v_i'^* \Omega_p^* v_j'^* \rangle - \langle v_j'^* \Omega_p^* v_i'^* \rangle \\ &+ \langle v_i'^* \Omega_p^* u_j'^* \rangle + \langle v_j'^* \Omega_p^* u_i'^* \rangle \end{aligned} \tag{5.10}$$

where $\omega^* \equiv \Omega_p^* - \langle \Omega_p^* \rangle$ is the modeled fluctuating response frequency of the dispersed phase defined with respect to the mean particle response frequency $\langle \Omega_p^* \rangle$, and $v_j'^* \equiv V_{p\,j}^* - \langle V_{p\,j}^* \rangle$ is the modeled fluctuating velocity of the dispersed phase defined with respect to the number–weighted mean velocity $\langle V_{p\,j}^* \rangle$ in the dispersed phase. The modeled evolution equation for k_d^* is then obtained by contracting indices Eq. (5.10):

$$\begin{aligned}\frac{dk_d^*}{dt} =& \langle v'^*_i \omega^* \rangle \left[\langle U_{f\,i} \rangle^* - \langle V_{p\,i}^* \rangle \right] - \langle v'^*_i \Omega_p^* v'^*_i \rangle \\ &+ \langle v'^*_i \Omega_p^* u_i'^* \rangle. \end{aligned} \tag{5.11}$$

For the case of zero mean slip, which is the case under consideration, Eq. (5.11) simplifies to

$$\frac{dk_d^*}{dt} = -\langle v'^*_i \Omega_p^* v'^*_i \rangle + \langle v'^*_i \Omega_p^* u_{f\,i}'^* \rangle. \tag{5.12}$$

Comparing Eq. (5.12) with Eq. (5.2), one can infer that if Eq. (5.6) is used as a particle velocity evolution equation, then the implied model for the acceleration-fluctuating velocity correlation $\langle A_i v_i'' \rangle$ is $-\langle v'^*_i \Omega_p^* v'^*_i \rangle + \langle v'^*_i \Omega_p^* u_{f\,i}' \rangle$. We can also expect that k_d^* in Eq. (5.12) could either decay or increase depending on the relative magnitudes of the terms on the right hand side of Eq. (5.12). Since these terms involve triple correlations among fluctuating quantities, it is hard to enforce any physical constraint on them such that k_d^* evolves according to trends seen in DNS or experiments.

Evolution of fluid–phase TKE

In the LE approach a modified k-ϵ model is used to evolve the turbulent kinetic energy and dissipation in the gas phase. The modeled equation for k_f^* (for the statistically homogeneous,

zero mean–slip case) used here is (Subramaniam, 2003; Amsden et al., 1989),

$$\frac{d(\rho_f \alpha_f k_f^*)}{dt} = -\rho_f \alpha_f \varepsilon_f^* + \left[\rho_d \alpha_d \left\{ \langle u_{f_j}'^* \Omega_p^* v_j'^* \rangle - \langle u_{f_j}'^* \Omega_p^* u_{f_j}'^* \rangle \right\}\right]. \tag{5.13}$$

The term in square brackets on the right hand side of Eq. (5.13) arises from a model that represents the rate at which the turbulent eddies do work in dispersing the spray droplets. This term represents the TKE transfer between the dispersed phase and the gas phase. The modeled equation for the dissipation (Subramaniam, 2003; Amsden et al., 1989) in the fluid phase ε_f is

$$\frac{d(\rho_f \alpha_f \varepsilon_f^*)}{dt} = -C_{\varepsilon 2} \rho_f \alpha_f \frac{\varepsilon_f^{*2}}{k_f^*} + \left[C_s \frac{\varepsilon_f^*}{k_f^*} \rho_d \alpha_d \left\{ \langle u_{f_j}'^* \Omega_p^* v_j'^* \rangle - \langle u_{f_j}'^* \Omega_p^* u_{f_j}'^* \rangle \right\}\right]. \tag{5.14}$$

The term in square brackets on the right hand side of Eq. (5.14) represents the contribution to the evolution of the modeled dissipation from the interphase TKE transfer.

It is important to note that most LE models (including KIVA) assume a volumetrically dilute spray $\alpha_d \ll 1$, and because $\alpha_f = 1 - \alpha_d$, it follows that $\alpha_f \approx 1$. On this basis, volume displacement effects are neglected (Amsden et al., 1989), and both Eq. (5.13) and Eq. (5.14) are solved with $\alpha_f = 1$, but with $\alpha_d \neq 0$.

5.5 Model predictions for the homogeneous problem

Predictions of normalized TKE in the fluid phase k_f^*, as a function of scaled time t/T_{ref}, are shown in Figs. 5.1 for increasing Stokes numbers St_η. These predictions are for the homogeneous problem using the KIVA drag model. Here $T_{\text{ref}} = u'/L_E$ is the large eddy turnover timescale (Sundaram and Collins, 1999). Also shown on the same plot is the evolution of k_f^* from the DNS (Sundaram and Collins, 1999) for increasing Stokes number. For a constant mass loading, it is expected that increasing Stokes number quickens the decay of TKE in the fluid phase, and hence the trend depicted by the DNS appears plausible. The predicted trend of k_f^* from KIVA for varying Stokes number does not match the trend depicted in the DNS.

Model prediction of normalized TKE in the dispersed phase k_d^*, as a function of scaled time t/T_{ref}, are shown in Figs. 5.2 for increasing Stokes numbers St_η, alongside results from DNS.

In KIVA, the dispersed phase TKE at the end of every time step is computed as

$$k_d^* = \frac{1}{2}\langle v_i'^* v_i'^* \rangle. \tag{5.15}$$

Again, for a constant mass loading, it is expected that the decay of TKE in the dispersed phase is more rapid for larger Stokes numbers. The model predictions for the evolution of k_d^* for varying Stokes numbers do not match the trends seen in the DNS.

One can make two important observations from the model predictions presented in Fig. 5.1 and 5.2. Firstly, the timescale of decay of k_f^* and k_d^* using the KIVA drag model is significantly lesser than that observed in the DNS. Secondly, an anomalous increase at $t/T_{\text{ref}} = 0.1$, (although slight, for the initial k_d/k_f ratio of unity used in this study), after an initial steep decrease, is seen in the evolution of k_d for $St_\eta = 1.6$. Later it will be shown that this anomalous increase is accentuated at larger initial k_d/k_f ratios. This behavior is deemed unphysical since the flow under consideration does not possess any mechanism to increase the TKE in the dispersed phase, and hence k_d should exhibit a monotonic decrease. On the other hand, the results from DNS show a monotonic decay in the TKE in the gas phase and dispersed phase, which is consistent with the flow physics.

Lagrangian-Eulerian model predictions can exhibit statistical variability due to randomness in initializing the particle properties (in this case, particle velocities). For different initial ensembles, model predictions of k_f^* and k_d^* can be different. Multiple independent simulations are performed with the model and it is observed that the statistical variability in the model predictions due to randomness in the initial conditions is less than 0.2% of the mean. Statistical variability in the model predictions is found to be insignificant compared to the differences observed due to the changing Stokes numbers St_η. It is found that the 95% confidence intervals corresponding to each St_η do not overlap in the model predictions shown in Figs 5.1 and 5.2. Since these confidence intervals are extremely small, they have been omitted in these figures.

5.6 Reason for the anomalous behavior in k_d

The unphysical increase in the k_d evolution can be explained by an exact analysis of the model equations that requires a few simplifying assumptions.

The analysis assumes that: (i) the particle response frequency (cf. Eq. (5.9)) is constant, and (ii) the fluctuating fluid–phase velocity (cf. Eq. (5.6)) is constant (this is true if the decay in the TKE of the fluid phase k_f^* is small over the time for which the analytical predictions are valid). A constant particle response frequency corresponds to a linear drag model. It is observed in the current simulations that a significant number of particles have $Re_p < 1$, a range wherein the Stokes drag is accurate (Bird et al., 2002). It must however be borne in mind that in the KIVA model, Ω_p^* does not remain constant and changes with $\mathbf{V}_p^*$.

Let the particle velocity $\mathbf{V}_p^*$ be distributed joint normally with mean $\langle \mathbf{V}_p^* \rangle = 0$ and covariance $(2/3)k_d(0)\delta_{ij}$. For constant Ω_p^*, the particle velocity evolution equation Eq. (5.6) can be solved to give an expression for the particle velocity $\mathbf{V}_p^*(t)$ at any time t as,

$$V_{p_j}^*(t) = u'^*_{f_j}(0) - [u'^*_{f_j}(0) - v'^*_j(0)]e^{-\Omega_p^* t} \tag{5.16}$$

where $u'^*_{f_j}(0)$ and $v'^*_j(0)$ are evaluated at initial time $t = 0$. The mean particle velocity $\langle V_{p_i}^* \rangle$ at any time t can be computed from Eq. (5.16) as,

$$\begin{aligned} \langle V_{p_i}^* \rangle(t) &= \left\langle u'^*_{f_i}(0) - [u'^*_{f_i}(0) - v'^*_{p_i}(0)]e^{-\Omega_p^* t} \right\rangle \\ &= 0, \end{aligned} \tag{5.17}$$

showing thereby that the mean particle velocity remains zero at all time.

Using Eq. (5.16), one can compute the dispersed–phase TKE $k_d^*(t)$ at any time t as

$$\begin{aligned} k_d^*(t) &= \langle v_i'^* v_i'^* \rangle \\ &= \frac{1}{2} \left\langle \left(V_{p_i}'^*(t) - \langle V_{p_i}'^*(t) \rangle(t) \right) \left(V_{p_i}'^*(t) - \langle V_{p_i}'^*(t) \rangle(t) \right) \right\rangle \\ &= \frac{1}{2} \langle [u'^*_{f_i}(0) - (u'^*_{f_i}(0) - v_i'^*(0))e^{-\Omega_p^* t}][u'^*_{f_i}(0) - (u'^*_{f_i}(0) - v_i'^*(0))e^{-\Omega_p^* t}] \rangle \\ &= \frac{1}{2} \langle u'^*_{f_i}(0)u'^*_{f_i}(0)(1 - e^{-\Omega_p^* t})^2 + v_i'^*(0)v_i'^*(0)e^{-2\Omega_p^* t} + 2u'^*_{f_i}(0)(1 - e^{-\Omega_p^* t})v_i'^*(0)e^{-\Omega_p^* t} \rangle \\ &= k_f(0)(1 - 2e^{-\Omega_p^* t} + e^{-2\Omega_p^* t}) + k_d(0)e^{-2\Omega_p^* t} \end{aligned} \tag{5.18}$$

The last equality follows from the following relations,

$$\langle {u'_{f_i}}^*(0){u'_{f_i}}^*(0)\rangle = 2k_f(0)$$
$$\langle {v'}_i^*(0){v'}_i^*(0)\rangle = 2k_d(0)$$
$$\langle {u'_{f_i}}^*(0){v'}_i^*(0)\rangle = 0.$$

We know that the samples ${u'_{f_i}}^*$ and ${v'}_i^*$ are independent at initial time, so the last relation follows from the fact that their covariance is equal to zero. We now have an analytical expression for the evolution of k_d^* in Eq. (5.18) that is applicable until the first renewal of ${\mathbf{u}'_f}^*$. Using Eq. (5.18), it is straightforward to compute the slope of the k_d^* evolution curve at time $t = 0$ that can explain the reason for the unusually steep initial descent in the evolution of k_d. Differentiating Eq. (5.18) with respect to time,

$$\frac{dk_d^*}{dt} = k_f(0)(2\Omega_p^* e^{-\Omega_p^* t} - 2\Omega_p^* e^{-2\Omega_p^* t}) - 2k_d(0)\Omega_p^* e^{-2\Omega_p^* t}, \tag{5.19}$$

At $t = 0$,

$$\frac{dk_d^*}{dt} = -2\Omega_p^* k_d(0) \tag{5.20}$$

Thus, k_d^* decays initially over a timescale that scales like the inverse of the particle response frequency ${\Omega_p^*}^{-1}$ and is the reason for the steep decay not seen in the DNS results (Sundaram and Collins, 1999). It is worthwhile to note that Eq. (5.18) has an inflection point at t_{infl} given by

$$t_{\text{infl}} = \frac{1}{\Omega_p^*} \ln\left(1 + \frac{k_d(0)}{k_f(0)}\right). \tag{5.21}$$

The decay in normalized k_d^* as predicted by Eq. (5.18) is shown in Fig. 5.3 alongside the evolution of predicted k_d^* from the KIVA drag model for $St_\eta = 1.6$ and two different initial k_d/k_f ratios. As the initial k_d/k_f ratio is decreased the reversal in the evolution of k_d^* is more prominent. The analytical point of inflection is close to the inflection point on the evolution curve of k_d^* from the KIVA drag model. The difference between the analytical and the numerical results until the point of inflection is because Ω_p^* and ${\mathbf{u}'_f}^*$ are not constant in the numerical simulations. The analytical expression predicts the initial steep decay very accurately, thereby illustrating that the unphysical model behavior is not an artifact of the numerical simulation.

Improved particle velocity evolution equation

We have shown that LE models for two–phase turbulence that are based on the particle response time (cf. Eq. (5.3)) result in anomalous evolution of averaged quantites like k_d^*. It is interesting therefore to understand why such particle velocity evolution equations when used in DNS of sub–Kolmogorov size particle–laden turbulent flows Sundaram and Collins (1999) yield plausible results. The answer simply lies in the fact that in the DNS, the particles interact with a range of time and length scales, where $\mathbf{U}_f^*$ appearing in Eq. (5.3) is no longer modeled but is an adequately resolved solution to the Navier–Stokes equation, with additional momentum source terms due to the presence of the particles (Sundaram and Collins, 1999). The particle response timescale is an *appropriate* timescale for the interphase momentum transfer terms that are added to the Navier–Stokes equations. Unfortunately, in LE models (Amsden et al., 1989; Ormancey and Martinon, 1984; Brown and Hutchinson, 1979; Gosman and Ioannides, 1983), the quantity $\mathbf{u}_f'^*$ represents a model for the fluctuating fluid–phase velocity that does not represent all the velocity scales that are captured in the DNS velocity field. Thus, the particle velocity evolution equation in LE computations needs modification to the interaction timescale in order to achieve results comparable with DNS.

5.7 Multiscale interaction timescale $\langle \tau_{\mathbf{int}} \rangle$

The fact that particles interact with a range of turbulence length and timescales—and that such a complex interaction cannot be adequately characterized by the particle response time alone in LE computations—motivates the development of a mean multiscale interaction time $\langle \tau_{\mathrm{int}} \rangle$ in place of $(1/\Omega_p^*)$ in Eq. (5.3). The angled brackets represent an interaction timescale averaged over all eddies, details of which follow. The fluctuating particle velocity relaxes to the local modeled fluctuating fluid velocity on the multiscale interaction timescale $\langle \tau_{\mathrm{int}} \rangle$ as

$$\frac{d\mathbf{v}'^*}{dt} = \frac{\mathbf{u}_f'^* - \mathbf{v}'^*}{\langle \tau_{\mathrm{int}} \rangle}. \tag{5.22}$$

The fluctuating gas phase velocity is modeled as in the original KIVA proposal (Amsden et al., 1989) by sampling from a Gaussian distribution with zero mean and variance $(2/3)k_f$. In

the homogeneous problem under consideration, the mean velocity in either phase is zero for all time. Hence, there is no need to evolve the mean velocities in this case. However, if the mean velocities are non–zero with non–zero mean slip, we hypothesize that the mean velocity in either phase would evolve over a timescale $1/\langle\Omega_p^*\rangle$ derived from Eq. (5.9) and C_D would depend on a mean particle Reynolds number.

The multiscale interaction timescale $\langle\tau_{\text{int}}\rangle$ was introduced by Pai and Subramaniam (2004) and has been successfully employed in the context of Eulerian–Eulerian two–phase turbulence modeling by Xu (2004) and Xu and Subramaniam (2005). This timescale is derived from the gas phase velocity field by first defining a Stokes number valid in the inertial range as

$$St_l = \frac{\tau_p}{\tau_l}, \tag{5.23}$$

where τ_l is computed as

$$\tau_l = \frac{|\mathbf{u}_f'^*|^2}{\varepsilon_f^*}. \tag{5.24}$$

Let us assume that $\mathbf{u}_f'^*$ obeys a joint normal distribution with zero mean and covariance $\sigma_f^2\delta_{ij}$, where $\sigma_f^2 = (2/3)k_f$. With this assumption, the pdf of $|\mathbf{u}_f'^*|$ is

$$f(z) = \sqrt{\frac{2}{\pi}}\frac{1}{\sigma_f^3}z^2\exp -z^2/2\sigma_f^2, \tag{5.25}$$

where z is the sample space variable corresponding to $|\mathbf{u}_f'^*|$. It is evident from Eq. (5.23) and (5.24) that

$$St_l \sim \frac{1}{|\mathbf{u}_f'^*|^2}. \tag{5.26}$$

A mean timescale of interaction $\langle\tau_{\text{int}}\rangle$ is derived from the pdf of $|\mathbf{u}_f'^*|$ as

$$\langle\tau_{\text{int}}\rangle = \int_{|\mathbf{u}_f'^*|^T}^{\infty}\tau_{\text{int}}f(z)dz + \int_0^{|\mathbf{u}_f'^*|^T}\tau_p f(z)dz, \tag{5.27}$$

where the timescale τ_{int} is hypothesized to be of the form

$$\tau_{\text{int}} = St_l\left(\tau_p - \tau\right) + \tau \tag{5.28}$$

for $|\mathbf{u}_f'^*|^T \leq |\mathbf{u}_f'^*| \leq \infty$. Here $\tau = k_f^*/\epsilon_f^*$ is the large eddy turnover timescale. The significance of the limit $|\mathbf{u}_f'^*|^T$ and the rationale behind the choice of a weighted–average timescale $\langle\tau_{\text{int}}\rangle$ in Eq. (5.27) is now discussed.

Equation (5.24) is based on an inertial sub–range scaling for eddies with a characteristic lengthscale l. The Stokes number St_l defined in Eq. (5.23) using the characteristic timescale τ_l determines how the droplets respond to these eddies. For a value of $St_l > 1$, it is hypothesized that the droplet responds slowly to the eddies and the timescale of energy transfer is influenced more by the particle response time τ_p. On the other hand, if $St_l < 1$, it is hypothesized that the droplet responds immediately to the flow, and the timescale of energy transfer is influenced more by the the eddy turnover timescale τ. Thus, the pdf of $|\mathbf{u}'^*_f|$ (See Fig.5.4) can be divided into two regions: one that represents $St_l > 1$ and the other that represents $St_l < 1$ with $|\mathbf{u}'^*_f|^T$ representing the transition between the two regions at $St_l = 1$. Therefore, $|\mathbf{u}'^*_f|^T$ is uniquely determined by the relation $\left(|\mathbf{u}'^*_f|^T\right)^2 = \tau_p\, \varepsilon^*_f$.

It is interesting to note that Eq. (5.27) has the correct behavior under limiting conditions of St_l and $|\mathbf{u}'^*_f|^T$. In the limit $|\mathbf{u}'^*_f|^T \to 0$, there are no eddies in the system with $St_l > 1$. The droplets are simply convected by the flow and the correct timescale for interphase TKE transfer in this limit is τ. In the limit $|\mathbf{u}'^*_f|^T \to \infty$, practically all the eddies in the system satisfy $St_l > 1$, which implies that there are no eddies energetic enough to convect the droplets. The correct timescale for interphase TKE transfer in this limit is the particle response timescale τ_p.

For a polydispersed droplet size distribution, each droplet has a different τ_p. Since the timescale $\tau_{\rm int}$ in Eq. (5.28) depends on τ_p, each droplet can have a different interaction timescale $\tau_{\rm int}$. So, a multiscale interaction timescale $\langle\tau_{\rm int}\rangle$ can be calculated for each droplet based on its particle response timescale. However, in the calculations presented in this work (see Chapter 7) we use the mean value of τ_p computed from the polydispersed droplet ensemble, in place of τ_p, to compute $\tau_{\rm int}$ in Eq. (5.28) to avoid prohibitively large computational run times.

5.7.1 Implementation of the multiscale interaction timescale in LE computations

The following algorithm outlines the procedure that can be used to implement the multiscale interaction time scale $\langle\tau_{\rm int}\rangle$ in LE computations of particle–laden flow.

1. An ensemble of N computational particles with velocity and radius $\{\mathbf{V}_p^{(i)}, R_p^{(i)}, i =$

$1, \ldots, N\}$ is sampled from a specific initial joint pdf of velocity and radius. The TKE k_f and dissipation rate ε_f in the fluid phasse are initialized.

2. The particle response time scale τ_p for each particle is computed using $\tau_p = (\rho_d d_p^2)/(\rho_f 18\nu_f)$. For a monodispersed ensemble, all particles will have an identical particle response time scale.

3. The transition value $|\mathbf{u}_f'^*|^T = \sqrt{\tau_p \varepsilon_f^*}$ is computed for each particle. All particles will have an identical value of $|\mathbf{u}_f'^*|^T$ for a monodispersed ensemble.

4. The multiscale interaction time scale $\langle \tau_{\text{int}} \rangle$ is computed by numerically integrating Eq. (5.27).

5. Each particle's velocity is evolved in time using Eq. (5.22).

6. Quantities k_d^*, k_f^* and ε_f^* are calculated at the new timestep, and steps (2)-(5) are repeated.

Note that for a polydispersed ensemble of particles, and for a spray with drop radii that is changing in time (as in the case of an evaporating spray), τ_p changes in time. In either case, $|\mathbf{u}_f'^*|^T$ will be different for each particle. Note also that if ε_f^* evolves in time, $|\mathbf{u}_f'^*|^T$ will also change in time.

5.7.2 Model results with multiscale interaction timescale

Predicted evolution of normalized k_f^* and k_d^* is shown in Figs. 5.5 and 5.6 respectively for KIVA drag model with $\langle \tau_{\text{int}} \rangle$, along with results from DNS. It can be inferred that the timescale of decay has improved significantly compared to the results using the KIVA drag model with τ_p (cf. Figs. 5.1 and 5.2). The decay trends of k_f^* and k_d^* with increasing Stokes number are also in the same direction as those depicted in the DNS, and the anomalous reversal in the evolution of k_d^* is also absent. A simple modification to the existing particle velocity evolution equation (Eq. 5.6) to incorporate a multiscale interaction timescale derived from the model for the fluctuating velocity has improved the decay characteristics of the TKE in the gas and dispersed phases significantly.

5.8 Discussion

The new multiscale interaction timescale correctly reproduces the trends in the decay of TKE in the fluid phase and dispersed phase, as observed in DNS of a homogeneous particle–laden turbulent flow. Implicit in the above statement is the assumption that the DNS data is itself an accurate representation of the problem physics. The point–particle assumption for the *particle drag* in such DNS is justified in a limited flow regime where particle Reynolds numbers $Re_p \ll 1$, dispersed phase to gas density ratios ρ_d/ρ_f are $\mathcal{O}(1000)$, and particles are sub–Kolmogorov size with negligible wake effects. Volume–displacement effects are neglected in such DNS and the gas phase velocity field is assumed to be solenoidal.

The homogeneous problem that forms the basis of the investigation in this work, and for which DNS datasets exist, corresponds to a flow regime where the assumptions mentioned earlier are valid. However, it is important to note that a good approximation to the particle drag in the DNS does not necessarily guarantee accurate calculation of the fluctuating velocity–acceleration correlation (cf. Eq. 5.2) or the fluid phase dissipation in the presence of particles. In the point–particle approximation, particle–particle interaction effects are not accounted for, and the effect of the point–particle approximation on the true pressure field is also not quantified. The only way to test these approximations is to perform *true* DNS where the flow around each particle is fully resolved and exact boundary conditions are imposed on each particle surface. Solenoidality of the gas phase (which in turn affects the fluid pressure field), and neglect of particle–particle interaction effects, can be tested in a true DNS. Recent studies by Moses and Edwards (2005) are emerging which seek to assess the consequences of the point–particle approximation. However, their study is in 2–d for considerably large cylinders (Reynolds number based on the diameter of cylinder = 26), with an emphasis on evaluating the effects of filtering the velocity field. Their study is relevant to examining the validity of LES based on the point–particle assumption. Similar studies are needed for DNS, although such simulations are still limited by computational expense. Therefore, the DNS datasets performed with the point–particle approximation that are used in this study are the best data available for model testing and validation. It appears very likely that the existing DNS

datasets *do* capture the major trends of the TKE variation with important non–dimensional parameters like Stokes number and mass loading. It is possible that true DNS might lead to revision in the exact quantitative predictions. Nevertheless, since our principal conclusions concern qualitative trends rather than an exact quantitative match between model predictions and DNS, it is reasonable to assert that the incorporation of the new multiscale interaction timescale leads to a better representation of the problem physics.

It is worthwhile to examine whether any experimental data can be used for model validation. Experimental investigations of nearly isotropic particle–laden turbulence include work by Friedman and Katz (2002) and Fallon and Rogers (2002). While, the former report only rise rate of droplets in the presence of two levels of turbulence intensity in the carrier phase, and the latter report preferential concentration of particles for varying Stokes numbers, both do not report kinetic energy in either phase that is required for model validation. While the data they report is useful for models that involve buoyancy effects and predict preferential concentration, information on the second moments of fluid and particle velocities is not reported.

5.9 Summary and Conclusions

Particle–turbulence interaction occurs over a range of length and timescales. DNS of homogeneous particle–laden turbulence report that the rate of decay of TKE increases with increasing Stokes number, with mass loading kept constant. A simple turbulent two–phase flow model problem that consists of monodispersed sub-Kolmogorov size solid particles (or non–evaporating droplets) evolving in zero–gravity homogeneous decaying turbulence is used to assess a class of particle velocity evolution equations in the LE modeling approach. LE turbulence models that use the particle response timescale as the timescale for interphase energy transfer fail to reproduce the correct trend of energy decay in both the fluid phase and the dispersed phase as observed in DNS. When the particle response timescale is replaced with a multiscale interaction timescale derived from an assumed representation of the gas phase turbulence, the trend of decay of fluid phase and dispersed phase TKE match those seen in DNS. This lends to support the hypothesis that the particle response timescale is inadequate

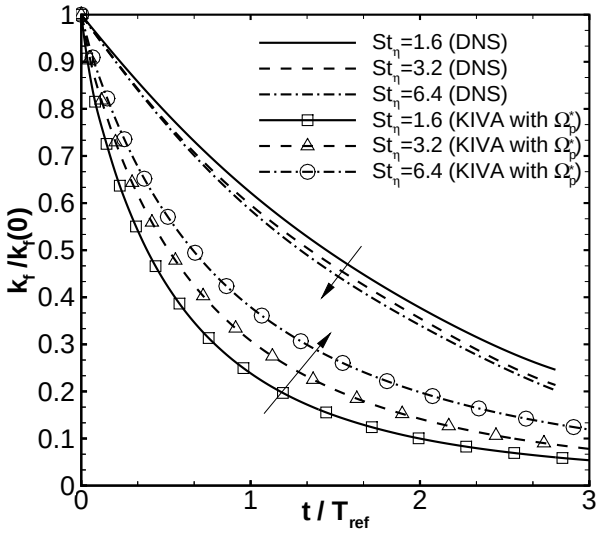

Figure 5.1 Evolution of normalized k_f for the homogeneous model problem (i) KIVA with Ω_p^* (ii) DNS of particle–laden freely decaying turbulence (Sundaram and Collins, 1999). Not only is the decay rate fast compared to the DNS result, but also the trend of decay in k_f is opposite to that seen in the DNS result. Arrow indicates direction of increasing Stokes number.

to represent the multiscale effects inherent in a two–phase flow system.

The principal conclusions of this study are:

1. LE models based on the particle response timescale do not capture the correct trends of decay in TKE with varying Stokes number in freely decaying particle–laden turbulence. The KIVA drag model with the particle response timescale also predicts an unphysical increase of dispersed phase energy in freely decaying turbulence. A simplified analysis assuming a constant particle response time reproduces the unphysical behavior, thereby illustrating that the non–monotonic behavior is not an artifact of the numerical simulation.

2. LE models with an improved multiscale interaction timescale predict the correct trends of decay in TKE with varying Stokes number in freely decaying particle–laden turbulence.

Predictions from the LE model with the multiscale interaction timescale can be assessed in other canonical flows like droplet–laden homogeneous shear and mixing layers.

Dispersed phase volume fraction α_d	1.8×10^{-4}
Fluid phase thermodynamic density ρ_f (kg/m^3)	1.1616
Dispersed phase thermodynamic density ρ_d (kg/m^3)	1045.44
Acceleration due to gravity $\mathbf{g}$ (m/s^2)	0.0,0.0,0.0
Initial mean slip (m/s)	0.0,0.0,0.0
(k_d/k_f) ratio at initial time	1

Table 5.1 Parameters of the particle–laden decaying turbulence test case.

$St_\eta = \tau_p/\tau_\eta$	u' (m/s)	v' (m/s)	ε_f (m^2/s^3)
1.6	0.80245	0.77250	0.36273
3.2	0.79371	0.73812	0.40309
6.4	0.79254	0.74360	0.43834

Table 5.2 Particle–laden decaying turbulence test case: Initial values of the turbulence intensities u' and v' in the fluid phase and dispersed phase, respectively, and dissipation rate in the fluid phase, for different Stokes numbers.

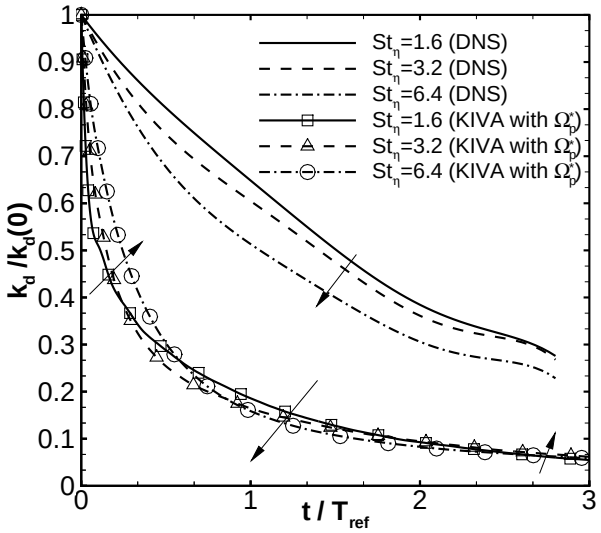

Figure 5.2 Evolution of normalized k_d for the homogeneous model problem (i) KIVA with Ω_p^* (ii) DNS of particle–laden freely decaying turbulence (Sundaram and Collins, 1999). The decay in k_d as predicted by the KIVA model is significantly faster than the DNS result. An unphysical cross–over in the predictions from KIVA is seen. Arrows indicate direction of increasing Stokes number.

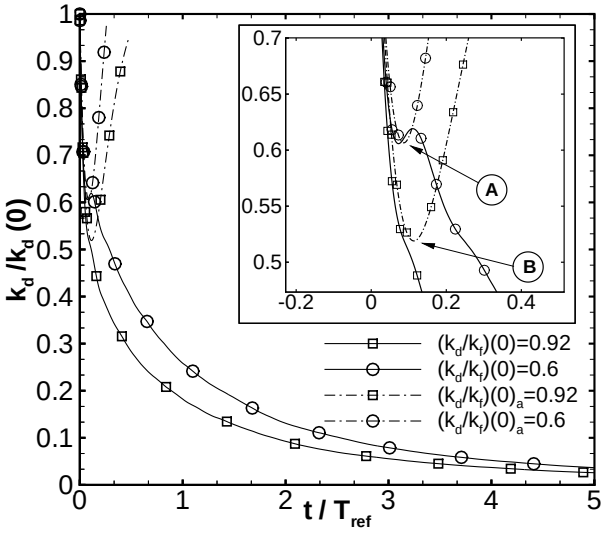

Figure 5.3 Results from a simple analysis assuming constant Ω_p^* (dot–dash lines and subscript 'a' in the legend) are shown alongside predictions from KIVA (solid lines) for two initial k_d/k_f ratios and a Stokes number of 1.6. The inset shows a blow–up of the region where the reversal in the decay of k_d^* (indicated by A and B) occurs. For a constant Ω_p^*, a decrease in the initial k_d/k_f ratio tends to aggravate the unphysical behavior.

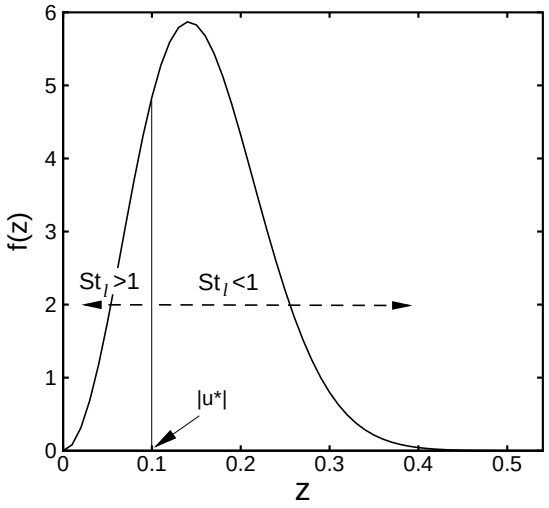

Figure 5.4 A schematic probability density function of $|\mathbf{u}_f'^*|$ used in the derivation of the multiscale interaction timescale $\langle\tau_{\text{int}}\rangle$. Here, z is the random variable corresponding to $|\mathbf{u}_f'^*|$. The transition value of $|\mathbf{u}_f'^*|$ – $|\mathbf{u}_f'^*|^T$ – is also indicated.

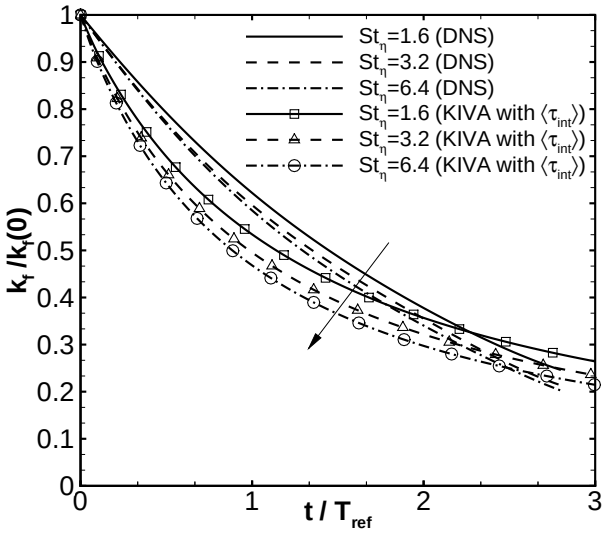

Figure 5.5 Evolution of normalized k_f for the homogeneous model problem (i) KIVA with $\langle\tau_{\rm int}\rangle$ (for clarity $\langle\tau_{\rm int}\rangle$ is written as $\langle\tau_i\rangle$ in the figure) (ii) DNS of particle–laden freely decaying turbulence (Sundaram and Collins, 1999). Not only has the timescale of decay in the evolution of k_f improved, but also the trend of decay with increasing Stokes number matches the DNS result. Arrow indicates direction of increasing Stokes number.

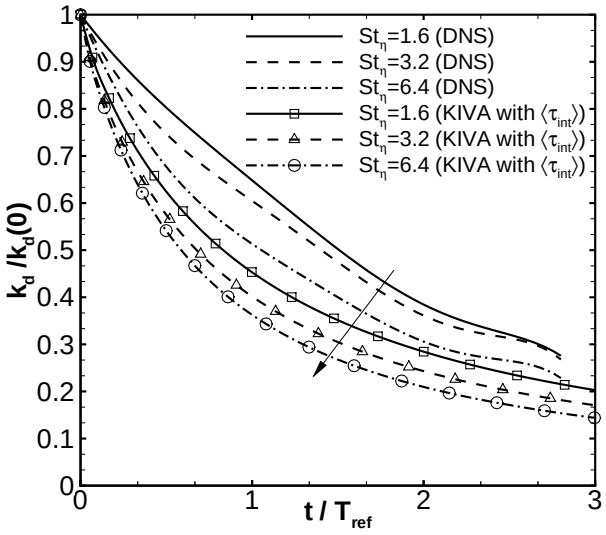

Figure 5.6 Evolution of normalized k_d for the homogeneous model problem (i) KIVA with $\langle\tau_{\rm int}\rangle$ (for clarity $\langle\tau_{\rm int}\rangle$ is written as $\langle\tau_i\rangle$ in the figure) (ii) DNS of particle–laden freely decaying turbulence (Sundaram and Collins, 1999). The timescale of decay with increasing Stokes numbers has improved significantly and is now closer to DNS results, and the trend of decay matches the DNS result. Arrows indicate direction of increasing Stokes number.

CHAPTER 6. A NEW DUAL-TIMESCALE LANGEVIN MODEL (DLM) FOR TWO–PHASE FLOWS

6.1 Desirable features for a two–phase model

Turbulent two–phase flows are characterized by the presence of multiple physical time and length scales. Models for a two–phase flow need to incorporate these fundamental time and length scales in their formulation in order to capture the essential physics of the fluid–particle interaction. Time and length scales in a homogeneous tubulent two–phase flow can be classified into (i) those related to fluid or carrier phase, and (ii) those related to the dispersed phase. Important time scales in such a flow are (i) the Kolmogorov timescale τ_η, which is the timescale corresponding to the smallest length scale of the eddy – the Kolmogorov length scale η given as $\tau_\eta = (\nu_f/\varepsilon_f)^{1/2}$, where ν_f and ε_f are the kinematic viscosity and the dissipation rate in the carrier phase, respectively, (ii) the eddy turnover timescale $\tau = k_f/\varepsilon_f$, where k_f is the TKE in the carrier phase, and (iii) particle response timescale $\tau_p = (\rho_d/\rho_f)d^2/(18\nu_f)$, where ρ_d and ρ_f are the densities of the dispersed phase and the carrier phase, respectively, and d is the particle diameter. Important length scales in the same two–phase flow are (i) η, (ii) eddy length scale $l = k_f^{3/2}/\varepsilon_f$ and (iii) the particle diameter d. In addition to these easily apparent physical timescales, there are other timescales that govern the evolution of two–phase flows. DNS of canonical two–phase flows report that TKE in each phase and the particle velocity autocorrelation evolve on timescales that behave differently with Stokes number St_η, defined as $St_\eta = \tau_p/\tau_\eta$. In particular, the TKE in the carrier and dispersed phase decays *faster* with increasing St_η in particle–laden freely decaying homogeneous turbulence (Sundaram and Collins, 1999), while the particle velocity autocorrelation decays *slower* with increasing St_η in droplet–laden, artificially forced stationary turbulence (Mashayek et al., 1997). A two–phase

flow model that is designed to be predictive in a range of two–phase flows must necessarily possess the capability to capture these disparate timescales in simple canonical two–phase DNS. It is noteworthy that two–phase models used in LE implementations (for instance, see Amsden et al. (1989)) that evolve the dispersed–phase velocity as

$$\frac{d\mathbf{V}_p}{dt} = \frac{\mathbf{U}_g - \mathbf{V}_p}{\tau_p} C_d(Re_p), \tag{6.1}$$

where $\mathbf{V}_p$ is the dispersed–phase velocity, $\mathbf{U}_g$ is the carrier–phase velocity, C_d is the drag coefficient which is a function of the particle Reynolds number Re_p, are incapable of capturing the observed trends in the decay of TKE with St_η noted earlier when tested in the canonical problem. The reason for the inability of such models to capture these trends observed in two–phase DNS was traced to the use of the particle–response timescale τ_p in Eq. (6.1). When τ_p was replaced by a multiscale interaction timescale, predicted trends of TKE decay from the LE model matched with DNS results (Pai and Subramaniam, 2006).

A two–phase model should also respect important limiting values of St_η and mass loading ϕ, which in this context is defined as $\phi = (\rho_d \alpha_d)/(\rho_f \alpha_f)$, where α_f and α_d are the carrier phase and dispersed–phase volume fractions. In the limit of $St_\eta \to 0$, the dispersed particles behave as fluid tracers since in this limit the particles possess negligible inertia. In this limit, predicted statistics such as TKE and velocity autocorrelation from a two–phase model corresponding to the dispersed phase must match those corresponding to the fluid phase. The limit of $St_\eta \to \infty$ is also important in that the particles are unaffected by the motion of the carrier phase. Such flows are collision dominated and are generally described by completely neglecting the presence of the fluid phase (eg. granular flows). Although the ability to capture this limit is a desirable feature of a two–phase flow model, the physics of the two–phase flow corresponding to this collision–dominated regime is not completely understood. In the limit of $\phi \to 0$, the fluid phase momentum source term becomes negligible. In this limit of one–way coupling, a two–phase model for the fluid phase must have neglible influence from the dispersed phase. On the other hand, as $\phi \to \infty$, two–way coupling effects become important and a two–phase model must possess the capability to capture the effects of two–way coupling in this limit.

6.2 General form of a coupled Langevin model for two–phase flows

Lagrangian models based on stochastic differential equations (SDE) have been successfully used in single–phase turbulent flows to model the velocity following a fluid particle (Pope, 1985). SDEs are amenable to analysis since properties of the Weiner process that appear in such equations are rigorously defined. We therefore extend models that have been successful in single–phase turbulent flows to two–phase flows.

In the most general form, a model for the fluctuating velocities in the fluid phase and dispersed phase in a two–phase flow system can be written as a matrix system of vector SDEs as

$$d\begin{pmatrix}\mathbf{u}\\ \mathbf{v}\end{pmatrix} = \underbrace{\begin{pmatrix}\mathbf{a}_{ff} & \mathbf{a}_{fd}\\ \mathbf{a}_{df} & \mathbf{a}_{dd}\end{pmatrix}}_{1}\begin{pmatrix}\mathbf{u}\\ \mathbf{v}\end{pmatrix}dt + \underbrace{\begin{pmatrix}\mathbf{b}_{ff} & \mathbf{b}_{fd}\\ \mathbf{b}_{df} & \mathbf{b}_{dd}\end{pmatrix}}_{2}\begin{pmatrix}d\mathbf{W}_f\\ d\mathbf{W}_d\end{pmatrix},$$

where

1. $\mathbf{u}$ and $\mathbf{v}$ are modeled fluctuating velocities in the fluid phase and dispersed phase, respectively,

2. the matrix denoted 1 is the the drift matrix whose elements have dimensions $[T^{-1}]$. Four submatrices viz. $\mathbf{a}_{ff}$, $\mathbf{a}_{fd}$, $\mathbf{a}_{df}$ and $\mathbf{a}_{dd}$ give the interaction timescales between combinations of carrier–f and dispersed–d phase,

3. the matrix denoted 2 is the diffusion [1] matrix whose elements have dimensions $[LT^{-3/2}]$. Four submatrices viz. $\mathbf{b}_{ff}$, $\mathbf{b}_{fd}$, $\mathbf{b}_{df}$ and $\mathbf{b}_{dd}$ represent the rate of change of TKE in each phase due to interphase TKE transfer and dissipation, and

4. $d\mathbf{W}_f$ and $d\mathbf{W}_d$ are independent Wiener processes. The usual properties of the Wiener process hold:

$$\langle \mathbf{W} \rangle = 0 \quad \langle \mathbf{W}_t \mathbf{W}_s \rangle = \min(t, s)$$

and at any time t and time step Δt, the increment $\mathbf{W}_{t+\Delta t} - \mathbf{W}_t$ is a Gaussian random variable with mean zero and variance Δt.

[1] The terms 'drift' and 'diffusion' are used in the sense of stochastic differential equation theory.

The fluid phase and particle phase fluctuating velocities can be coupled through the drift and diffusion coefficients. In general, the drift and diffusion coefficients can be functions of the mean velocity gradients in either phase, TKE and viscous dissipation in either phase, in addition to non–dimensional quantities, such as particle Reynolds number, mass loading, volume fraction, particle to fluid density ratio. In summation convention, the above system can be rewritten as

$$du_i = \left(a_{ik}^{ff} u_k + a_{ik}^{fd} v_k\right) dt + b_{ik}^{ff}\, dW_{f\,k} + b_{ik}^{fd}\, dW_{dk} \tag{6.2}$$

$$dv_i = \left(a_{ik}^{df} u_k + a_{ik}^{dd} v_k\right) dt + b_{ik}^{df}\, dW_{f\,k} + b_{ik}^{dd}\, dW_{dk} \tag{6.3}$$

6.3 Dual–timescale Langevin model

We explore one possible specification of the general form of the coupled Langevin model given by Eq. (6.2)–(6.3) with isotropic drift and diffusion coefficients, and with $\mathbf{a}_{fd} = \mathbf{a}_{df} = \mathbf{b}_{fd} = \mathbf{b}_{df} = \mathbf{0}$. For a homogeneous turbulent two–phase flow, the proposed form for the new model is:

$$du_i = -\left(A(t)\delta_{ij} + \frac{\partial \langle U_i \rangle}{\partial x_j}\right) u_j dt + B(t)\delta_{ij} dW_{f\,j} \tag{6.4}$$

$$dv_i = -\left(C(t)\delta_{ij} + \frac{\partial \langle V_i \rangle}{\partial x_j}\right) v_j dt + D(t)\delta_{ij} dW_{p\,j}, \tag{6.5}$$

where

$$\begin{aligned}
A(t) &= \left[\frac{1}{2\tau_1} + \left(\frac{1}{2} + \frac{3}{4}C_0\right)\frac{\varepsilon_f}{k_f}\right], \\
B(t) &= \left[C_0\varepsilon_f + \frac{2}{3}\frac{k_f}{\tau_1} + \frac{2}{3}\left(\frac{k_f^e - k_f}{\tau_2}\right)\right]^{1/2}, \\
C(t) &= \frac{1}{2\tau_3}, \\
D(t) &= \left[\frac{2}{3}\frac{k_d}{\tau_3} + \frac{2}{3}\left(\frac{k_d^e - k_d}{\tau_4}\right)\right]^{1/2}.
\end{aligned}$$

Here, τ_1 and τ_3 are timescales that appear in the drift coefficients, while τ_2 and τ_4 are timescales that appear in the diffusion coefficients of each SDE. We refer to the above model as the Dual–timescale Langevin model (DLM) in the rest of this work. The TKE in the dispersed phase is denoted k_d with a superscript 'e' to denote 'equilibrium' values (the same holds for the TKE

in the fluid phase k_f). The gas–phase dissipation enhanced by the presence of the dispersed phase is denoted ε_f. Reasons for this particular choice of the drift and diffusion coefficients, and the reason for the use of the phrase 'equilibrium' will become clear in due course. Mean velocity gradients in the fluid phase $\partial\langle U_i\rangle/\partial x_j$ and dispersed phase $\partial\langle V_i\rangle/\partial x_j$ are incorporated into the drift coefficients, analogous to models in single–phase flows.

The fluid–phase SDE can be viewed as an extension of the simplified Langevin model (SLM) (Pope, 2000; Haworth and Pope, 1986) to two–phase flows, but with an important difference being the introduction of drift and diffusion timescales that are different from each other. Additional terms that represent interphase interactions have been added. In this model, the coupling between the two phases is only through mean fields like TKE (k_f and k_d) and ε_f, and not explicitly through u_i and v_i.

The reason to choose SLM as a basis for DLM is manifold. The simplified Langevin model performs well in the context of single–phase flows (Pope, 2000). In particular, in single–phase stationary turbulence the Lagrangian integral timescale matches well with DNS results (Yeung and Pope, 1989). The form of the second–order structure function as implied by SLM is linear in time separation, which is consistent with Kolmogorov's hypotheses. In single–phase homogeneous shear flows, SLM is a reasonable model for the Lagrangian velocity of a fluid particle (Pope, 2002). However, in homogeneous shear flows when the Reynolds stresses and the Lagrangian integral time scale from DNS (Sawford and Yeung, 2001) are employed to arrive at the implied diffusion coefficient in SLM, Pope (Pope, 2002) does find that this coefficient is significantly anisotropic; although it is not clear if the anisotropy is an effect of the low Reynolds number regime studied in the DNS. A value of $C_0 = 3.4$ has also been used by Pope in the same study with better agreement of model predictions with DNS results, than with $C_0 = 2.1$.

In this study, the primary emphasis is to match trends of important two–phase statistics in canonical two–phase flows with varying non–dimensional parameters, such as Stokes number and mass loading, with those observed in DNS. We also do not seek an exact quantitative match between model predictions and DNS data for reasons discussed in Section 6.8. Therefore, we

use the simplest form of the single–phase Langevin model in this study with $C_0 = 2.1$. It is expected that the ideas proposed in this paper on extending single–phase models to two–phase flows can be incorporated into recent model developments and recommendations in the context of single–phase flows (Lamorgese et al., 2007).

6.3.1 Implied evolution equation for the Reynolds stresses

The evolution equations of key statistics in a two–phase flow as implied by DLM are now derived. From Eqs. (6.4)–(6.5), the evolution equations for the Reynolds stresses implied by DLM can be derived in the usual manner (Pope, 2000) to be

$$\frac{d}{dt}\langle u_i u_j\rangle = -2A(t)\langle u_i u_j\rangle - \left(\langle u_k u_j\rangle \frac{\partial\langle U_i\rangle}{\partial x_k} + \langle u_i u_k\rangle \frac{\partial\langle U_j\rangle}{\partial x_k}\right) + B(t)^2\delta_{ij} \tag{6.6}$$

$$\frac{d}{dt}\langle v_i v_j\rangle = -2C(t)\langle u_i u_j\rangle - \left(\langle v_k v_j\rangle \frac{\partial\langle V_i\rangle}{\partial x_k} + \langle v_i v_k\rangle \frac{\partial\langle V_j\rangle}{\partial x_k}\right) + D(t)^2\delta_{ij}. \tag{6.7}$$

6.3.2 Implied evolution equations for the TKE

Contracting like indices in Eq. (6.6) and Eq. (6.7) results in the evolution equations for the TKE in the fluid phase, defined as $k_f = (1/2)\langle u_i u_i\rangle$, (where the averaging is performed over an ensemble of realizations) and the TKE in the dispersed phase, defined as $k_d = (1/2)\langle v_i v_i\rangle$, respectively:

$$\frac{dk_f}{dt} = -2A(t) - \langle u_k u_i\rangle \frac{\partial\langle U_i\rangle}{\partial x_k} + \frac{3}{2}B(t)^2 \tag{6.8}$$

$$\frac{dk_d}{dt} = -2C(t) - \langle u_k u_i\rangle \frac{\partial\langle V_i\rangle}{\partial x_k} + \frac{3}{2}D(t)^2 \tag{6.9}$$

Simplfying the above equation using the prescribed form of the drift and diffusion coefficients in Eqs. (6.4) and (6.5) results in

$$\frac{dk_f}{dt} = -\frac{k_f - k_f^e}{\tau_2} - \langle u_k u_i\rangle \frac{\partial\langle U_i\rangle}{\partial x_k} - \varepsilon_f \tag{6.10}$$

$$\frac{dk_d}{dt} = -\frac{k_d - k_d^e}{\tau_4} - \langle u_k u_i\rangle \frac{\partial\langle V_i\rangle}{\partial x_k} \tag{6.11}$$

The first term on the right hand side of the above equations represents the modeled interphase TKE transfer term. For the case of particle–laden homogeneous turbulence with no mean

velocity gradients, the evolution equations for the TKE in each phase given by Eq. (6.10) and Eq. (6.11) simplify to

$$\frac{dk_f}{dt} = -\frac{k_f - k_f^e}{\tau_2} - \varepsilon_f \tag{6.12}$$

$$\frac{dk_d}{dt} = -\frac{k_d - k_d^e}{\tau_4}. \tag{6.13}$$

6.3.3 Implied Lagrangian velocity autocorrelation

The Lagrangian velocity autocorrelation in phase β, denoted $\rho_{\beta_{ij}}(t,s)$, is defined as

$$\rho_{\beta_{ij}}(t,s) = \frac{\langle \gamma_i(t)\gamma_j(t+s)\rangle}{(\langle \gamma_i(t)\gamma_i(t)\rangle)^{1/2}\langle \gamma_j(t+s)\gamma_j(t+s)\rangle^{1/2}} \tag{6.14}$$

(no summation is implied over repeated indices) where γ stands for either u or v. Here β indicates the phase: f for the fluid phase or d for the dispersed phase. The Lagrangian autocorrelation is simply a normalized autocovariance and gives a measure of how quickly the phase velocity loses correlation with its value at some earlier time. In stationary [2] particle–laden turbulence, $\rho_{\beta_{ij}}$ depends only on the *separation* time s, and not on t:

$$\rho_{\beta_{ij}}(s) = \frac{\langle \gamma_i(t_0)\gamma_j(t_0+s)\rangle}{(\langle \gamma_i(t_0)\gamma_i(t_0)\rangle)^{1/2}\langle \gamma_j(t_0+s)\gamma_j(t_0+s)\rangle^{1/2}} \tag{6.15}$$

where t_0 can be any initial time after the system reaches stationarity. In decaying turbulence, the velocity autocorrelation also depends on the time t_0.

Assuming stationarity, the evolution equations for the fluid–phase velocity autocovariance and the dispersed–phase velocity autocovariance derived from Eq. (6.4) and Eq. (6.5) are

$$\frac{d}{dt}\langle u_i(t_0)u_j(t)\rangle = -\left[\frac{1}{2\tau_1} + \left(\frac{1}{2} + \frac{3}{4}C_0\right)\frac{\varepsilon_f}{k_f}\right]\langle u_i(t_0)u_j(t)\rangle - \frac{\partial\langle U_j\rangle}{\partial x_k}\langle u_i(t_0)u_k(t)\rangle \tag{6.16}$$

and

$$\frac{d}{dt}\langle v_i(t_0)v_j(t)\rangle = -\frac{1}{2\tau_3}\langle v_i(t_0)v_j(t)\rangle - \frac{\partial\langle V_j\rangle}{\partial x_k}\langle v_i(t_0)v_k(t)\rangle, \tag{6.17}$$

respectively.

[2] Stationarity in particle–laden flows can be ascertained by observing the evolution of statistics such as TKE in either phase.

For homogeneous particle–laden turbulence without any mean velocity gradients the evolution equations for the velocity autocovariance in each phase given by Eq. (6.16) and Eq. (6.17) simplify to

$$\frac{d}{dt}\langle u_i(t_0)u_j(t)\rangle = -\left[\frac{1}{2\tau_1} + \left(\frac{1}{2} + \frac{3}{4}C_0\right)\frac{\varepsilon_f}{k_f}\right]\langle u_i(t_0)u_j(t)\rangle \tag{6.18}$$

$$\frac{d}{dt}\langle v_i(t_0)v_j(t)\rangle = -\frac{1}{2\tau_3}\langle v_i(t_0)v_j(t)\rangle, \tag{6.19}$$

where for stationary turbulence, the half in paranthesis in Eq. (6.18) is dropped.

A striking feature of DLM is that in each of the four equations Eqs. (6.8), (6.9), (6.18), (6.19), only one of the four timescales τ_1, τ_2, τ_3 and τ_4 appear. Each of these timescales can be constructed in such a way that they behave independently from each other. Thus in DLM, the evolution of TKE can be constructed to behave *differently* from the evolution of the velocity autocovariance. It is therefore possible to incorporate the capability of capturing the disparate timescale trends observed in two–phase DNS into DLM. It is noteworthy that in model proposals based on the generalized Langevin model (Pozorski and Minier, 1999) the implied TKE and the velocity autocorrelation evolve over a single timescale, namely the Lagrangian integral timescale.

The equilibrium energies k_f^e and k_d^e in Eqs. (6.4) and (6.5) are related to one another as shown next, and so the evolution of k_f and k_d are coupled through these terms. The proposed form of the TKE evolution equations Eqs. (6.10) and (6.11) and the relation between the equilibrium energies is based on an underlying model for the interphase TKE transfer. We briefly review this model next.

6.4 Equilibration of Energy concept

To explain the EoE concept, which was proposed recently by Xu and Subramaniam (2006), the following model system of equations for the evolution of TKE in a dilute homogeneous two–

phase flow system are assumed to hold:

$$\frac{de_f}{dt} = \Pi_{k_f} - \rho_f \alpha_f \varepsilon_f \tag{6.20}$$

$$\frac{de_d}{dt} = \Pi_{k_d}, \tag{6.21}$$

where $\Pi_{k_f} = (e_f^e - e_f)/\tau_\pi$ and $\Pi_{k_d} = (e_d^e - e_d)/\tau_\pi$ are the interphase TKE transfer terms [3]. Here, τ_π is the interphase TKE transfer timescale, $e_f = \rho_f \alpha_f k_f$ and $e_d = \rho_d \alpha_d k_d$ are the *specific* carrier phase and dispersed phase energies, respectively and $e_f^e = \rho_f \alpha_f k_f^e$ and $e_d^e = \rho_d \alpha_d k_d^e$ are the equilibrium *specific* TKEs in the carrier phase and dispersed phase, respectively. Collisions among particles are assumed to be elastic and hence no dissipation is considered in the dispersed phase.

The EoE concept states that if

$$\frac{de_m}{dt} = -\rho_f \alpha_f \varepsilon_f + \mathcal{F}_f = 0, \tag{6.22}$$

where $\mathcal{F}_f$ is the external artificial forcing required to balance the dissipation in order to maintain $de_m/dt = 0$, then the specific dispersed phase TKE and specific fluid phase TKE evolve to their respective equilibrium values. In the above equation, $e_m = \rho_m k_m = e_f + e_d = \rho_f \alpha_f k_f + \rho_d \alpha_d k_d$ is the mixture energy in the two–phase flow system and ρ_m is the mixture density defined as $\rho_m = \rho_d \alpha_d + \rho_f \alpha_f$. Note that the dissipation in the carrier phase is the sum of the single–phase dissipation rate and an additional dissipation due to the presence of boundary layers around the dispersed particles. Implicit in the above expression is that assumption that $\Pi_{k_f} = -\Pi_{k_d}$, which implies that the interphase TKE transfer is conservative. This assumption is valid for rigid particle–laden turbulent flows (Xu and Subramaniam, 2007).

Equilibrium values of the specific fluid–phase TKE e_f^e and specific dispersed–phase TKE e_d^e are determined by a model constant C_k which is defined as

$$\frac{e_d^e}{e_m} = C_k, \quad \text{or} \quad \frac{e_f^e}{e_m} = 1 - C_k. \tag{6.23}$$

Since C_k represents the fraction of the specific mixture energy present in the dispersed phase at equilibrium, it must lie between zero and unity.

[3] There is an implicit assumption of sub–Kolmogorov size particles in the above equations. This is because large particles can shed wakes that can in turn lead to production in the carrier phase. Production due to particle wakes is considered negligible in this study.

An implicit dependence of C_k on mass loading ϕ of the two–phase system can be ascertained by rewriting Eq. (6.23) as

$$C_k = \frac{\rho_d \alpha_d k_d^e}{\rho_m k_m} = \frac{\rho_d \alpha_d k_d^e}{\rho_f \alpha_f k_f^e + \rho_d \alpha_d k_d^e} = \frac{\phi \frac{k_d^e}{k_f^e}}{1 + \phi \frac{k_d^e}{k_f^e}}, \tag{6.24}$$

where $\phi = \rho_d \alpha_d / (\rho_f \alpha_f)$ is the mass loading of the two–phase system. The constant C_k can also depend on other non–dimensional quantities such as Stokes number St_η, particle Reynolds number Re_d, initial k_d/k_f ratio, the ratio of the droplet diameter d_p to Kolmogorov length scale η, and dispersed–phase volume fraction α_d.

For a constant mass loading ϕ, decreasing Stokes number should drive the dispersed–phase equilibrium TKE closer to the fluid phase equilibrium TKE, and in the limit of zero Stokes number, the two equilibrium energies should match. This observation imposes a constraint on C_k in the limiting case of zero Stokes number and from Eq. (6.24) we get

$$C_k|_{St_\eta = 0} = \frac{\phi}{1 + \phi}. \tag{6.25}$$

The EoE concept can be extended to the case where the turbulence decays in time (no artificial forcing of the mixture energy in the two–phase flow system). However, a model for the dissipation rate needs to be added to the system of equations (cf. Eqs. (6.20)–(6.21)), which now reads

$$\begin{aligned}
\frac{de_f}{dt} &= \Pi_{k_f} - \rho_f \alpha_f \varepsilon_f \\
\frac{de_d}{dt} &= \Pi_{k_d} \\
\frac{d\varepsilon_f}{dt} &= -C_{\varepsilon 2} \frac{\varepsilon_f^2}{k_f} + C_s \frac{\varepsilon_f}{k_f} \left(\frac{k_f^e - k_f}{\tau_\pi} \right) - C_{\varepsilon 1} \langle u_i u_j \rangle \frac{\partial \langle U_i \rangle}{\partial x_j} \frac{\varepsilon_f}{k_f},
\end{aligned} \tag{6.26}$$

where ε_f is the fluid–phase dissipation evolving according to a modified single–phase ε equation (Xu and Subramaniam, 2006) with the production term due to mean velocity gradients. The model constants $C_{\varepsilon 2}$ and $C_{\varepsilon 1}$ are proposed to be 1.92 and 1.44, respectively. The constant C_s is chosen to be 3.0 in this work, compared to 1.2 in Xu and Subramaniam (2006), as this value gave a better agreement of model predictions with DNS results in this case. A detailed discussion on the extension of the EoE concept to inhomogeneous flows in the context

of Eulerian–Eulerian statistical representation of two–phase flows can be found in Xu and Subramaniam (2006).

6.5 Model constants in DLM

6.5.1 Specification of C_k

The EoE model constant C_k defined in Eq. (6.24) represents the ratio of specific TKE in the dispersed phase to that in the two–phase mixture. As noted in Section 6.4, C_k can depend on the mass loading ϕ, Stokes number St_η, particle Reynolds number Re_d, initial k_d/k_f ratio and the dispersed–phase volume fraction α_d. The droplet Reynolds numbers considered in this study are of $\mathcal{O}(1)$, dispersed–phase volume fractions are of $\mathcal{O}(10^{-3})$ and the initial k_d/k_f ratio is of $\mathcal{O}(1)$. Hence, dependence of C_k on these parameters is neglected in this study. However, if the above non–dimensional parameters vary by an order of magnitude across the test cases considered, we expect that the dependence of C_k on these parameters will need to be taken into account.

The dependence of C_k on mass loading and Stokes number St_η [4] is accounted for in this study. Since the ratio of the equilibrium TKEs k_d^e/k_f^e (cf. Eq. (6.24)) is not known *a priori*, a model for C_k is required. The following model for C_k is proposed:

$$C_k = \frac{\phi}{1 + \phi + St_\eta}. \tag{6.27}$$

Note that this specification obeys the correct limiting behavior of C_k as $St_\eta \to 0$ (cf. Eq. (6.25).) In order to improve the model for C_k, datasets from carefully controlled DNS of particle–laden turbulent flows that report the fraction of the mixture energy in each phase are required. Also, the DNS should quantify the effect of non–dimensional parameters in a two–phase flow system, as noted earlier, on the fraction of specific TKE in each phase. To the knowledge of the authors, no such DNS datasets are as yet available in the literature.

[4] Henceforth, "Stokes number" refers to St_η, the Stokes number based on the Kolmogorov timescale, unless mentioned otherwise.

6.5.2 Drift timescales in DLM

The form of the drift timescales τ_1 and τ_3 in Eqs. (6.4)–(6.5), respectively, is now developed depending on how we expect the system of SDEs to behave in limiting cases.

Zero Stokes number limit

As noted earlier in Sec.6.1, in the limit of zero Stokes number the dispersed particles respond immediately to the surrounding fluid. In this limit, the fluid–phase velocity autocovariance and the dispersed–phase velocity autocovariance must match. Therefore we require that, in the limit of vanishing Stokes number, the timescale τ_3 in Eq. (6.17) should tend to the evolution timescale of the velocity autocovariance in Eq. (6.16).

A simple specification for τ_3 is

$$\frac{1}{\tau_3} = 2\left[\frac{1}{2\tau_1} + \left(\frac{1}{2} + \frac{3}{4}C_0\right)\frac{1}{\tau}\right]\frac{1}{1 + St_\eta C_3}, \tag{6.28}$$

where C_3 is a model constant ($C_3 = 0.1$). Although there is no explicit dependence of the timescale τ_3 on mass loading ϕ, we shall show next that the dependence on ϕ does appear through the timescale τ_1.

The timescale obeys the limiting behavior as $St_\eta \to 0$ viz.

$$\lim_{St_\eta \to 0}\left\{\left[\frac{1}{2\tau_1} + \left(\frac{1}{2} + \frac{3}{4}C_0\right)\frac{1}{\tau}\right]\frac{1}{1 + St_\eta C_3}\right\} = \frac{1}{2\tau_1} + \left(\frac{1}{2} + \frac{3}{4}C_0\right)\frac{1}{\tau}.$$

Currently, particle velocity autocorrelation data for large Stokes number (say, $St_\eta > 10$) is not available from DNS or experiments that can help determine the behavior of τ_3 in the large St_η limit. Furthermore, there is an limit to which datasets from DNS that use the point–particle approximation can be used for model validation. It can be shown that if the density ratio ρ_d/ρ_f is of $\mathcal{O}(1000)$, then the maximum value of St_η for which the point–particle approximation is valid is around 10. (See the analysis in L'vov et al. (2003)). It is surmised that this limit of St_η can also be taken to be the upper limit for the validity of DLM, although this claim needs to be validated by comparison with DNS.

Zero mass loading limit

In the limit of zero mass loading, the effect of the dispersed–phase on the fluid–phase momentum is negligible, which leads to the concept of one–way coupling (See Sec.6.1). Regardless of the Stokes number, the fluid timescales remain unaffected by the presence of the dispersed phase and are identical to those seen in a single–phase flow. In this limit, the timescale τ_1, which essentially represents the modification to the fluid velocity autocorrelation timescale due to the presence of dispersed phase, should tend to zero. Therefore, we require that the drift timescale in Eq. (6.4) should approach the specification for the single–phase SLM (Pope, 2000).

Using available data from DNS of particle–laden flows (Truesdell and Elghobashi, 1994; Ahmed and Elghobashi, 2001) we propose the following form of τ_1:

$$\frac{1}{\tau_1} = \frac{C_1 \phi \, St_\eta}{\tau},$$

where C_1 is a model constant ($C_1 = 2.5$). This specification obeys the correct limiting behavior as $\phi \to 0$ viz.

$$\lim_{\phi \to 0} \left[\frac{1}{2\tau_1} + \left(\frac{1}{2} + \frac{3}{4} C_0 \right) \frac{1}{\tau} \right] = \left(\frac{1}{2} + \frac{3}{4} C_0 \right) \frac{1}{\tau}.$$

For a constant mass loading, and in the limit $St_\eta \to 0$, the dispersed phase velocity autocorrelation behavior is identical to that of the fluid phase. In this limit, the timescale for the decay of velocity autocorrelation is the single–phase velocity autocorrelation decay timescale. Hence, the above specification of τ_1 ensures that as $St_\eta \to 0$, the timescale $1/\tau_1 \to 0$.

6.5.3 Diffusion timescales in DLM

The timescales τ_2 and τ_4 govern the evolution of TKE in each phase (cf. Eq. (6.12) and Eq. (6.13)). In accordance with the EoE concept, and to introduce the capability to capture the multiscale nature of a turbulent two–phase mixture into DLM, the timescales τ_2 and τ_4 are chosen to be equal to $\tau_\pi = \langle \tau_i \rangle / C_\pi$, where $\langle \tau_i \rangle$ is a multiscale interaction timescale for interphase TKE transfer first proposed by (Pai and Subramaniam, 2006). It was shown in that study that the new timescale accurately captures the dependence of the interphase TKE transfer on St_η. This timescale has been successfully employed in the context of EE two–

phase turbulence modeling by (Xu and Subramaniam, 2006). The constant C_π is chosen to be 1.0 in this study. Details of the derivation relevant to the DLM timescale specification are reviewed here for the sake of completeness. The development of the timescale is given in Pai and Subramaniam (2006) and Xu and Subramaniam (2006), and is not repeated here for the sake of brevity. Only important results are reviewed here.

Details of the derivation of the multiscale interaction timescale was presented earlier in Chapter 5, Section 5.7. Using DLM the pdf of absolute fluctuating velocity in the multiscale interaction timescale can be computed from the simulation. However, we retain the analytical form for the pdf of absolute value of fluctuating velocity as in Section 5.7.

6.5.4 Model summary and comparison with desirable features

Based the discussion heretofore DLM possesses the following desirable features of two–phase models:

1. The ingredients of DLM and Equilibration of Energy concept are important non–dimensional parameters for two–phase flows, such as St_η, mass loading ϕ and volume fraction α_d. Important time and length scales observed in a two–phase system are incorporated into the formulation of the multiscale interaction timescale $\langle \tau_{\text{int}} \rangle$.

2. DLM possesses the capability of capturing the disparate timescale trends of TKE and velocity autocorrelation decay with St_η that are observed in DNS of particle–laden decaying and particle–laden stationary turbulence.

3. DLM has the correct limiting behavior as $St_\eta \to 0$ and $\phi \to 0$, and also in the limit $\phi \to \infty$. DLM may not perform well in the limit $St_\eta \to \infty$ since the validity of DLM is restricted to the range over which the point–particle approximation is valid. Moreover, as the St_η number increases, it is expected that the physics of the particle–carrier phase interaction will not be identical to that when $St_\eta \to 0$, primarily due to enhanced collisions as $St_\eta \to \infty$.

In summary, DLM along with the Equilibration of Energy concept possesses some of the necessary features desirable of two–phase models for the parameter range considered in this study.

6.6 DNS datasets for model validation

Several researchers (Sundaram and Collins, 1999; Mashayek et al., 1997; Boivin et al., 1998) have performed DNS of particle–laden homogeneous turbulence. However, such DNS are not *true* DNS, where the flow around each particle is accurately resolved, but are based on the point–particle assumption. This assumption holds for density ratios of $\rho_d/\rho_f \sim \mathcal{O}(1000)$ and $d/\eta < 1$, where η is the Kolmogorov length scale of turbulence – conditions which are satisfied by the test cases investigated in this study. In this parameter range, the only significant contribution to the particle acceleration is through particle drag. Although such DNS cannot capture the additional dissipation due to the boundary layers around the paricles, we do expect that they qualitatively capture the correct trends in key statistics, such as TKE, with varying Stokes number and mass loading.

'True' DNS of particle–laden flows are becoming commonplace thanks to the advances in numerical techniques and computational power. Recent advances in numerical techniques have the capability of accurately quantifying the increased dissipation in the carrier phasse due to the presence of the particles, and the modulation of the carrier–phase TKE by the dispersed particles. However, no such DNS datasets are available to validate DLM in the parameter range explored in this study.

In this study, two important test cases are considered. Particle–laden freely–decaying turbulence is an important canonical two–phase problem and a necessary test for two–phase models, especially since models based the momentum–response timescale fail to capture accurate trends of TKE decay with varying Stokes number that are observed in DNS, when tested in this problem (Pai and Subramaniam, 2006). It will therefore be interesting to ascertain if DLM can capture these trends. Since dispersion and dynamics (interphase TKE transfer) are two coupled phenomena in any two–phase flow, it will also be interesting to check if DLM

Dispersed phase volume fraction α_d	1.8×10^{-4}
Fluid phase thermodynamic density ρ_f (kg/m^3)	1.1616
Dispersed phase thermodynamic density ρ_d (kg/m^3)	1045.44
Kinematic viscosity of fluid ν_f (m^2/s)	6.761×10^{-3}

Table 6.1 Parameters of the test case corresponding to particle–laden decaying turbulence used in this study. Acceleration due to gravity and initial mean slip between phases is zero for all cases.

can capture trends of velocity autocorrelation with varying particle inertia. Another important test case is particle–laden homogeneous shear wherein there is an interplay of production due to mean velocity gradients, interphase TKE transfer and carrier–phase dissipation. Although particle–laden stationary turbulence is also an important canonical problem, we direct the reader to Chapter 7 (also, Pai and Subramaniam (2007)) where DLM has been validated against DNS datasets of evaporating and non–evaporating droplet–laden flow in stationary turbulence. In that study DLM was shown to capture trends of TKE and particle velocity autocorrelation with varying St_η depicted in DNS.

6.6.1 Decaying turbulence: Turbulence modification and dispersion statistics

Sundaram and Collins (1999) have performed a study on particle–laden freely decaying turbulence in the absence of gravity for several Stokes numbers. The system is volumetrically dilute, with particles in the sub–Kolmogorov size range and collisions among particles, if any, are assumed to be elastic. Two–way coupling is assumed, i.e., the effect of the particles on fluid–phase momentum conservation is also accounted for. Parameters of the homogeneous model problem are given in Tables 6.1-6.2. In Table 6.1, u' is the initial turbulence intensity in the fluid phase and v' is the initial turbulence intensity in the dispersed phase. These intensities are related to the respective TKE in each phase at initial time through $u'^2 = (2/3)k_f(0)$ and $v'^2 = (2/3)k_d(0)$. Initial conditions for the particles are given in Table 6.2 and are taken from the DNS dataset at $T = 0.8$. This test case is hereafter referred to as SC.

Truesdell and Elghobashi (1994) (hereafter referred to as TE) have performed DNS of particle dispersion in freely decaying turbulence with two–way coupling effects included. The

$St_\eta = \tau_p/\tau_\eta$	u' (m/s)	v' (m/s)	ε_f (m^2/s^3)
1.6	0.80245	0.77250	0.36273
3.2	0.79371	0.73812	0.40309
6.4	0.79254	0.74360	0.43834

Table 6.2 Particle–laden decaying turbulence test case: Initial values of the turbulence intensities u' and v' in the fluid phase and dispersed phase, respectively, and dissipation rate in the fluid phase, for different Stokes numbers.

St_η	ρ_d/ρ_f	d	α_d	ϕ
1.27	909	9.295×10^{-5}	2.5×10^{-4}	0.23
2.54	1818	9.295×10^{-5}	2.5×10^{-4}	0.45
5.09	3636	9.295×10^{-5}	2.5×10^{-4}	0.91

Table 6.3 Particle–laden decaying turbulence test case to investigate particle dispersion (Truesdell and Elghobashi, 1994). For this test case, the following (unscaled) parameter values are chosen: initial dissipation: $\varepsilon_f = 0.03713$ m^2/s^3; initial TKE in both phases: $k_f = k_d = 8.62 \times 10^{-3}$ m^2/s^2; kinematic viscosity $\nu_f = 1.634 \times 10^{-5}$ m^2/s.

range of Stokes numbers St_η considered in this study were from 1.27 to 5 and the mass loading was 2.5×10^{-4}. Initial conditions for the model comparison are taken from the DNS dataset at the time when the particles are introduced into the simulation. Parameters of the DNS dataset are given in Tables 6.3. TE report evolution of the velocity autocorrelation of the dispersed phase and the fluid in the vicinity of the dispersed phase. Information on the fluid velocity autocorrelation in the vicinity of the dispersed particle is not available from the one–point description of the two–phase flow pursued in this study. More importantly, a one–point description of a two–phase flow cannot distinguish between a point in the vicinity of a particle and in the bulk; such affects could be captured however by using information from a two–point model. Furthermore, the velocity autocorrelation of the fluid in the vicinity of the particle is not the same as the fluid–particle velocity autocorrelation given by Eq. (6.16)), and therefore we do not compare this result with model predictions.

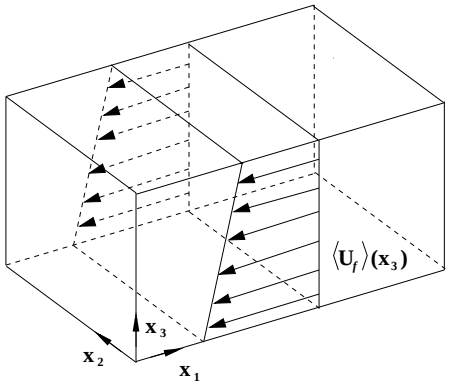

Figure 6.1 Schematic of the DNS of turbulent homogeneous shear laden with particles (Ahmed and Elghobashi, 2000)

6.6.2 Homogeneous shear: Turbulence modification

Ahmed and Elghobashi (2000) have performed DNS of homogeneously sheared turbulence laden with rigid particles. Of the several test cases analyzed in that study, only the test cases involving varying mass loading and varying particle inertia, in the absence of gravity, are considered here. A constant shear rate given by $\partial\langle U_1\rangle/\partial x_3 = \partial\langle V_1\rangle/\partial x_3 = \mathcal{S}$ is imposed on the fluid phase and the dispersed phases, respectively. The point–particles are evolved as per the equation due to Maxey and Riley (1983), with an additional contribution due the mean shear. For the varying mass loading test case, parameters of the DNS datasets are given in Table 6.5 and for the varying particle inertia test case, parameters are given in Table 6.4. This test case is hereafter referred to as AE–1.

6.7 Model predictions

This section summarizes model predictions from DLM for the canonical test cases cited earlier. Comparison of model predictions are performed with DNS results.

	d	ρ_d/ρ_f	St_η	d/η	α_d	ϕ
C	6.0×10^{-4}	525	0.233	0.0887	1.9×10^{-4}	0.1
I	1.0×10^{-3}	472.5	0.583	0.1479	2.1×10^{-4}	0.1
H	1.0×10^{-3}	945	1.165	0.1479	1.0×10^{-4}	0.1
F	1.0×10^{-3}	1890	2.33	0.1479	5.0×10^{-5}	0.1

Table 6.4 Particle–laden homogeneous shear test case: Varying particle inertia

	d	ρ_d/ρ_f	St_η	d/η	α_d	ϕ
B	1.0×10^{-3}	1890	2.33	0.1479	5.0×10^{-4}	1
G	1.0×10^{-3}	1890	2.33	0.1479	2.5×10^{-4}	0.5
F	1.0×10^{-3}	1890	2.33	0.1479	5.0×10^{-5}	0.1

Table 6.5 Particle–laden homogeneous shear test case: Varying mass loading

6.7.1 CASE I: Decaying turbulence

6.7.1.1 Prediction of TKE in particle–laden decaying turbulence

For the case of homogeneous decaying turbulence, the implied evolution equations for the TKE in the fluid phase and dispersed phases are given by Eq. (6.12) and Eq. (6.13), respectively. The only two terms that govern the evolution of the TKE in the fluid–phase are the interphase TKE transfer term Π_{k_f} and the fluid–phase dissipation ε_f.

Figure (6.2) shows the predicted evolution of the fluid–phase TKE by DLM for varying initial Stokes numbers St_η. Shown alongside are corresponding results from DNS data SC. In this particle size range and in the absence of production, the higher the particle inertia, the faster is the decay of energy in the carrier and dispersed phases. This behavior is clearly depicted by the DNS results, implying that the timescale of decay of TKE *decreases* with increasing Stokes number. DLM accurately reproduces the trend of TKE evolution for varying Stokes number. The evolution of the dispersed–phase TKE is shown in Fig. (6.3), which again illustrates that DLM accurately captures the trends of TKE evolution with Stokes number.

The reason why DLM successfully captures this trend correctly is due to incorporation of the multiscale interaction timescale τ_π as the timescale for interphase TKE transfer. As mentioned earlier, drag models based on the particle–response timescale fail to capture this trend of TKE decay with increasing Stokes number (Pai and Subramaniam, 2006).

6.7.1.2 Prediction of particle velocity autocorrelation in particle–laden decaying turbulence

Figure (6.4) shows the predicted evolution of the particle velocity autocorrelation in decaying turbulence given by Eq. (6.15) for a range of Stokes numbers for the test case TE. Also shown on the same plot are corresponding results from DNS (Truesdell and Elghobashi, 1994). With increasing particle Stokes number, the decay in particle velocity autocorrelation is slower since particles with larger inertia lose correlation with their earlier velocities slower. This implies that the timescale of decay of particle velocity autocorrelation *increases* with increasing Stokes number. DLM accurately captures this trend of decay of particle velocity autocorrelation with varying Stokes numbers. Interestingly, the particle velocity autocorrelation behaves in an identical manner in stationary turbulence (Pai and Subramaniam, 2007), where DLM is again successful in reproducing trends observed in DNS.

It is noteworthy to recapitulate at this point that two–phase turbulence models in which the interphase TKE transfer evolves on the particle response timescale τ_p (see Pai and Subramaniam (2006)) do not possess the capability to *simulaneously* capture the decay trend in the TKE and the decay trend in particle velocity autocorrelation with varying Stokes number. Models employed in LE statistical implementations of two–phase flows fall in this category (Amsden et al., 1989).

6.7.2 CASE II: Homogeneous shear

6.7.2.1 Prediction of TKE in particle–laden homogeneous shear

For a uniformly imposed mean shear in the 1–3 direction as $\partial\langle U_i\rangle/x_j = \partial\langle V_i\rangle/x_j = \mathcal{S}\delta_{i1}\delta_{j3}$, the implied evolution equations given in Eq. (6.8) and Eq. (6.9) can be written as

$$\frac{d}{dt}\langle u_i u_j\rangle = -2A(t)\langle u_i u_j\rangle - (\langle u_k u_j\rangle \mathcal{S}\delta_{1i}\delta_{k3} + \langle u_i u_k\rangle \mathcal{S}\delta_{j1}\delta_{k3}) + B(t)^2\delta_{ij} \tag{6.29}$$

$$\frac{d}{dt}\langle v_i v_j\rangle = -2C(t)\langle u_i u_j\rangle - (\langle v_k v_j\rangle \mathcal{S}\delta_{1i}\delta_{k3} + \langle v_i v_k\rangle \mathcal{S}\delta_{j1}\delta_{k3}) + D(t)^2\delta_{ij}, \tag{6.30}$$

which simplify to

$$\frac{dk_f}{dt} = -\frac{k_f - k_f^e}{\tau_2} - \langle u_k u_i\rangle \mathcal{S}\delta_{1i}\delta_{k3} - \varepsilon_f \tag{6.31}$$

$$\frac{dk_d}{dt} = -\frac{k_d - k_d^e}{\tau_4} - \langle u_k u_i\rangle \mathcal{S}\delta_{1i}\delta_{k3} \tag{6.32}$$

in the case of DLM. The dissipation equation Eq. (6.26) simplifies to

$$\frac{d\varepsilon_f}{dt} = -C_{\varepsilon 2}\frac{\varepsilon_f^2}{k_f} + C_s\frac{\varepsilon_f}{k_f}\left(\frac{k_f^e - k_f}{\tau_\pi}\right) - C_{\varepsilon 3}\langle u_1 u_3\rangle \mathcal{S}\frac{\varepsilon_f}{k_f}. \tag{6.33}$$

The computations are initialized at time $\mathcal{S}t = 1$ when, as per the DNS (Ahmed and Elghobashi, 2000), the carrier–phase turbulence is fully developed. At this time, the stochastic particles that represent the fluid and the dispersed phases are initialized with mean zero and covariance given by $\langle u_i u_j\rangle = 2k_f[b_{ij} + (1/3)\delta_{ij}]$ and $\langle v_i v_j\rangle = 2k_d[b_{ij} + (1/3)\delta_{ij}]$, respectively. The components of the initial anisotropic tensor b_{ij}, which is the same for both the phases, are $b_{11} = 0.036186$, $b_{22} = -0.044069$, $b_{33} = 0.007883$ and $b_{13} = b_{31} = -0.121595$ at $\mathcal{S}t = 1$. The fluid–phase dissipation ε_f at this scaled time is 0.00057678, and the fluid kinematic viscosity ν_f is 0.000105. Test cases investigated in this study are the denoted B, G, F, C, I, H and F, and parameter corresponding to these test cases are given in Tables 6.5 and 6.4.

Figure (6.5) shows the predicted evolution of the fluid–phase TKE by DLM for varying Stokes numbers (particle inertia) and constant mass loading of $\phi = 0.1$. These test cases correspond to cases C, I, H and F in the DNS AE–1. It is difficult to predict the evolution of the TKE based on intuition as is possible in CASE I for particle–laden homogeneous decaying turbulence. This is primarily because there are competing effects of fluid–phase dissipation

and production due to the mean shear, coupled with interphase TKE transfer. It appears from the DNS that with increasing particle inertia and for a constant mass loading, the increase in the fluid–phase TKE is slower, a trend that is accurately captured by DLM. This trend with increasing particle inertia is identical to that observed in CASE I for homogeneous decaying turbulence. It is interesting to note that EE drag models based on the particle–response timescale are unable to capture this trend in particle–laden homogeneous shear flow (See Fig. (16) of Xu and Subramaniam (2006)), thereby supporting the need to ascertain the behavior of two–phase models in the freely–decaying turbulence canonical problem. Figure (6.6) shows that the trend of fluid–phase dissipation predicted by Eq. (6.33) for varying Stokes numbers matches with DNS results, although there is slight cross over at initial time.

Figure (6.7) shows the predicted evolution of the fluid–phase TKE by DLM for varying mass loading and constant particle response time $\tau_p = 1.0$. These test cases correspond to the cases B, G and F in the DNS AE–1. For increasing mass loading the DNS depicts a slower increase in k_f. DLM predicts the trends accurately after scaled time $t/T_{\text{ref}} = 1.2$, but predicts a cross over at initial time. Close inspection of the DNS results (see Figure (46) in AE–1) in fact reveals a similar cross over, although not as conspicuous as predicted by DLM. The fluid–phase dissipation as predicted by Eq. (6.33) for this test is also close to the DNS results as is depicted in Fig. (6.8). The initial increase in the dissipation for $\phi = 1.0$ that is observed in the DNS results is also predicted well by the dissipation model.

To quantify the contribution to each term in the fluid–phase TKE evolution equation, the budgets of each term on the right hand side of Eq. (6.31) are shown in Fig. (6.9) for the case where $\tau_p = 1.0$ and $\phi = 1.0$ (case B in AE–1). In the figure, Π_{kf} is the interphase TKE transfer (first term on the right hand side of Eq. (6.31)). The general trend in the evolution of the budgets agree with the DNS results. However, the predicted magnitude of the interphase TKE transfer term Π_{k_f} is different from the DNS results. In Xu and Subramaniam (2006), a similar plot for the EEM model predictions (see Fig. (13) in that reference) shows a much smaller magnitude of Π_{k_f}. The difference in the magnitude of Π_{k_f} between this study and Xu and Subramaniam (2006) can be traced to two sources: (i) the expression for C_k is $C_k = 0.6\phi$

in Xu and Subramaniam (2006), which does not contain an explicit dependence on St_η, and (ii) the model for $\langle u_1 u_3 \rangle$ is different from that implied by DLM (compare Eqs. (28)–(29) in Xu and Subramaniam (2006) and Eqs. (6.29)–(6.30)).

6.8 Discussion

In all the test case presented above, DLM is able to capture trends of important statistics in particle–laden freely–decaying turbulence and homogeneous shear. In particular, the ability of DLM to capture the trends of TKE decay in freely–decaying turbulence for varying Stokes number is noteworthy since drag models based on the particle response timescale are incapable of capturing this trend (Pai and Subramaniam, 2006). DLM also has the capability to capture the correct behavior of the dispersion timescale in particle–laden freely decaying turbulence, thereby illustrate the ability to capture the disparate timescale associated with dispersion and dynamics of a two–phase flow. In particle–laden homogeneous shear, DLM is able to capture the correct evolution of fluid–phase TKE. In such flows, there are competing effects of production due to mean velocity gradients, interphase TKE transfer, and dissipation. Although the dissipation is modeled, it appears that DLM performs well in predicting the production $\langle u_1 u_3 \rangle \mathcal{S}$ and the interphase TKE transfer.

The reasons for the emphasis in this study on predicting only the trends correctly rather than seeking an exact quantitative match are manifold. In DNS of particle-laden flow (Sundaram and Collins, 1999; Mashayek et al., 1997; Squires and Eaton, 1991a), although the gas phase is treated accurately by solving the full Navier–Stokes equations, the no–slip condition on the surface of each particle is not enforced. Also, since the flow around each particle is not resolved, a drag model of the form derived by Maxey and Riley (1983) is used to evolve particle velocities in time. The influence of the particle on the fluid–phase momentum equation is included by means of a modeled source term. It is important to recognize that the point–particle assumption for the *particle drag* in such DNS is justified in a limited flow regime where particle Reynolds numbers Re_d are $\mathcal{O}(1)$, dispersed phase to fluid density ratios ρ_d/ρ_f are $\mathcal{O}(1000)$, and particles are sub–Kolmogorov size with negligible wake effects. The homogeneous prob-

lem that forms the basis of the investigation in this work and for which DNS datasets exist corresponds to a flow regime where the assumptions mentioned earlier are valid.

However, volume–displacement effects are neglected in such DNS and the carrier–phase velocity field is assumed to be solenoidal. Also, particle–particle (or drop–drop) interaction effects are not accounted for in such DNS, and the effect of the point–particle approximation on the true pressure field is also not quantified. The only way to test whether these approximations are justified is to perform *true* DNS where the flow around each particle is fully resolved and exact boundary conditions are imposed on each particle surface. The assumption of solenoidality of the gas–phase velocity (which in turn affects the fluid pressure field), and neglect of particle–particle interaction effects, can only be tested in a true DNS. Recent studies by Ten Cate et al. (2004) are emerging which seek to assess the consequences of the point–particle approximation. They perform fully resolved simulations of particle–laden stationary turbulence in the same particle Stokes number and particle mass loading range as in the DNS study by Boivin et al. (1998) which uses a point–particle approximation for the dispersed phase. Ten Cate et al. (2004) find that the decrease in the rate of energy dissipation at the large scales is of the same order as that found by Boivin et al. (1998). However, one should note that the particle diameter is smaller than the Kolmogorov length scale, particle to fluid density ratios are $\mathcal{O}(1000)$ and the particle Reynolds numbers are $\mathcal{O}(1)$ in the DNS performed by Boivin et al. (1998). On the other hand, the particle diameters are larger than the Kolmogorov length scale, particle to fluid density ratios are $\mathcal{O}(1)$ and particle Reynolds numbers are $\mathcal{O}(10)$ in the fully resolved DNS performed by Ten Cate et al. (2004) and their simulations do not fall in the regime of two–phase flows investigated in this study.

Therefore, the DNS datasets performed with the point–particle approximation that are used in this study are the best data available for model testing and validation. It appears very likely that the existing DNS datasets *do* capture the major trends of the TKE variation and autocorrelation evolution with important non–dimensional parameters like Stokes number and mass loading. It is possible that true DNS such as the one performed by Ten Cate et al. (2004) might lead to revision in the exact quantitative predictions. Owing to all the reasons cited

above, our principal conclusions concern qualitative trends predicted by DLM, rather than an exact quantitative match with available DNS data.

6.9 Conclusions

Direct numerical simulations of particle–laden flow confirm the existence of two disparate timescales, one governing particle dispersion and the other governing the interphase TKE transfer, that behave differently with Stokes number. In this context, the principal conclusions and achievements of this study are:

1. Two–phase flow turbulence models should possess the capability to capture these disparate timescales observed in simple two–phase flow DNS. They should also possess the capability to capture the trends of these timescales with varying Stokes number in these simple flow configurations in order to be predictive in more complex spray computations.

2. A new Dual–timescale Langevin Model, based on the Equilibration of Energy concept is proposed. A novel feature of the proposed model is the incorporation of dual timescales, which can be specified to match the disparate trends in the evolution of TKE and velocity autocorrelation with varying Stokes number and mass loading.

3. DLM predicts the evolution of TKE and particle dispersion in freely–decaying turbulence which are in good agreement with DNS data.

4. DLM predicts the evolution of TKE in particle–laden homogeneous shear, wherein there is an interplay between interphase TKE transfer, dissipation and production due to mean velocity gradients.

In summary, a new model that can simultaneously capture important two–phase flow phenomena is proposed. Such a feature is as yet unavailable in two–phase flow models in literature. The next chapter will investigate the behavior of DLM in predicting dynamics and dispersion in evaporating and non–evaporating droplet–laden stationary turbulence.

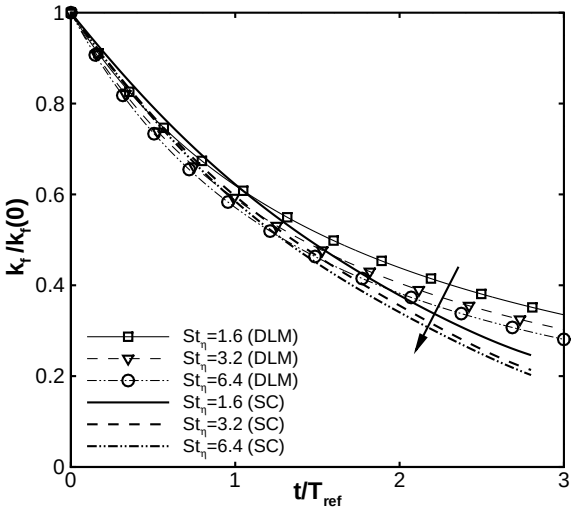

Figure 6.2 Evolution of TKE in the fluid phase (CASE I). Arrow indicates direction of increasing Stokes number.

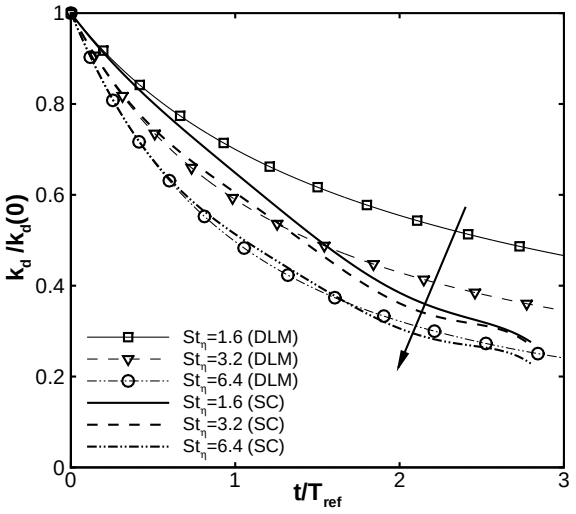

Figure 6.3 Evolution of TKE in the dispersed phase (CASE I). Arrow indicates direction of increasing Stokes number.

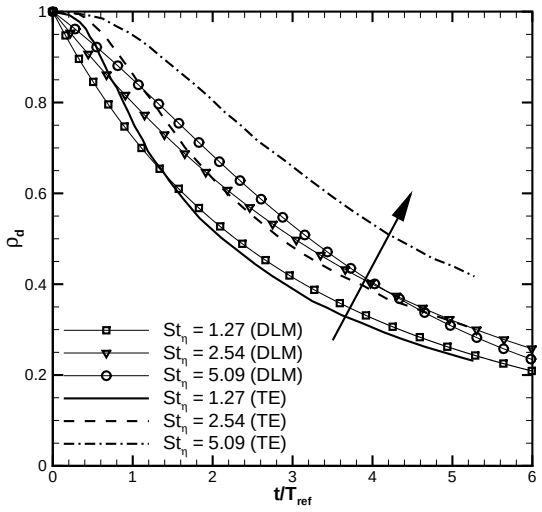

Figure 6.4 Evolution of dispersed–phase velocity autocorrelation for varying Stokes number St_η in particle–laden decaying turbulence alongside results from DNS Truesdell and Elghobashi (1994). Arrow indicates direction of increasing Stokes number.

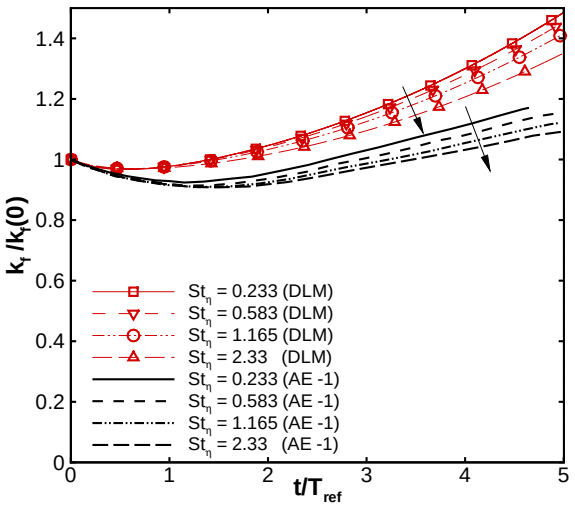

Figure 6.5 Evolution of fluid–phase TKE for varying particle inertia and constant mass loading $\phi = 0.1$ (CASE II). Arrow indicates direction of increasing particle inertia.

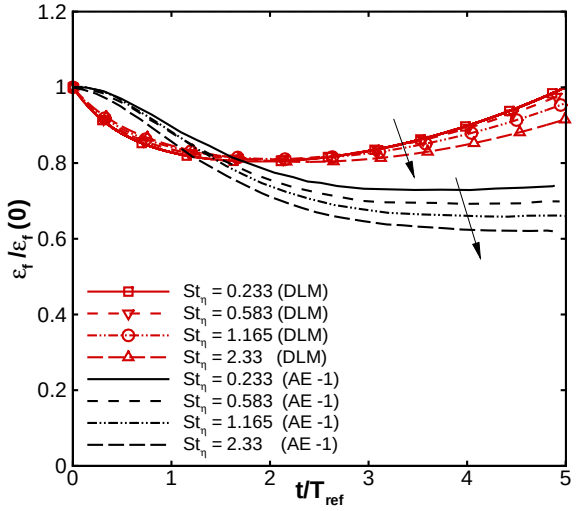

Figure 6.6 Evolution of fluid–phase dissipation for varying particle inertia for constant mass loading. Arrow indicates direction of increasing particle inertia.

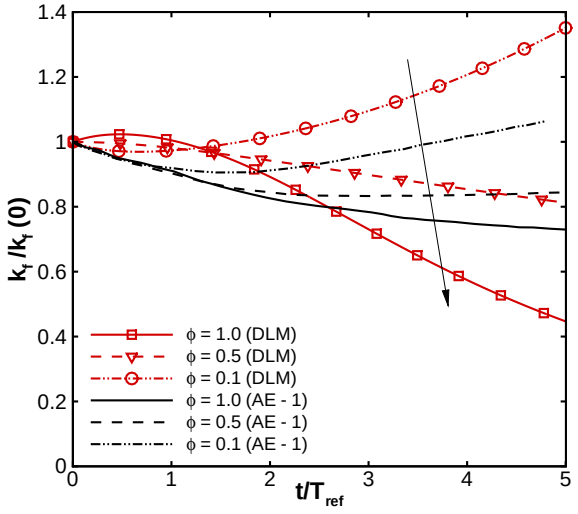

Figure 6.7 Evolution of fluid–phase TKE for varying mass loading and constant particle inertia $\tau_p = 1.0$ (CASE II). Arrow indicates direction of increasing mass loading.

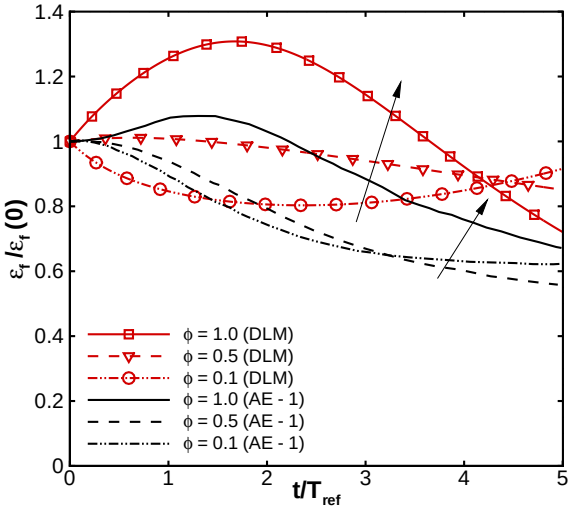

Figure 6.8 Evolution of fluid–phase dissipation for varying mass loading. Arrows indicate direction of increasing mass loading for the DLM predictions and DNS results.

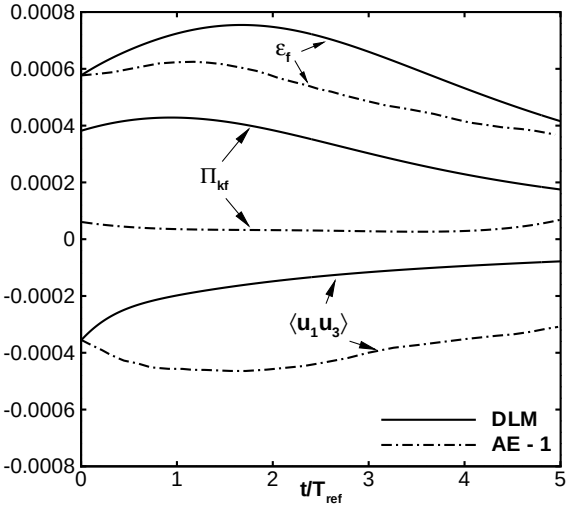

Figure 6.9 Comparison of budgets of each term on the right hand side of the fluid–phase TKE evolution equation Eq. (6.31) predicted by DLM with DNS results.

CHAPTER 7. MODELING DROPLET DISPERSION AND INTERPHASE TURBULENT KINETIC ENERGY TRANSFER USING DLM

A significant part of this chapter has appeared in 'M. G. Pai and S. Subramaniam (2007). Modeling droplet dispersion and interphase turbulent kinetic energy transfer using a new dual-timescale Langevin model, Intl. J. Multiphase Flow, 33(3):252–281.'

Dispersion of spray droplets and the modulation of turbulence in the ambient gas by the dispersing droplets are two coupled phenomena that are closely linked to the evolution of global spray characteristics, such as the spreading rate of the spray and the spray cone angle. Direct numerical simulations (DNS) of turbulent gas flows laden with sub–Kolmogorov size particles, in the absence of gravity, report that dispersion statistics and turbulent kinetic energy (TKE) evolve on different timescales. Furthermore, each timescale behaves differently with Stokes number, a non–dimensional flow parameter (defined in this context as the ratio of the particle response time to the Kolmogorov timescale of turbulence) that characterizes how quickly a particle responds to turbulent fluctuations in the carrier or gas phase. A new dual–timescale Langevin model (DLM) composed of two coupled Langevin equations for the fluctuating velocities, one for each phase, is proposed. This model possesses a unique feature that the implied TKE and velocity autocorrelation in each phase evolve on different timescales. Consequently, this model has the capability of simultaneously predicting the disparate Stokes number trends in the evolution of dispersion statistics, such as velocity autocorrelations, and TKE in each phase. Predictions of dispersion statistics and TKE from the new model show good agreement with published DNS of non–evaporating and evaporating droplet–laden turbulent flow.

7.1 Background

The evolution of a fuel spray in an internal combustion engine is strongly influenced by its interaction with the rapidly changing turbulent gas phase in the combustion chamber. Turbulence in the ambient gas directly affects the spreading rate of a spray which in turn affects the spray penetration length and spray cone angle. Dispersing droplets in turn amplify or suppress the turbulence in the ambient gas, thereby coupling the effects of turbulence and droplet dispersion.

Direct numerical simulations (DNS) of particle–laden decaying turbulence performed in the absence of gravity report that the timescale for interphase turbulent kinetic energy (TKE) transfer is different from the timescale associated with particle dispersion, and that the trends of these timescales are also different for varying Stokes numbers. Particles with high Stokes number lose energy *faster* than particles with low Stokes number in freely decaying turbulence (Sundaram and Collins, 1999). On the other hand, particles with high Stokes number lose correlation with their initial velocities *slower* than particles with low Stokes number in stationary turbulence (Mashayek et al., 1997; Squires and Eaton, 1991a). The disparate behavior of the velocity autocorrelation and TKE timescales affects the dispersion characteristics of a spray. Turbulence models for spray computations (or particle–laden turbulent flows, in general) must be capable of simultaneously capturing these disparate timescale trends with Stokes number, in order to be predictive.

Experimental evidence for the dependence of the evolution timescales of velocity autocorrelation and interphase TKE transfer on Stokes number is available in literature (Snyder and Lumley, 1971; Wells and Stock, 1983; Groszmann and Rogers, 2004). However, unlike in the DNS studies, it is difficult to isolate physical mechanisms that affect these timescales in experiments. Snyder and Lumley (1971), in their particle–laden grid–generated turbulence experiments in gravity, report a particle–velocity autocorrelation timescale that shows a trend that is opposite to that reported in the DNS (Sundaram and Collins, 1999; Mashayek et al., 1997; Squires and Eaton, 1991a). They find that particles with higher inertia lose correlation with their initial velocities faster than particles with lower inertia. However, they acknowledge

that the observed trend in the autocorrelation timescale with Stokes number may be due to the predominant effect of crossing trajectories in their experiments. They also report that particles with larger inertia lose TKE faster than particles with lower inertia. Wells and Stock (1983) used two sets of charged particles evolving in an electric field to control the effects of particle drift in their experiments of particle–laden grid–generated turbulence. Based on the size of the 95% confidence intervals one may conclude that the reported long time dispersion coefficient of the higher–inertia particles are around the same as that for particles with lower inertia. Thus, one cannot infer a dependence of the autocorrelation timescale on Stokes number from this observation. While they acknowledge the presence of experimental uncertainty in their results, they mention that the higher inertia particles had a lower fluctuating velocity than the lower inertia particles which appears to agree with the DNS results cited earlier. In order to negate the effects of gravity, Groszmann and Rogers (2004) have performed experiments in microgravity and reported mean squared displacements for Stokes numbers 1, 50 and 100. However, due to limitations in observation time during microgravity experiments, it is difficult to extract velocity autocorrelations and long–time diffusion coefficients from such experiments for a range of Stokes numbers for valid conclusions to be made. They also acknowledge the presence of sampling errors in the results for Stokes numbers around unity.

Given the uncertainty involved in experiments in extracting velocity autocorrelations and TKE in dispersed two–phase flows, the canonical DNS cited earlier are of intrinsic value to the modeling community for two principal reasons. Firstly, crossing trajectory effects due to particle drift, and particle inertia effects are easily isolated in numerical computations. Secondly, models for individual terms in the governing equations for dispersed two–phase flows, like the interphase TKE and mass transfer, can be tested in isolation by comparing with corresponding terms extracted from DNS. The same is not possible with experiments. Thus, reproducing results from such canonical two–phase DNS constitutes an important first step in validating multiphase flow turbulence models.

In the Lagrangian–Eulerian (LE) representation of two–phase flows, the dispersed phase is modeled using *computational* particles whose velocities evolve according to a drag model of

the form

$$\frac{d\mathbf{V}_p}{dt} = \frac{\mathbf{U}_f - \mathbf{V}_p}{\tau_p} C_d(Re_d) + \mathbf{F}_{\text{add}}, \tag{7.1}$$

and whose positions evolve according to

$$\frac{d\mathbf{X}_p}{dt} = \mathbf{V}_p, \tag{7.2}$$

where $\mathbf{V}_p$ is the instantaneous particle velocity, $\mathbf{U}_f$ is the instantaneous gas–phase velocity [1], $\tau_p = (\rho_d d_p^2)/(\rho_f 18\nu_f)$ is the particle response timescale, $\mathbf{X}_p$ is the particle position and $\mathbf{F}_{\text{add}}$ represents additional terms that include lift and body forces. The instantaneous gas–phase velocity $\mathbf{U}_f$ is decomposed into a mean $\langle \mathbf{U}_f \rangle$ and a fluctuating component $\mathbf{u}'_f$). Here, ρ_d and ρ_d are the thermodynamic densities of the dispersed phase and fluid phase, respectively, d_p is the particle or droplet diameter and ν_f is the kinematic viscosity of the fluid phase. A drag coefficient C_d that depends on the droplet Reynolds number Re_d is generally included as shown. The major research effort in modeling turbulent two–phase flows using the LE representation has been directed towards arriving at a suitable model for $\mathbf{U}_f$. The principal LE modeling studies that are relevant to dispersion and TKE evolution are reviewed here.

Lu (1995) uses a time–series analysis involving fluid–phase temporal and spatial Eulerian velocity correlations to arrive at a stochastic model for the fluid velocity at the particle location, in the limit of one–way coupled turbulence. Spray droplet interactions with the gas phase are, however, strongly two–way coupled. Nevertheless, testing the behavior of a two–phase model in the limit of one–way coupled spray configurations is indeed necessary. Lu reports good agreement between model results and theoretical results of Csanady (1963), and particle–laden grid–generated turbulence results of Snyder and Lumley (1971) in predicting particle diffusion coefficients and velocity autocorrelations. Mashayek (1999) used Lu's time–series approach to predict particle–velocity autocorrelation functions and asymptotic diffusion coefficients for non-evaporating and evaporating droplets laden in one–way coupled stationary turbulence, again reporting overall reasonable agreement with DNS data (Mashayek et al., 1997). An extension of the time–series model has been tested by Gao and Mashayek (2004b) in compressible homogeneous shear flows with interphase mass transfer due to evaporating droplets.

[1] Also sometimes referred to as the gas–phase velocity "seen" by the particles.

They report good agreement of predicted droplet velocity correlations and droplet–fluid velocity cross correlations with DNS of evaporating droplets in a low Mach number turbulent shear flow (Mashayek, 1998). Pozorski and Minier (1999) modified the Lagrangian integral timescale in the generalized Langevin model proposed by Haworth and Pope (1986) to arrive at the fluid velocity "seen" by the particles. To our knowledge, no validation tests are available in literature that quantify the predictive capability of this model in canonical particle–laden flows. Chagras et al. (2005) employ a Langevin–type equation that uses the Lagrangian integral timescale of the fluid "seen" by the particles and the fluid–phase Reynolds stresses to arrive at a model for $\mathbf{u}'_f$. They analyze several cases of two–way coupled gas–solid pipe flow with large mass loading reporting overall agreement of temperature profiles and instantaneous velocities with experimental results. Chen and Periera (1997) use an assumed probability density function (pdf) for the spatial distribution of the particles whose variance evolves in time by an ordinary differential equation containing an assumed fluid–phase Lagrangian autocorrelation of the Frenkiel form (Gouesbet and Berlemont, 1999). They report good match of predicted dispersed–phase velocities from their two–way coupled simulations with results from experiments conducted on particle–laden planar mixing layers and co–flowing planar jets.

With the exception of Mashayek (1999), there is no evidence in literature of tests conducted with the aforementioned models in simple canonical two–phase flows (like stationary or freely decaying particle–laden turbulence) to test their capability in simultaneously capturing the energy and dispersion timescales as observed in DNS. However, the time series model (Lu, 1995) used by Mashayek (1999) relies on statistics of the fluid phase that are valid only in the limit of one–way coupled two–phase flows. Extending the time series model to two–phase flows with significant two–way coupling effects will require the knowledge of the Eulerian spatial correlation of gas–phase velocity which is a non–trivial quantity to measure or model in such flows. Also, the extension of the time–series model proposed by Gao and Mashayek (2004a,b) involves correlations among the velocity components, temperature and mass fraction, with the assumption that all these correlations evolve on the same Eulerian fluid integral timescale.

Another common feature of the LE models cited above is the use of the particle response

time τ_p as the timescale for both interphase momentum and TKE transfer. Recently, a representative LE model (Amsden et al., 1989) was tested in freely decaying turbulence laden with sub–Kolmogorov size particles (Pai and Subramaniam, 2006). It was shown in that study that LE models based on the particle response timescale fail to accurately capture trends in the evolution of TKE in both phases with varying Stokes numbers, when tested in the canonical problem. This observation pointed to a need for improvement in the predictive capability of existing LE models. A multiscale interaction timescale was proposed (Pai and Subramaniam, 2006), to replace τ_p, that captured trends in the evolution of TKE with varying Stokes number as seen in the DNS.

The primary objective of this work is to propose a new model called the Dual–timescale Langevin model (DLM). In this model we adopt a Lagrangian–Lagrangian description of both the fluid and dispersed phases. Unlike the models cited earlier, we do not use Eq.(7.1) to evolve the particle velocities, and also the implied TKE in either phase evolves on a timescale derived by taking into account the multiscale nature of droplet–turbulence interaction (Pai and Subramaniam, 2006). Furthermore, the novel feature of this model is the existence of dual timescales in a single model that enables the model to *simultaneously* capture the disparate Stokes number trends in the evolution of TKE and also particle dispersion characteristics in both phases. It is important to note that although Langevin models have been successful in predicting turbulent reactive flows (Pope, 2000, 1985), extending these models to two–phase flows is not straightforward. This is because single–phase Langevin models are based on a single timescale and such models are clearly incapable of simultaneously capturing the disparate timescales of TKE and autocorrelation observed in two–phase DNS. However, Langevin models have the advantage that they are more amenable to analysis than existing LE models based on stochastic white noise (Gosman and Ioannides, 1983; Amsden et al., 1989). A second objective of this work, and a guiding principle for the model development, is to clearly identify terms in the governing equations of the dispersed phase that require modeling.

The rest of the paper is organized as follows. The new stochastic model is introduced and implied evolution equations for the statistics of the fluid and dispersed phases are derived in

Section 7.2. A new hypothesis for modeling the interphase TKE transfer called the Equilibration of Energy (EoE) concept is presented in Section 7.3. The rationale underlying the specification of model constants is explained in Section 7.4. Test cases for which DNS data are available from Mashayek et al. (1997) for both non–evaporating and evaporating droplet–laden stationary turbulence are described in Section 7.5. Model predictions for these test cases are reported in Section 7.6. An assessment of the model and the DNS data is presented in Section 6.8. The final section presents the principal conclusions of the study.

7.2 Dual–timescale Langevin model (DLM)

A new stochastic model called the Dual–timescale Langevin model (DLM) is proposed for homogeneous turbulent two–phase flows. This model consists of a system of stochastic differential equations (SDE) for the modeled fluctuating Lagrangian gas–phase velocity $\mathbf{u}$ and fluctuating Lagrangian dispersed–phase velocity $\mathbf{v}$. The proposed system of SDEs is

$$du_i = -\left[\frac{1}{2\tau_1} + \left(\frac{1}{2} + \frac{3}{4}C_0\right)\frac{\varepsilon_f}{k_f}\right]u_i dt + \left[C_0\varepsilon_f + \frac{2}{3}\frac{k_f}{\tau_1} + \frac{2}{3}\left(\frac{k_f^e - k_f}{\tau_2}\right)\right]^{1/2} dW_i^u \tag{7.3}$$

$$dv_i = -\frac{1}{2\tau_3}v_i dt + \left[\frac{2}{3}\frac{k_d}{\tau_3} + \frac{2}{3}\left(\frac{k_d^e - k_d}{\tau_4}\right)\right]^{1/2} dW_i^v, \tag{7.4}$$

where τ_1, τ_2, τ_3 and τ_4 are timescales that appear in the drift and diffusion coefficients[2] of each SDE, while dW_i^u and dW_i^v are independent Wiener processes (Kloeden and Platen, 1992). The subscript i denotes the Cartesian components. The TKE in the dispersed phase is denoted k_d and the TKE in the gas phase is denoted k_f, with a superscript 'e' to denote their 'equilibrium' values (the concept of 'equilibrium' is explained in Section 7.3)[3]. Also, ε_f is the gas–phase dissipation enhanced by the presence of the dispersed phase. The constant $C_0 = 2.1$, which is identical to that used in the Simplified Langevin model (SLM) (Pope, 2000). Mean velocity and, hence mean slip in either phase is assumed to be zero for simplicity, although this is not an inherent limitation of DLM. The fluid–phase SDE can be viewed as an extension of the SLM (Pope, 2000; Haworth and Pope, 1986) to two–phase flows, but with an important difference being the introduction of drift and diffusion timescales that are different from each

[2]The terms 'drift' and 'diffusion' are used in the sense of stochastic differential equation theory.

[3]The subscript f stands for the gas phase or fluid phase, and the subscript d stands for the dispersed phase.

other. Also, additional terms involving k_f^e and k_d^e (in parentheses) that represent interphase interactions have been added. The coupling between the two phases is only through moments of the velocities in each phase like TKE (k_f and k_d) and the dissipation ε_f, and not explicitly through the instantaneous values of u_i and v_i.

One can derive the implied evolution equations for the TKE in the fluid phase, defined as $k_f = (1/2)\langle u_i u_i \rangle$, (where the averaging is performed over an ensemble of realizations) and the TKE in the dispersed phase, defined as $k_d = (1/2)\langle v_i v_i \rangle$, from Eq.(7.3) and Eq.(7.4), respectively, to be

$$\frac{dk_f}{dt} = \left(\frac{k_f^e - k_f}{\tau_2} \right) - \varepsilon_f \tag{7.5}$$

$$\frac{dk_d}{dt} = \left(\frac{k_d^e - k_d}{\tau_4} \right). \tag{7.6}$$

Of the four timescales present in Eq.(7.3) and Eq.(7.4), only τ_2 and τ_4 appear in the above equations. The equilibrium energies, k_f^e and k_d^e, are related to each other as will be shown later, and so the evolution of k_f and k_d are coupled through these terms. It has to be emphasized here that the interphase TKE transfer timescales τ_2 and τ_4 are not *equal* to τ_p, although they do depend on this timescale. Note that for widely–used LE models, the interphase TKE transfer evolves on the particle response timescale τ_p, which was found to be inadequate to capture the multiscale nature of particle–turbulence interaction (Pai and Subramaniam, 2006). The exact form of these timescales will be presented in Section 7.4.

Stationary turbulence limit

In the context of two–phase flows, an important canonical problem is homogeneous turbulence in which the fluid phase turbulence is artificially forced to remain stationary, while the dispersed phase evolves to its stationary state. Several studies have been performed in this important limiting case using DNS (Squires and Eaton, 1991a; Mashayek et al., 1997), making it an ideal case for model validation.

In the limit of stationary turbulence, the drift coefficient in the fluid phase SDE in Eq.(7.3) is modified along the lines of the SLM proposed for single–phase stationary turbulence (Pope,

2000) as

$$du_i = -\left(\frac{1}{2\tau_1} + \frac{3}{4}C_0\frac{\varepsilon_f}{k_f}\right)u_i dt + \left[C_0\varepsilon_f + \frac{2}{3}\frac{k_f}{\tau_1} + \frac{2}{3}\left(\frac{k_f^e - k_f}{\tau_2}\right)\right]^{1/2} dW_i^u. \tag{7.7}$$

With this modification, the fluid phase dissipation drops out of the implied evolution equation for the TKE in the fluid phase, which now reads

$$\frac{dk_f}{dt} = \left(\frac{k_f^e - k_f}{\tau_2}\right). \tag{7.8}$$

In the limit of two–way coupled homogeneous particle–laden stationary turbulence, Eq.(7.8) and Eq.(7.6) form the modeled governing equations for the TKE in the fluid and dispersed phases, respectively. The only term appearing on the right hand side of these equations is the TKE transfer due to inter–phase interactions.

Equation(7.8) is a physically consistent model for k_f in an artificially forced two–phase flow system where energy is added at the large scales to exactly balance the viscous dissipation, which now includes additional dissipation due to the presence of the particles in the fluid phase. DLM predicts that, in the case of stationary turbulence, the TKE in the fluid phase would evolve to an equilibrium value k_f^e over a timescale τ_2. Statistics related to dispersion of spray droplets, as implied by DLM, are derived next.

7.2.1 Implied Lagrangian velocity autocorrelation

In stationary isotropic turbulence, which is the main focus of this study, the Lagrangian velocity autocorrelation denoted $R_{\beta_{ij}}(s)$ is given as (Hinze, 1975):

$$R_{\beta_{ij}}(s) = \frac{\langle\gamma_i(t_0)\gamma_j(t_0+s)\rangle}{\langle\gamma_i(t_0)\gamma_j(t_0)\rangle}, \tag{7.9}$$

where t_0 can be any initial time after the system reaches stationarity and s is the *separation* time. No summation is implied over repeated indices. Here, γ stands for either u or v. The Lagrangian autocorrelation is simply a normalized autocovariance and gives a measure of how quickly the fluid–particle or droplet loses correlation with its velocity at some earlier time. Note that for isotropic turbulence, $R_{\beta_{ij}} = 0$ for $i \neq j$, and $R_{\beta_{ii}} = R_{\beta_{jj}}$ for $i, j \in \{1, 2, 3\}$.

The evolution equation for the fluid velocity autocovariance implied by DLM for the stationary case is

$$\frac{d\langle u_i(t_0)u_j(t)\rangle}{dt} = -\left(\frac{1}{2\tau_1} + \frac{3}{4}C_0\frac{\varepsilon_f}{k_f}\right)\langle u_i(t_0)u_j(t)\rangle, \tag{7.10}$$

while the evolution equation for the dispersed–phase velocity autocovariance is

$$\frac{d\langle v_i(t_0)v_j(t)\rangle}{dt} = -\frac{1}{2\tau_3}\langle v_i(t_0)v_j(t)\rangle, \tag{7.11}$$

where $t = t_0 + s$.

A striking feature of DLM is that Eqs.(7.5)–(7.6) depend on the timescales τ_2 and τ_4, respectively, while Eqs.(7.10)–(7.11) depend on timescales τ_1 and τ_3, respectively. In DLM, therefore, the evolution of TKE can be constructed to behave *differently* from the evolution of the velocity autocovariance. In model proposals that use the generalized Langevin model (Pozorski and Minier, 1999), however, the implied TKE in the fluid phase and the velocity autocorrelation evolve over the same timescale, namely the Lagrangian integral timescale.

The dispersion of droplets or fluid particles is characterized by the diffusion coefficient tensor associated with phase β, denoted $\alpha_{\beta_{ij}}$. In the isotropic case, the diagonal components of the diffusion coefficient tensor are all identical viz. $\alpha_{\beta_{11}} = \alpha_{\beta_{22}} = \alpha_{\beta_{33}} = \alpha_\beta$. In the stationary case, the diffusion coefficient tensor and the Lagrangian velocity autocorrelation tensor are related by

$$\alpha_{\beta_{ij}}(t) = \langle\gamma_i(t_0)\gamma_j(t_0)\rangle\int_0^t R_{\beta_{ij}}(t')dt' \tag{7.12}$$

(again, no summation is implied over repeated indices) [4].

7.3 Equilibration of Energy (EoE) concept

The right hand sides of Eq. (7.8) and Eq. (7.6) are models for the interphase TKE transfer, and are based on the EoE concept that was proposed by Xu and Subramaniam (2006). This concept is briefly reviewed here for the sake of completeness.

[4] In order to be consistent with the published journal article (Pai and Subramaniam, 2007), the diffusion coefficients corresponding to the fluid phase and dispersed phase are denoted α_f and α_d, respectively, in the rest of this chapter, while the volume fraction is denoted θ.

In order to explain the EoE concept, the following system of model equations for the evolution of TKE in a dilute homogeneous two–phase flow system (with no interphase mass transfer) is proposed:

$$\frac{de_f}{dt} = \Pi_{k_f} - \rho_f \theta_f \varepsilon_f \tag{7.13}$$

$$\frac{de_d}{dt} = \Pi_{k_d}, \tag{7.14}$$

where $\Pi_{k_f} = (e_f^e - e_f)/\tau_\pi$ and $\Pi_{k_d} = (e_d^e - e_d)/\tau_\pi$ are the interphase TKE transfer terms. Here, τ_π is the interphase TKE transfer timescale, while $e_f = \rho_f \theta_f k_f$ and $e_d = \rho_d \theta_d k_d$ are the *specific* fluid phase and dispersed phase energies, respectively, and $e_f^e = \rho_f \theta_f k_f^e$ and $e_d^e = \rho_d \theta_d k_d^e$ are the equilibrium *specific* TKEs in the gas phase and dispersed phase, respectively. The volume fractions of the fluid phase and dispersed phase are denoted θ_f (see Footnote 4) and $\theta_d = 1 - \theta_f$, respectively. Collisions among particles are elastic and hence no dissipation is considered in the dispersed phase.

Adding Eqs.(7.13) and (7.14) results in

$$\frac{de_m}{dt} = -\rho_f \theta_f \varepsilon_f,$$

where $e_m = \rho_m k_m = e_f + e_d = \rho_f \theta_f k_f + \rho_d \theta_d k_d$ is the mixture energy in the two–phase flow system and ρ_m is the mixture density defined as $\rho_m = \rho_d \theta_d + \rho_f \theta_f$. It is assumed that $\Pi_{k_f} = -\Pi_{k_d}$, which implies that the interphase TKE transfer is conservative. This assumption is valid for rigid particle–laden turbulent flows. However, as will be shown later, this assumption can be extended to the droplet–laden turbulent flow considered in this study.

The EoE concept states that if

$$\frac{de_m}{dt} = -\rho_f \theta_f \varepsilon_f + \mathcal{F}_f = 0, \tag{7.15}$$

where $\mathcal{F}_f$ is the external artificial forcing required to balance the dissipation in order to maintain $de_m/dt = 0$, then the specific dispersed phase TKE and specific fluid phase TKE evolve to their respective equilibrium values. Note that the modeled dissipation in the carrier phase is the sum of the single–phase dissipation rate and the additional dissipation due to the presence of boundary layers around the dispersed particles.

Equilibrium values of the specific fluid–phase TKE e_f^e and specific dispersed–phase TKE e_d^e are determined by a model constant C_k defined as,

$$\frac{e_d^e}{e_m} = C_k \qquad \frac{e_f^e}{e_m} = 1 - C_k. \tag{7.16}$$

Since C_k represents the fraction of the specific mixture energy present in the dispersed phase at equilibrium, it must lie between zero and unity.

An implicit dependence of C_k on mass loading ϕ of the two–phase system can be deduced by rewriting Eq.(7.16) as

$$C_k = \frac{\rho_d \theta_d k_d^e}{\rho_m k_m} = \frac{\rho_d \theta_d k_d^e}{\rho_f \theta_f k_f^e + \rho_d \theta_d k_d^e} = \frac{\phi \frac{k_d^e}{k_f^e}}{1 + \phi \frac{k_d^e}{k_f^e}}, \tag{7.17}$$

where $\phi = \rho_d \theta_d / (\rho_f \theta_f)$ is the mass loading of the two–phase system. The constant C_k can also depend on other non–dimensional quantities that characterize this homogeneous turbulent two–phase flow system such as Stokes number $St_\eta = \tau_p / \tau_\eta$ (where τ_η is the Kolmogorov timescale), particle Reynolds number Re_d, initial k_d/k_f ratio, d_p/η ratio (where η is Kolmogorov length scale of turbulence) and θ_d.

For a constant mass loading ϕ, decreasing Stokes number should drive the dispersed–phase equilibrium TKE closer to the fluid–phase equilibrium TKE and in the limit of zero Stokes number, the two equilibrium energies k_f^e and k_d^e should match. This observation imposes a constraint on C_k in the limiting case of zero Stokes number and from Eq.(7.17) we find

$$C_k|_{St_\eta = 0} = \frac{\phi}{1 + \phi}. \tag{7.18}$$

The EoE concept can be extended to the case where the turbulence decays in time (no artificial forcing of the mixture energy in the two–phase flow system). However, a model for the dissipation rate needs to be added to the system of equations (cf. Eqs.(7.13)–(7.14)), which now reads

$$\begin{aligned}
\frac{de_f}{dt} &= \Pi_{k_f} - \rho_f \theta_f \varepsilon_f \\
\frac{de_d}{dt} &= \Pi_{k_d} \\
\frac{d\varepsilon_f}{dt} &= -C_{\varepsilon 2} \frac{\varepsilon_f^2}{k_f} + C_s \frac{\varepsilon_f}{k_f} \left(\frac{k_f^e - k_f}{\tau_\pi} \right),
\end{aligned}$$

where ε_f is the fluid–phase dissipation evolving according to a modified single–phase ε equation (Xu and Subramaniam, 2006). The model constant C_s is chosen to be 1.5 and $C_{\varepsilon 2}$ is 1.92.

7.3.1 Applicability of the EoE concept to droplet–laden turbulent flows

7.3.1.1 Non–evaporating droplets

Certain assumptions, like conservative interphase TKE transfer and zero dissipation in the dispersed phase, that are used in arriving at the model equations Eqs.(7.13)–(7.14) for flows with rigid solid particles need to be revisited and carefully understood when applied to non–evaporating droplet–laden flows. For this we take as reference the exact evolution equation for the dispersed–phase TKE using the Eulerian–Eulerian (EE) approach Eq. (D.4) presented in the Appendix (see Xu (2004) for more details) for a homogeneous two–phase flow. The important terms that appear in this equation are:

(a) the interphase TKE transfer $\langle u''_{di}(S_{Mdi} - U_i S_{\rho_d})\rangle$, where S_{Mdi} is the interphase momentum transfer given by Eq. (D.6) in Appendix D, U_i is the instantaneous velocity in the two–phase flow system, and S_{ρ_d} is the interphase mass transfer given by Eq. (D.7) in Appendix D,

(b) contribution to the dispersed phase TKE due to interphase mass transfer $(1/2)\langle u''_{di}u''_{di}S_{\rho d}\rangle - \tilde{k}_d\langle S_{\rho d}\rangle$, where $\tilde{k}$ is the density–weighted TKE in the dispersed phase given by Eq. (D.3), and

(c) the term $\langle u''_{di}\partial(I_d\tau_{ki})/\partial x_k\rangle$ that contains the dissipation in the dispersed phase, where u''_{di} is the fluctutating velocity with respect to the volume–averaged velocity in the dispersed phase given by Eq. (D.5) in Appendix D, I_d is the indicator function (Drew, 1983) which is unity in the dispersed phase and zero in the fluid phase and $I_d\tau_{ki}$ is the stress tensor in the dispersed phase.

The reader is referred to Appendix D for more details on these terms. For non–evaporating droplets, S_{ρ_d} is zero.

The system is assumed to be dilute so that collisions and coalescence of droplets are neglected. Break–up of droplets is also neglected. Since the focus of this study is on droplets that are smaller than the Kolmogorov length scale, dissipation inside the droplet can be considered negligible as the flow in the interior of such droplets is in the laminar regime. One could, on the other hand, consider a Hill's vortex (Batchelor, 1971; Clift et al., 1978) inside the droplets to get an estimate of the dissipation. If the velocity inside the droplet is assumed to be composed of only fluctuations, then one can estimate the dissipation $\varepsilon_{d,in}$ inside the droplet using $\varepsilon_{d,in} = 2\nu_f \langle s_{ij} s_{ij} \rangle$, where s_{ij} is the fluctuating strain rate tensor, using the prescribed stream–function for the Hill's vortex (Batchelor, 1971; Clift et al., 1978). It can be shown that the dissipation inside the droplet scales like r^2, where r is the radius of the droplet, implying that dissipation is small for small droplets. Thus, the term $\langle u''_{di} \partial(I_d \tau_{ki})/\partial x_k \rangle$ in Eq. (D.4) is assumed to be negligible for non–evaporating droplets in the two–phase flow regime considered here.

Experiments on single droplets in quiescent (Greene et al., 1993; Warnica et al., 1995a) and turbulent gas fields (Warnica et al., 1995b) have reported that, for droplet Reynolds numbers in the range 10^{-3} to 100, and in the absence of drop oscillation or deformation, the drag on droplets is not different from drag on solid spheres in quiescent conditions. The droplet Reynolds numbers in the current study are $\mathcal{O}(1)$ and well within the range of Reynolds numbers explored in the experiments. Under such conditions, the term S_{Mdj}, representing the instantaneous interphase momentum transfer, is equal and opposite in both the phases. Under conditions of zero mean slip velocity in either phase, the fluctuating velocity at the droplet surface u''_{di} is the same as the fluctuating gas–phase velocity u''_{fi} at the same location. These arguments allow us to assume that conservative interphase TKE transfer, and hence the EoE hypothesis, is valid for the class of flows laden with non–evaporating droplets analyzed in this study.

7.3.1.2 Evaporating droplets

To understand the contribution to the TKE in either phase due to interphase mass transfer in evaporating droplet–laden flows, we again resort to the dispersed–phase TKE evolution equation derived using the EE approach Eq. (D.4) in the Appendix. The term $(S_{Mdi} - U_i S_{\rho_d})$ in the second term on the right hand side of Eq. (D.4) essentially works out to a stress contribution, namely $-\tau_{ij}\frac{\partial I_d}{\partial x_j}$, at the interface. One can decompose the fluctuating velocity in the dispersed phase u''_{di} into a part that is equal to u''_{f_i} and a stochastic part ξ_i (which we assume to be an isotropic Wiener process). Substituting this decomposition into the dispersed–phase TKE evolution equation (cf. Eq. (D.4)), we get

$$\theta_d \rho_d \frac{d}{dt}\tilde{k}_d = \left\langle u''_{di}\frac{\partial(I_d\tau_{ki})}{\partial x_k}\right\rangle - \langle(u''_{f_i} + \xi_i)\tau_{ij}\frac{\partial I_d}{\partial x_j}\rangle + (1/2)\langle u''_{di}u''_{di}S_{\rho_d}\rangle - \tilde{k}_d\langle S_{\rho_d}\rangle. \tag{7.19}$$

We assume that the correlation $\langle\xi_i\tau_{ij}\frac{\partial I_d}{\partial x_j}\rangle$ in the second term on the right hand side of Eq. (7.19) is zero for the droplet–laden isotropic turbulence considered in this study. With this simplification, the interphase TKE transfer term in the fluid–phase TKE evolution equation is equal and opposite in sign to that in the dispersed–phase TKE evolution equation(cf. Eq. (D.4)), since

$$-\langle u''_{f_i}\tau_{ij}\frac{\partial I_d}{\partial x_j}\rangle = \langle u''_{f_i}\tau_{ij}\frac{\partial I_f}{\partial x_j}\rangle.$$

Thus, the interphase TKE transfer is conservative for this two–phase system. Again, based on a similar argument as for non–evaporating droplets, the dissipation inside an evaporating droplet is assumed to be negligible. The other two terms remaining on the right hand side of the above equation are the interphase mass transfer terms. No special treatment is required for these terms because in DLM or other Lagrangian models for droplets, a model for the droplet vaporization rate in turn implies a model for the interphase mass transfer terms (see Appendix D for more details).

7.4 Model constants in DLM

7.4.1 Specification of C_k

The test case chosen in this study is particle–laden one–way coupled stationary turbulence. DLM is a model primarily constructed for the limit of two–way coupling. We noticed that the model constants need to be changed slightly compared to Section 6.5 in order to give good agreement with the one–way coupled DNS used in this study. This should not be misinterpreted as a failure of DLM to model a range of two–phase flows with the same model constants. Models for C_k and timescales τ_1, τ_3 (and even τ_π) can be improved only by resorting to carefully controlled DNS datasets that provide information on these quantities. We believe that a more refined model of C_k and the timescales could lead to more accurate estimates of model constants. These model constants will hopefully be the same for a wide class of two–phase flows that can be modeled by DLM.

In this study, the following model for C_k is proposed:

$$C_k = \frac{\phi(1 - 0.1St_\eta)}{1 + \phi(1 - 0.1St_\eta)}. \tag{7.20}$$

Note that this specification obeys the correct limiting behavior of C_k as $St_\eta \to 0$ (cf. Eq.(7.18)). Other functional forms of C_k were also considered but the above specification gave the best agreement with the DNS dataset used in this study.

7.4.2 Drift timescales in DLM

A novel feature of the proposed DLM is the presence of two different timescales in each SDE for the drift and diffusion terms. The form of the drift timescales τ_1 and τ_3 in Eqs.(7.3)–(7.4), respectively, is now developed. For a discussion on the procedure to derive the drift timescales in DLM, the reader is directed to Section 6.5. The model constant C_3 is chosen to be 0.1 in this case.

We neglect the dependence of τ_1 on St_η and prescribe τ_1 to be

$$\frac{1}{\tau_1} = \frac{C_1\phi}{\tau},$$

where C_1 is a model constant ($C_1 = 0.5$) and τ is the fluid–phase eddy turnover timescale.

7.4.3 Diffusion timescales in DLM

For a discussion on the procedure to arrive at a diffusion timescale, the reader is directed to Section 6.5. We noticed that a constant $C_\pi = 2.5$ gives the best results in this study.

Table 7.1 summarizes the model constants and timescales used in DLM.

7.5 Test cases for model validation

Direct numerical simulations of non–evaporating and evaporating droplets in stationary turbulence have been performed by Mashayek et al. (1997). Simulation parameters used in the DNS are summarized in Table 7.2. We compare predictions from DLM against this DNS dataset since the DNS reports both TKE in each phase, and statistics related to droplet dispersion. In addition, since a simplified evaporating droplet regime is simulated, the behavior of DLM with temporally–evolving droplet radii can be ascertained. The DNS (Mashayek et al., 1997) has been performed under the following assumptions:

Non–evaporating droplets:

1. Droplets are in the sub-Kolmogorov size range
2. The point–particle approximation is employed to represent the droplets in the system.
3. The droplets do not affect the fluid–phase momentum equation which implies that the simulations are one–way coupled.

Evaporating droplets:

In addition to the assumptions for non–evaporating droplets, the following assumptions hold for the evaporating droplets.

Spherically–symmetric droplet vaporization is assumed, and constant–temperature droplets are assumed to vaporize in an infinite, isothermal gas phase. It is also assumed that the vaporizing droplets do not significantly alter the density of the surrounding gas, and all fluid–phase transport properties are assumed to be constant.

The d^2–law of vaporization is assumed wherein the rate of change of droplet surface area is a linear function of time (Faeth, 1977):

$$d_p^2(t) = d_{p0}^2 - \kappa t, \tag{7.21}$$

where $d_p(t)$ is the droplet diameter at time t, d_{p0} is the droplet diameter at some initial time t_0, and κ is the evaporation rate given by relation (Faeth, 1977)

$$\kappa = 8\Gamma_f \ln(1 + B_M) C_{\mathrm{Re}}. \tag{7.22}$$

Here Γ_f is the fuel–vapor diffusivity coefficient (Lewis number of unity is assumed) and B_M is the Spalding transfer number. The correlation factor C_{Re} of the form

$$C_{\mathrm{Re}} = 1 + 0.3\mathrm{Re}_d^{0.5}\mathrm{Sc}_d^{0.33} \tag{7.23}$$

proposed by Ranz and Marshall (1952) accounts for convective effects.

The droplet Reynolds number Re_d is defined as

$$Re_d = \frac{|\mathbf{U}_f(\mathbf{X}_d, t) - \mathbf{V}_d| d_p}{\nu_f}, \tag{7.24}$$

where $\mathbf{U}_f$ is the gas–phase velocity at the location $\mathbf{X}_d$, $\mathbf{V}_d$ is the droplet velocity and $Sc_d = \nu_f/\Gamma_f$ is the droplet Schmidt number (Faeth, 1977). The evaporation constant κ varies in time only due to change in C_{Re}, which in turn depends on the temporal variation in Re_d.

Incorporating the d^2–law into the expression for the particle time constant defined as

$$\tau_p(t) = \frac{\rho_d}{\rho_f} \frac{d_p^2}{18\nu_f} \tag{7.25}$$

results in

$$\tau_p(t) = \tau_{p0} - \tau_e t, \tag{7.26}$$

where the initial particle time constant

$$\tau_{p0} = \frac{\rho_d}{\rho_f} \frac{d_{p0}^2}{18\nu_f}. \tag{7.27}$$

The non–dimensional quantity τ_e can be related to the momentum response time by

$$\tau_e = \frac{\rho_d \kappa}{\rho_f 18\nu_f} = \frac{\tau_p(t)\kappa}{d_p(t)^2} = \frac{\tau_p(t)}{\tau_{\mathrm{evap}}}. \tag{7.28}$$

Thus, τ_e is the ratio of the mechanical response time of the particle to the remaining droplet lifetime $\tau_{\text{evap}} = d_p(t)^2/\kappa$, if the droplet evaporated at a constant vaporization rate from time t. A value of $\tau_e < 1$ implies that the time taken by the droplet to equilibrate with the flow is larger than the droplet lifetime. The ratio τ_e can be expressed in terms of C_{Re} as

$$\tau_e = C_{Re}\tau_{e0}, \tag{7.29}$$

where

$$\tau_{e0} = \frac{\rho_d}{\rho_f}\frac{4\Gamma_f}{9\nu_f}\ln(1+B_M) = \frac{\rho_d}{\rho_f}\frac{\kappa}{18\nu_f C_{Re}}. \tag{7.30}$$

Mashayek et al. (1997) report initial vaporization rates in terms of a parameter τ_{ec} that they relate to τ_{e0} by the relation

$$\tau_{e0} = 0.29\tau_{ec}/\tau. \tag{7.31}$$

More details on the parameter τ_{ec} and the reason for the coefficient 0.29 can be found in Mashayek et al. (1997). The initial evaporation rate is reported by specifying τ_{ec} in multiples of the Kolmogorov timescale τ_k. For a given value of τ_{ec}, τ_{e0} and κ are found using Eq.(7.31) and Eq.(7.30), successively.

The non–evaporating test case is denoted **TNE**. Of the several test cases reported in the DNS with evaporating droplets, only three representative test cases are chosen in this work for the sake of brevity:

1. Varying initial vaporization rates, constant initial particle response time, constant C_{Re} (**TE1**)

2. Varying initial vaporization rates, varying initial particle response time, varying C_{Re} by changing Re_d, keeping $Sc_d = 1$ (**TE2**)

3. Varying initial vaporization rates, varying initial particle response time, varying C_{Re} by changing both Re_d and Sc_d (**TE3**)

The other two cases analyzed in the DNS are (a) the effect of spray size and (b) the effect of initial drop size distribution. Since we restrict our study to a homogeneous evaporating spray, we do not analyze the effect of initial spray size. Additional terms including the change

in mean velocity along and transverse to the axis of the spray need to be taken into account to study an inhomogeneous spray completely. Since such information is not reported in the DNS (Mashayek et al., 1997), we do not analyze this test case. Although the DLM is capable of considering effects of initial spray size, for the sake of brevity, we do not analyze the test case involving varying drop size distributions. Also, drift effects due to gravity are not investigated in this study.

7.5.1 DLM in the limit of one–way coupling

If the mass loading $\phi \to 0$ in a two–phase flow system, then it is reasonable to assume one–way coupling. At the edges of an evolving spray, where the volume fraction of the liquid $\theta_d \ll 1$, the limit of one–way coupling could be achieved and it is important for a two–phase flow turbulence model to behave reasonably well in the one–way coupled limit. In this limit, the TKE in the fluid phase can be assumed to remain unaffected by the presence of the dispersed phase. Thus, terms representing interphase interaction in the evolution equation for the fluid–phase TKE Eq. (7.13) can be neglected.

An interesting feature of DLM is that, by virtue of the EoE hypothesis, it has the correct one–way coupled limiting behavior as the mass loading $\phi \to 0$. The interphase TKE transfer term in Eq.(7.8) turns out to be negligible in this limit. In other words, no additional treatment is necessary to introduce the physics governing the two–phase flow mixture in the one–way coupled limit into DLM. This observation can be explained as follows.

The specific equilibrium TKE in the fluid phase e_f^e defined in Eq.(7.16) can be rewritten as

$$\begin{aligned} k_f^e &= (1 - C_k)\frac{\rho_m k_m}{\rho_f \theta_f} \\ &= (1 - C_k)(k_f + \phi k_d). \end{aligned}$$

From Eq.(7.17), one can infer that for $\phi \to 0$ (limit of one–way coupling), $C_k = \phi k_d^e / k_f^e$ (since k_d^e / k_f^e is finite). This results in

$$\lim_{\phi \to 0} k_f^e = k_f,$$

which essentially implies that $dk_f/dt \sim 0$ in Eq.(7.8).

7.6 Model predictions

In this section, details of the numerical implementation and integration of the SDEs given by Eqs.(7.3)–(7.4) are first presented. Next, predictions from DLM are compared with DNS results for the test cases **TNE**, **TE1**, **TE2** and **TE3**. It is noted at the outset that we do not seek an exact match between predicted results and the DNS dataset used in model validation, rather we assess the capability of the new model in capturing trends of important two–phase flow statistics with varying Stokes number. A more detailed discussion is presented in Section 6.8.

7.6.1 Initialization of the computational ensemble

The fluid–phase turbulence simulated in the DNS (Mashayek et al., 1997) is isotropic at initial time, and owing to one–way coupling, remains isotropic in time. Corresponding to this initial condition, in DLM the initial velocity of a stochastic particle that represents the fluid phase is sampled from a joint normal distribution with zero mean and covariance matrix $(2/3)k_f\delta_{ij}$. In the DNS, the droplets are introduced into the fluid phase with the same velocity as the surrounding fluid. This fact affects the evolution of statistics like droplet Reynolds number that depend on velocities in both phases at the same position and time. However, since in DLM the particle Reynolds number calculation procedure (see next) randomly reorders the stochastic particles at every time step, it does not matter if particles with like indices across the phases have identical velocities at initial time or not. Nevertheless, we do ensure that $k_f(t=0) = k_d(t=0)$.

7.6.2 Computational details for the system of SDEs

An Euler–Maruyama (EM) scheme (Kloeden and Platen, 1992), which is the stochastic equivalent of the deterministic Euler scheme, is used to evolve the system of vector SDEs (cf. Eq.(7.3) and (7.4)) in time. Since we are interested in mean quantities in this study, and

because the weak order of convergence of the EM scheme is unity (Kloeden and Platen, 1992), we choose this scheme to integrate the SDEs in time. Twenty multiple independent simulations (MIS) are performed for each case, and statistics are obtained by averaging over these MIS to reduce statistical error. The number of stochastic particles that represent each phase is the same, and equal to 10000. The statistical variability in the moments of the velocity, like TKE in the fluid phase k_f and dispersed phase k_d, and velocity autocorrelations in the both phases (cf. Eq. 7.10 and 7.11), across the twenty MIS is less than 3%. The time step required for accurate numerics is determined by performing a series of simulations with successively decreasing time steps. It is observed that for $\Delta t \leq 0.002 \min(\tau_p, \tau)$, the predicted moments did not change in a statistical sense. Therefore, this value of Δt is chosen for all the simulations. The runs for the evaporating cases are stopped when the minimum of the particle response times of all droplets is (1/20)th of the initial particle response time, in order to avoid prohibitively large computational times.

We estimate the droplet Reynolds number from the ensemble of stochastic particles in the following manner. The computational particles that represent the fluid phase are randomly paired with those that represent the dispersed phase at the beginning of each time step (note that the number of stochastic particles that represent each phase is the same). The Reynolds number estimate for the mth stochastic particle that represents the dispersed phase is computed as

$$Re_{d,(m)} = \frac{|\mathbf{u}_{(m)} - \mathbf{v}_{(m)}| d_{p,(m)}}{\nu_f}, \tag{7.32}$$

where $d_{p,(m)}$ is the diameter property associated with the mth stochastic particle. The mean droplet Reynolds number is calculated by averaging Eq. (7.32) over the stochastic particles that represent the dispersed phase as[5]

$$\langle Re_d \rangle = \frac{1}{N_p} \sum_{m=1}^{N_p} Re_{d,(m)}. \tag{7.33}$$

where $N_p = 10000$. We adopt this procedure to calculate $\langle Re_d \rangle$ since each stochastic particle represents only a realization of a stochastic process (cf. Eqs.(7.3)–(7.4)). Moreover, in the

[5]In inhomogeneous computations, the same procedure can be applied to the computational particles in each phase that occupy the same Eulerian grid cell.

homogeneous ensemble of particles considered, each particle that represents the dispersed phase is equally likely to be next to a particle that represents the fluid phase.

7.6.3 Test case TNE

Mashayek et al. (1997) perform a test for stationarity in the non–evaporating case by reporting the evolution of the mean droplet Reynolds number $\langle Re_d \rangle$ (see Eq.(7.24) for the definition of Re_d). In the DNS, the angled brackets represent an averaging done over all droplets.

Predicted evolution of droplet Reynolds number for increasing Stokes number using DLM is shown in Fig. 7.1 against scaled time t/T_{ref}. Here $T_{\text{ref}} = l/u'$, where l is the Eulerian integral length scale and u' is the initial turbulence intensity in the fluid phase, both reported in the DNS (Mashayek et al., 1997)[6]. From the figure it can be observed that the system reaches stationarity after $t/T_{\text{ref}} = 3.0$. As a result of the random pairing of particles to determine $\langle Re_d \rangle$, the initial evolution of $\langle Re_d \rangle$ does not start from zero as in the DNS. Although the trend with increasing Stokes number is predicted accurately, DLM overestimates the stationary value of $\langle Re_d \rangle$. To check whether this overestimation is a problem of numerical resolution, an analytical expression for $\langle Re_d \rangle$ as implied by DLM is derived in Appendix 7.9 where it is shown that the predictions from DLM are consistent with the analytical results (the analytical stationary value of $\langle Re_d \rangle$ is shown in Fig. 7.1 for each Stokes number).

Scaled equilibrium dispersed–phase TKE predicted by DLM is compared in Fig. 7.2 with results from DNS for increasing Stokes number. Since the turbulence in the fluid phase is forced to remain constant, the stationary TKE of the fluid phase is identical to the initial TKE $k_f(t_0)$. With decreasing Stokes number, the equilibrium TKE in the dispersed phase should approach the equilibrium TKE in the fluid phase, a trend observed in the DNS. From the figure one can conclude that predictions of dispersed–phase equilibrium energies from DLM agree well with the DNS results.

[6] An alternative scaling of the time coordinate is the Eulerian integral timescale τ_E estimated by $(C_5/C_6)(u'^2/\varepsilon)$, where $C_5 = 0.212$ and $C_6 = 0.36$ (See Lu (1995),Hinze (1975)). It turns out that $\tau_E \sim T_{\text{ref}}$. However, the emphasis in this study is to match trends rather than seek an exact quantitative match with DNS results. Therefore, T_{ref} is retained as an appropriate scaling of the time co-ordinate.

Predicted droplet–velocity autocorrelations from DLM using Eq. (7.9) are presented in Fig.7.3 against scaled time t/T_{ref}. With increasing Stokes number, a droplet takes more time to lose correlation with its initial velocity resulting in larger timescales of droplet–velocity autocorrelation decay. Predicted trend in the autocorrelation decay with increasing Stokes number by DLM matches well with corresponding results from DNS.

Predictions from DLM for the asymptotic dispersed–phase diffusion coefficients $\alpha_d(\infty)$ computed using Eq.(7.12), scaled by the product of the initial turbulence intensity u' and the Eulerian integral length scale l, are reported in Fig.7.4. Although DLM overestimates the asymptotic diffusion coefficient of the dispersed phase, the trend with increasing Stokes number matches DNS results. Also, shown on the same figure is the fluid–phase asymptotic diffusion coefficient $\alpha_f(\infty)$ computed using DLM. As predicted by theoretical calculations (See G. Gouesbet and Picart (1984) for a discussion on Tchen's analysis (Chen, 1947)), the dispersed–phase asymptotic diffusion coefficient matches with that of the fluid–phase as $St_\eta \to 0$. Again, to see if the overestimation of $\alpha_d(\infty)$ is a problem of numerical resolution, an analytical estimate of the asymptotic diffusion coefficient as implied by DLM is given in Appendix 7.10. It is seen that DLM predictions are consistent with the analytical estimates.

7.6.4 Test case TE1

In this test case, the radii of initially monodispersed droplets evolve according to the d^2–law given by Eq.(7.21). All droplets evolve by a constant vaporization rate such that each droplet's radius reduces by the same amount in time. This is accomplished by assuming that C_{Re} remains at unity (or $Sc_d = 0$, which implies infinitely fast diffusion of the fuel vapor in the gas). The initial particle response time is the same across all the runs. As the droplet radii decrease in time their Stokes numbers St_η decrease and the droplets respond faster to the flow disturbances, thereby losing correlation with their initial velocity faster. Thus, when vaporization is included, droplet–velocity autocorrelations decay faster compared to the case with no evaporation ($\tau_{ec} = 0$). The faster decay in autocorrelations is accentuated at higher initial vaporization rates.

Predicted evolution of droplet–velocity autocorrelations for different initial vaporization rates and for an initial particle time constant $\tau_{p0} = 5\tau_\eta$ ($St_\eta = 5$) using DLM is shown in Fig. 7.5. DLM shows a reasonable match with the autocorrelations from DNS and also matches the trend with increasing vaporization rate.

7.6.5 Test case TE2

Droplet vaporization rates, which were constant in time for each droplet in test case **TE1**, are allowed to change in this test case by allowing for a non–zero Sc_d (in this case $Sc_d = 1$). The dependence of vaporization rate on Re_d through the assumed correlation Eq. (7.23) results in a radius evolution that is different for each droplet. Consequently, an initially monodispersed ensemble of droplets becomes polydispersed in time. Evolution of particle response time normalized by its initial value averaged over all the particles is shown in Fig. 7.6. A linear decay in the scaled particle response time is observed in DLM which is consistent with the DNS results.

The d^2–law predicts that, for constant vaporization rate κ, droplets with smaller radii evaporate faster than ones with larger radii. Since κ depends on Re_d through the correlation for C_{Re} in Eq. (7.23), each droplet has different initial vaporization rates at initial time due to different droplet Reynolds numbers arising from the initial distribution of droplet velocities (cf. Eq. (7.24)). As d_p decreases, Re_d decreases which slows down the vaporization rate. Once a droplet starts to evaporate, a competition between the d^2–law and the vaporization rate is observed. The DNS predicts that the standardized pdf of d_p becomes more Gaussian as τ_p increases. A negative value of skewness in the standardized pdf of d_p is expected, since owing to the d^2–law, the probability of finding large particles in the computational domain is higher than finding smaller ones at long time [7]. From Fig. 7.7 one can infer that in the DNS the skewness of the standardized pdf of d_p remains largely on the negative side, becoming more negative towards the end. Also, the DNS shows that the kurtosis is closer to Gaussian,

[7]The skewness and kurtosis of the standardized pdf of the particle diameter d_p characterizes the polydispersity of the spray droplets. Skewness measures the degree of asymmetry of a distribution (Abramowitz and Stegun, 1964). Skewness for a Gaussian random variable is 0. The kurtosis characterizes the peakedness of the distribution. Kurtosis for a Gaussian random variable is 3.

especially in between $t/T_{\text{ref}} = 1$ and $t/T_{\text{ref}} = 2$.

Skewness and kurtosis predictions from DLM are shown in Fig.7.7. DLM predicts a larger particle Reynolds number compared to the DNS (see Fig.7.1 for the stationary case), thereby overestimating the vaporization rate. This results in a larger negative skewness compared to the DNS results. The effect of an overestimated vaporization rate is also seen in the kurtosis predicted by DLM showing a value much larger than 3. This implies that the pdf of d_p predicted by DLM is more peaked than that seen in the DNS. However, the approximate flattening of the kurtosis in between $t/T_{\text{ref}} = 0.5$ and $t/T_{\text{ref}} = 1.5$ illustrates that DLM does capture the competing effects of vaporization rate and the d^2–law as the droplets evolve. DLM predicts a trend of an increasing kurtosis and decreasing skewness towards the end of the simulation, similar to that seen in DNS, although the trends are more pronounced in the DLM predictions. Droplets with smaller initial vaporization rate and Stokes number tend to remain longer in the DNS, a trend that is captured by DLM. A comparison of the pdf of $\tau_p^{(1/2)}$ (or d_p) for an initial $St_\eta = 5$ and $\tau_{ec} = 5\tau_\eta$ with that from the DNS results is shown in Fig. 7.8 for different scaled times [8]. As suggested by the higher (positive) kurtosis and a negative skewness of $\tau_p^{1/2}$ from DLM (cf. Fig.7.7) compared to the DNS, the pdf of $\tau_p^{1/2}$ is more peaked with longer left tails than the corresponding DNS results.

7.6.6 Test case TE3

The effect of changing Sc_d for different initial vaporization rates and particle response times is now considered. Mashayek et al. (1997) present two sets of results in this test case depending on how the simulation is initialized: in the first case, the relative velocity between the droplets and the surrounding fluid is zero (non–stationary initial state) and in the second case, the initial state of the droplet–laden turbulent flow is stationary. The value of $\langle C_{Re} - 1 \rangle$ is tracked in these cases which for a constant Sc_d measures how $\langle Re_d^{1/2} \rangle$ (cf. Eq. (7.23)) evolves in time.

For the non–stationary initial state, the droplet Reynolds number at initial time is zero

[8] The exact scaling of the ordinate for the pdf plot reported in the DNS is not clear, since the pdf from the DNS does not appear to integrate to unity. So we make a qualitative comparison of the pdf of $\tau_p^{(1/2)}$ from DLM with that from the DNS on the same plot with different ordinates.

in the DNS. Once the droplets start to evolve the Reynolds number increases due to a finite relative velocity. At the same time, the droplet diameter is decreasing due to vaporization. A maximum value in the evolution of Reynolds number is reached, analogous to that seen in case **TNE** (see Fig.7.1). In time, the effect of the decreasing diameter offsets the increase in the relative velocity and the particle Reynolds number starts to decrease. As is evident from the DNS results presented in Figs. 7.9 and 7.10 for initial Stokes numbers $St_\eta = 0.5$ and 5, respectively, increasing Sc_d increases the rate of evolution of $\langle C_{Re} - 1 \rangle$ although the maximum is reached at almost the same scaled time.

Figure 7.9 shows the predicted trend in the evolution of $\langle C_{Re} - 1 \rangle$ by DLM for $St_\eta = 0.5$. As observed in the non–evaporating case, the droplet Reynolds number is overestimated by DLM in this case. This results in an overestimate of $\langle C_{Re} - 1 \rangle$. Again as a result of the random pairing of particles to determine $\langle Re_d \rangle$ in DLM, $\langle C_{Re} - 1 \rangle$ does not start from zero as in the DNS. However, the trend with increasing Sc_d is identical to that seen in the DNS. The same behavior is seen in the predicted trends of $\langle C_{Re} - 1 \rangle$ for initial $St_\eta = 5$ in Fig. 7.10.

For the stationary initial condition and a value of $Sc_d = 1$, the droplets have a attained stationary mean Reynolds number and the flow has reached a stationary state prior to the start of vaporization. Once vaporization is initiated, the particle Reynolds number begins to decrease due to a decrease in the diameter. Fig. 7.11 shows that the predicted trend for the two initial particle response times from DLM matches with DNS results.

7.6.7 Interphase mass transfer terms in the dispersed–phase TKE evolution equation

With no interphase mass transfer, as in the test case **TNE**, the only term that governs the evolution of the dispersed–phase TKE is the interphase TKE transfer term $\widetilde{\langle A_i v_i'' \rangle}$ (cf. Eq. (D.1) in the Appendix). However, in the presence of interphase mass transfer, as in the test cases **TE1**–**TE3**, additional terms appear in the evolution equation for the dispersed–phase TKE. These additional terms, namely, $3n\langle R^3 \rangle \left\langle \widetilde{v_i'' v_i''} \Gamma | t \right\rangle$ and $6n\langle R^3 \rangle \tilde{k}_d \left\langle \tilde{\Gamma} | t \right\rangle$ in Eq.(D.1) in the Appendix, represent the contribution to the dispersed–phase TKE due to interphase mass

transfer. It has to be borne in mind that two–phase models may give correct predictions for the dispersed–phase TKE in flows with mass transfer even if the individual contributions in the TKE evolution equation (cf.Eq. (D.1)) are not accurately modeled. DNS of evaporating two–phase flows possess the capability to quantify these terms. However, to our knowledge the DNS datasets available in literature do not report budgets of the interphase mass transfer terms. Therefore, we do not quantify these terms from DLM since we do not have any datasets to compare with. If available, model predictions of these individual terms can be compared with DNS data, thereby resulting in a more rigorous validation of any two–phase flow turbulence model.

7.7 Discussion

In all the test cases presented above, it is clear that DLM captures the correct trend in the evolution of certain key statistics related to both non–evaporating and evaporating droplet–laden two–phase turbulent flow. It is fair to conclude that even though DLM has been derived taking two–way coupling into consideration, it has performed reasonably well in predicting droplet dispersion characteristics and TKE in the limit of one–way coupled droplet–laden turbulence.

The one–way coupled case considered is a simplified test case, applicable only in certain dilute spray regimes. Nevertheless, the one–way coupled limiting behavior of a two–phase flow turbulence model can be analyzed and also the behavior of certain important model constants can be ascertained through this comparison.

The reasons for the emphasis in this study on predicting only the trends correctly rather than seeking an exact quantitative match have been discussed in Section 6.8.

7.8 Conclusions

In addition to the conclusions presented in Section 6.9, principal conclusions and achievements of this study on the behavior of DLM in stationary turbulence are:

1. DLM predicts correct trends in stationary dispersed–phase TKE, dispersed–phase velocity autocorrelation decay and asymptotic droplet diffusion coefficients in droplet–laden stationary turbulence for a range of Stokes numbers.

2. In the evaporating–droplet test case, DLM predicts pdf and moments of the droplet diameter that are in reasonable agreement with DNS results. Thus, DLM performs well in the simplified evaporating droplet regime accessed by the DNS.

Important terms in the evolution equation of the dispersed–phase TKE are identified in both the LE and EE statistical representations of two–phase flow. This exercise can serve as a guiding framework for generating datasets from future DNS of evaporating droplet–laden flow that are helpful to the two–phase flow modeling community.

7.9 Mean droplet Reynolds number estimate from DLM

Using standard methods to solve a time–dependent Ornstein–Uhlenbeck process (Gardiner, 1983) one can show that for a stochastic differential equation of the form

$$dU(t) = -A(t)U(t)dt + B(t)dW(t), \tag{7.34}$$

where $A(t)$ and $B(t)$ are the drift and diffusion terms, respectively, and $dW(t)$ is a Wiener process, the pdf of $U(t)$ is Gaussian with the mean and variance evolving according to

$$\langle U(t)\rangle = \mu \exp[-\int_0^t A(t')dt'] \tag{7.35}$$

$$\mathrm{Var}[U(t)] = \sigma^2 \exp[-2\int_0^t A(t')dt'] + \int_0^t \exp[-2\int_{t'}^t A(s)ds]B^2(t')dt', \tag{7.36}$$

for an initial Gaussian velocity field $U(t)$ with mean μ and variance σ^2. Note that Eqs.(7.3)–(7.4) are of the same form as Eq. (7.34).

One can then derive the probability density function of the absolute value of the relative velocity $W = |\mathbf{u} - \mathbf{v}|$ as

$$f_W(w) = \sqrt{\frac{2}{\pi}} \left(\frac{2}{3}S\right)^{-3/2} w^2 \exp\left(-w^2/[\frac{4}{3}S]\right),$$

where

$$S = k_f(t) + k_d(t) - 2\rho(t)\sqrt{k_f(t)k_d(t)}$$

and

$$\rho(t) = \frac{\langle u(t)v(t)\rangle}{\sqrt{\langle u(t)^2\rangle\langle v(t)^2\rangle}} = \frac{\langle u(t)v(t)\rangle}{\frac{2}{3}\sqrt{k_f(t)k_d(t)}}$$

is the correlation coefficient between like components of velocities u and v[9]. The mean of the absolute relative velocity W at any time t is

$$\langle W\rangle(t) = \frac{4}{\sqrt{3\pi}}\sqrt{S}.$$

So, the analytical mean droplet Reynolds number as implied by DLM for the non–evaporating case is

$$\begin{aligned}\langle Re_d\rangle(t) = \frac{\langle W\rangle d_p}{\nu_f} &= \frac{4}{\sqrt{3\pi}}\sqrt{S}\,\frac{d_p}{\nu_f} \\ &= \frac{4\sqrt{6}}{\sqrt{\pi}}St_\eta\sqrt{\left(\frac{\tau}{\tau_p}\right)\left(1 + \frac{k_d(t)}{k_f(t)} - 2\rho(t)\sqrt{\frac{k_d(t)}{k_f(t)}}\right)\left(\frac{\rho_f}{\rho_d}\right)}. \qquad (7.37)\end{aligned}$$

The above expression shows that $\langle Re_d\rangle$ can be written as a function of Stokes number St_η, ratio of τ $(= k_f/\varepsilon_f)$ and particle response time τ_p, and the k_d/k_f ratio. The same expression is true when a system reaches stationarity, where $k_f(t) = k_f^e$ and $k_d(t) = k_d^e$. It can be shown that the correlation coefficient $\rho(t)$ decreases exponentially to zero for DLM.

Using the analytical expression for the variance Eq. (7.36), one can compute the ratio k_d^e/k_f^e for various Stokes numbers, which are in fact close to the DLM predictions reported in Fig. 7.2. For a Stokes number $St_\eta = 5$, the ratio $k_d^e/k_f^e \sim 0.52$. Substituting this value in the expression for $\langle Re_d\rangle$ above, along with $k_f = k_f^e = 1.5u'^2$ and the other non–dimensional ratios, the magnitude of $\langle Re_d\rangle \sim 1.97$, which matches with DLM predictions. Thus, predictions from DLM are consistent with analytical results.

7.10 Asymptotic diffusion coefficient estimate from DLM

For the droplet–laden stationary turbulence case considered in this study, an analytical solution to the evolution of the dispersed phase velocity autocovariance given by Eq.(7.11)

[9]Since the turbulence is isotropic, $\rho(t)$ is the same for all the three like components of velocities.

can be derived as follows. If we assume that the fluid–phase TKE k_f and the fluid–phase dissipation ε_f remain constant in artificially forced turbulence, then the eddy turnover time τ remains constant. Owing to the constant τ_p in the non–evaporating case and constant τ_η, the Stokes number St_η remains constant. Consequently, τ_3 remains constant in time. The analytical solution to Eq.(7.11) is thus (dropping the subscripts i for brevity)

$$\langle v(t_s)v(t)\rangle = \langle v(t_s)v(t_s)\rangle e^{-t/(2\tau_3)}$$

where $t > t_s$ and t_s is the time at which the system reaches stationarity. Substituting the above expression into Eq.(7.12) and in the limit $t \to \infty$

$$\alpha_d(\infty) = 2\langle v(t_s)v(t_s)\rangle\tau_3 = \frac{4}{3}k_d(t_s)\tau_3 = \frac{4}{3}k_f^e\left(\frac{k_d^e}{k_f^e}\right)\tau_3.$$

The substitution $k_d(t_s) = k_d^e$ has been made in the above development. Using the expression for analytical variance derived in Appendix 7.9, one can compute the ratio of equilibrium TKE k_d^e/k_f^e. For $St_\eta = 5$, it is found that $\tau_3 = 56.9$ and $k_d^e/k_f^e = 0.57$, for which scaled $\alpha_d = 1.15$. For $St_\eta = 0.4$, it is found that $\tau_3 = 44.8$ and $k_d^e/k_f^e = 0.97$, for which scaled $\alpha_d = 1.54$. Both these values for analytical α_d are close to predictions from DLM.

The reason for the large magnitude of α_d compared to DNS results, especially at small Stokes numbers, lies in limiting value of τ_3 reached as $St_\eta \to 0$. In this limit, τ_3 evaluates to $[(3/2)C_0(\varepsilon_f/k_f]^{-1}$, since $1/\tau_1 \to 0$ in the one–way coupled limit assumed in this study. In this limit and for the parameters used in this study, the magnitude of $\tau_3 = 43.2$ and the corresponding dispersion coefficient $\alpha_d(\infty) = 1.536$. These results are consistent with the predictions from DLM. It is noteworthy that in the limit $St_\eta \to 0$, $2\tau_3$ evaluates to the Lagrangian integral timescale (LIT) in the gas phase (Pope, 2000), and $\alpha_d(\infty) = \alpha_f(\infty)$ (cf. Fig. 7.4). It has been verified in the DNS of Yeung and Pope (1989) (see also Pope (2000)) that the SLM specification of the drift coefficients gives reasonable estimates for the LIT in the range of $Re_\lambda = 40$–60, which is the range of Re_λ studied in the DNS. However, no information on the LIT is reported by the DNS (Mashayek et al., 1997) used in this study for any quantitative comparisons of this timescale to be made.

Model constant	Stationary case	Decaying case
C_k	$\frac{\phi\,(1-0.1St_\eta)}{1+\phi\,(1-0.1St_\eta)}$	same
$1/\tau_1$	$C_1\phi/\tau$	same
$1/\tau_2 = 1/\tau_4 = 1/\tau_\pi$	$C_\pi/\langle\tau_{\rm int}\rangle$	same
$1/\tau_3$	$2\left[\frac{1}{2\tau_1} + \left(\frac{3}{4}C_0\right)\frac{1}{\tau}\right]\frac{1}{1+St_\eta C_3}$	$2\left[\frac{1}{2\tau_1} + \left(\frac{1}{2} + \frac{3}{4}C_0\right)\frac{1}{\tau}\right]\frac{1}{1+St_\eta C_3}$

Table 7.1 Specification of model constants that appear in DLM for homogeneous particle–laden decaying and stationary turbulence. The constants $C_1 = 0.5$, $C_\pi = 2.5$ and $C_3 = 0.1$.

Volume fraction	5.5×10^{-5}
Fluid–phase thermodynamic density	1.00
Dispersed–phase thermodynamic density	1000.00
Acceleration due to gravity	0.0
Initial mean slip	0.0,0.0,0.0
Turbulence intensity in fluid phase	0.019
Dissipation rate in fluid phase	3.98×10^{-6}
Kinematic viscosity of fluid	2.692×10^{-4}
Taylor scale Reynolds number	41

Table 7.2 Parameters used in the DNS

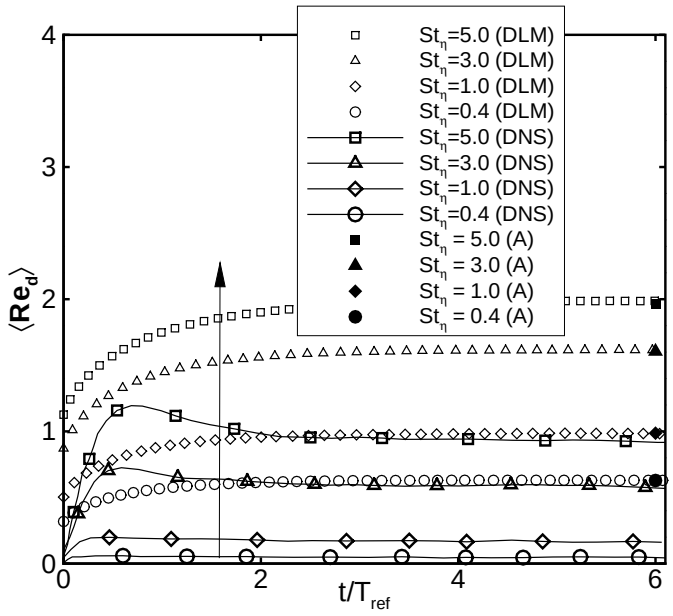

Figure 7.1 Evolution of particle Reynolds number for the test case **TNE** (i) DLM (ii) DNS results (Mashayek et al., 1997). Arrow indicates direction of increasing Stokes number. The letter '(A)' in the legend denotes analytical values computed using Eq. (7.37).

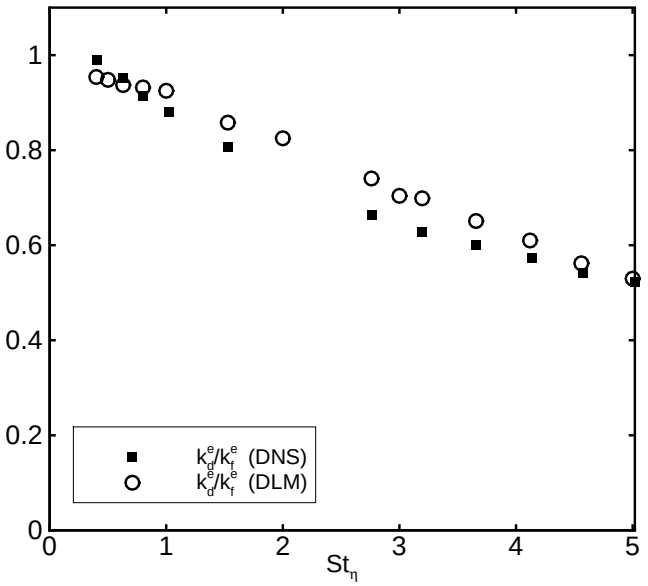

Figure 7.2 Trend of equilibrium dispersed–phase turbulent kinetic energy k_d^e scaled by equilibrium fluid–phase turbulent kinetic energy k_f^e with increasing Stokes number St_η for the test case **TNE** (i) DLM (ii) DNS results (Mashayek et al., 1997).

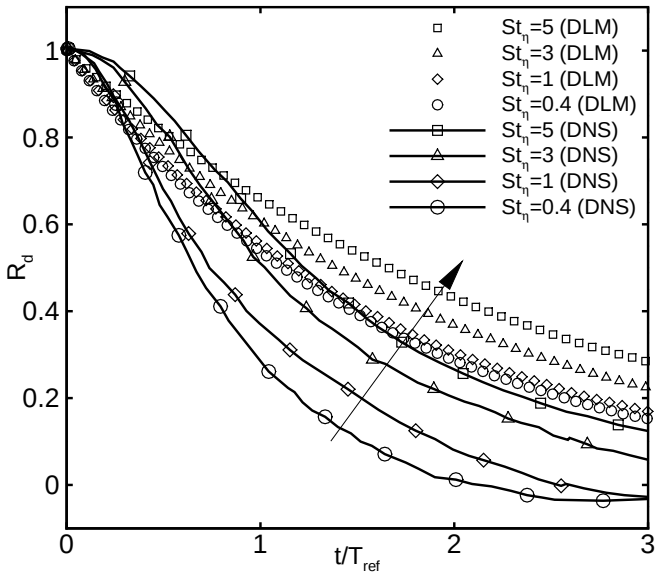

Figure 7.3 Evolution of dispersed–phase velocity autocorrelation R_d given by Eq. (7.9) for the test case **TNE** (i) DLM (ii) DNS results (Mashayek et al., 1997). Arrow indicates direction of increasing Stokes number.

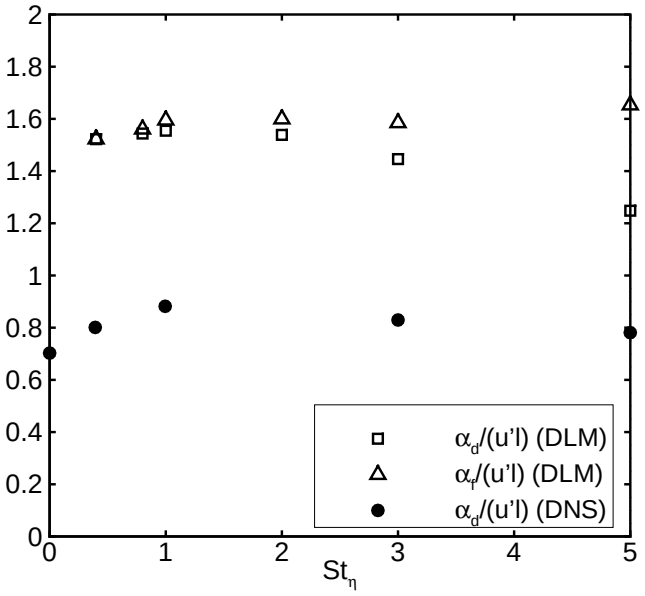

Figure 7.4 Trend of asymptotic diffusion coefficient $\alpha_d(\infty)$ in the dispersed phase with increasing Stokes number St_η for the test case **TNE** (i) DLM (ii) DNS results (Mashayek et al., 1997). Also shown is the trend of asymptotic fluid–phase diffusion coefficient $\alpha_f(\infty)$ as predicted by DLM for this range of Stokes numbers.

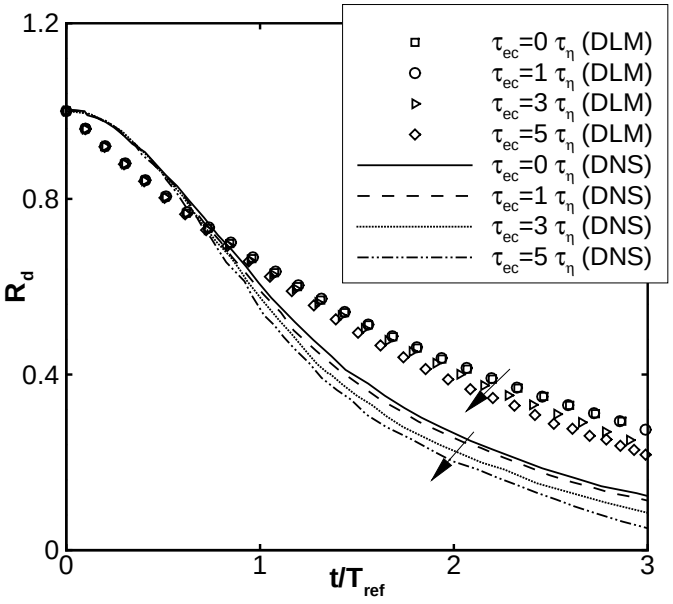

Figure 7.5 Evolution of dispersed–phase velocity autocorrelation R_d given by Eq. (7.9) for a constant initial Stokes number $St_\eta = 5.0$ and varying vaporization rates for test case **TE1** (i) DLM (ii) DNS results (Mashayek et al., 1997). Arrow indicates direction of increasing initial vaporization rate.

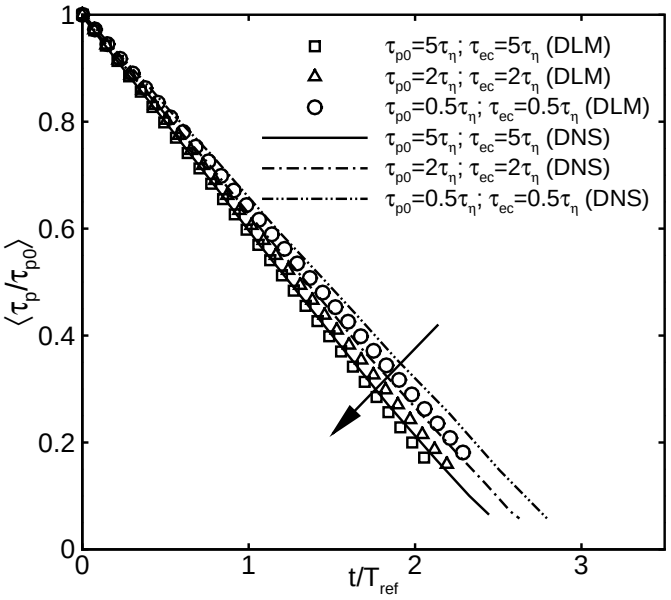

Figure 7.6 Predicted trend of scaled particle response time for varying initial vaporization rates and varying initial particle response time for for the test case **TE2** (i) DLM (ii) DNS results (Mashayek et al., 1997). Arrow indicates direction of increasing initial Stokes number St_η and initial vaporization rate.

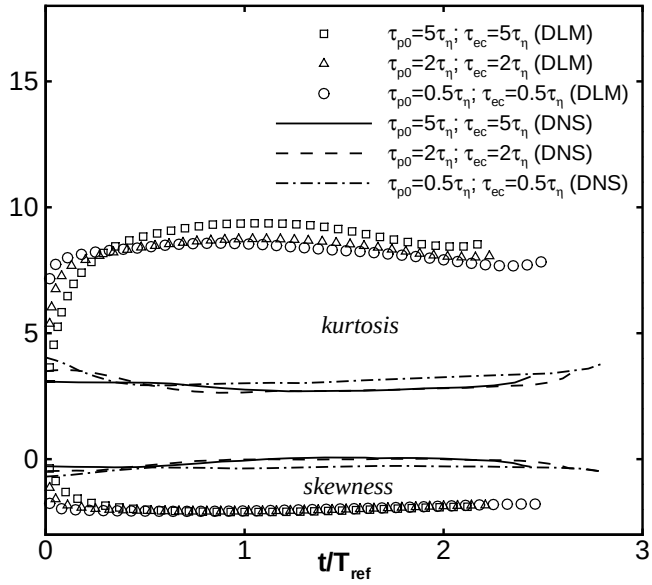

Figure 7.7 Evolution of skewness and kurtosis of droplet diameter d_p for varying initial vaporization rates and varying initial particle response time for the test case **TE2** (i) DLM (ii) DNS results (Mashayek et al., 1997).

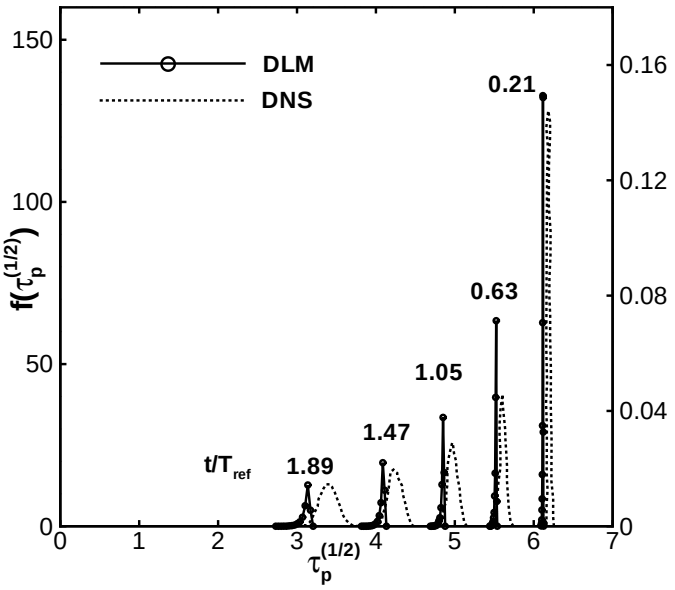

Figure 7.8 Predicted evolution of the probability density function of $\tau_p^{1/2}$ for $St_\eta = 5$, $\tau_{ec} = 5\tau_\eta$ and $Sc_d = 1$ for the test case **TE2** (i) DLM (ii) DNS results (Mashayek et al., 1997). The right hand side ordinate is taken from the DNS results while the left hand side ordinate is from DLM.

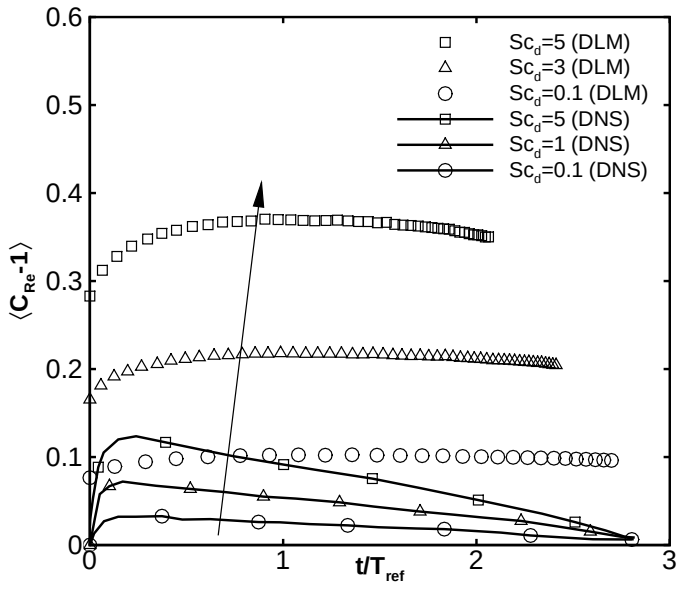

Figure 7.9 Predicted trend of $\langle C_{Re} - 1 \rangle$ for varying Sc_d and $\tau_{p0} = 0.5\tau_k$, $\tau_{ec} = 0.5\tau_k$ evolving from a non–stationary initial state, for **TE3** (i) DLM (ii) DNS (Mashayek et al., 1997). Arrow shows direction of increasing Sc_d.

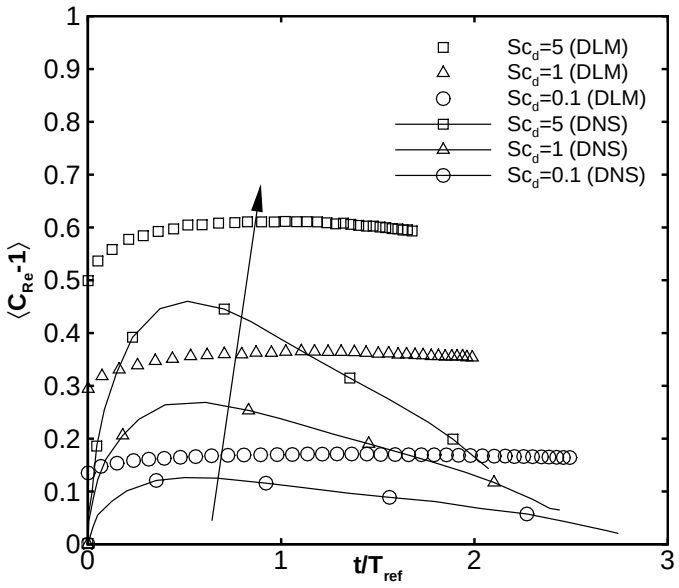

Figure 7.10 Predicted trend of $\langle C_{Re} - 1 \rangle$ for varying Sc_d and $\tau_{p0} = 5\tau_k$, $\tau_{ec} = 5\tau_k$ evolving from a non–stationary initial state, for **TE3** (i) DLM (ii) DNS (Mashayek et al., 1997). Arrow shows direction of increasing Sc_d.

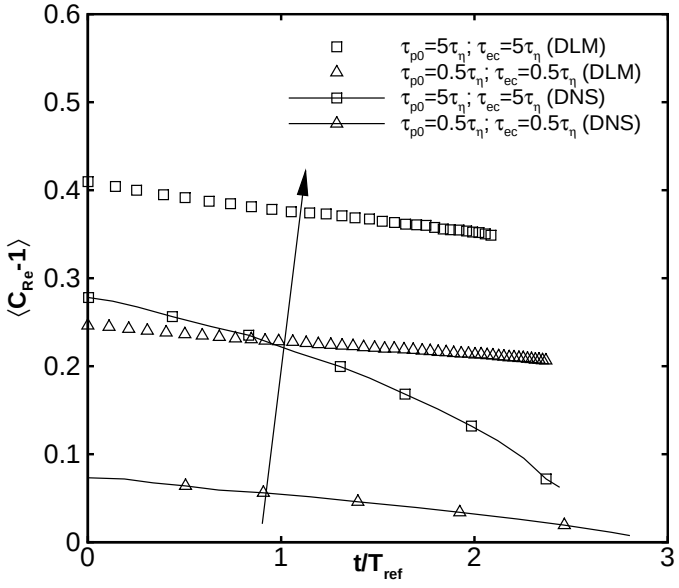

Figure 7.11 Predicted trend of $\langle C_{Re} - 1 \rangle$ for $Sc_d = 1$ with two initial values of particle response time and vaporization rates, evolving from a stationary initial state, for **TE3** (i) DLM (ii) DNS (Mashayek et al., 1997). Arrow shows direction of increasing initial Stokes number St_η.

CHAPTER 8. CONCLUSIONS AND FUTURE WORK

The foundation for the fundamental probability density function that forms the basis of the Eulerian–Eulerian (EE) and Lagrangian–Eulerian (LE) statistical representations has been presented in this work. A new statistical representation based on the Lagrangian description of the fluid phase namely the Lagrangian–Lagrangian (LL) representation is proposed. A multiscale interaction timescale in the context of the LE representation and a new dual–timescale Langevin model in the context of the LL representation are proposed. In this context, the highlights and principal conclusions of this work are enumerated below. Following the conclusions, some possible extensions of the current study are identified.

A comprehensive mathematical framework for the pdf formalism of multiphase flows is essential to further our understanding of this complex and challenging physical system. This disseration is an attempt to provide a single reference for such a complete theoretical framework for the single–point description of multiphase flows. This goal has been achieved by synthesizing existing work, and completing several missing pieces in the framework. The missing pieces from the framework that form an original contribution of this dissertation are enumerated below:

1. Definition and evolution of the mass density $\mathcal{F}_{\mathbf{U}|I_\beta}$, along with the subsequent derivation and verification of the consistency of the mean equations with the ensemble–averaged EE equations.

2. Definition of the density–weighted phasic mean and mixture velocities, and the nature of their fields.

3. Derivation of the mean mixture pressure evolution.

4. Identification of advantages and limitations of the EE and LE statistical representations.

5. Theory underlying the new Lagrangian–Lagrangian statistical representation.

6. Multiscale interaction timescale in the context of modeling two–phase flows.

7. New Dual–timescale model Langevin model in the context of modeling two–phase flows.

In addition to the above, the original contribution of this dissertation also comprises the other theoretical details that surface during the process of synthesis.

Nevertheless, the summary and conclusions of the work are now enumerated as an organic whole which includes the aforementioned original contributions of this dissertation. Interspersed in these conclusions the reader would find references to the work already done.

8.1 Summary and Conclusions

8.1.1 Theoretical description

1. Fundamental events associated with an EE description of a two–phase flow are presented in Chapter 3. A clear understanding of the fundamental events associated with a two–phase flow is essential in order to propose a rigorous probability density function formalism. The mininimal and complete single–point Eulerian description of a two–phase flow (Subramaniam, 2005) is identified; it is shown that the phasic pdfs and one of the volume fractions of either phase constitute such a description. The knowledge of fundamental events and corresponding probabilities provides a convenient framework to derive the evolution equation for the mass density corresponding to a particular phase of the two–phase flow.

2. The droplet distribution function (ddf) which forms the basis for the description of the dispersed phase in the LE representation (Subramaniam, 2001c, 2000) is presented in Chapter 3. It is important to note that the ddf is correctly interpreted as a summation over a sequence of surrogate droplet densities (Subramaniam, 2000). The notion of a single droplet is lost in the process of the derivation of the ddf. A unique single–particle pdf corresponding to the symmetrized Liouville density can be obtained, however, this

pdf has to be interpreted as corresponding to "surrogate" particles, not droplets (Subramaniam, 2000).

3. The relationship between phasic joint pdf of velocity and radius in the EE representation and the conditional joint pdf of velocity and radius in the LE representation is presented (Subramaniam, 2001b,a). In particular, the two pdfs are not equal in general, but are simply related only in the case of monodispersed size distribution and homogeneous number density. The relationship between the volume fraction and the number density is presented, and again a simple relationship between these quantities exists only for integrable forms of number density fields and homogeneous radius pdfs (Subramaniam, 2001b,a).

4. The phasic mass density evolution equation in the EE representation contains terms that represent its evolution in position space and velocity space. Source terms that represent interphase mass exchange appear in this equation that are required to ensure the normalization property of the phasic pdf corresponding to the mass density. Governing equations for the mean mass, mean momentum and second–moment of velocity in each phase are straightforward to derive in each phase. It is shown that these mean equations are identical to the widely–used ensemble–averaged equations for a two–phase flow that are derived using the indicator–function formalism. Galilean invariant forms of unclosed terms that need to be modeled are identified (Subramaniam, 2001a).

5. The evolution equation of the ddf, which is the spray equation, is presented (Subramaniam, 2001c) in Chapter 3. Important terms in the spray equation are the expected conditional acceleration and expected conditional vaporization rate, which is different from the "single" droplet or particle acceleration and vaporization rate (Subramaniam, 2001c). Evolution equations for the mean mass and mean momentum corresponding to the dispersed phase are derived from the spray equation. In order to derive the second–moment equations, the volume–weighted ddf of fluctuating velocity is defined (Subramaniam, 2001a, 2003).

6. The correspondence between unclosed terms in the governing equations in the EE and LE representations is established. Such a correspondence ensures a seamless and unambiguous transfer of statistical information from the EE to the LE representation (Subramaniam, 2001a).

7. A description of the carrier phase in the Lagrangian reference frame results in a new representation called the Lagrangian–Lagrangian (LL) statistical representation. The symmetrization of the multiparticle Liouville density in the dispersed phase implies a corresponding symmetrization of the multipoint Eulerian density. In the process, the notion of a "fluid" particle is lost. Thus, the carrier phase is correctly viewed as being composed of "surrogate" fluid particles. Since these notional particle paths can cross, it is useful to view these particles as computational particles. The modeled mass density implied by these computational particles is presented, and conditions that ensure that these notional particles evolve consistently with the Eulerian mass density in the EE representation are derived.

In essence, the theoretical contribution of this dissertation can be summarized as follows. The Eulerian description of the carrier phase in the EE description and the Eulerian description of the carrier phase in the LE description are identical. The Eulerian description of the dispersed phase in the EE description is different from the Lagrangian description of the dispersed phase in the LE description, and are related only under restrictive conditions of spatial homogeneity. The Lagrangian description of the dispersed phase in the LL description is identical to the Lagrangian description of the dispersed phase in the LE representation. However, the Lagrangian description of the carrier phase is in terms of "surrogate" fluid particles and serves as the theoretical basis for constructing Lagrangian models for the carrier phase in two–phase flows.

8.1.2 Modeling

1. Particle turbulence interactions are multiscale in nature. In widely–used LE implementations, the drag model and the interphase turbulent kinetic energy (TKE) transfer evolve

over the particle response timescale. It is illustrated in Chapter 5 through comparison with datasets from DNS of freely–decaying turbulence that this timescale fails to capture the multiscale interaction of particles and turbulence. A multiscale interaction timescale is proposed, which when used in place of the particle response timescale, is shown to capture the trends of important two–phase statistics in DNS of freely–decaying turbulence.

2. Particle dispersion and modulation of the carrier phase turbulence by the dispersing particles are two important phenomena that govern the evolution of a two–phase flow. DNS of canonical two–phase flows reveal that these two phenomena evolve on timescales that behave differently with Stokes number, an important non–dimensional quantity in a two–phase flows. Thus, any two–phase model must be able to capture these disparate timescales in a two–phase flow. A new dual–timescale Langevin model (DLM) is proposed in Chapter 6 which possesses the unique capability of being able to *simultaneously* capture the disparate timescales corresponding to particle dispersion and interphase TKE transfer. DLM is tested in the following canonical particle–laden flows: (*i*) freely–decaying turbulence, (*ii*) homogeneous shear, and (*iii*) stationary turbulence (in Chapter 7). DLM is shown to be able to capture the trends of important two–phase flows statistics with Stokes number and mass loading that are observed in the DNS of the canonical two–phase flows. This level of versatility of a two–phase flow model has not been demonstrated in literature.

In summary, new multiscale models that can capture the evolution of fundamental phenomena in a two–phase flow are proposed in this work to complement the theoretical contributions.

8.2 Future work

8.2.1 New class of hybrid EE-LE computations of two–phase flows

Recently, several researchers have been studying various hybrid EE–LE computations that represent a certain region of the two–phase flow using a EE representation, while the remaining

two–phase flow region is represented using the LE formalism. A clear understanding of the details underlying a consistent transfer of information from one representation to the other at the boundary of the two regions is absent in these studies. It is in such simulations that the work presented in this thesis is poised to make a significant impact, primarily because this work clearly brings out the necessary relations that are required in such an information transfer (See Chapter 3 and Subramaniam (2001a) for more details). As a part of the future work, one could explore such an implementation and probe its advantages and limitations in terms of accuracy in the description of a two–phase flow and computational requirements. The success of such an implementation will inevitably rest on the numerical techniques adopted to implement the hybrid scheme. Nevertheless with the advent of improved numerical techniques, such as particle number density control in two–phase flow computations, it is expected that hybrid EE–LE computations along with the modeling advances proposed in this work will be able to describe phenomena that cannot be captured by using solely a EE, or solely a LE description of the two–phase flow.

8.2.2 Sub–grid modeling of velocity in LES of two–phase flows

There is a huge thrust towards developing Large Eddy Simulations (LES) of two–phase flows, primarily owing to the prohibitive computational expense of direct numerical simulations, and inaccuracies involved in current Reynolds–averaged Navier–Stokes compuations. A principal unknown in such computations is the sub–grid scale carrier phase velocity contribution to evolution of the dispersed phase. It is known that the instantaneous carrier–phase velocities are characterized by spatial velocity correlations. Thus, one may expect that the filtered carrier–phase velocity field and the sub–grid velocity fluctuations also have spatial correlations associated with them. However, such sub–grid velocity fluctuations are currently modeled using single–point closures available from single–phase flow theory. A popular single–point closure for the sub–grid scale velocities seen by the particles is the Generalized Langevin model (GLM) usually employed in the same form as given in Haworth and Pope (1986). In this form, GLM does not contain scale information. Moreover, such closures for the sub–grid

scale velocity do not contain any dependence on the Stokes number and mass loading of the two–phase flow. Particles dispersed in a turbulent velocity field are affected by the spatial correlations of the underlying velocity field. *A priori* DNS of two–phase flows reveal that Stokes number has a non–neglible effect on the sub–grid scale velocity. It is thus interesting to investigate if DLM is a good model for the sub–grid scale velocity fluctuations in LES of two–phase flows. Although DLM is essentially based on GLM, its form as presented in this work contains modeled contributions due to interphase TKE transfer, Stokes number, mass loading and a multiscale interaction timescale. In particular, the multiscale interaction timescale is derived from a timescale associated with eddies of a characteristic length scale, and implicitly has modeled length scale information in it.

8.2.3 Incorporating scale information in moment closures

Moment equations presented in Chapter 3 contain unclosed terms that need non–local closures. Such terms can be quantified using "true" direct numerical simulations of particle–laden flows. In this work, a multiscale interaction timescale was proposed to capture the effect of the non–local interaction of particles and turbulence on the timescale governing interphase TKE transfer. In order to efficiently model these unclosed terms in inhomogeneous two–phase flows, however, one may need to resort to models that contain "second–order" information (Stoyan et al., 1995), or information on the spatial location of particle centers. Statistics of simple point fields can be used to incorporate scale information into existing single–point models for the unclosed terms, or new models proposed. Such second–order models are poised to make a significant impact on the ability to model particle–laden flows, especially in the dense regimes.

APPENDIX A. DERIVATION OF THE SECOND-MOMENT EQUATION FROM THE PHASIC PDF

In order to derive the evolution equation for $\tilde{R}_{ij}^{(\beta)}$, we multiply Eq. (3.57) by $v'^{(\beta)}_i v'^{(\beta)}_j$, where $v''^{(\beta)}_i \equiv u_i - \widetilde{\langle U_i^{(\beta)} \rangle}$, and integrate over $\mathbf{u}$ space to obtain

$$\underbrace{v'^{(\beta)}_i v'^{(\beta)}_j \frac{\partial \mathcal{F}_{\mathbf{U}|I_\beta}}{\partial t}}_{1} + \underbrace{v'^{(\beta)}_i v'^{(\beta)}_j u_k \frac{\partial \mathcal{F}_{\mathbf{U}|I_\beta}}{\partial x_k}}_{2} = \underbrace{- v'^{(\beta)}_i v'^{(\beta)}_j \frac{\partial}{\partial V_k}\left[\left\langle \rho I_\beta \frac{DU_k}{Dt}\Big|\mathbf{u}\right\rangle \frac{\mathcal{F}_{\mathbf{U}|I_\beta}}{\langle \rho I_\beta|\mathbf{u}\rangle}\right]}_{3}$$
$$\underbrace{+ v'^{(\beta)}_i v'^{(\beta)}_j \frac{\mathcal{F}_{\mathbf{U}|I_\beta}}{\langle \rho I_\beta|\mathbf{u}\rangle}\left\langle \rho\left(U_i - U_i^{(I)}\right)\frac{\partial I_\beta}{\partial x_i}\Big|\mathbf{u}\right\rangle}_{4} \tag{A.1}$$

The first term simplifies to

$$v'^{(\beta)}_i v'^{(\beta)}_j \frac{\partial \mathcal{F}_{\mathbf{U}|I_\beta}}{\partial t} = \frac{\partial v'^{(\beta)}_i v'^{(\beta)}_j \mathcal{F}_{\mathbf{U}|I_\beta}}{\partial t} - \mathcal{F}_{\mathbf{U}|I_\beta}\frac{\partial v'^{(\beta)}_i v'^{(\beta)}_j}{\partial t} \tag{A.2}$$

The second term simplifies to

$$v'^{(\beta)}_i v'^{(\beta)}_j u_k \frac{\partial \mathcal{F}_{\mathbf{U}|I_\beta}}{\partial x_k} = \frac{\partial v'^{(\beta)}_i v'^{(\beta)}_j u_k \mathcal{F}_{\mathbf{U}|I_\beta}}{\partial x_k} - \underbrace{u_k \mathcal{F}_{\mathbf{U}|I_\beta}\frac{\partial v'^{(\beta)}_i v'^{(\beta)}_j}{\partial x_k}}_{a}$$

Taking term a in the above expression

$$u_k \mathcal{F}_{\mathbf{U}|I_\beta}\frac{\partial v'^{(\beta)}_i v'^{(\beta)}_j}{\partial x_k} = -u_k \mathcal{F}_{\mathbf{U}|I_\beta}\left\{ v''^{(\beta)}_i \frac{\partial \langle U_j^{(\beta)}\rangle}{\partial x_k} + v''^{(\beta)}_j \frac{\partial \langle U_i^{(\beta)}\rangle}{\partial x_k}\right\}$$

Part 3 above simplifies to

$$\begin{aligned} v'^{(\beta)}_i v'^{(\beta)}_j \frac{\partial}{\partial V_k}\left[\left\langle \rho\frac{DU_k}{Dt}\Big|\mathbf{u}\right\rangle \frac{\mathcal{F}_{\mathbf{U}|I_\beta}}{\langle \rho I_\beta|\mathbf{u}\rangle}\right] &= \frac{\partial}{\partial V_k}\left[v'^{(\beta)}_i v'^{(\beta)}_j \left\langle \rho I_\beta \frac{DU_k}{Dt}\Big|\mathbf{u}\right\rangle \frac{\mathcal{F}_{\mathbf{U}|I_\beta}}{\langle \rho I_\beta|\mathbf{u}\rangle}\right] \\ &\quad - \left\{\left\langle \rho I_\beta \frac{DU_k}{Dt}\Big|\mathbf{u}\right\rangle \frac{\mathcal{F}_{\mathbf{U}|I_\beta}}{\langle \rho I_\beta|\mathbf{u}\rangle}\right\}\frac{\partial}{\partial V_k}\left[v'^{(\beta)}_i v'^{(\beta)}_j\right] \\ &= \frac{\partial}{\partial V_k}\left[v'^{(\beta)}_i v'^{(\beta)}_j \left\langle \rho I_\beta \frac{DU_k}{Dt}\Big|\mathbf{u}\right\rangle \frac{\mathcal{F}_{\mathbf{U}|I_\beta}}{\langle \rho I_\beta|\mathbf{u}\rangle}\right] \\ &\quad - \left\{ v''^{(\beta)}_i \left\langle \rho I_\beta \frac{DU_j}{Dt}\Big|\mathbf{u}\right\rangle + v''^{(\beta)}_j \left\langle \rho I_\beta \frac{DU_i}{Dt}\Big|\mathbf{u}\right\rangle\right\}\frac{\mathcal{F}_{\mathbf{U}|I_\beta}}{\langle \rho I_\beta|\mathbf{u}\rangle} \end{aligned}$$

The last term on the right hand side of Eq. (A.2) simplifies to

$$\begin{aligned}
\mathcal{F}_{\mathbf{U}|I_\beta}\frac{\partial v_i'^{(\beta)}v_j'^{(\beta)}}{\partial t} &= \mathcal{F}_{\mathbf{U}|I_\beta}\frac{\partial}{\partial t}\left[(V_i-\widetilde{\langle U_i^{(\beta)}\rangle})(V_j-\widetilde{\langle U_j^{(\beta)}\rangle})\right] \\
&= \mathcal{F}_{\mathbf{U}|I_\beta}\frac{\partial}{\partial t}\left[V_iV_j - V_j\widetilde{\langle U_i^{(\beta)}\rangle} - V_i\widetilde{\langle U_j^{(\beta)}\rangle} + \widetilde{\langle U_i^{(\beta)}\rangle}\widetilde{\langle U_j^{(\beta)}\rangle}\right] \\
&= \mathcal{F}_{\mathbf{U}|I_\beta}\left[-V_j\frac{\partial\widetilde{\langle U_i^{(\beta)}\rangle}}{\partial t} - V_i\frac{\partial\widetilde{\langle U_j^{(\beta)}\rangle}}{\partial t} + \frac{\partial\widetilde{\langle U_i^{(\beta)}\rangle}\widetilde{\langle U_j^{(\beta)}\rangle}}{\partial t}\right]
\end{aligned}$$

When integrated over all $\mathbf{u}$ space, the term in square brackets evaluates to zero.

The second moment equation is then

$$\begin{aligned}
&\frac{\partial}{\partial t}\langle I_\beta\rho\rangle\widetilde{R}_{ij}^{(\beta)} + \frac{\partial}{\partial x_k}\langle\rho I_\beta u_i''^{(\beta)}u_j''^{(\beta)}u_k''^{(\beta)}\rangle + \frac{\partial}{\partial x_k}\langle\rho I_\beta\rangle\widetilde{R}_{ij}^{(\beta)}\widetilde{\langle U_k^{(\beta)}\rangle} = \\
&\quad + \left\{\langle\rho I_\beta u_i''^{(\beta)}u_k''^{(\beta)}\rangle\frac{\partial\widetilde{\langle U_j^{(\beta)}\rangle}}{\partial x_k} + \langle\rho I_\beta u_j''^{(\beta)}u_k''^{(\beta)}\rangle\frac{\partial\widetilde{\langle U_i^{(\beta)}\rangle}}{\partial x_k}\right\} \\
&\quad + \left\langle\rho I_\beta u_i''^{(\beta)}\frac{DU_j}{Dt}\right\rangle + \left\langle\rho I_\beta u_j''^{(\beta)}\frac{DU_i}{Dt}\right\rangle
\end{aligned} \tag{A.3}$$

The second term on the right hand side can be written as follows:

$$\left\langle\rho I_\beta u_i''^{(\beta)}\frac{DU_j}{Dt}\right\rangle = \left\langle\rho u_i''^{(\beta)}\frac{\partial(I_\beta\tau_{kj})}{\partial x_k}\right\rangle - \left\langle\rho u_i''^{(\beta)}\tau_{kj}\frac{\partial I_\beta}{\partial x_k}\right\rangle$$

The same treatment can be applied to the last term on the right hand side of Eq. (A.3). Using the product rule on the temporal derivative, and the spatial derivative (third term on left hand side), rearranging and using the mean mass conservation equation, we obtain Eq.(3.107).

APPENDIX B. SIMPLIFIED RELATIONS BETWEEN THE EE AND LE REPRESENTATIONS

In this section, details of the simplified relationships between $\alpha_d(\mathbf{x},t)$ and $n(\mathbf{x};t)$, and between $f^E_{\mathbf{U}R|I_d}(\mathbf{u},r\ ;\mathbf{x},t)$ and $f^c_{\mathbf{V}R}(\mathbf{v},r\mid\mathbf{x};t)$, that were presented in Section 3.3 are given. Combinations of statistically homogeneous number density, statistically homogeneous radius pdf and statistically homogeneous $f^c_{\mathbf{V}\,|\,R}(\mathbf{v}\mid r,\mathbf{x};t)$ are considered. Two–phase flows with monodisperse DPE's are included as a special subset of the homogeneous radius pdf case.

The assumption of spherical DPE's implies an isotropic point process [1] and leads to the following isotropic form of Eq. (3.26) that is convenient for simplification under special conditions:

$$\alpha_d(\mathbf{x},t)\ =\int_{r=0_+}^{\infty}\int_{r'=0}^{r}K'_D\ {r'}^{D-1}n(\mathbf{x}+\mathbf{e}\,r';t)\,f^c_R(r\mid\mathbf{x}+\mathbf{e}\,r',t)\,dr'\,dr, \tag{B.1}$$

where $\mathbf{e}$ is the unit vector in the radial direction. The above expression has been written in a general form for D–dimensional space ($1\le D\le 3$) with $K'_1=2, K'_2=2\pi$, and $K'_3=4\pi$.

Similarly, the assumption of an isotropic point process in Eq. (3.30) results in the simplification:

$$f^E_{\mathbf{U}R|I_d}(\mathbf{v},r\ ;\mathbf{x},t)=\frac{1}{\alpha_d(\mathbf{x},t)}\int_{r'=0}^{r}K'_D\ {r'}^{D-1}n(\mathbf{x}+\mathbf{e}\,r';t)\,f^c_{\mathbf{V}R}(\mathbf{v},r\mid\mathbf{x}+\mathbf{e}\,r',t)\,dr'. \tag{B.2}$$

[1] Non–spherical shapes could still result in an isotropic point process but those are not considered here.

HNHP: Homogeneous number density and homogeneous, polydisperse radius pdf

If the number density is homogeneous ($n(\mathbf{x}';t) = n(t)$), but the DPE's have a statistically homogeneous size distribution represented by $f_R^c(r;t)$, then Eq.(B.1) simplifies to

$$\begin{aligned}\alpha_d(\mathbf{x},t) &= \int_{r=0_+}^{\infty}\int_{r'=0}^{r} K'_D\; r'^{D-1} n(t)\, f_R^c(r;t)\, dr'\, dr \\ &= n(t)\, K_D \int_{[r_+]} r^D f_R^c(r;t)\, dr \\ &= n(t)\, \overline{\mathcal{V}}_D(t), \end{aligned} \tag{B.3}$$

where $\overline{\mathcal{V}}_D(t)$ is the average volume occupied by a DPE in D–dimensional space given by

$$\overline{\mathcal{V}}_D(t) = K_D\; \langle R^D(t)\rangle = K_D \int_{[r_+]} r^D f_R^c(r;t)\, dr, \tag{B.4}$$

where $\langle R^D(t)\rangle$ is the Dth moment of the radius pdf. The above expression has been written in a general form for D–dimensional space ($1 \le d \le 3$) with $K_1 = 2, K_2 = \pi$, and $K_3 = 4\pi/3$, and $K'_D = DK_D$. In $\mathbb{R}^3$ this reduces to the well–known result

$$\alpha_d(t) = n(t)\frac{4}{3}\pi\langle R^3(t)\rangle. \tag{B.5}$$

If $f^c_{\mathbf{V}\,|\,R}(\mathbf{v} \mid r, \mathbf{x}';t)$ is also statistically homogeneous then the expression (Eq. B.2) for the Eulerian jpdf of velocity and radius conditional on the dispersed phase, $f^E_{\mathbf{U}R|I_d}(\mathbf{v}, r\,; \mathbf{x}, t)$ simplifies in this case to

$$\begin{aligned} f^E_{\mathbf{U}R\,|\,d}(\mathbf{v},r;t) &= \frac{1}{\alpha_d(t)}\int_{r'=0}^{r} K'_D\; r'^{D-1} n(t)\, f_R^c(r;t)\, f^c_{\mathbf{V}\,|\,R}(\mathbf{v} \mid r\,;t)\, dr' \\ &= \frac{1}{\langle R^D(t)\rangle} r^D f^c_{\mathbf{V}R}(\mathbf{v},r;t) \\ &= \tilde{f}^c_{\mathbf{V}R}(\mathbf{v},r;t), \end{aligned} \tag{B.6}$$

where the expression for $\alpha_d(\mathbf{x},t)$ from Eq.(B.3) has been substituted and $\tilde{f}^c_{\mathbf{V}R}(\mathbf{v},r;t)$ is the (DPE) volume–weighted–pdf corresponding to $f^c_{\mathbf{V}R}(\mathbf{v},r;t)$ defined as

$$\tilde{f}^c_{\mathbf{V}R}(\mathbf{v},r;t) \equiv \frac{r^D\, f^c_{\mathbf{V}R}(\mathbf{v},r;t)}{\langle R^D(t)\rangle}. \tag{B.7}$$

Integrating both sides of Eq. (B.6) over $\mathbf{v}$ space results in

$$f^E_{R\,|\,d}(r;t) = \frac{1}{\langle R^D(t)\rangle} r^D f_R^c(r;t), \tag{B.8}$$

which provides a relationship between the Eulerian radius pdf conditional on the dispersed phase and the size distribution in the LE approach.

HNHM: Homogeneous number density and homogeneous, monodisperse radius pdf

If the number density is homogeneous then $n(\mathbf{x}';t) = n(t)$, and if the DPE's are monodisperse then they all have the same radius r_0, so that $f_R^c(r \mid \mathbf{x}';t) = \delta(r - r_0)$. Substituting these simplifications into Eq. B.1 results in the following expression for $\alpha_d(\mathbf{x},t)$:

$$\begin{aligned}\alpha_d(\mathbf{x},t) &= \int_{r=0_+}^{\infty}\int_{r'=0}^{r} K_D'\ r'^{D-1} n(t)\,\delta(r-r_0)\,dr'\,dr, \\ &= n(t)\int_{r=0_+}^{\infty} K_D\ r^D \delta(r-r_0)\,dr \\ &= n(t) K_D\ r_0^D, \end{aligned} \tag{B.9}$$

This yields the result

$$\alpha_d(t) = n(t)\frac{4}{3}\pi r_0^3 \tag{B.10}$$

in $\mathbb{R}^3$. Note that $\alpha_d(\mathbf{x},t)$ in both Eqs.(B.5) and (B.10) depends on the dimensionality D of physical space, whereas $n(\mathbf{x};t)$ does not. This alone is evidence that the point–process and random–field statistical representations contain different information.

Although the relation between $\alpha_d(\mathbf{x},t)$ and $n(\mathbf{x};t)$ only requires assumptions concerning the number density and the radius pdf $f_R^c(r \mid \mathbf{x};t)$ because $\alpha_d(\mathbf{x},t)$ does not depend on the statistical properties of the velocity of the DPE's, further assumptions are needed to relate $f_{\mathbf{U}R}^E(\mathbf{v},r\,;\mathbf{x},t)$ and $f_{\mathbf{V}R}^c(\mathbf{v},r \mid \mathbf{x};t)$. If $f_{\mathbf{V}\mid R}^c(\mathbf{v} \mid r,\mathbf{x}';t)$ is also assumed to be statistically homogeneous, then the expression (Eq. B.2) for the Eulerian jpdf of velocity and radius conditional on the dispersed phase, $f_{\mathbf{U}R|I_d}^E(\mathbf{u},r\,;\mathbf{x},t)$ simplifies in this case to

$$\begin{aligned} f_{\mathbf{U}R|I_d}^E(\mathbf{v},r;t) &= \frac{1}{\alpha_d(t)}\int_{r'=0}^{r} K_D'\ r'^{D-1} n(t)\,\delta(r-r_0) f_{\mathbf{V}\mid R}^c(\mathbf{v} \mid r;t)\,dr' \\ &= \frac{1}{\alpha_d(t)} n(t)\,K_D\ r^D\ f_{\mathbf{V}\mid R}^c(\mathbf{v} \mid r\,;t)\,\delta(r-r_0) \\ &= \delta(r-r_0) f_{\mathbf{V}\mid R}^c(\mathbf{v} \mid r;t), \end{aligned} \tag{B.11}$$

where the simplified expression for $\alpha_d(\mathbf{x},t)$ given by Eq.(B.9) has been substituted above.

Thus, for the case of statistically homogeneous number density and statistically homogeneous radius pdf, the following relations hold:

$$\alpha_d(t) = n\overline{\mathcal{V}}_D \tag{B.12}$$

$$\overline{\mathcal{V}}_D = K_D\langle R^D\rangle \tag{B.13}$$

$$f^E_{\mathbf{U}R|d}(\mathbf{v}, r\,; t) = \frac{r^D}{\langle R^D\rangle} f^c_{\mathbf{V}R}(\mathbf{v}, r\,; t) \tag{B.14}$$

$$\alpha_d(t) f^E_{\mathbf{U}R|d}(\mathbf{v}, r\,; t) = K_D r^D f(\mathbf{v}, r, t) \tag{B.15}$$

$$f^E_X(t) = \frac{1}{\langle V_d(t)\rangle}\alpha_d(t) \tag{B.16}$$

$$f^E_{\mathbf{U}R|d}(\mathbf{v}, r\,; t) f^E_X(t) = \frac{r^D}{\langle R^D(t)\rangle\langle N_s(t)\rangle} f(\mathbf{v}, r, t), \tag{B.17}$$

where $f^E_X(t)$ is the position pdf of the dispersed phase, $\langle V_d(t)\rangle$ is the volume occupied by the dispersed phase and $\langle N_s(t)\rangle$ is the mean number of DPEs in the domain.

It is not enough to just define α_d or f^E_R independently in terms of n and f^c_R, but rather they must jointly form a consistent definition so that a quantity like mean momentum in a control volume makes sense. Although one might be tempted to write $\alpha_d(\mathbf{x}, t) \approx n(\mathbf{x}; t)\ \overline{\mathcal{V}}_D(\mathbf{x}, t)$ and $f^E_{\mathbf{U}R|I_\beta}(\mathbf{u}, r\,; \mathbf{x}, t)\ \approx r^D f^c_{\mathbf{V}R}(\mathbf{v}, r \mid \mathbf{x}; t)\ /\langle R^D(\mathbf{x}, t)\rangle$ under conditions of local homogeneity of the number density $l_n > R_{\max}$ and $l_{f^c_R(r\,|\,\mathbf{x};t)}\ > R_{\max}$, such relations are only approximate and useful for scaling purposes. They cannot hold as strict equalities simultaneously, and therefore unlike the statistically homogeneous cases presented earlier, they cannot form a consistent basis for comparing the two statistical representations. In the inhomogeneous case we must conclude that the two statistical representations are indeed different, and cannot be related.

APPENDIX C. EVOLUTION EQUATION FOR THE VOLUME–WEIGHTED DDF OF FLUCTUATING VELOCITY

The evolution equation for the volume–weighted ddf of fluctuating velocity $\tilde{g}$ that was introduced in Section 3.5.3 is derived in this section. Using the chain rule, we first form the time and spatial derivatives of the r^3–weighted ddf $\tilde{f}$:

$$\frac{\partial \tilde{f}}{\partial t} = \frac{\partial \tilde{g}}{\partial t} + \frac{\partial \tilde{g}}{\partial w_j}\frac{\partial \widetilde{\langle V_j \rangle}}{\partial t} \tag{C.1}$$

$$\frac{\partial \tilde{f}}{\partial x_k} = \frac{\partial \tilde{g}}{\partial x_k} + \frac{\partial \tilde{g}}{\partial w_j}\frac{\partial \widetilde{\langle V_j \rangle}}{\partial x_k} \tag{C.2}$$

The above two expressions can be combined as follows:

$$\frac{\partial \tilde{f}}{\partial t} + \left(\widetilde{\langle V_k \rangle} + w_k\right)\frac{\partial \tilde{f}}{\partial x_k} = \frac{\partial \tilde{g}}{\partial t} + \left(\widetilde{\langle V_k \rangle} + w_k\right)\frac{\partial \tilde{g}}{\partial x_k} + \frac{\partial \tilde{g}}{\partial w_j}\left[\frac{\partial \widetilde{\langle V_j \rangle}}{\partial t} + \left(\widetilde{\langle V_k \rangle} + w_k\right)\frac{\partial \widetilde{\langle V_j \rangle}}{\partial x_k}\right]. \tag{C.3}$$

Multiplying Eq. (3.130) on both sides by r^3, the evolution equation for $\tilde{f} = r^3 f$ can be derived:

$$\frac{\partial \tilde{f}}{\partial t} + v_k\frac{\partial \tilde{f}}{\partial x_k} = -\frac{\partial}{\partial v_k}\left[\langle A_k|\mathbf{x},\mathbf{v},r;t\rangle \tilde{f}\right] - \frac{\partial}{\partial r}\left[\langle \Theta|\mathbf{x},\mathbf{v},r;t\rangle \tilde{f}\right] + 3r^2\langle \Theta|\mathbf{x},\mathbf{v},r;t\rangle. \tag{C.4}$$

Note that since v_k is a sample space variable, it can be taken outside the derivative in the second term on the left hand side. Equating the right hand sides of Eq. (C.3) and Eq. (C.4), and rearranging results in the transport equation for the r^3–weighted ddf of fluctuating velocity Eq.3.111.

APPENDIX D. EXACT EQUATION FOR THE DISPERSED–PHASE TKE IN THE LE APPROACH

The primary objective of this section is to identify unclosed terms in the evolution equation for the dispersed–phase TKE that need to be modeled. The connection between DLM and the LE approach will also be explained here.

The droplet distribution function $f(\mathbf{x}, \mathbf{v}, r, t)$ and the corresponding r^3–weighted ddf of fluctuating velocity $\tilde{g}(\mathbf{x}, \mathbf{w}, r, t)$ was presented in Chapter 3. From $\tilde{g}$, the evolution equation for the Reynolds stresses in the dispersed phase can be derived (cf. Eq. (3.112)).

In particle method solutions to the ddf evolution equation (see for example Amsden et al. (1989)) and in DLM, the triple velocity correlation in Eq. (3.112) is in closed form. If there is no interphase mass transfer, then the terms representing the change in the velocity covariance due to interphase mass transfer are zero, and the only remaining term to be modeled in the LE approach is the correlation of acceleration with fluctuating velocity.

Contracting indices in Eq. (3.112) and dropping terms involving the spatial gradients (assuming spatial homogeneity) results in an evolution equation for the r^3–weighted TKE in the dispersed phase $\tilde{k}_d = (1/2)\widetilde{\langle v_i'' v_i'' \rangle}$ as

$$2n\langle R^3\rangle \frac{\partial}{\partial t}\tilde{k}_d = 2\langle R^3\rangle n\widetilde{\langle A_i v_i''\rangle} + 3n\langle R^3\rangle\widetilde{\langle v_i'' v_i''\Gamma|t\rangle} - 6n\langle R^3\rangle\tilde{k}_d\langle\widetilde{\Gamma}|t\rangle. \tag{D.1}$$

With no interphase mass transfer, as in non–evaporating or solid particle-laden turbulent flow, and mono–dispersed particles, the terms involving Γ are zero. Also, volume–weighted quantities are the same as their number–weighted counterparts. The above equation then simplifies to

$$\frac{\partial}{\partial t}k_d = \left\langle A_i v_i'' \right\rangle .$$

Thus, in a homogeneous two–phase flow with *no interphase mass transfer*, the evolution of the dispersed–phase TKE is governed only by the acceleration–fluctuating velocity covariance.

Relationship between the ddf and DLM

Subramaniam (2001c) has shown that the ddf can be related to the single surrogate–droplet density $f_{1s}^{(m)}(\mathbf{x}, \mathbf{v}, r; t)$ as

$$f(\mathbf{x}, \mathbf{v}, r, t) = \sum_{m \geq 1} p_m m f_{1s}^{(m)}(\mathbf{x}, \mathbf{v}, r; t), \tag{D.2}$$

where p_m is the probability that the number of droplets in the system at any time t is equal to m. The single surrogate droplet–density is the density of identically distributed surrogate droplets in phase space. This density has important implications in particle method solutions, like the one used in this study, of the spray equation where each *computational* particle is assumed to be an identically distributed realization of the spray. The Lagrangian joint probability density function of velocity and radius implied by a stochastic model like DLM can be identified with $f_{1s}^{(m)}$, and hence every model for the particle velocity in turn implies a modeled spray equation. Models for particle velocity and droplet vaporization in turn imply models for $\langle A_i \rangle$ and $\langle \Theta \rangle$. In particle–based LE approaches like DLM (also Amsden et al. (1989)), the terms on the right hand side of Eq. (3.112) are closed and can be determined from the solution.

Correspondence between the governing equations in the EE and LE statistical representations

For a homogeneous two–phase flow, there is a correspondence between the governing equations for the dispersed–phase TKE derived using the LE and Eulerian–Eulerian (EE) representation of two–phase flow. This correspondence allows one to estimate an unclosed term on the EE side using the corresponding term on the LE side.

Under assumptions of statistical homogeneity, one can derive the evolution equation for the density–weighted dispersed–phase TKE, defined as

$$\tilde{k}_d = \langle I_d \rho u_{di}'' u_{di}'' \rangle / \langle I_d \rho \rangle, \tag{D.3}$$

in the EE representation as (Drew, 1983; Subramaniam, 2003; Xu, 2004) as

$$\theta_d\rho_d\frac{d}{dt}\tilde{k}_d = \left\langle u''_{di}\frac{\partial(I_d\tau_{ki})}{\partial x_k}\right\rangle + \langle u''_{di}(S_{Mdi} - U_iS_{\rho d})\rangle + (1/2)\langle u''_{di}u''_{di}S_{\rho d}\rangle - \tilde{k}_d\langle S_{\rho d}\rangle, \qquad \text{(D.4)}$$

where U_i is the instantaneous velocity in the two–phase system. The dispersed–phase fluctuating velocity u''_{di} is defined with respect to the density–weighted mean as

$$u''_{di} = U_i - \langle\tilde{U}_{i,d}\rangle. \qquad \text{(D.5)}$$

Here, the density–weighted mean velocity in the dispersed phase is given as

$$\langle\tilde{U}_{i,d}\rangle = \frac{\langle I_d\rho U_i\rangle}{\langle I_d\rho\rangle},$$

where ρ is the density of the two–phase flow field. The corresponding equations for the fluid phase are obtained by replacing d by f. In the above equations, I_d is the indicator function which is unity in the dispersed phase and zero in the fluid phase. The interphase momentum transfer S_{Mdi} is (Subramaniam, 2003; Xu, 2004)

$$S_{Mdi} = \rho U_i(U_j - U_j^{(I)})\frac{\partial I_d}{\partial x_j} - \tau_{ji}\frac{\partial I_d}{\partial x_j}, \qquad \text{(D.6)}$$

where $U_j^{(I)}$ is the interface velocity (for example, the regression velocity of the droplet surface) and τ_{ji} is the stress tensor in the dispersed phase. The presence of $\partial I_d/\partial x_j$ in the terms on the right hand side imply that such terms are defined only at the interface. The interphase mass transfer term S_{ρ_d} can be written as (Subramaniam, 2003; Xu, 2004)

$$S_{\rho d} = \rho(U_i - U_i^{(I)})\frac{\partial I_d}{\partial x_i}. \qquad \text{(D.7)}$$

With no interphase mass transfer, Eq.(D.4) simplifies to

$$\theta_d\rho_d\frac{d}{dt}\tilde{k}_d = \left\langle u''_{di}\frac{\partial(I_d\tau_{ki})}{\partial x_k}\right\rangle + \langle u''_{di}S_{Mdi}\rangle. \qquad \text{(D.8)}$$

The correspondence between the dispersed–phase TKE evolution equation in the LE and EE representations is given below by comparing the the right hand sides of Eq. (D.1) and Eq. (D.4):

$$\begin{aligned}
2\left\langle u''_{di}\frac{\partial(I_d\tau_{ki})}{\partial x_k}\right\rangle + 2\langle u''_{di}(S_{Mdi})\rangle &\Longleftrightarrow \frac{4}{3}\pi\rho_d n\langle R^3\rangle 2\left\langle\widetilde{A_iv''_i}\right\rangle \\
\langle u''_{di}u''_{di}S_{\rho d}\rangle &\Longleftrightarrow \frac{4}{3}\pi\rho_d n\langle R^3\rangle\left(3\left\langle\widetilde{v''_iv''_i\Gamma}|t\right\rangle\right) \\
-2\tilde{k}_d\langle S_{\rho d}\rangle &\Longleftrightarrow -\frac{4}{3}\pi\rho_d n\langle R^3\rangle\langle\widetilde{v''_iv''_i}\rangle\left(6\langle\widetilde{\Gamma}|t\rangle\right).
\end{aligned}$$

where $\Longleftrightarrow$ denotes the correspondence between the terms. For the case with zero interphase mass transfer, the correspondence simplifies to

$$\left\langle u''_{di}\frac{\partial(I_d\tau_{ki})}{\partial x_k}\right\rangle + \langle u''_{di}(S_{Mdi})\rangle \Longleftrightarrow \frac{4}{3}\pi\rho_d n\langle R^3\rangle \left\langle \widetilde{A_i v''_i}\right\rangle .$$

Using DLM, the terms on the right hand side involving Γ are in closed form since such terms can be easily computed from the solution. The above development enables one to estimate from the LE representation the corresponding unclosed term in the EE representation.

BIBLIOGRAPHY

Abramowitz, M. and Stegun, I. A. (1964). *Handbook of Mathematical Functions with Formulas, Graphs, and Mathematical Tables*. Dover, New York.

Ahmed, A. M. and Elghobashi, S. (2000). On the mechanisms of modifying the structure of turbulent homogeneous shear flows by dispersed particles. *Phys. Fluids*, 12(11):2906–2930.

Ahmed, A. M. and Elghobashi, S. (2001). Direct numerical simulation of particle dispersion in homogeneous turbulent shear flows. *Phys. Fluids*, 13(11):3346–3364.

Amsden, A. A. (1993). KIVA–3: A KIVA Program with Block–Structured Mesh for Complex Geometries. Technical Report LA–12503–MS, Los Alamos National Laboratory.

Amsden, A. A., O'Rourke, P. J., and Butler, T. D. (1989). KIVA–II: A Computer Program for Chemically Reactive Flows with Sprays. Technical Report LA–11560–MS, Los Alamos National Laboratory.

Aplin, C. and Subramaniam, S. (2003). A fundamental property of phase averaging: implications for averaged equations of multiphase flow (Unpublished).

Batchelor, G. K. (1971). *An introduction to Fluid dynamics*. Cambridge University Press, Port Chester, NY.

Bird, R. B., Stewart, W. E., and Lightfoot, E. N. (2002). *Transport Phenomena*. John Wiley and Sons, Inc., New York, 2nd edition.

Blokkeel, G., Borghi, R., and Barbeau, B. (2003). A 3d Eulerian Model to Improve the Primary Breakup of Atomizing Jet. *SAE Technical Papers*, (2003-01-0005).

Boivin, M., Simonin, O., and Squires, K. (1998). Direct numerical simulation of turbulence modulation by particles in isotropic turbulence. *J. Fluid Mech.*, 375:235–263.

Brown, D. J. and Hutchinson, P. (1979). The Interaction of Solid or Liquid Particles and Turbulent Fluid Flow Fields – A Numerical Simulation. *J. Fluids Engineering*, 101:265–269.

Chagras, V., Oesterle, B., and Boulet, P. (2005). On the heat transfer in gas–solid pipe flows: Effects of collision induced alterations of the flow dynamics. *Intl. J. Heat Mass Transfer*, 48:1649–1661.

Chapman, S. and Cowling, T. G. (1990). *The mathematical theory of non–uniform gases*. Cambridge University Press, New York.

Chen, C. M. (1947). *Mean value and correlaton problems connected with the motion of small particles suspended in a turbulent fluid*. PhD dissertation, University of Delft, The Hague.

Chen, X.-Q. and Periera, J. C. F. (1997). Efficient computation of particle dispersion in turbulent flows with a stochastic–probabilistic model. *Intl. J. Heat Mass Transfer*, 40(8):1727–1741.

Clift, R., Grace, J. R., and Weber, M. E. (1978). *Bubbles, Drops and Particles*. Academic Press, New York.

Crowe, C. T., Troutt, T. R., and Chung, J. N. (1996). Numerical models for two–phase turbulent flows. *Annu. Rev. Fluid Mech.*, 28:11–43.

Csanady, G. T. (1963). Turbulent diffusion of heavy particles in the atmosphere. *J. Atmos. Sci.*, 20:201–208.

D. Goldstein, R. H. and Sirovich, L. (1993). Modeling a no-slip flow boundary with an external force field. *J. Comp. Phys.*, 105:354–366.

Derevich, I. V. (2000). Statistical modeling of mass transfer in turbulent two–phase dispersed flows – 1. Model development. *Intl. J. Heat Mass Transfer*, 43(19):3709–3723.

Derevich, I. V. and Zaichik, L. I. (1988). Particle deposition from a turbulent flow. *Fluid. Dyn.*, 23:722–729.

Dreeben, T. D. and Pope, S. B. (1997a). Probability density function and Reynolds–stress model ing of near–wall turbulent flows. *Phys. Fluids*, 9:154–163.

Dreeben, T. D. and Pope, S. B. (1997b). Probability density function and Reynolds-stress modeling of near-wall turbulent flows. *Phys. Fluids*, 9:154–163.

Drew, D. A. (1983). Mathematical modeling of two–phase flow. *Annu. Rev. Fluid Mech.*, 15:261–291.

Drew, D. A. and Passman, S. L. (1999). *Theory of multicomponent fluids*. Springer–Verlag, New York.

Edwards, C. F. (2000). Towards a comprehensive theory of dense spray flows. *Atomization and Sprays*, 10(3–5):335–353.

Edwards, C. F. and Marx, K. D. (1996). Single–point statistics of ideal sprays, Part I: Fundamental descriptions and derived quantities. *Atomization and Sprays*, 6(5):499–536.

Faeth, G. M. (1977). Current status of droplet and liquid combustion. *Prog. Energy Combust. Science*, 3:191–224.

Fallon, T. and Rogers, C. B. (2002). Turbulence–induced preferential concentration of solid particles in microgravity conditions. *Exp. Fluids*, 33:233–241.

Friedman, P. D. and Katz, J. (2002). Mean Rise Rate of Droplets in Isotropic Turbulence. *Phys. Fluids*, 14(9):3059–3073.

G. Gouesbet, A. B. and Picart, A. (1984). Dispersion of discrete particles by continuous turbulent motions. Extensive discussion of the Tchen's theory, using a two–parameter family of Lagrangian correlation functions. *Phys. Fluids*, 27(4):827–837.

Gao, Z. and Mashayek, F. (2004a). Stochastic model for nonisothermal droplet-laden turbulent flows. *AIAA Journal*, 42(2):255–260.

Gao, Z. and Mashayek, F. (2004b). Stochastic modeling of evaporating droplets polydispersed in turbulent flows. *Intl. J. Heat Mass Transfer*, 47:4339–4348.

Gardiner, C. W. (1983). *Handbook of Stochastic Methods*. Springer–Verlag, New York.

Gosman, A. D. and Ioannides, E. (1983). Aspects of Computer Simulation of Liquid Fueled Combustors. *Journal of Engine Research*, 6(7):482–490.

Gouesbet, G. and Berlemont, A. (1999). Eulerian and Lagrangian approaches for predicting the behaviour of discrete particles in turbulent flows. *Prog. Energy Combust. Science*, 25:133–159.

Greenberg, J. B., Silverman, I., and Tambour, Y. (1993). On the origins of spray sectional conservation equations. *Combustion and Flame*, 93(1–2):90–96.

Greene, G. A., T. F. Irvine, J., Gyves, T., and Smith, T. (1993). Drag relationships for liquid droplets settling in a continuous Liquid. *A.I.Ch.E.J.*, 29(1):37–41.

Groszmann, D. E. and Rogers, C. B. (2004). Turbulent scales of dilute particle–laden flows in microgravity. *Phys. Fluids*, 16(12):4671–4684.

Haworth, D. C. and Pope, S. B. (1986). A Generalized Langevin model for turbulent flows. *Phys. Fluids*, 29:387–405.

Hinze, J. O. (1975). *Turbulence*. McGraw–Hill series in Mechanical Engineering, New York, 2^{nd} edition.

Hwang, W. and Eaton, J. K. (2006). Homogeneous and isotropic turbulence modulation by small heavy particles ($St \sim 50$) particles. *J. Fluid Mech.*, 564:361–393.

Hyland, K. E., McKee, S., and Reeks, M. W. (1999a). Derivation of a pdf kinetic equation for the transport of particles in turbulent flows. *J. Phys. A: Math. Gen.*, 32:6169–6190.

Hyland, K. E., McKee, S., and Reeks, M. W. (1999b). Exact analytic solutions to turbulent particle equations. *Phys. Fluids*, 11(5):1249–1261.

Jones, W. P. (1980). *Prediction methods for turbulent flows*. von Karman Institute (VKI) for Fluid Dynamics. Hemisphere.

Kashiwa, B. A. and Gaffney, E. S. (2003). Design Basis for CFDLib. Technical Report LA–UR-03–1295, Los Alamos National Laboratory.

Kashiwa, B. A. and Rauenzahn, R. M. (1994). A Multimaterial Formalism. Technical Report LA–UR-94–771, Los Alamos National Laboratory.

Kataoka, I. and Serizawa, A. (1989). Basic equations of turbulence in gas-liquid two-phase flow. *Intl. J. Multiphase Flow*, 15(5):843–855.

Kim, D., Desjardins, O., Herrmann, M., and Moin, P. (2006). Toward two-phase simulation of the primary breakup of a round liquid jet by a coaxial flow of gas. *Annual Res. Briefs, Center for Turbulence Research*, pages 185–195.

Kloeden, P. and Platen, E. (1992). *Numerical solution of stochastic differential equations*. Springer-Verlag, New York.

Kraichnan, R. H. (1965). Lagrangian-history closure approximation for turbulence. *Phys. Fluids*, 8(4):575–598.

Kraichnan, R. H. (1977). Eulerian and lagrangian renormalization in turbulence theory. *J. Fluid Mech.*, 83(22):349–374.

Krol, S., Pekediz, A., and de Lasa, H. (2000). Particle clustering in down flow reactors. *Powder Technology*, 108:6–20.

Lamorgese, A. G., Pope, S. B., Yeung, P. K., and Sawford, B. L. (2007). A conditionally cubic-Gaussian stochastic Lagrangian model for acceleration in isotropic turbulence. *J. Fluid Mech.*, 582:423–448.

Lázaro, B. J. and Lasheras, J. C. (1992a). Particle dispersion in the developing free shear layer. Part 1. Unforced flow. *J. Fluid Mech.*, 235:143–178.

Lázaro, B. J. and Lasheras, J. C. (1992b). Particle dispersion in the developing free shear layer. Part 2. Forced flow. *J. Fluid Mech.*, 235:179–221.

Libby, P. A. (1976). Prediction of the intermittent turbulent wake of a heated cylinder. *Phys. Fluids*, 19(4):494–501.

Libby, P. A. and Williams, F. A., editors (1980). *Turbulent Reacting Flows*. Topics in Applied Physics. Springer–Verlag, Berlin.

Libby, P. A. and Williams, F. A., editors (1993). *Turbulent Reacting Flows*. Combustion Treatise. Academic Press, Harcourt Brace and Co., New York.

Lu, Q. Q. (1995). An approach to modeling particle motion in turbulent flows – I. Homogeneous, isotropic turbulence. *Atmos. Environ.*, 29(3):423–436.

Lundgren, T. S. (1969). Model equation for nonhomogeneous turbulence. *Phys. Fluids*, 12:485.

L'vov, V. S., Ooms, G., and Pomyalov, A. (2003). Effect of particle inertia on turbulence in a suspension. *Phys. Rev. E*, 67:046314.

Mashayek, F. (1998). Droplet–turbulence interactions in low–Mach number homogeneous shear two–phase flows. *J. Fluid Mech.*, 367:163–203.

Mashayek, F. (1999). Stochastic simulations of particle–laden isotropic turbulent flow. *Intl. J. Multiphase Flow*, 25:1575–1599.

Mashayek, F., Jaberi, F. A., Miller, R. S., and Givi, P. (1997). Dispersion and polydispersity of droplets in stationary isotropic turbulence. *Intl. J. Multiphase Flow*, 23:337–355.

Mashayek, F. and Pandya, R. V. R. (2003). Analytical description of particle/droplet–laden turbulent flows. *Prog. Energy Combust. Science*, 29:329–378.

Maxey, M. R. and Riley, J. J. (1983). Equation of motion for a small rigid sphere in a non–uniform flow. *Phys. Fluids*, 26:883–889.

Monin, A. S. and Yaglom, A. M. (1971). *Statistical Fluid Mechanics: Mechanics of Turbulence; Vol. 1.* The MIT Press, Cambridge, Massachusetts.

Moses, B. and Edwards, C. (2005). LES–style filtering and partly–resolved particles. In *Proceedings of the Eighteenth Annual Conference on Liquid Atomization and Spray Systems*. Intl. Liquid Atomization and Spray Systems Soc.

Ning, W., Reitz, R. D., Lippert, A. M., and Diwakar, R. (2007). Development of a next–generation spray and atomization model using an Eulerian–Lagrangian methodology. In *Proceedings of the* 20*th Annual Conference on Liquid Atomization and Spray Systems*, Chicago, IL. Intl. Liquid Atomization and Spray Systems Soc.

Okong'o, N. and Bellan, J. (2004). Consistent Large Eddy Simulation of a temporal mixing layer laden with evaporating drops. Part 1: Direct Numerical Simulation, formulation and *a priori* analysis. *J. Fluid Mech.*, 499:1–47.

Ormancey, A. and Martinon, J. (1984). Prediction of particle dispersion in turbulent flows. *PhysicoChemical Hydrodynamics*, 3/4(5):229–244.

O'Rourke, P. J. (1981). *Collective drop effects on vaporizing liquid sprays*. PhD dissertation, Princeton University, New Jersey.

Pai, M. G. and Subramaniam, S. (2004). Analysis of turbulence models in Lagrangian–Eulerian spray computations. In *Proceedings of the Seventeenth Annual Conference on Liquid Atomization and Spray Systems*. Intl. Liquid Atomization and Spray Systems Soc.

Pai, M. G. and Subramaniam, S. (2006). Modeling interphase turbulent kinetic energy transfer in Lagrangian–Eulerian spray computations. *Atomization and Sprays*, 16(7):807–826.

Pai, M. G. and Subramaniam, S. (2007). Modeling droplet dispersion and interphase turbulent kinetic energy transfer using a new dual-timescale Langevin model . *Intl. J. Multiphase Flow*, 33(3):252–281.

Pandya, R. V. R. and Mashayek, F. (2001). Probability density function modeling of evaporating droplets dispersed in isotropic turbulence. *AIAA Journal*, 39:1909–1915.

Pandya, R. V. R. and Mashayek, F. (2003). Kinetic Equation for Particle Transport and Heat Transfer in Nonisothermal Turbulent Flows. *AIAA Journal*, 41:841–847.

Patankar, N. A., Singh, P., Joseph, D. D., Glowinski, R., and Pan, T.-W. (2000). A new formulation of the distributed Lagrange multiplier/fictitious domain method for particulate flows. *Intl. J. Multiphase Flow*, 26(9):1509–1524.

Peirano, E. and Minier, J.-P. (2002). Probabilistic formalism and hierarchy of models for polydispersed turbulent two–phase flows. *Phys. Rev. E*, 65:046301.

Poelma, C. and Ooms, G. (2006). Particle–turbulence interaction in a homogeneous, isotropic turbulent suspension. *App. Mech. Rev.*, 59(2):78–90.

Pope, S. B. (1985). PDF methods for turbulent reactive flows. *Prog. Energy Combust. Science*, 11:119–192.

Pope, S. B. (2000). *Turbulent Flows*. Cambridge University Press, Port Chester, NY.

Pope, S. B. (2002). Stochastic Lagrangian models of velocity in homogeneous turbulent shear flow. *Phys. Fluids*, 14(5):1696–1702.

Pozorski, J. and Minier, J.-P. (1999). Probability density function modeling of dispersed two–phase turbulent flows. *Phys. Rev. E*, 59(1):855–863.

Ranz, W. E. and Marshall, W. R. (1952). Evaporation from drops. Parts I and II. *Chem. Engr. Prog.*, 48:141–146, 173–180.

Reeks, M. W. (1991). On a kinetic equation for the transport of particles in turbulent flows. *Phys. Fluids*, 3(3):446–456.

Reeks, M. W. (1992). On the continuum equations for dispersed particles in nonuniform flows. *Phys. Fluids*, 4(6):1290–1303.

Sawford, B. L. and Yeung, P. K. (2001). Lagrangian statistics in uniform shear flow: Direct numerical simulation and Lagrangian stochastic models. *Phys. Fluids*, 13:2627.

Sethian, J. A. (1996). *Level Set Methods*. Cambridge University Press, New York.

Shirolkar, J. S., Coimbra, C. F. M., and McQuay, M. Q. (1996). Fundamental aspects of modeling turbulent particle dispersion in dilute flows. *Prog. Energy Combust. Science*, 22:363–399.

Simonin, O. (1996). Combustion and turbulence in two–phase flows. Technical report, Von Karman Institute of Fluid Dynamics Lecture Series.

Snyder, W. H. and Lumley, J. L. (1971). Some measurements of particle velocity autocorrelation functions in a turbulent flow. *J. Fluid Mech.*, 48:41–71.

Squires, K. D. and Eaton, J. K. (1991a). Measurements of particle dispersion obtained from direct numerical simulations of isotropic turbulence. *J. Fluid Mech.*, 226:1–35.

Squires, K. D. and Eaton, J. K. (1991b). Preferential concentration of particles by turbulence. *Phys. Fluids*, 3(5):1169–1178.

Stoyan, D., Kendall, W. S., and Mecke, J. (1995). *Stochastic geometry and its applications*. J. Wiley and Sons, New York, 2nd edition.

Subramaniam, S. (2000). Statistical representation of a spray as a point process. *Phys. Fluids*, 12(10):2413–2431.

Subramaniam, S. (2001a). Consistent modeling of two–phase flows based on the relationship between point–process and random-field statistical representations (unpublished).

Subramaniam, S. (2001b). Relationship between Lagrangian Statistical Spray Models and Eulerian Statistical Models of Two–phase Flow. In *Proceedings of the Fourteenth Annual Conference on Liquid Atomization and Spray Systems*, pages 34–40. Intl. Liquid Atomization and Spray Systems Soc.

Subramaniam, S. (2001c). Statistical modeling of sprays using the droplet distribution function. *Phys. Fluids*, 13(3):624–642.

Subramaniam, S. (2003). Modeling Turbulent Two–phase flows. In *Proceedings of the Sixteenth Annual Conference on Liquid Atomization and Spray Systems*. Intl. Liquid Atomization and Spray Systems Soc.

Subramaniam, S. (2005). The role of particle–fluid velocity correlation in single–point statistical closures of dispersed turbulent two–phase flows (unpublished).

Subramaniam, S. and O'Rourke, P. (1998). Numerical Convergence of the KIVA-3 code for sprays and its implications for modeling. Technical Report LA-UR-98-5465, Los Alomos Scientific Laboratory, Los Alamos, NM 87545.

Sundaram, S. and Collins, L. R. (1994a). Spectrum of density fluctuations in a particle–fluid system – i. Monodisperse spheres. *Intl. J. Multiphase Flow*, 20(6):1021–1037.

Sundaram, S. and Collins, L. R. (1994b). Spectrum of density fluctuations in a particle–fluid system – ii. Polydisperse spheres. *Intl. J. Multiphase Flow*, 20(6):1039–1052.

Sundaram, S. and Collins, L. R. (1999). A numerical study of the modulation of isotropic turbulence by suspended particles. *J. Fluid Mech.*, 379:105–143.

Ten Cate, A., Derksen, J. J., Portela, L. M., and Van Den Akker, H. E. A. (2004). Fully resolved simulations of colliding monodisperse spheres in forced isotropic turbulence. *J. Fluid Mech.*, 519:233–271.

Truesdell, G. C. and Elghobashi, S. (1994). On the two–way interaction between homogeneous turbulence and dispersed solid particles. II. Particle dispersion. *Phys. Fluids*, 6(3):1405–1407.

Van Kampen, N. G. (1992). *Stochastic processes in Physics and Chemistry*. North–Holland, Amsterdam.

Warnica, W. D., Renksizbulut, M., and Strong, A. B. (1995a). Drag coefficients of spherical liquid droplets Part 1: Turbulent gaseous fields. *Exp. Fluids*, 18:258–264.

Warnica, W. D., Renksizbulut, M., and Strong, A. B. (1995b). Drag coefficients of spherical liquid droplets Part 2: Turbulent gaseous fields. *Exp. Fluids*, 18:265–276.

Wells, M. R. and Stock, D. E. (1983). The effects of crossing trajectories on the dispersion of particles in a turbulent flow. *J. Fluid Mech.*, 136:31–62.

Williams, F. A. (1958). Spray combustion and atomization. *Phys. Fluids*, 1(6):541–545.

Xu, Y. (2004). An improved multiscale model for dilute turbulent gas particle flows based on the equilibration of energy concept. Master's thesis, Iowa State University, USA.

Xu, Y. and Subramaniam, S. (2005). An improved multiscale model for dilute turbulent gas–particle flows based on the Equilibration of Energy concept. In *Proceedings of the ASME FED Summer Meeting and Exhibition*.

Xu, Y. and Subramaniam, S. (2006). A multiscale model for dilute turbulent gas–particle flows based on the equilibration of energy concept. *Phys. Fluids*, 18:033301(1–17).

Xu, Y. and Subramaniam, S. (2007). Conservative interphase turbulent kinetic energy transfer in particle–laden flows. *Phys. Fluids (to appear)*.

Yeung, P. K. and Pope, S. B. (1989). Lagrangian statistics from direct numerical simulations of isotropic turbulence. *J. Fluid Mech.*, 207:531–586.

Yusof, M. J. (1996). *Interaction of massive particles with turbulence*. PhD dissertation, Cornell University, Ithaca, NY.

Zaichik, L. I. (1999). A statistical model of particle transport and heat transfer in turbulent shear flows. *Phys. Fluids*, 11(6):1521–1534.

Zhang, D. Z. and Prosperetti, A. (1994). Averaged equations for inviscid dispersed two–phase flow. *J. Fluid Mech.*, 267:185–219.

Zhu, M., Bray, K. N. C., Rumberg, O., and Rogg, B. (2000). Pdf transport equations for two–phase reactive flows and sprays. *Combustion and Flame*, 122:327–338.